

NATIONAL AERONAUTICS AND SPACE ADMINISTRATION

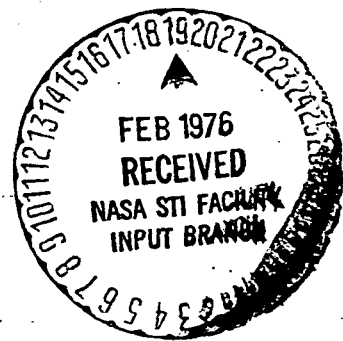
Technical Memorandum 33-734

Volume II

*Mariner Venus-Mercury 1973 Project
Final Report*

Extended Mission—Mercury II and III Encounters

(NASA-CR-145935) MARINER VENUS-MERCURY 1973 N76-17168
PROJECT. VOLUME 2: EXTENDED
MISSION-MERCURY 2 AND 3 ENCOUNTERS Final
Report (Jet Propulsion Lab.) 117 p HC \$5.50 Unclass
CSCL 22C G3/13 13614



JET PROPULSION LABORATORY
CALIFORNIA INSTITUTE OF TECHNOLOGY
PASADENA, CALIFORNIA

December 1, 1975

NATIONAL AERONAUTICS AND SPACE ADMINISTRATION

Technical Memorandum 33-734

Volume II

*Mariner Venus-Mercury 1973 Project
Final Report*

Extended Mission—Mercury II and III Encounters

JET PROPULSION LABORATORY
CALIFORNIA INSTITUTE OF TECHNOLOGY
PASADENA, CALIFORNIA

December 1, 1975

PREFACE

The Mariner 10 spacecraft passed within approximately 48,000 km (29,830 miles) of the bright side surface of the planet Mercury during its second encounter which occurred on September 21, 1974. This encounter was designed primarily for television science. The third Mercury encounter, which occurred on March 16, 1975, was on the dark side of the planet at a distance of approximately 327 km (203 miles) from the planet surface. The third encounter was primarily designed for nonimaging science. Both encounters were highly successful.

The scientific information, both television and non-imaging science, contained in this document was derived from status bulletins published during the mission under the direction of the Mariner Venus/Mercury 1973 Project. The data in these bulletins were obtained from the Principal Investigators in near-real-time in relationship to the events discussed, and as such are to be interpreted as preliminary. For detailed scientific discussions of the Mariner 10 results, the reader is referred to the reference and bibliographic sections in this document.

The work described in this report was performed by the Mariner Venus/Mercury 1973 Extended Mission Project of the Jet Propulsion Laboratory whose membership was composed of personnel from the Jet Propulsion Laboratory and The Boeing Aerospace Company.

**ORIGINAL PAGE IS
OF POOR QUALITY**

ACKNOWLEDGMENTS

The Spacecraft Team, composed of both Boeing and JPL people, put forth great personal efforts and solved perplexing problems with ingenuity. Their development of a workable solar sailing control technique is a major accomplishment in spaceflight technology. Boeing design engineers are to be commended for incorporating the flexibility into the spacecraft without which Mariner 10 could not have survived for a third encounter. The Sequence Generation and Navigation Teams responded to the spacecraft anomalies and emergencies in a professional and outstandingly innovative manner. All Science Team members extend their gratitude to W. Eugene Giberson, who directed the Mariner Venus-Mercury Project from its inception to its second Mercury encounter, to Robert J. Parks who was Acting Project Manager from the post-Mercury II period through the end of the mission, to James A. Dunne, who was deputized to provide project direction on a day-to-day basis, and to the Mariner Mission Operations Team under the direction of Dallas Beauchamp, Chief of Mission Operations, and everyone involved in this accomplishment. For several days, many worked around the clock to make the third Mercury encounter a success.

Those involved in the encounter science made great scientific strides in proving that Mercury possesses an intrinsic magnetic field and a magnetosphere that is remarkably similar in structure to that of the Earth, providing the groundwork for new theoretical work on planetary magnetism and new insights into the physics of the interaction between the solar wind and magnetic carriers.

The cooperation of the Deep Space Network and the Helios and Pioneer Projects personnel in yielding their scheduled tracking time during critical periods is deeply appreciated.

Grateful appreciation is extended to the Mariner 10 Extended Mission Operations Teams for the preparation of this document. Acknowledgment is made to the following Mariner 10 personnel:

M. H. Bantell	Maneuvers
D. F. Beauchamp	Chief of Mission Operations
R. T. Cowley	Propulsion
G. E. Danielson	Television Science
E. K. Davis	DSN Manager
J. A. Dunne	Project Scientist
M. D. Ebben	Telecommunications
P. Esposito	Celestial Mechanics
R. D. Garcia	Temperature Control
M. Gray	Assistant Chief of Mission Operations
J. M. Hardman	Guidance and Control
L. A. Hughes	Data Storage Subsystem
W. N. Jensen	Assistant Chief of Mission Operations
J. B. Jones	Navigation Team Chief
K. P. Klaasen	Television Science
R. E. Koch	Tracking and Orbit Determination
L. Koga	Central Computer and Sequencer
C. C. La Baw	Television Subsystem
J. G. Leisenring	Power Subsystem
A. Messner	Flight Data Subsystem
W. I. Purdy	Spacecraft Team Chief
M. J. Sander	MCCC Manager
J. Schmidling	Data Records
L. L. Schumacher	Attitude Control and Articulation and Pointing
J. H. Thomas	TCM Analysis
J. R. Tupman	Data Records
B. H. Walton	Facilities Operations Project Engineer
R. F. Wong	Central Computer and Sequencer
C. M. Yeates	Non-Imaging Science
A. R. Zieger	Mission Sequence Working Group
V. S. Zum Brunnen	Spacecraft Buss Chief

CONTENTS

I. Introduction	1
A. Purpose	1
B. Background	1
C. Scope	2
II. Extended Mission Summary	3
A. Sequence Summary	3
B. Mission Major Events Time Line	3
III. Science Objectives and Results	9
A. Television Subsystem and Science	9
B. Television Subsystem Performance	14
C. Non-Imaging Science—Mercury II	15
D. Non-Imaging Science—Mercury III	15
IV. Mission Sequence Working Group	23
A. Organization	23
B. Software Functions	23
C. Scheduling	23
D. Sequence Structure	23
E. Problems and Critical Items	25
F. Functions Performed Correctly	25
V. Mission Operations	26
A. Operation Philosophy and Technique	26
B. Recommendations	27
C. Command System	27
VI. Spacecraft Extended Mission Performance	31
A. Telecommunications Systems	31
B. Guidance and Control	43
C. Thermal Control	55
D. Data Control and Processing	59
E. Propulsion Subsystem Performance	62
F. Mariner 10 Power Subsystem	63
VII. Navigation	66
A. Introduction	66
B. Radiometric Tracking	67
C. Orbit Determination	74
D. Maneuver Analysis	92

VIII. DSN Mission Support	103
A. The Period April 15 to Oct. 15, 1974	103
B. Program Control	104
C. Implementation Activities	104
D. The Period Oct. 15, 1974 to Feb. 15, 1975	105
E. The Period Feb. 15 to April 15, 1975	106
IX. Mission Control and Computing Center	109
A. Extended Mission Planning	109
B. MCCC Extended Mission Support	109
C. MCCC Operations	109
D. Mission Support Area	109
E. MSA for Extended Missions	111
X. Data Records	112
A. Science Data Team Activities	112
B. EDR Activities	112
C. SEDR Activities	112
D. Mercury II and III Predicts	113
E. Real-Time Support of Mission Activities	113
F. Recommendations	113
References	114
Bibliography	115

TABLES

1. Extended Mission summary	3
2. Successful commands by mission phase	28
3. Command anomalies by mission phase	30
4. Extended Mission successful commands by command system	30
5. Summary of Extended Mission TCM parameters	51
6. Attitude control estimates of TCM pointing errors — TCM pointing error estimate (bias $\pm 3\sigma$ deg)	51
7. Temperature at Mercury I, II, and III	58
8. Trajectory correction maneuvers	59
9. Mariner 10 TCM summary	63
10. Deep Space Stations used to support Mariner 10	67
11. DSN data types used to support navigation	68
12. Trajectory correction maneuver and flyby summary for the Extended Mission	94
13. Trajectory correction maneuver parameter summary for the Extended Mission	96

14.	Goldstone antenna arraying experiment key characteristics and comments	105
15.	Significant project/DSN Mission achievements	108

FIGURES

1.	Mariner 10 trajectory showing maneuver and encounter events	2
2.	Sequence summary	7
3.	Major mission events time line	8
4.	TV discriminability limits	10
5.	TV Mercury areal coverage	11
6.	TV Mercury wide-angle view	12
7.	TV Mercury south polar region	13
8.	Mosaicked photo of Discovery Scarp	16
9.	Magnetic field lines	16
10.	Spacecraft's path at Mercury III	16
11.	Magnetic field magnitude	16
12.	Mercury's magnetosheath	18
13.	Mercury's magnetosheath and plasma sheet	18
14.	Two views of Mercury I and Mercury III encounters showing bow shock waves	18
15.	Charged particle count profile	20
16.	Spiraling solar magnetic field line	20
17.	Ultraviolet spectrometer limb drift data	20
18.	Mariner 10's ground track across Mercury	20
19.	Third Mercury encounter geometry	20
20.	Doppler variation during Mercury III encounter	22
21.	Representative doppler residuals within Mercury III encounter ± 12 h	22
22.	Extended Mission organization	24
23.	Schedule/logic diagram for typical encounter sequence development	24
24.	Monthly manpower chart	29
25.	TCM 4A downlink AGC	32
26.	Sun-Earth-probe angle	32
27.	33-1/3 bits/s SNR and AGC, May 22 to June 11, 1974	33
28.	33-1/3 bits/s SNR and AGC, June 19-29, 1974	35
29.	X-band downlink AGC mean and standard variation	36
30.	S-band uplink AGC	37
31.	Uplink carrier power mean and standard variation	37

32.	DSN antenna array configuration	38
33.	117 kbits/s BER-Mercury II	40
34.	LGA performance comparison	40
35.	LGA performance, Oct. 15, 1974	41
36.	LGA performance, Jan. 8, 1975	41
37.	TCM 7 predict LGA pattern	42
38.	TCM 7 performance plot	44
39.	Mercury III 22.05 kbits/s bit error rate	44
40.	Mariner 10 articulated members configuration	45
41.	Solar pressure forces on solar panel	45
42.	Earth track and HGA torque versus clock and cone angles	47
43.	Extended mission gas predicts and actual usage	47
44.	Limit cycle torques	49
45.	Limit cycle and torque versus gas consumption	49
46.	Gas Jet pulse rate	56
47.	Roll axis gyro-structural interaction excitation- celestial (roll inertial)	56
48.	Roll axis gyro-structural interaction excitation- celestial (gyro rate)	57
49.	Equivalent Sun hours from launch	57
50.	Solar panel degradation	65
51.	Block diagram to generate two-way doppler (F2)	69
52.	Tracking data flow block diagram	70
53.	Data quality analysis edit procedure	73
54.	Univac 1557/1558 display device	73
55.	Theory of range calibration at a deep space station	73
56.	DSS range residuals	75
57.	F2 data on day of superior conjunction	76
58.	Assumed plasma-corrupted F2 residuals	76
59.	Plasma-corrupted F2 residuals	77
60.	Clean F2 residuals data	78
61.	Uncorrected F2 residuals	79
62.	Roll-corrected F2 residuals	80
63.	Significant navigation events	83
64.	Definition of B-plane	84
65.	Mercury II B-plane solutions	84
66.	TCM 4 in Mercury B-plane	85
67.	Doppler noise versus Sun-Earth-probe angle	88

68.	TCM 5 in Mercury II B-plane	88
69.	Pre-TCM 6 Mercury B-plane	89
70.	TCM 6 in Mercury III B-plane	90
71.	TCM 7 orbit determination in Mercury III B-plane	90
72.	TCM 7 post-maneuver estimates in Mercury III B-plane	91
73.	TCM 6 Mercury III flyby	98
74.	TCM 7 Mercury III flyby	100
75.	TCM 8 Mercury III flyby	101
76.	Goldstone DSSC antenna array block diagram	101
77.	Mission support area layout	110

ABSTRACT

This report describes the Mariner Venus/Mercury 1973 mission operations Extended Mission. Prepared by the Mission Operations Team, this report encapsulates the activities from shortly after Mercury I through the end of mission. The operational activities are reported by Mission Operations Systems functions providing a brief summary from each discipline. Based on these experiences, recommendations for future projects are made.

**ORIGINAL PAGE IS
OF POOR QUALITY**

DEFINITION OF ABBREVIATIONS

ACE-1	Operational designation for the on-duty ACMO
ACMO	Assistant Chief of Mission Operations
ADC	Analog-to-digital converter
AGC	Automatic gain control
APS	Articulation and pointing subsystem
BER	Bit error rate
B/R	Booster regulator
CA	Closest approach
CC&S	Central computer and sequencer
CMO	Chief of Missions Operations
COMGEN	Command generation
COPY	Program for copying SEDRs
CPT	Charged particle telescope
CMRS	Celestial Mechanics and Radio Science
DCMO	Deputy Chief of Mission Operations
DN	Data number
DPODP	Double Precision Orbit Determination Program
DPTRAJ	Double Precision Trajectory Program
DSN	Deep Space Network
DSS	Data Storage System, also Deep Space Station (Table 10)
DSCC	Deep Space Communications Complex
ECO	Engineering change order
EDR	Experimental data records
EDRGEN	Experimental data record generator
EM	Mercury encounter
EPIM	Magnetometer EDR Program
ESH	Equivalent Sun hours
FE	Far encounter
FDS	Flight data subsystem
FDSC	Flight Data System Count (Program)
FIP	Fixed Instrument Pointing (Program)
FLICONS	Flight path software control (1108)
GMT	Greenwich Mean Time
GPCF	General-Purpose Computing Facility
HGA	High-gain antenna

LIBPOG	LIBRARY POGASIS Program
LGA	Low-gain antenna
LSB	Least significant bit
MCCC	Mission Control and Computing Center
MCCF	Mission Control and Computing Facility
MDS	Modulation-demodulation subsystem
MOAT	Mission Operations Analysis Team
MOPS	Maneuver Operations Program system
MOS	Mission Operations System
MSA	Mission Support Area
MSWG	Mission Sequence Working Group
MTC	Mission and test computer
MTCF	Mission and Test Computer Facility
NCS	Network Control System
NIS	Non-Imaging science
NSP	NASA Support Plan
OD	Orbit determination
ODR	Original Data Record
OPSCOP	Operations Control Program
OVT	Operational verification test
PAFUVS	Particle and fields ultraviolet spectrometer
PET	Probe ephemeris tape
PLOP	Planetary operations
POGASIS	Planetary observation geometry and science instrument sequencer
POR	Power on reset
PRA	Planetary ranging assembly
PSE	Plasma science experiment
PS&L	Power switching and logic
RFMT	Reformat
SCE	Spacecraft event
SEDR	Supplementary experiment data
SEG	Sequence of events generator
SEP	Sun-Earth-probe
SES	Scanning electron spectrometer
SIRD	Support Instrumentation Requirements Document
SOFCNS	Software control
SPOP	Scan Platform Operations Program

SOE	Sequence of events
SSA	Symbol synchronizer assembly
SSG	Science Steering Group
STUFF	Computer program to complete engineering minor frames
TCA	Time of closest approach
TCM	Trajectory correction maneuver
TMU	Telemetry modulation unit
TPAP	Telecommunications prediction and analysis program
TSOST	TV science operational sequence table
TVS	Television subsystem
TVCA	Thrust Vector Control Assembly
UVSAG	Ultraviolet spectrometer – airglow

I. INTRODUCTION

This is the final report for the Extended Mission of the Mariner Venus/Mercury 1973 (MVM '73) Program. Preparation of this report is in accordance with a request from the MVM '73 Mission Project Office.

A. Purpose

The purpose of this report is to document a brief summary of the MVM '73 Extended Mission and describe the unique operational features utilized. Sections of the document list operational items performed correctly and others which were considered disadvantageous. All items are intended to be constructive. In the hope of helping future mission operations, the special techniques which resulted in time and cost savings are specifically emphasized.

B. Background

The MVM '73 Extended Mission began at the culmination of the primary mission, April 15, 1974. Project decision was made to attempt a Mercury II and possibly Mercury III encounter based on having sufficient onboard consumables. Figure 1 shows maneuver and encounter events plotted on the mission trajectory curve. At this time it was readily apparent that the most critical consumable item was attitude-control gas. Due to problems encountered during the primary mission, most of the gas had been depleted. Hence, it became mandatory that a scheme for efficient use of attitude-control gas be devised.

Maximum television science at a Mercury encounter was attainable with a bright-side flyby, whereas a dark-side flyby was desirable for non-imaging science (NIS). Another dark-side pass, similar to the first Mercury encounter would yield very little additional science for TV. In order to maximize science return, a decision

was reached to make the Mercury II encounter a bright-side pass followed by a dark-side encounter for Mercury III. Also, having the bright-side encounter first fulfilled propulsion constraints (discussed later).

During Mercury I, excellent TV coverage was obtained of the incoming and outgoing visible portions of the planet; but, due to the nature of the dark-side flyby, it was not possible to obtain coverage of the planetary areas directly facing the Sun. Hence, the TV Team requested a bright-side pass which would provide coverage of one of the poles. Since the Mercury II return trajectory was below the planet, the Navigation Team recommended altering the trajectory for a southern hemisphere pass. Thus, the primary objective for Mercury II became: OBTAIN IMAGING DATA OF THE SOUTHERN HEMISPHERE PROVIDING PHOTOGRAPHIC COVERAGE TO OVERLAP WITH THE DATA ALREADY OBTAINED.

The Mercury II flyby would be too far from the planet to achieve NIS data other than ultraviolet spectrometer - airglow (UVSAG) data.

The Mercury I encounter unexpectedly revealed a planet-related magnetic field. With a single dark-side flyby, there remained a question as to whether the field was intrinsic or induced. It was quite conceivable that the magnetic field measurements could be stronger than expected due to solar interaction in the immediate vicinity of the planet. To detect an intrinsic magnetic field, it would be necessary to have a close dark-side encounter. Hence, the primary objective of the Mercury III flyby was: OBTAIN NIS DATA DURING A CLOSE DARK-SIDE FLYBY WITH PRIMARY EMPHASIS ON THE MAGNETOMETER MEASUREMENTS.

Imaging data was of secondary priority with the objectives of obtaining higher resolution pictures of areas previously covered and possibly the highest resolution pictures of the mission.

C. Scope

This report provides a summary of the operational aspects of the MVM '73 Extended Mission.

Chronologically it covers mission operations from April 15, 1974 to the end of mission, which occurred at 05:21 PDT March 24, 1975. The report is organized according to MOS disciplines with each section containing problem areas and recommendations. A bibliography of relevant documents pertaining to more detailed analysis of some of the problems is included for reference.

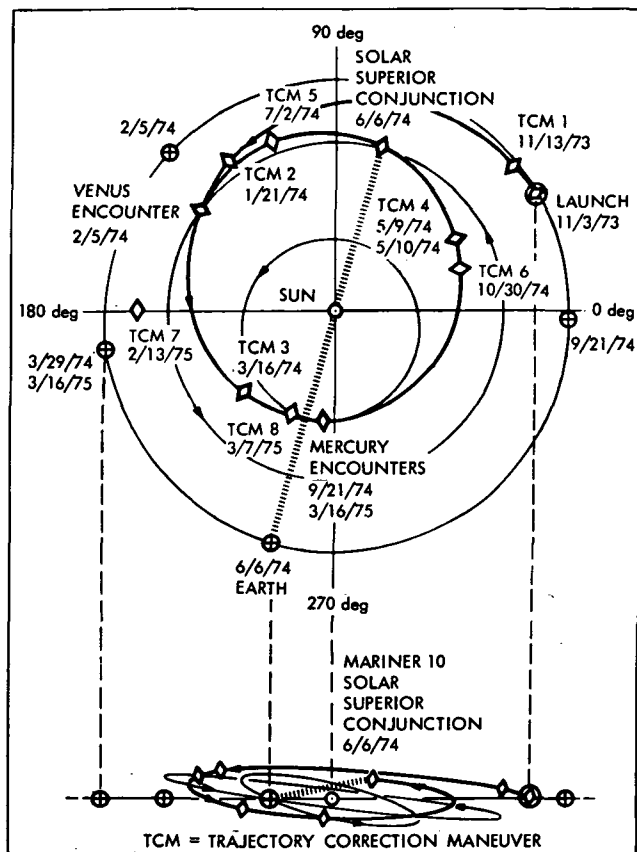


Figure 1. Mariner 10 trajectory showing maneuver and encounter events

II. EXTENDED MISSION SUMMARY

A. Sequence Summary

Figure 2 presents the overall MVM '73 mission summary showing the period of the Extended Mission. The Extended Mission comprises about two thirds of the total mission, since the primary mission was about six months duration. Table 1

lists the key extended mission items and descriptive comments.

B. Mission Major Events Time Line

Figure 3 presents the major events sequence and a brief summary of the spacecraft subsystem activity periods.

Table 1. Extended Mission summary

Item	Time	Comment
Begin extended mission	April 15, 1974	Began routine use of DSS (tape recorder) to obtain data during DSN tracking gaps. Some DSS cycling controlled by CC&S routines. Beginning in May tape recorder playbacks were suspended due to poor link performance as a result of increasing range to the spacecraft
TCM-4 A/B	May 9, 10, 1974	TCM performed on back-to-back days due to propulsion constraints. CC&S parameters were reloaded between maneuvers
Superior conjunction period	May 24 start June 6 conj. July 20 end	Performed dual frequency S/X band radio science experiments
TCM-5	July 2, 1974	TCM provided precise navigation to Mercury II aim point. Last successful use of onboard tape recorder.
Magnetometer and CPT calibration	July 5, 1974	First magnetometer calibration and flips and CPT calibration after superior conjunction. Calibrations performed on weekly basis when possible
UVSAG slit cal and scan platform engineering test	July 22, 1974	Performed to support Mercury II encounter preparation
PSE/SES status check	Aug. 5, 1974	Determine the response of the channeltrons
DSS tape failure	Aug. 14, 1974	Tape recorder not slewing properly; tape motion sluggish. Appeared to be stuck past parking window
Subreflector, antenna off-point, and dichroic reflector test	Aug. 12, 1974	Performed in preparation for Mercury II encounter. Telecommunications/DSN preparing for antenna arraying at Goldstone during this period
Magnetometer sensitivity check	Aug. 19, 1974	Determination magnetometer performance
DSS failed	Aug. 20, 1974	DSS test performed, tape motion obtained but stuck again during test, unable to move tape again
MCCC OVT	Sept. 9, 1974	Verified readiness of facility
Array test DSS 14 DSS 12 DSS 13	Sept. 11, 1974	Verified array concept and performance using 117.6 kbits/s data from the spacecraft

Table 1 (contd)

Item	Time	Comment
Goldstone DSCC test DSS 14 DSS 43	Sept. 11, 1974	Checkout of the DSN stations for encounter operations
Array test DSS 14 DSS 12 DSS 13	Sept. 12, 1974	Further verification and performance measurement
CC&S load U-26.0 EM2 encounter sequence	Sept. 13, 1974	Full load (about 500 words) of the Central Computer and Sequencer (CC&S) requiring approx. 10 hours of continuous ground commanding
Goldstone DSCC test DSS 63	Sept. 15, 1974	Checkout of DSS 63 for 22.05 kbits/s sequences
TV and UVSAG on	Sept. 16, 1974	Science instruments turn on
Array test DSS 14 DSS 12 DSS 13	Sept. 16, 1974	Final array test prior to encounter
Goldstone DSCC test DSS 14	Sept. 16, 1974	Goldstone DSCC supergroup test to validate ability to receive 117.6 kbits/s in real time at MCCC
Optical navigation	Sept. 17, 1974	Perform optical navigation sequences via ground commands every 3 hours
Far encounter TV mosaic and UVSAG slews	Sept. 17, 1974	73 km far encounter TV mosaic and UVSAG slews
Optical navigation	Sept. 18, 1974	Two sets of optical navigation sequences to obtain planet/star relative geometry pictures
Real time TV mosaics	Sept. 18, 1974	Data mode 4 (117.6 kbits/s) with filter wheel stepping followed by UVSAG slews
Jupiter TV pix and UVSAG slews	Sept. 19, 1974	First pictures of Jupiter taken by Mariner spacecraft for TV calibration purposes followed by UVSAG slews of Mercury
TV mosaic	Sept. 20, 1974	Final far encounter 117.6 kbits/s TV mosaics prior to encounter
UVSAG step and drift	Sept. 20, 21, 1974	UVSAG step and drift sequence to obtain slow scans across the planet due to spacecraft planet relative motion
UVS collector high-voltage and CPT priority inhibit	Sept. 21, 1974	UVSAG and CPT to proper enc mode at EM2-8 hrs
CC&S control	Sept. 21, 1974	Begin onboard computer control of the encounter sequence
UVSAG slews	Sept. 21, 1974	Performed from EM2-7 h to EM2-2 h and after closest approach from EM2+2 h to EM2+7 h
Encounter TV	Sept. 21, 1974	Primary encounter pictures were obtained for EM2 \pm 2 h pictures received were of excellent quality providing new coverage of the south pole region. The antenna array technique used for the first time during this encounter made possible the receipt of full frame pictures at acceptable bit error rates. Ranging was off during encounter. The CC&S sequence terminated at EM2+8 h

Table 1 (contd)

Item	Time	Comment
UVSAG step and drift	Sept. 22, 1974	UVSAG data obtained during outgoing encounter similar to the incoming sequence
TV mosaic	Sept. 22, 1974	Final outgoing far encounter TV mosaic to complement the corresponding incoming mosaic
Optical navigation	Sept. 22, 1974	Final three optical navigation sequences followed by TV and UVSAG off
CC&S load U-28.0	Sept. 23, 1974	Onboard computer programmed for cruise functions such as HGA pointing, solar panel tilts, Canopus cone steps
Acquisition lost	Oct. 5, 1974	Loss of Canopus due to particle
Acquisition lost	Oct. 6, 1974	Loss of Canopus due to particle. Difficulty reacquiring without using major portion of remaining attitude-control gas. Decision to stay in roll drift mode to conserve attitude-control gas.
CC&S load U-28.2	Oct. 28, 1974	TCM-6 maneuver sequence and FDS reprogramming
TCM-6	Oct. 30, 1974	First TCM performed with rolling spacecraft maneuver consisted of stopping at proper roll angle and performing pitch-burn-pitch CC&S controlled sequence, then return to roll drift mode
1 year in flight	Nov. 3, 1974	Mariner 10 was launched Nov. 3, 1973 at 05:45 GMT
NIS-2 using LGA magnetometer roll calibration maneuver NIS checkout		During spacecraft closest distance to Earth data mode 13 was used to obtain low rate NIS data over the LGA with the spacecraft in the roll drift mode
Aim point selection	December and January	Meetings were held to determine best aim point for science. SSG selected high north latitude darkside pass as close as possible with primary emphasis on magnetic field measurements
CC&S load U-28.6	Feb. 10, 1975	TCM-7 maneuver sequence loaded for another pitch-burn-pitch maneuver strategy similar to TCM-6
TCM-7 aborted	Feb. 12, 1975	Uncertainties in Canopus identification made aborting mandatory
TCM-7	Feb. 13, 1975	Executed as planned. Entire maneuver sequence was retargeted and implemented by working around the clock. Spacecraft remained roll drift mode before and after CC&S controlled maneuver
EM3 sequence preparation	December through February	Varying aim point selection created the need for developing several Mercury III encounter sequences. The sequence was very sensitive to pointing due to the close approach
CC&S load U-28.8	Mar. 6, 1975	Small CC&S load to perform TCM-8 sunline maneuver
TCM-8 sunline	Mar. 7, 1975	Executed as planned. Performed to provide assurance of not impacting. Created need for another complete iteration through sequence software

Table 1 (contd)

Item	Time	Comment
EM3 encounter load, part 1	Mar. 8, 1975	Due to multiple project demands of DSN stations MVM was forced to use one pass per day consequently it was elected to uplink the encounter load in 3 parts using DSS 63
EM3 encounter load, part 2	Mar. 9, 1975	
EM3 encounter load, part 3	Mar. 10, 1975	
Canopus acquisition	Mar. 13 to Mar. 15	Tremendous difficulties in acquisition are attributable to a series of problems. See Sect. VI-B for details
TV sequence and NIS checkout	Mar. 15, 1975	Far encounter TV in edit mode was obtained. Magnetometer and PSE checkout sequences were performed
CC&S load to tweak encounter sequence	Mar. 15, 1975	Redefinition of the aim point from orbit determination after performing TCM 8 created the need for a final restructuring of certain parts of the encounter sequence
Mercury III encounter	Mar. 16, 1975 22:39:24 GMT	Closest approach was about 327 km above the surface. Primary objectives of obtaining critical NIS data were achieved. High resolution pictures of Mercury were obtained, although optimum TV data was not achieved because the TV edit mode was used due to station not being able to receive imaging 1 data (117.6 kbits/s) at the required bit error rate
TV color mosaic and TV off	Mar. 17, 1975	Outgoing far encounter TV mosaic was performed with filter wheel stepping. This obtained the data required for preparing a color mosaic. Following the mosaic the TV was turned off
UVSAG slit calibration and astronomy	Mar. 17 to Mar. 20, 1975	The UVSAG slit was calibrated and several UVS astronomy sequences were performed with good results
Engineering tests	Mar. 21, 1975	See engineering test results in Sect. VI
End of mission	Mar. 24, 1975 12:21:00 GMT	Spacecraft attitude control gas was depleted. Radio subsystem was turned off using DC-55

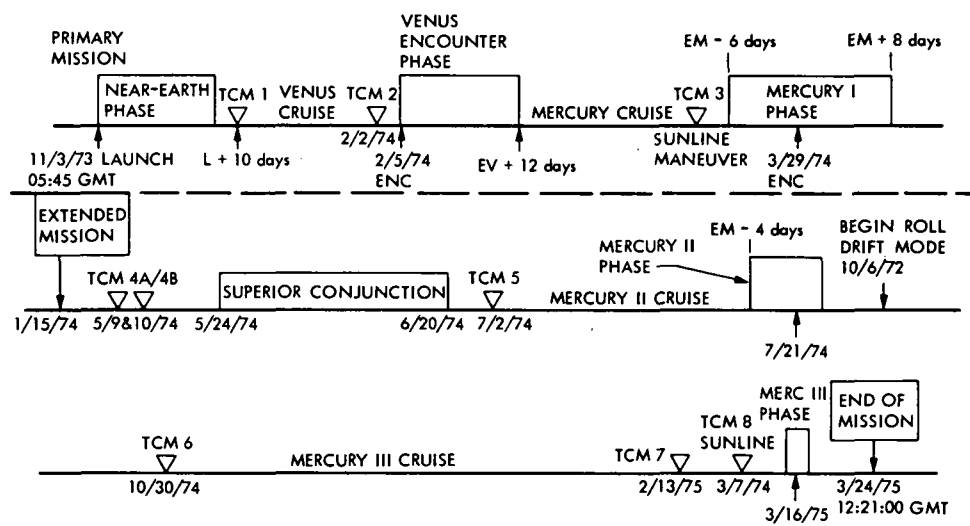


Figure 2. Sequence summary

ORIGINAL PAGE IS
OF POOR QUALITY

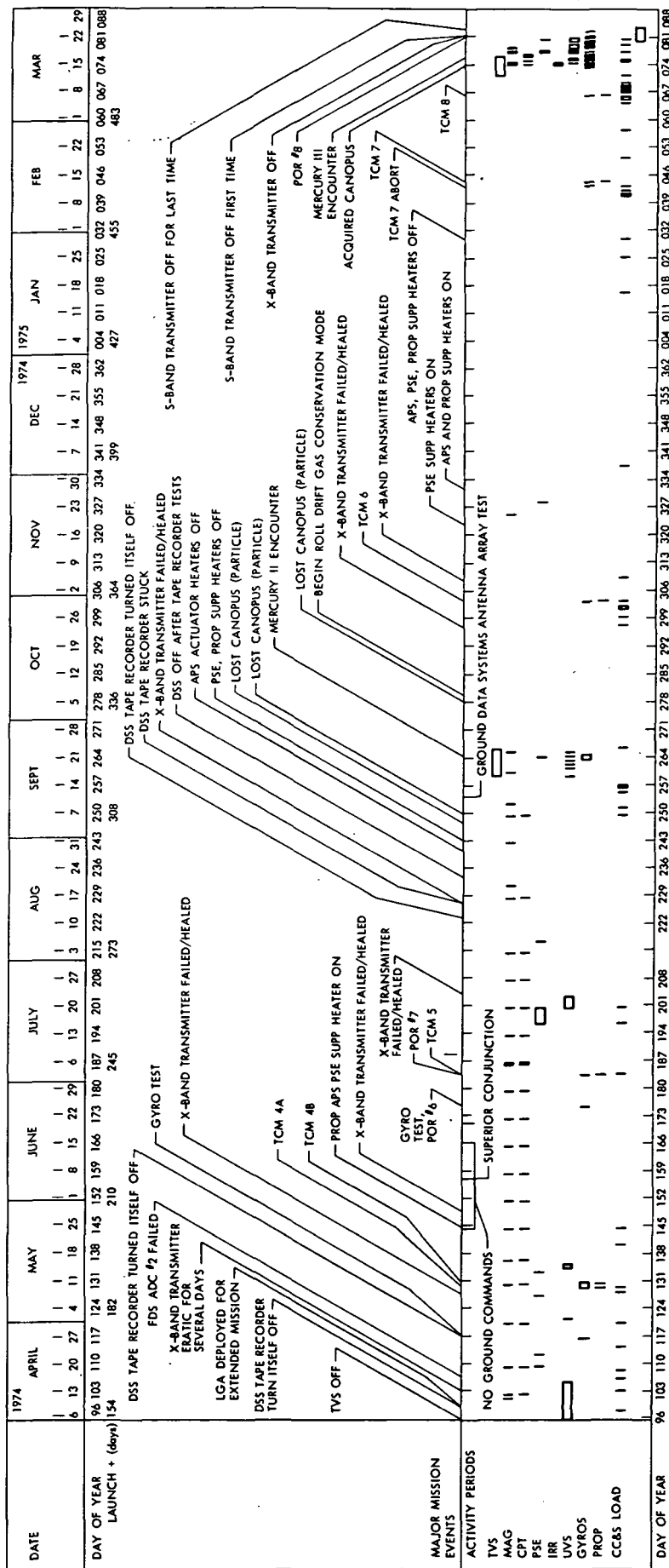


Figure 3. Major mission events time line

III. SCIENCE OBJECTIVES AND RESULTS

A. Television Subsystem and Science

1. Mercury II. The first encounter of Mercury was targeted for a dark-side flyby in order to maximize the science return from all the experiments onboard the spacecraft. The second encounter provided a unique opportunity to greatly enhance the return from the television science experiment by selecting a bright-side aim point. Synchronisms between the spacecraft orbit, Mercury's orbit, and Mercury's rotation rate caused the identical portion of Mercury to be sunlit for both encounters. Although no new terrain was lit, much valuable imaging data could still be added to that obtained during the first encounter. Severe foreshortening and high solar illumination angles precluded accurate interpretation of the surface structure near the limb regions of Mercury as viewed on the first encounter (Fig. 4). The bright-side pass allowed continuous television coverage of these regions and provided for a geologic and cartographic tie between the two sides.

In order to obtain continuous coverage of the regions of interest with the long focal length (1500 mm) cameras, the periapsis point was chosen with a range of about 50,000 km. Although this large miss distance meant a sacrifice in surface resolution, the greater areal coverage allowed was deemed more desirable. An aim point about 35 deg South of the equator minimized the velocity change needed for a possible third encounter of Mercury. Television science preferred an aim point farther South to allow unfore-shortened photography of the Southern terminator region. The final aim point was chosen to be about 40 deg South of the equator.

With this aim point selection, the following objectives were adopted for the television science experiment:

- (1) Obtain a geologic and cartographic tie in the Southern hemisphere between the two sides of Mercury photographed during the first encounter.
- (2) Search for new types of terrain not seen during the first encounter and determine the extent of previously recognized types.
- (3) Search for basins in the size range 450 to 1300 km, none of which were recognized on the first encounter pictures.
- (4) Obtain stereographic coverage of a large portion of the Southern hemisphere for quantitative topographic information.
- (5) Improve knowledge of the Mercurian photometric function through observations at different phase angles.

In order to achieve these objectives, an imaging sequence was designed that consisted of a far-encounter sequence for instrument checkout and calibration, and a real-time imaging sequence at 117.6 kbits/s in the six-hour period around encounter. To meet the photometry objective, the far-encounter sequence included photography of

Mercury at up to seven exposure levels through the various color filters to characterize the camera sensitivity at cold temperatures (the optics heaters had failed just after the first Mercury encounter) and photography of Jupiter to give an independent check of absolute system sensitivity. The planned encounter sequence consisted of coverage of the entire sunlit Southern hemisphere at surface resolutions between 1 and 3 km in an attempt to meet the other objectives. One picture through the wide-angle optics (50-mm focal length) was planned near periapsis to obtain photometric data at the minimum possible phase angle.

The entire television science sequence was accomplished as planned. Pointing was excellent; scan platform backlash was compensated for very well. The telemetry bit error rate was about 1/35, as expected. Figure 5 shows the approximate area covered during the second encounter at between 1 and 1.5 km resolution (shaded) overlaid on a map of the coverage obtained during the first encounter. Areal coverage at good discriminability was increased by about 50%. Figure 6 shows the wide-angle view of Mercury obtained near encounter and compares this view to those from the first encounter. Figure 6(a) is the Mercury I outgoing view, 6(b) is the Mercury I incoming view, and (c) is the Mercury II view.

The pictures obtained of the Southern hemisphere have provided the coverage necessary to make a reliable geologic and cartographic tie between the two sides of Mercury seen on the first encounter. In general, the South polar regions consist of a heavily cratered surface very similar in appearance to the inbound side seen on the first encounter (Fig. 7). The surface is crossed by numerous bright rays. Several large basins, often multiringed, were observed in the size range of 200 to 600 km. Lobate scarps are abundant in the South polar regions, which supports the concept of an early episode of global compression. With appropriate image processing, excellent stereoscopic viewing can be achieved over the majority of the lit Southern hemisphere that will be extremely valuable in deciphering Mercurian topographic, stratigraphic, and structural relationships.

2. Mercury III. The aim point for the third encounter of Mercury was again on the dark side to maximize the return from the particles and fields experiments. Periapsis was chosen to be about 200 km above the surface at about 70 deg North latitude. Again, the identical portion of Mercury's surface was illuminated.

Although the trajectory passed far to the North at periapsis, the view of the planet outside of approximately 20 min on either side of encounter was changed only slightly from that of the first encounter because of the close flyby point. Therefore, essentially no new area could be photographed on the third encounter. The objectives of the television science experiment for the third Mercury encounter were thus chosen to be:

- (1) Increase the resolution of the photography of selected targets of interest.

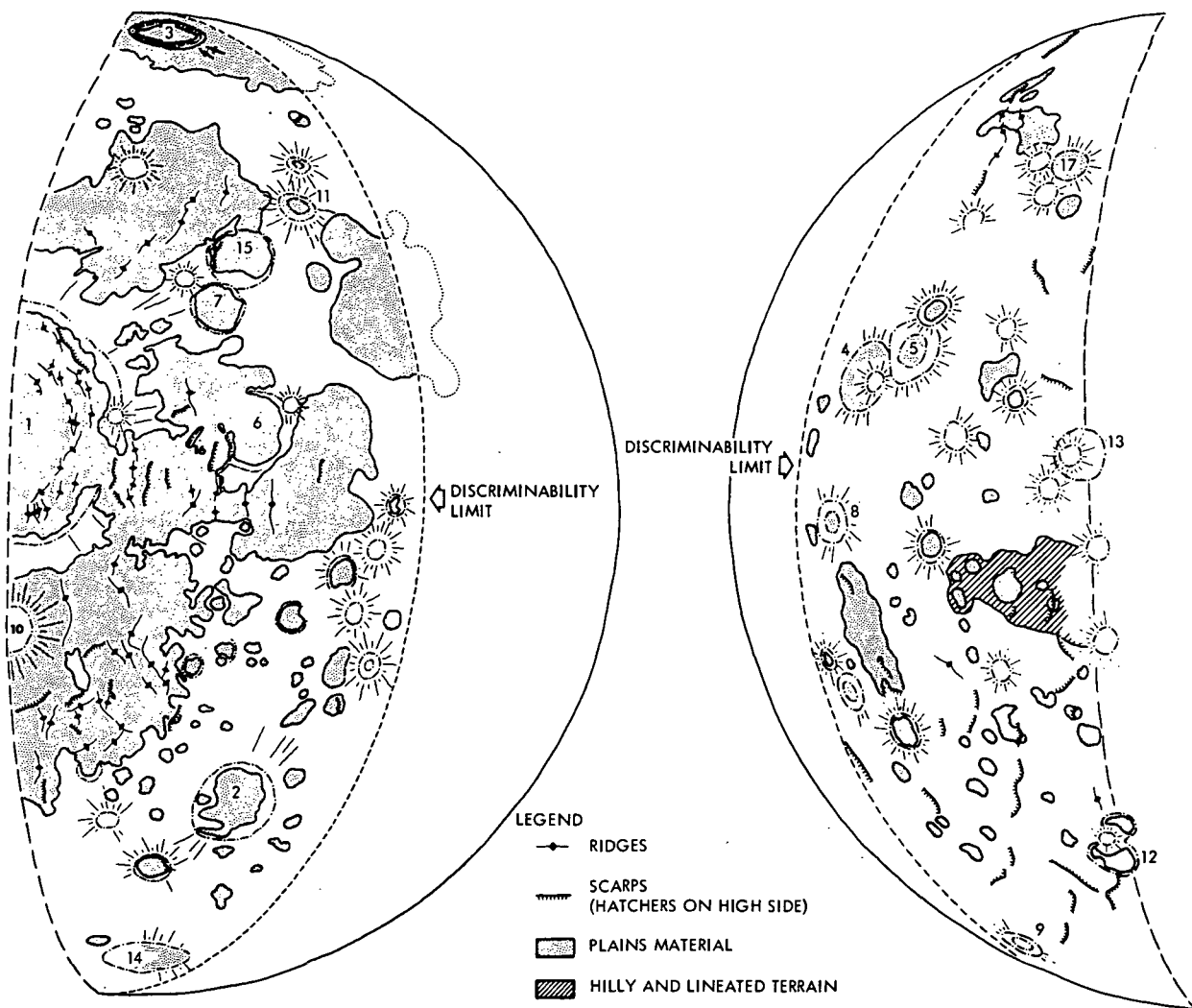
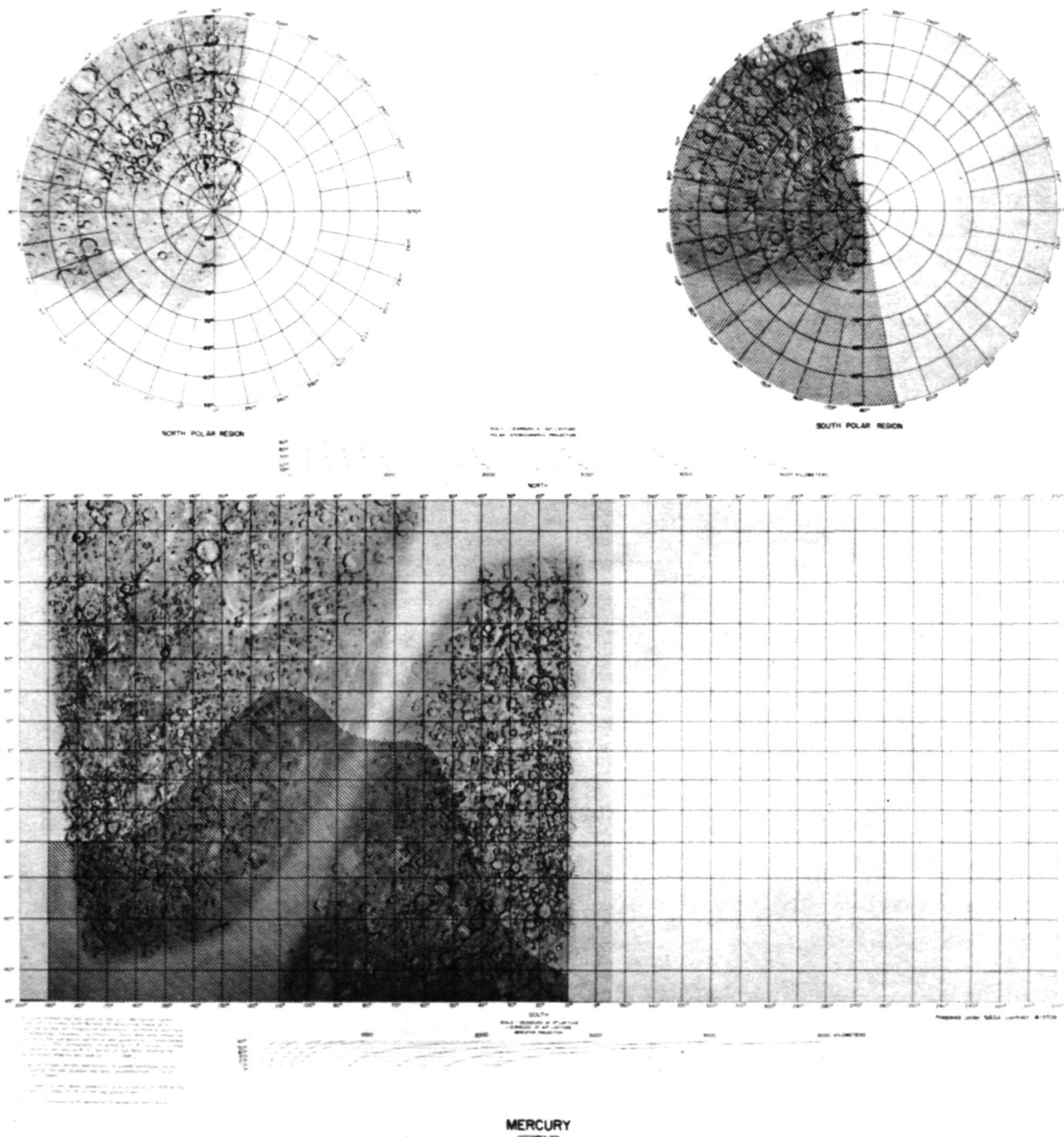


Figure 4. TV discriminability limits



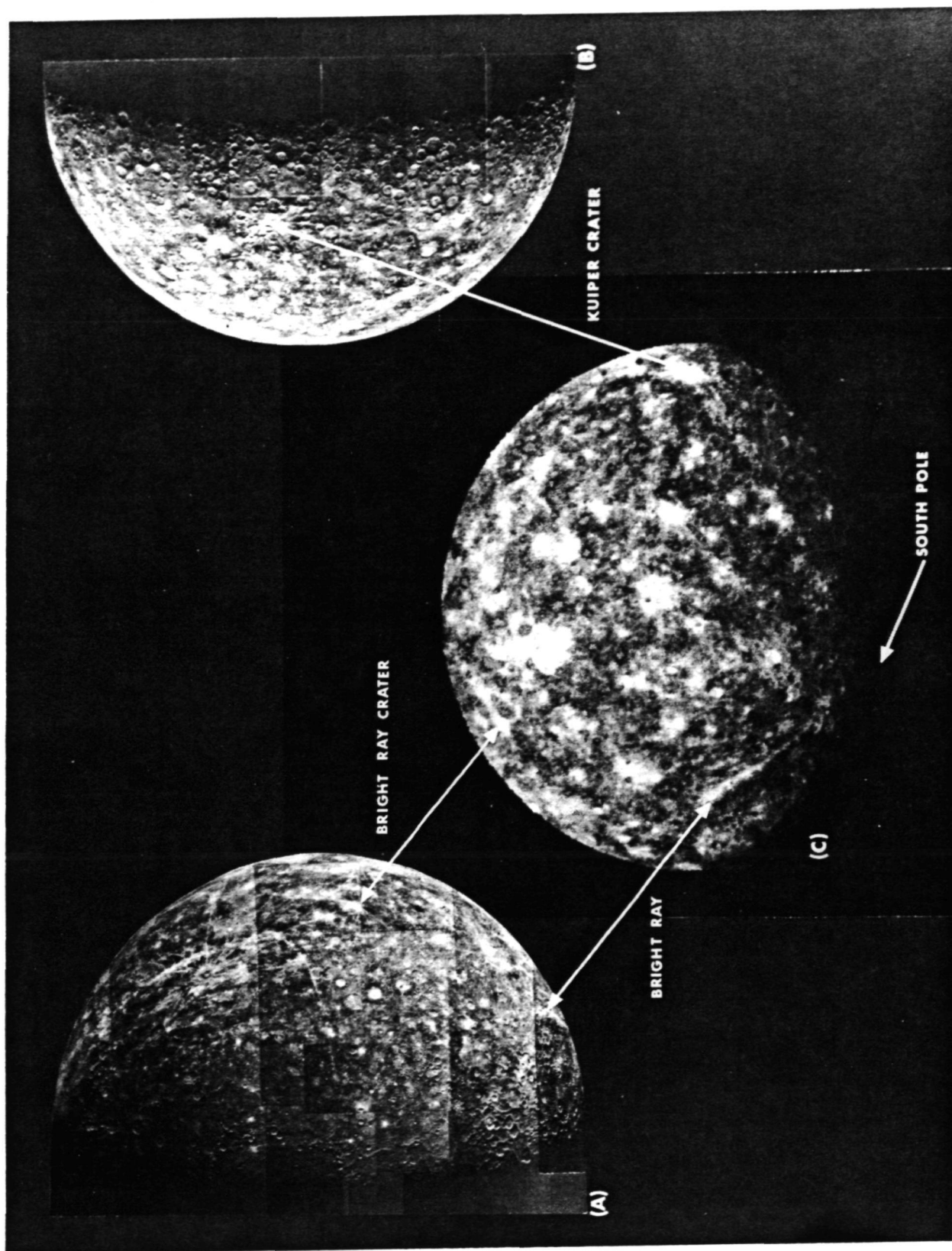


Figure 6. TV Mercury wide-angle view

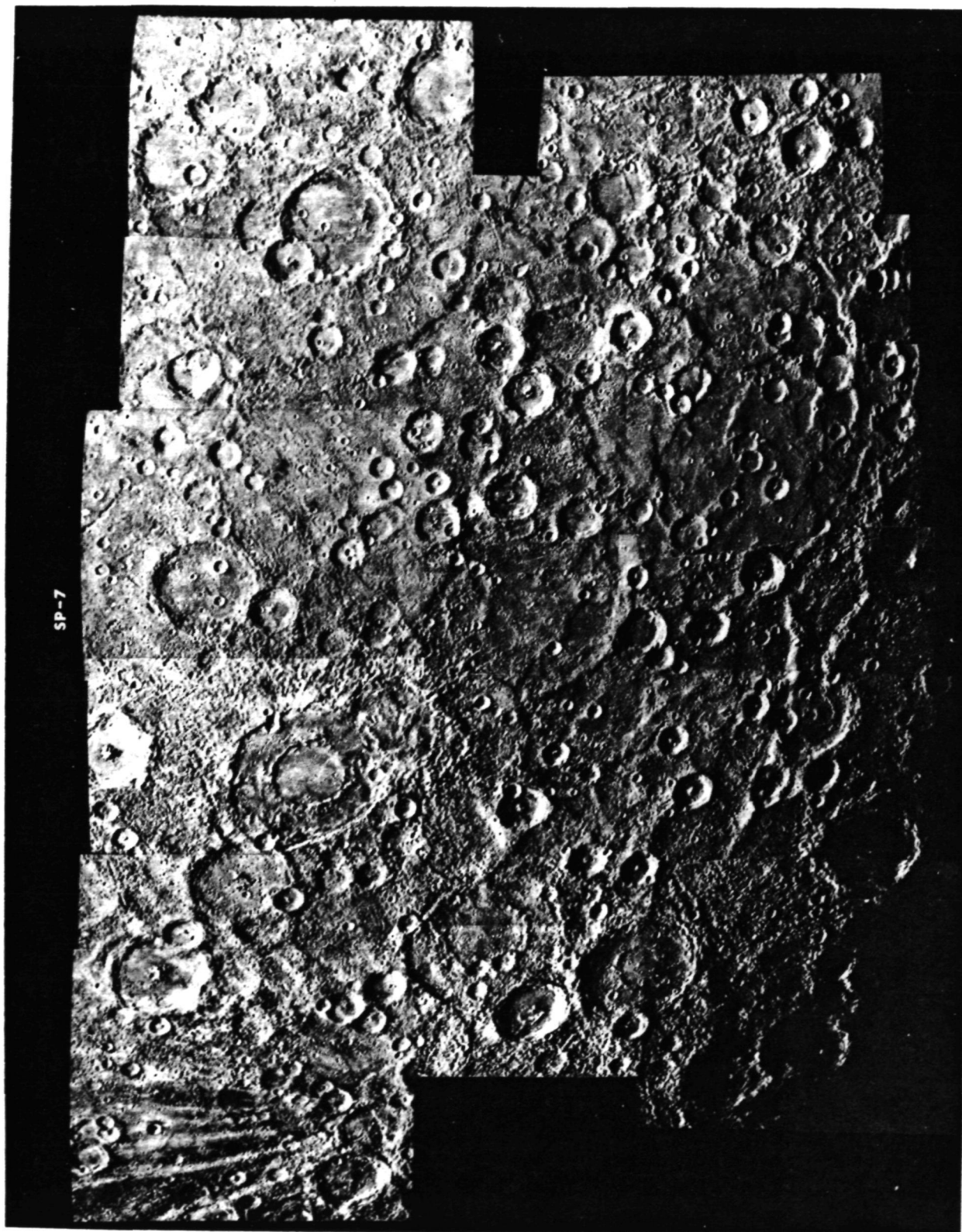


Figure 7. TV Mercury south polar region

- (2) Fill in gaps in the high-resolution coverage obtained on the first encounter.
- (3) Improve the color ratio data in the terminator regions.

The planned imaging sequence consisted of a far-encounter sequence for instrument checkout and calibration, mosaics in orange and ultra-violet wavelengths covering the terminator regions about six hours out on either side of encounter, and high-resolution photography at 117.6 kbits/s of selected points and areas in the four-hour period around encounter.

The actual television sequence only partially fulfilled the objectives. Difficulties in acquiring Canopus caused deletion of the early portions of the far-encounter sequence, although enough data were obtained after acquisition to calibrate the system. Difficulties in resetting the roll position gyro prior to encounter forced delay of the color ratio mosaic scheduled for 6 h before encounter. When the mosaic was actually begun, the command system at DSS 14 failed and the mosaic was canceled. The real-time encounter sequence then had to be performed at 22.05 kbits/s in the center-strip edit mode because DSS 43 had hardware problems and could not cool their maser sufficiently to achieve an acceptable bit-error rate at 117.6 kbits/s. Scan platform pointing control appeared good. However, only a few of the high-resolution targets were actually photographed, partly because of the quarter-frame coverage and partly because periapsis was higher than predicted, and the outgoing trajectory asymptote was somewhat changed. High-resolution pictures were received of Discovery Scarp, the "weird terrain," and the floor and mountains of the Caloris Basin. The color ratio mosaic on the outbound leg was obtained. Picture processing and scientific analysis of the data is underway.

Figure 8 is a mosaic of four frames taken during the Mercury III encounter. Although only the center quarter of each frame was received, fortuitous spacecraft limit cycling caused these four frames to fall close enough together to be mosaicked. The highest resolution pictures (600 m) of Discovery Scarp, the target of interest for this planned mosaic, are shown here. This scarp, located near 38°W longitude and 55°S latitude, is over 500 km long and 2 to 3 km high and presents some evidence for an early episode of crustal shortening on Mercury. The distance from top to bottom of this mosaic is about 300 km.

B. Television Subsystem Performance

1. Mercury II. Television power was turned on by ground command at 15:40 GMT, September 16, 1974. The beams and light flooding were enabled at 07:13 GMT, September 17, 1974. The resulting beam currents were:

A = 73 DN read, 122 DN erase

B = 96 DN read, 175 DN erase

Normal operation was observed during the entire encounter period.

Statistics for the encounter was as follows:

Power ON	277.3 h
Beams ON	63.6 h
Filter steps	A = 48 B = 64
Shutters	1436 each

The television subsystem was turned OFF at 04:39 GMT, September 23, 1974.

2. Mercury III. TV power was turned on by ground command at 10:47 GMT, March 12, 1975. Power on was confirmed by a change in the +X solar panel current. Temperatures rose through the next three days, finally stabilizing at -5°C for the A vidicon and -14° and -15°C for the B optics (rear) and the Auxiliary Electronics Subassembly, respectively. Data Mode 1 on March 15, 1975 provided housekeeping data indicating that all TVS operating parameters were correct. The beams and light flood were enabled at 1008 GMT, and the resulting beam currents (A = 77 DN read, 130 DN erase; B = 94 DN read, 170 DN erase) were virtually the same as at turn-off after Mercury II.

Near-encounter proceeded without difficulty, although the inability to receive 117.6 kbits/s imaging resulted in the loss of picture side lap due to the use of the center strip edit mode to recover some high-resolution imagery. This also caused some data loss in the very early outgoing pictures, as the short exposures to prevent smear resulted in data that was active in the LSBs; the two least of which are truncated in 22.05 kbits/s data.

The outgoing mosaics were conducted properly with the exception of one filter wheel step command being overridden by another entered by command form. A few A camera orange filter pictures of the final mosaics were lost until this was corrected.

At 10:30 GMT on March 17, 1975, the TVS power was turned off. The beam currents at that time were: A = 71,116 and B = 91,163. The measurement of concern, the A vidicon read beam current, at that time was 9 DN above the beam starvation level. Cumulative statistics for TVS operations are as follows:

	<u>Mercury III</u>	<u>Total mission</u>
Power on	119.7 h	3077.5 h
Beam on	36.7 h	866.3 h
Filter steps	A, 32; B, 24	A, 363; B, 409
Shutters	700 each	6157 each

The television experiment was conducted by a team of fourteen investigators under the leadership of Dr. B. C. Murray, California Institute of Technology, Principal Investigator. Coinvestigators included Dr. M. J. S. Belton of the Kitt Peak Observatory, M. E. Davies of Rand Corporation, G. E. Danielson of the Jet Propulsion

Laboratory, D. E. Gault of Ames Research Center, Dr. B. C. Hapke of the University of Pittsburgh, Dr. B. T. O'Leary of Hampshire College, R. G. Strom of the University of Arizona, Dr. V. E. Suomi of the University of Wisconsin and Dr. N. J. Trask of the United States Geological Survey. Associates include J. L. Anderson of the California Institute of Technology, Dr. A. Dollfus of the Paris Observatory, Dr. J. E. Guest of the University of London Observatory, and Dr. G. P. Kuiper (deceased) of the University of Arizona.

C. Non-Imaging Science - Mercury II

This imaging encounter enabled the collection of data from the other instruments. The data system was configured so that the priority for real-time data was given to imaging. As of this writing the Charged Particle Telescope and Magnetometer experimenters have not completed analysis of data. The Plasma Science investigators saw some interesting changes. Details must await the correlation with the magnetic field experimenters as to whether they are planet-related phenomena.

1. Magnetometer. The instrument was on and operating normally. However, due to the large flyby distance, very little data of value was obtained.

2. Charged Particle Telescope. The Mercury II trajectory passed too far from the planet to allow any field and particle measurements of the Mercury interaction with the solar wind. Since it was a bright-side pass, the infrared radiometer did not see Mercury.

3. Ultraviolet Spectrometer. Ultraviolet spectrometer measurements were taken from a distance of about 50,000 km on both the bright and dark side of Mercury, with a predominance of dark-side measurements. The data has not yet been analyzed in detail.

D. Non-Imaging Science - Mercury III

1. Magnetometer Experiment. The magnetic field experiment on Mariner 10 during the third encounter dramatically confirmed and extended the results obtained a year earlier at the Mercury I encounter. The magnetic field, which is responsible for deflecting the flow of solar wind, is unquestionably intrinsic to the planet and is not associated with any complex or exotic induction process associated with the solar wind interaction with the planet.

Based upon the Mercury I encounter results and a mathematical analysis, a modest planetary magnetic field with a strength of 350 gamma at the equator and 700 gamma in the polar region was identified (Fig. 9). The magnetic dipole axis was tilted 7 deg from the axis of rotation of the planet. The Mercury III encounter trajectory (Fig. 10) was very carefully selected to enhance the ability of the data to illuminate more fully the characteristics of the planetary magnetic field and its deformation by the solar wind. A model magnetosphere was constructed which permitted predictions of the expected bow shock and magnetopause crossings as well as the maximum magnetic field to be measured.

The actual observations of the characteristic bow shock and magnetopause show a perfect correspondence with predictions (Fig. 11). The maximum field measured was 400 gamma, only slightly less than the 500 gamma value predicted pre-encounter. The difference is understood, since the actual flyby occurred at an altitude approximately 127 km higher than predicted pre-encounter and used in the model.

The composite results of the magnetic field measurements establish unequivocally that the planet Mercury is one of the few magnetized terrestrial planets in our solar system. Neither Venus nor the Moon has even a modest magnetic field. The results on Mars, due to investigations by the USSR, are somewhat equivocal, partially associated with the less than ideal trajectory of the spacecraft Mars II, III and V.

The origin of the magnetic field is definitely associated with the planetary interior. Whether it is due to permanently magnetized rocks or an active dynamo mechanism in a fluid core is at present unclear. However, the permanent magnetization theory requires a very special sequence of events occurring during the formation and evolution of the planet. The active dynamo mechanism faces some difficulties because of the uncertainty about the exact structure of the planetary interior. It is expected that careful analyses of the magnetic field measurements at Mercury III and comparison with those of Mercury I shall contribute to a resolution of this issue. The existence of the planetary magnetic field places specific constraints on the planetary interior in either model, which can be tested with other complementary data including other measurements by Mariner 10. For example, the distribution of mass within the interior may be estimated by a careful analysis of the tracking data following the deflection of the spacecraft's trajectory by Mercury.

The magnetic field experiment was conducted by a team of investigators from the Goddard Space Flight Center in Greenbelt, Maryland. Dr. Norman F. Ness is the principal investigator, and coinvestigators are Mr. K. W. Behannon and Dr. R. P. Lepping of GSFC and Prof. Y. C. Whang of the Catholic University in Washington, D. C.

2. Plasma Science Experiment. Data obtained with the plasma science instruments on Mariner 10 provided definite indications that the interaction between the solar wind and Mercury's magnetic field, to a remarkable degree of detail, appears to be a scaled-down version of the interaction of the solar wind and Earth's magnetic field. Magnetosphere boundary locations and the bow shock (Fig. 10) observed during Mercury III are consistent with the locations that were previously scaled from Earth's magnetosphere on the basis of the Mercury I field and particle observations. In addition, the cool and hot regions of the plasma sheet and also a polar low-flux region (similar to that at Earth's polar cap or the high-latitude magnetotail) are all consistent with a similar scaling on the basis of the magnetic field model deduced from Mercury I data. This new evidence strongly supports the idea

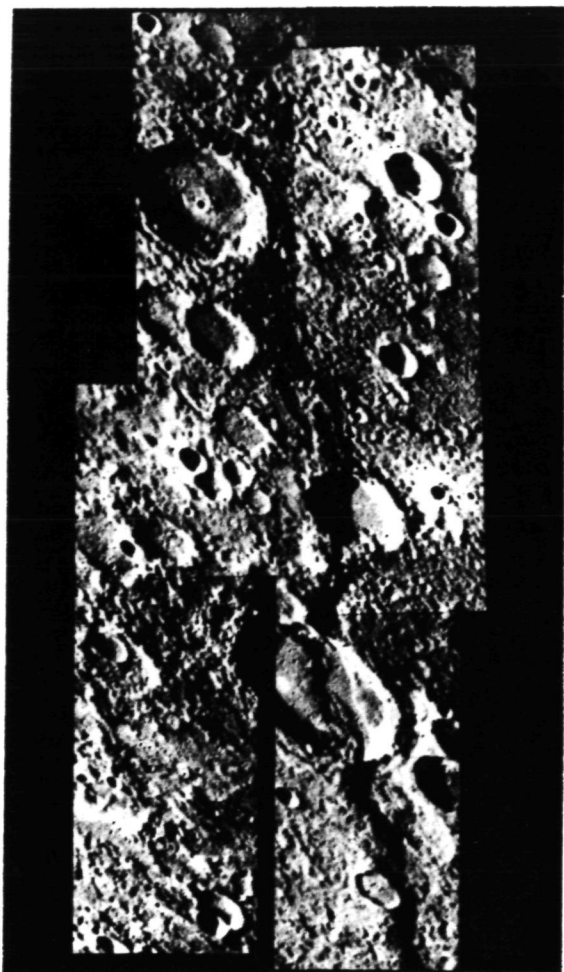


Figure 8. Mosaicked photo of Discovery Scarp

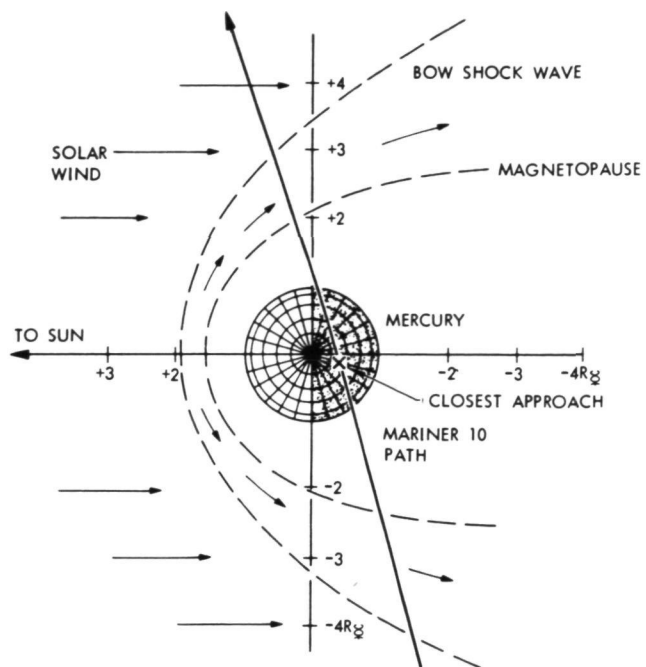


Figure 10. Spacecraft's path at Mercury III

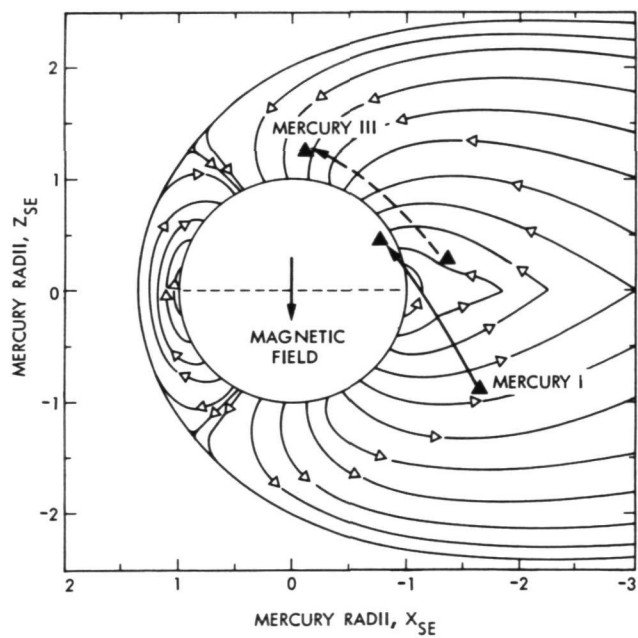


Figure 9. Magnetic field lines

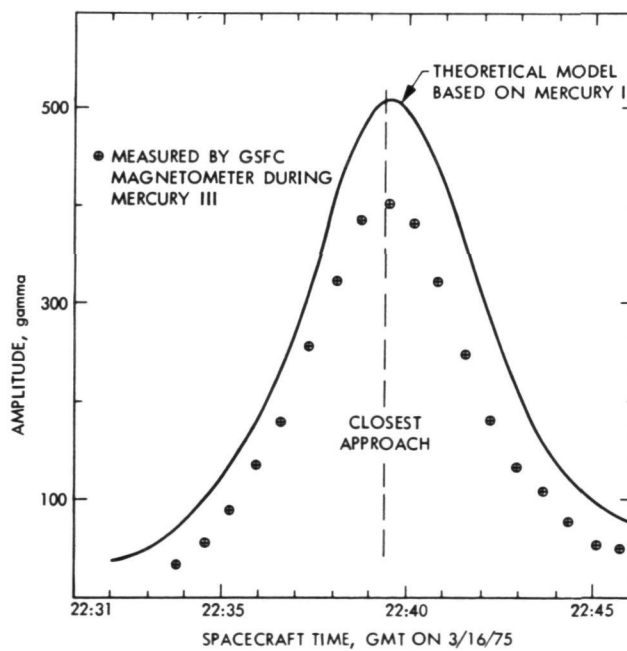


Figure 11. Magnetic field magnitude

that Mercury's magnetic field is largely of intrinsic planetary origin. The polar low-flux region was observed for the first time during Mercury III. Distinctions between the cool and hot plasma sheets became apparent from a comparison of the Mercury I and III data.

Figure 12 shows the trajectories of both the Mercury I and III encounters by Mariner 10 together with the orientation of Mercury's magnetospheric equator, given by the model of Ness et al. Predicted locations of the magnetopause and of the bow shock are shown for Mercury III as well as the observed boundaries and plasma regions on both encounters. The inbound crossings of the magnetopause and the bow shock occur at almost precisely the predicted locations; the outbound crossings were only slightly farther out than predicted. After crossing the inbound magnetopause, Mercury III encountered a region of fairly intense but relatively low energy electron population (spectral peak at ~150 eV, e-folding energy ~50 eV), very similar to the cool plasma sheet seen in Earth's magnetic tail at appreciable distances from the magnetospheric equator. A similar region was seen on the inbound pass of Mercury I. In Fig. 12, it should be noted that Mercury I is well below the magnetospheric equator, and Mercury III is well above. The intensities and energy spectra seen in Mercury I and III are similar when allowances are made for the fact that during Mercury III the instrument (or spacecraft) appears to be at a positive potential of about 40 V relative to the plasma. This difference is tentatively attributed to aging effects.

Near the center of the Mercury III encounter trajectory, where the projection of the spacecraft on the magnetospheric equator is behind (or within) the planet (Fig. 13), a region of very low electron flux was observed, having a very soft energy spectrum (e-folding energy <10 V). However, this region was not encountered during Mercury I because at this point the spacecraft was close to the magnetospheric equator; whereas in Mercury III, it was nearly at its maximum height of about one planetary radius above the magnetospheric equator. If the magnetosphere is scaled relative to Earth, this region corresponds to about 7 Earth radii. At such a location in Earth's magnetosphere, very low particle intensities are also observed, this region corresponding to magnetic field lines that emanate from Earth's polar cap. The origin of these few observed low-energy particles is still an unsettled and controversial question in the case of Earth and is equally uncertain for Mercury; they could originate from Mercury's magnetosheath or from its tenuous atmosphere. Further study of the observed spectra should help clarify this question. During Mercury III, significant time variations are seen in this low-intensity population.

The outbound traversal of the magnetosphere on Mercury III is similar to the inbound, as expected because the spacecraft is at nearly the same height above the magnetospheric equator. By contrast, on Mercury I the electron population seen on the outbound traversal was quite hot (spectral peak above the instrument range, e-folding energy at hundreds of electron volts),

much hotter than the corresponding portion of the inbound traversal. As can be seen from Fig. 12, the spacecraft while outbound was nearly at the magnetospheric equatorial plane, indicating that the plasma behavior is the same as in the case of Earth, where the plasma near the equator is hotter than at the outer regions of the plasma sheet in the magnetotail.

The plasma science experiment was conducted by a team of nine investigators from five organizations under the leadership of Dr. H. S. Bridge, MIT Center for Space Research, Principal Investigator. Coinvestigators included Dr. C. M. Yeates of JPL, Dr. H. A. Lazarus of MIT, Dr. K. W. Ogilvie of GSFC, Dr. J. D. Scudder of GSFC, Dr. R. E. Hartle of GSFC, Dr. G. L. Siscoe of UCLA, Dr. J. R. Asbridge of Los Alamos, and Dr. S. J. Bame of Los Alamos.

3. Charged Particle Experiment. In the discussion of magnetic fields and plasma observations, the emphasis was the major magnetic field that exists around the planet Mercury and the interaction of that field with the solar wind plasma (Fig. 13) which has relatively low energy; i.e., 10 to 150 eV. The charged particle experiment measures the intensities of protons and electrons that range from a few percent to very close to the velocity of light; i.e., 0.5 to 2 MeV. Although these high-energy particles do not carry enough energy to distort a planet's magnetic field, they are at the core of energy conversion from magnetic fields into high-energy particles by an acceleration process.

The high-energy particles come from distant reaches of a planet's magnetic field which cannot be reached by the spacecraft itself. Therefore these particles can be used as probes of a much larger region of a planet's environment than by the actual probing of a magnetometer. Interesting features about the scale properties of a magnetic field can be deduced.

A preliminary examination of the charged particle data revealed two interesting phenomena. The first was that intense bursts of radiation were observed by the Charged Particle Experiment as Mariner 10 approached and passed by Mercury during the first encounter. The magnitude or intensity of this event was very great and the duration very brief. Such events are apparently related to solar electromagnetic storms that have been observed on Earth. The second phenomenon was a fortuitous first actual test of the idea that the Sun is emitting a steady stream of nuclear particles along its magnetic field lines that extend outward from the Sun and are in corotation with it.

During the first Mercury Encounter bursts of high-energy radiation were observed that extended several orders of magnitude in intensity, dying away very rapidly as the spacecraft passed into the occultation region. As the particle intensities died down, they appeared to ring or oscillate at 6-sec intervals. This phenomenon may be due to a resonant flapping of the magnetic tail like a flag waving in a breeze. Both low-energy protons and electrons appear to be accelerated and taking part in this mechanism. This phenomenon

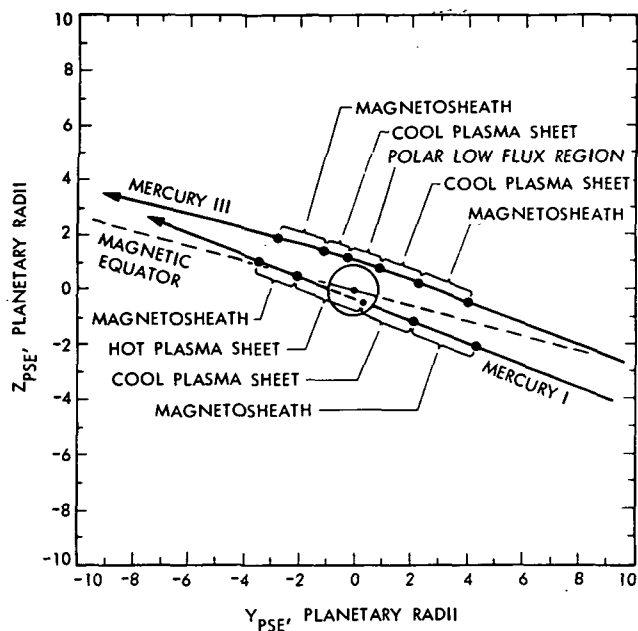


Figure 12. Mercury's magnetosheath

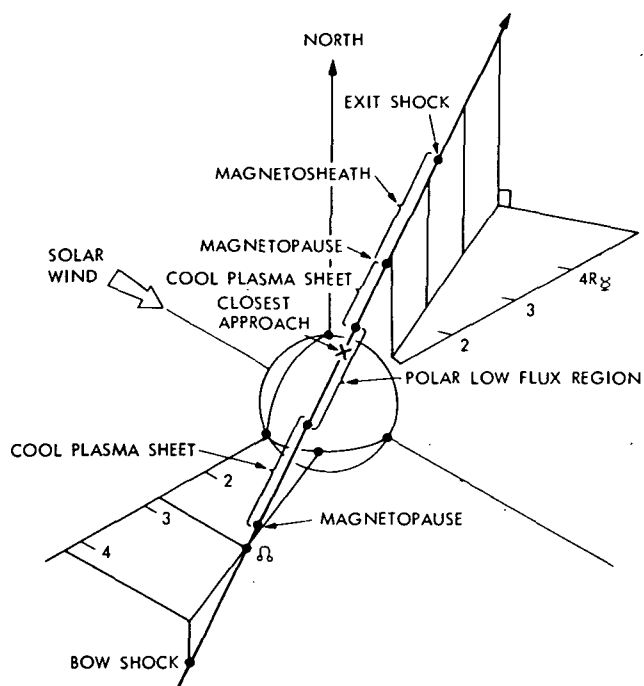


Figure 13. Mercury's magnetosheath and plasma sheet

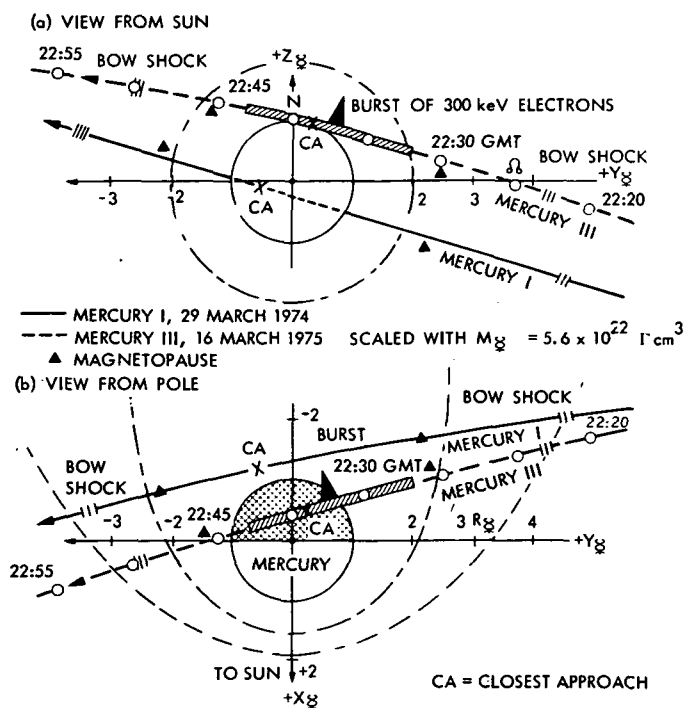


Figure 14. Two views of Mercury I and Mercury III encounters showing bow shock waves

occurs so rapidly that there is not enough time to accelerate them by a process as in a bevatron or cyclotron. There is hardly enough time to execute even one gyro radius in a typical magnetic field. It must be an unstable and explosive event that promptly dies away. It is related to the generation of a momentary strong electric field. During Mercury I, the pass was on the dark side, close to the planet's magnetic equator, which is a relatively weak region near the neutral sheet or the merging region for the magnetic field. This merging can be considered as an energy source for particle acceleration.

In Fig. 14, the results of the charged particle experiments during Mercury I are compared with those of Mercury III. During the cross-polar flight of Mercury III, no unusual data were expected. The particles would have to fan out and reach the higher latitudes where the field was expected to be stronger. However, a giant burst of 300 keV electron radiation was experienced. The Mercury III data are shown in Fig. 15.

About 2 days before Mariner 10 encountered Mercury, the interplanetary radiation of protons was observed to be rising gradually to a factor of 10 above the normal background level in interplanetary space. Then, as Mariner 10 passed behind Mercury, the particle energy level dropped to the quiet level. In Fig. 16, the spacecraft are looking down on the Sun, and the magnetic field lines are seen to spiral outward, where they are frozen into the plasma. One curved line passes Earth where it is being observed by the IMP-8 satellite orbiting around Earth. About 4 days later, a particle burst of the identical energy range was detected by the Charged Particle Experiment on board Mariner 10. The Sun's 13.3 deg/day rotation rate is seen to shift the plasma radiation line, which has a broad sector structure, about 55 deg in 4 days, and this same line then passes Mercury with protons having 10 times the normal background energy.

In addition to the Sun being a source of occasional impulsive events like solar flares, the Sun also has many active centers that emit an almost continuous particle population distribution. For almost 9 years, this problem has been studied at the University of Chicago at a distance of 1 AU from the Sun. Now, Mariner 10 has provided a test situation that demonstrated the dropout of the burst particles as the spacecraft passed behind Mercury. As the particles flow outward along the Sun's field lines, they spiral or loop around these frozen-in magnetic fields. The radius of this spiraling action does not appear to differ greatly from the radius of Mercury. Nature provided us with a giant shutter of the right size to give evidence of the continual emission of nuclear matter from the Sun. The energy spectrum of the helium component emitted appears to be 0.1 of the proton level and has the same spectral pattern. Figure 14 is an equatorial plane view of the Mariner 10 flight path showing the region in which the burst event occurred. The collapse of the magnetic fields occurred in about 100 sec. This collapse may serve as an energy conversion source to accelerate nuclear particles. This information may help increase our knowledge of the effects of magnetic storms on Earth.

The charged particle experiment was conducted by Dr. J. A. Simpson, principal investigator and Mr. James E. Lamport, co-investigator, both of the Enrico Fermi Institute at the University of Chicago.

4. Ultraviolet Spectrometer. Extensive UVS observations were taken on the limbs, across the terminator, and on the night side, with particular coverage on the north polar cap region. Preliminary curves of Lyman Alpha 1216 Å and HeI 584 Å are shown in the Fig. 17. These are the results of a slow drift of the UVS slit across the bright limb of Mercury, near the equatorial region. Considerable HeI is again observed as before during Mercury I encounter. The source of the helium is still an open question. Three very slow high-resolution scans were obtained on approach and three on the outbound portion of the trajectory.

5. Celestial Mechanics Experiment. The determination of the mass and low-order coefficients in the gravitational potential of Mercury is one of the major objectives of the celestial mechanics experiment. During Mariner 10's second flyby of Mercury, the encounter altitude was approximately 47,000 km and consequently radio metric data received from the spacecraft was of little or no value for celestial mechanics purposes. However, the encounter trajectory at Mercury III was favorable for deducing celestial mechanics information.

Figures 18 and 19 reveal geometric characteristics of the third encounter. In particular, the altitude of the spacecraft was 327 km, the spacecraft's hyperbolic trajectory was inclined 76 deg to Mercury's equator and a geocentric occultation did not occur.

Radiometric data received from Mariner 10 consisted of high quality coherent two-way doppler and round-trip time delay measurements. The variation of the doppler within 20 hours of encounter is shown in Fig. 20. Several features are immediately apparent: (1) the overall trend represents the geocentric motion of the spacecraft, (2) the individual curves represent the characteristic signature caused by the diurnal motion of the tracking station due to the Earth's rotation and (3) the distinct signature at encounter is due to Mercury's dominant gravitational influence on the flyby trajectory.

Preliminary results for the mass and gravity field were obtained as follows. The basic data arc consisted of radiometric data from 3 days before to 3 days after encounter. Precise tracking station coordinates and ephemerides of the Earth, Mercury and other planets were used in the analysis and are the result of extensive and accumulative research conducted at JPL and MIT. Basic forces acting on the spacecraft (solar radiation pressure, etc.) were modeled, the influence of the troposphere on the radio signal was accounted for, and ground and spacecraft calibrations were applied to the time-delay data. Typically the analysis involved estimating the six orbital parameters of the Mariner 10 trajectory, the mass of Mercury, and various subsets of the low-order gravity coefficients. The results of

¹Reference numbers refer to Bibliography entries.

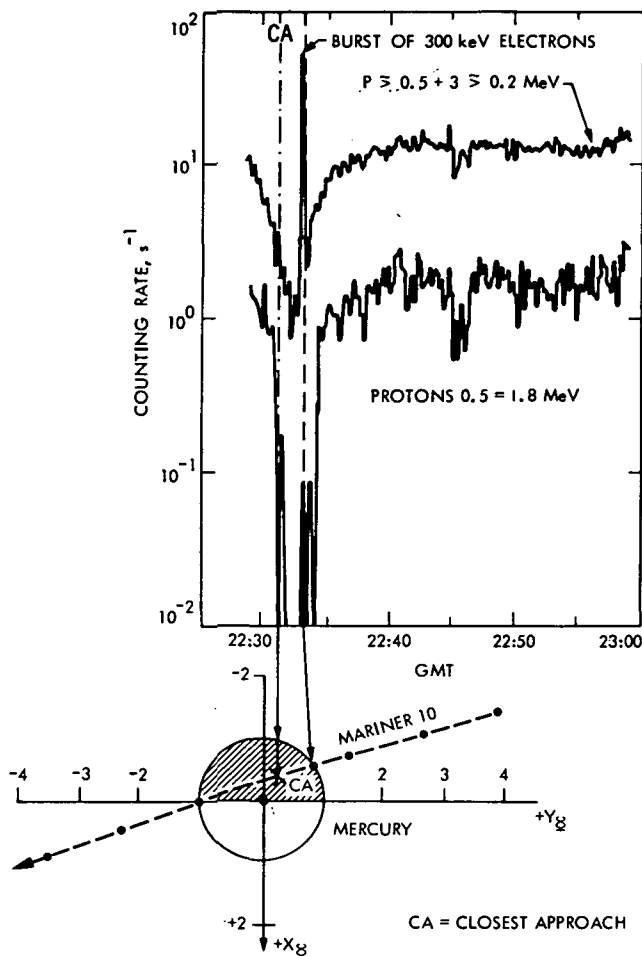


Figure 15. Charged particle count profile

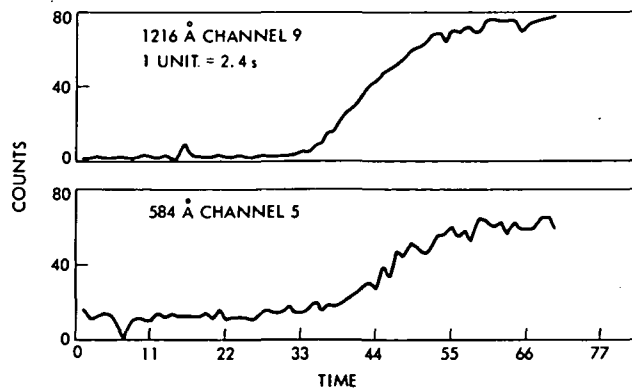


Figure 17. Ultraviolet spectrometer limb drift data

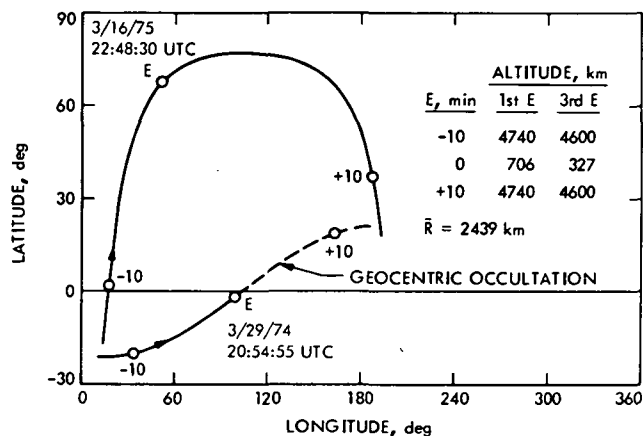


Figure 18. Mariner 10's ground track across Mercury

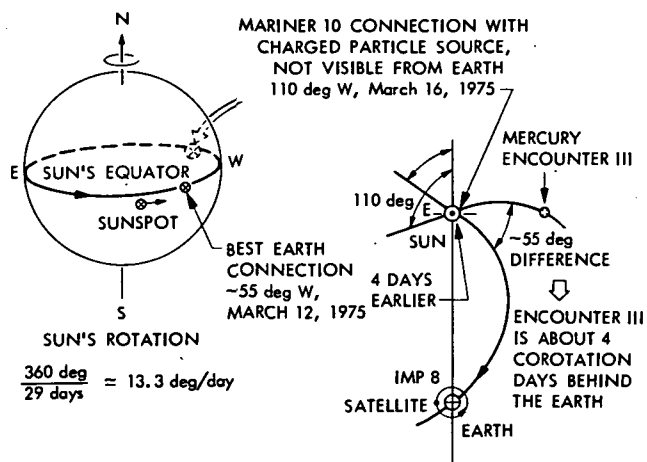


Figure 16. Spiraling solar magnetic field line

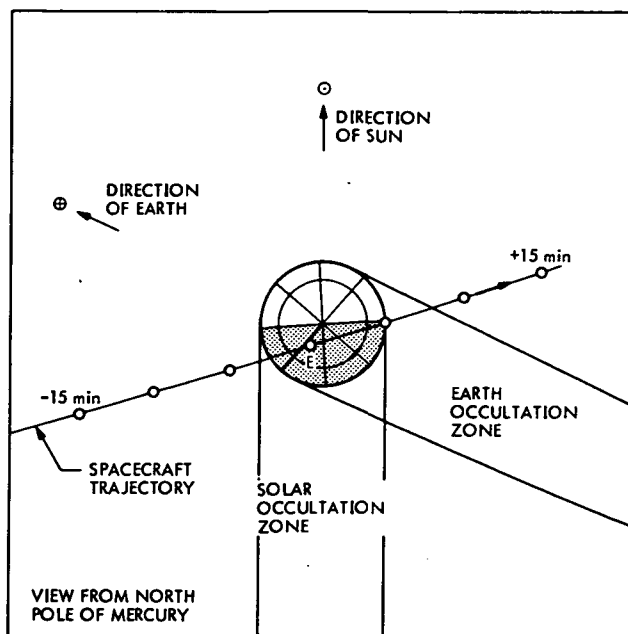


Figure 19. Third Mercury encounter geometry

the preliminary analysis thus far concluded are (1) the ratio of the mass of the Sun to that of the mass of Mercury is $6\,023\,700 \pm 300$ (corresponding to a planetary gravitational constant of $GM = 22031.8 \pm 1.0 \text{ km}^3 \text{ sec}^{-2}$) and (2) there are strong indications that the oblateness of Mercury (J_2) is approximately one half of the value of the lunar oblateness. The mass solution is in excellent agreement with the mass deduced from the first Mercury flyby (Ref. 23¹). Furthermore, the uncertainty associated with the mass may be reduced by about a factor of five, once data received from both encounters have been analyzed in detail. Analysis of the third encounter data for Mercury's oblateness is complicated by the influence of other gravity effects and the correlation of J_2 with other parameters. Thus, at this preliminary stage of the analysis and in view of the above difficulties, it is advisable to place a conservative uncertainty on J_2 of 100%. However, in order to indicate the sensitivity of the oblateness parameter to the data, we find a standard deviation of 6% or less when one assumes that the influence of all other gravity coefficients is negligible. Clearly more work is necessary before the proper value and uncertainty of J_2 can be determined with definitiveness.

A representative set of doppler residuals is shown in Fig. 21. The rms residual for doppler average over 60 sec is about 5 mHz. Doppler within encounter ± 20 min was averaged over 10 sec and this fact, in part, accounts for the increased noise noted in this region. In addition, within encounter ± 3 min, the residuals exhibit a systematic trend with an amplitude of roughly 80 mHz. Presently, this trend is being attributed to the influence of other gravity terms in the potential expansion. However, other possible causes are also under investigation.

This brief report represents the status of the analysis after a very preliminary examination of the Mercury III data. A good deal of additional work needs to be accomplished. Finally, although the analysis has concentrated on the doppler data, high-quality time-delay data were measured throughout the encounter period. These data will improve the Mariner 10 encounter trajectory and will determine the distance between Mercury and the Earth at the time of the encounter. This distance will be used to improve the ephemeris of Mercury, and it will contribute to tests of general relativity which rely on precision orbits for the inner planets.

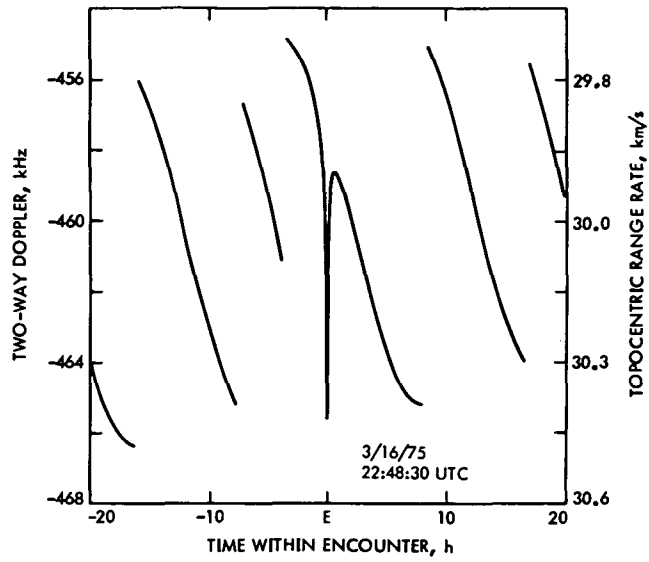


Figure 20. Doppler variation during Mercury III encounter

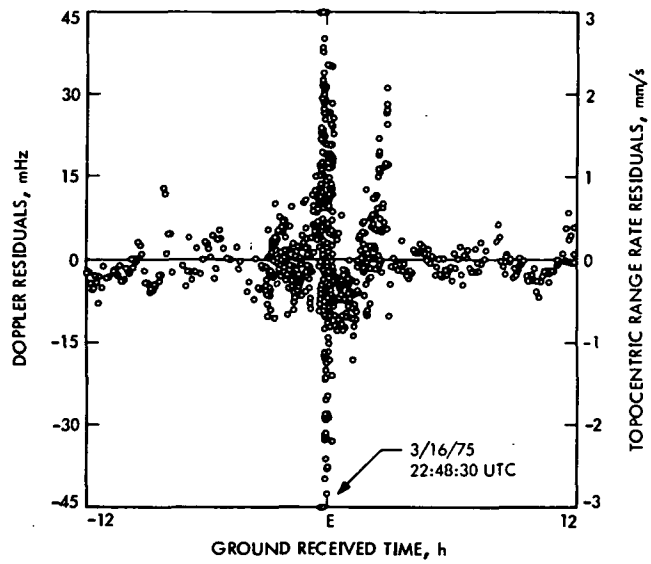


Figure 21. Representative doppler residuals within Mercury III encounter ± 12 h

IV. MISSION SEQUENCE WORKING GROUP

The MVM '73 Mission Sequence Working Group (MSWG) prepared all MOS sequences beginning with simulation exercises prior to launch. The same concept was continued during the extended mission. The extended mission MSWG, composed of key individuals from each functional sequence area, developed and implemented sequences similar to the primary mission. A significant difference in operating procedure was the structuring of a single major sequence during any one period. As a result of "scoping down" sequence development to a series concept, the necessary team membership was reduced to nine key personnel. Sequence reviews afforded critique opportunities for the entire MOS team, generally consisting of about thirty personnel.

A. Organization

Figure 22 presents the MOS organization depicting the relationship of the MSWG with other MOS teams. MSWG team members played dual roles in the operations organization, since many members were also members of another team. The primary function performed in MSWG activities was nonreal-time planning and preparation of executable sequences. Generally, the final product being the CC&S load and associated ground commands to perform the sequence. Non-MSWG functions were centered around performing the planned sequences and reacting to any problems occurring during sequence execution. This proved to be a very valuable working arrangement since MSWG members were aware of spacecraft idiosyncracies and any difficulties that might be encountered during implementation.

B. Software Functions

The most significant aspect of sequence development is the proper use of all the software programs. Each program performs a specific task and links one or more individuals to getting each job accomplished. The MSWG software set and functions performed are as follows:

1. TSOST (Div. 82). General-purpose science input program providing basic sequence structure. Interfaces with SEG, POGASIS, SPOP, and COMGEN. Used primarily for generating first cut at encounter sequences. Also, provided critical interface from POGASIS to SPOP. Performs rudimentary constraint checking. Used SCOUT conic trajectory program for trajectory information.

2. SEG (Div. 29). Merges the spacecraft command files with other sequence inputs to provide the integrated sequence output. Used to prepare planning sequences for review/critique by using TSOST card interface for the bulk of spacecraft sequence inputs. This technique provided planning sequences in the same format as flight sequences.

3. POGASIS (Div. 39). Precision navigational pointing supplied by plot outputs to provide accurate pointing analysis. Employed after initial sequence development and for final trajectory tweaks to obtain initial pointing parameters.

4. SPOP (Div. 34). Generates proper scan platform pointing values considering offsets, biases, and backlash compensation. Final pointing parameters input to COMGEN. In the processing mode, SPOP uses the COMGEN spacecraft command files to provide an as-programmed spacecraft command pointing profile for LIBPOG.

5. COMGEN (Div. 36). Provides final spacecraft command files. Integrates all spacecraft commands for both CC&S and ground commands. Performs the bulk of sequence generation activities by simulating CC&S, APS, FDS, and DSS spacecraft subsystems. Provides the command deck for ground commanded sequences and interface files for SEG and SPOP.

6. LIBPOG (Div. 39). Produces the final pointing values with a plot capability to show pointing results from those actually obtained from COMGEN files. Performs extremely important function of checking programmed values, in particular, initial positions and backlash compensation.

C. Scheduling

The very nature of sequence development being tied with software programs used by cognizant team members lends itself to milestone scheduling. Each software program performs one or more functions in the sequence development process. Figure 23 combines the schedule with a logic diagram approach. This technique was utilized often to maintain visibility. Extreme difficulty is usually encountered in trying to keep the sequence development process on schedule. Operating the software identifies many items which are not foreseeable in the early planning phase. This often requires modification and reiteration through some of the software processes.

D. Sequence Structure

The major spacecraft constraint to sequence design was the limitation due to CC&S program-mable storage (512 words). Tradeoffs were continually performed between the desired sequence and the implementable sequence. Two ways to partially overcome this problem are to reload the CC&S and to augment the CC&S using ground commanded sequences. For Mercury encounters, augmentation with ground commands proved to be the more desirable choice. Both extended mission encounters were executed with hybrid sequences composed of ground commanded far encounters and CC&S-controlled near encounters. Mercury III near encounter utilized ground commands for UVSAG slew sequences to enhance science return during predetermined pauses in CC&S-controlled slew sequences.

Trajectory Correction Maneuver sequences and specialty items, such as UVS astronomy contained ground commands in order to provide real-time sequence flexibility. TCM's 6, 7, and 8 were initiated by ground commands which, in turn, started CC&S-controlled maneuvers. In the case of UVS astronomy, the desire was to be able to control the initial pointing by ground

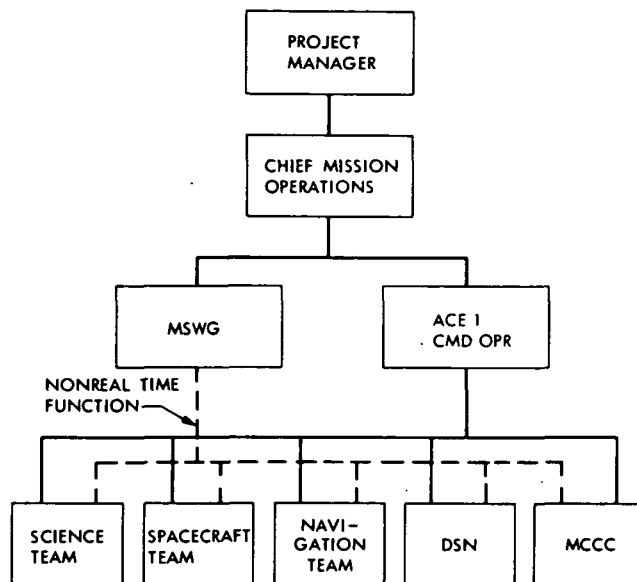


Figure 22. Extended Mission organization

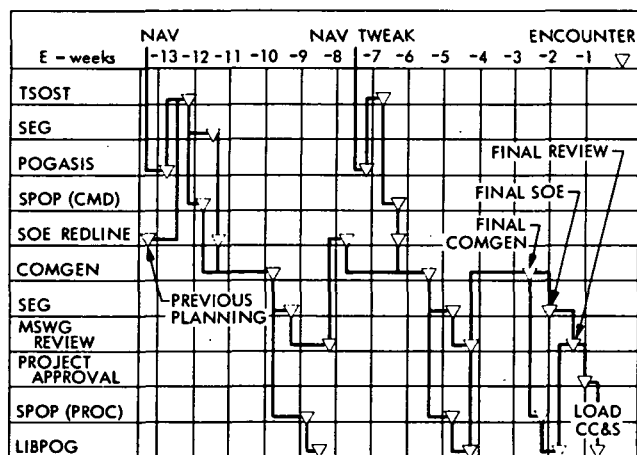


Figure 23. Schedule/logic diagram for typical encounter sequence development

command, and let the CC&S execute the lengthy incremental slew sequences. Utilization of these types of sequence structure made possible the implementation of complex sequences within extended mission MOS limitations.

E. Problems and Critical Items

Mercury II encounter preparation was hampered by SPOP backlash compensation corrections. Results from the first Mercury encounter revealed that the backlash was a major item which must be properly taken into account. Performing a scan platform engineering pointing test provided new backlash parameters and identified nonlinearity in the backlash values. For example, near cone angles of 90 deg, a value of 4 incremental steps was adequate; whereas at higher cone angles 7 or 10 steps might be required. This posed problems in programming the CC&S mosaic routines and in the post processing to obtain LIBPOG plots. Extra iterations with COMGEN were required late in the preparation process to overcome this problem. However, as a result of understanding this operational idiosyncrasy, the most accurately pointed pictures of the mission were obtained during the Mercury II encounter.

Mercury III problems consisted mostly of uncertainties in the aim point. Although this was a tradeoff that science was willing to make for a close approach, it made encounter sequence preparation difficult, due to the many sequence iterations required. This problem occurred since TCM 8 was necessary to decrease the probability of impact. To overcome this problem, the MSWG prepared two sequences and then selected the proper sequence after determination of the aim-point parameters. This approach created an additional hardship on personnel, since most members performed the dual work role of sequence development and sequence execution.

F. Functions Performed Correctly

In retrospect, there are several key items which contributed to the success of the MVM extended mission:

- (1) MSWG staffing was at the minimum level. Most areas were represented by a single cognizant engineer. Interfaces were well defined.
- (2) Personnel comprising the MSWG were selected from the primary mission. In some cases, these individuals had been involved in sequence design since two years before launch.
- (3) Although very informal in many areas, the MSWG maintained signature approval requirements for flight sequences. This type of approval meant each area had reviewed the sequence and added their comments where appropriate.
- (4) The MVM software was inherited from MM '71 and modified to fill the requirements of MVM. Many operational problems were fixed, and the users understood their software extremely well. The program interfaces worked smoothly. In planning stages card interfaces allowed easy access for changes between programs. During final sequence development phase tapes and files with additional input by cards were exclusively used. Good software is available only after many hours of testing and operational use; hence, MVM was blessed with second-generation software. In addition, MSWG personnel were well aware of software idiosyncrasies and limitations.

V. MISSION OPERATIONS

The Mission Operations Organization for the extended MVM Mission did not differ from the MOS Organization except for its relative size. It consisted of five teams, as follows:

- (1) Mission Control Team
- (2) Spacecraft Team
- (3) Navigation Team
- (4) Sequence Development Team
- (5) Science Team

This section of the final report will deal primarily with the Mission Control Team.

The Mission Control Team consisted of two elements: the flight control element and the data processing element. The flight control element provided overall control and execution of flight operations including all commanding of the spacecraft. The data processing element provided the necessary interface between the MCCC data-processing facilities (i.e., the MTC, MTCF, and MCCF) and the Project.

For the extended mission of MVM '73, it was necessary to drastically reduce the manpower levels from the prime mission. For example, the Mission Control Team was reduced as follows:

ACMOs (ACE-1s)	From 5 to 2
Command operators	From 3 to 0
Deputy CMOs	From 1 to 0
Secretarial support	From 1 to 0
Data chiefs	From 5 to 2
SOFCONs	From 5 to 1
FLICONs	From 3 to 1

In order to provide the same prime mission functions at an acceptable level of support, the extended Mission Control Team staff was extensively cross-trained to perform other functions. For example, both ACMOs were cross-trained to be Command Operators.

The Data Chiefs, SOFCONs and FLICONs became familiar with one another's functions and performed the other functions as required.

A. Operation Philosophy and Technique

The reduced manpower along with limitations on the number of tracking passes that could be provided by the DSN (DSN had commitment to Pioneer, Helios, Radio Astronomy, and Viking) forced the extended mission operational philosophies and techniques to change from those of the prime mission. Basically, 24 h/per day around-the-clock tracking and spacecraft monitoring was no longer possible. Another constraint was that the MTC would support cruise phases on a 40-hour 5-day week basis. This constraint was somewhat flexible in that during high activity periods such as TCMs and encounters the MTC

supported as required. The constraint was primarily leveled to allow MTC to reconfigure for the Viking Project and to complete their prime mission sequence data records generation.

The operational technique used from Mercury I to Mercury II was to place the spacecraft in a rather quiescent cruise mode and track it at least once a day. The operations teams would monitor the spacecraft in real time from Monday through Friday during normal working hours. During off hours and on weekends key personnel were on emergency-call basis with a reaction time, portal to portal, of no more than 60 min. This was accomplished by assignment of Page Boy II beepers (effective range radius of 80 miles) to on-call personnel. Operations requiring extended coverage such as TCMs, CC&S loading, and science calibrations required that many personnel work extended shifts such as 12 h on, 12 h off.

For the Mercury II Encounter some personnel from the prime mission were recruited to staff their old operational position during the periods of lower activity, thus allowing the main crew to concentrate their efforts on the high activity periods. Specifically, two ACMOs and one command operator were brought back temporarily to fill in as required.

The extended mission operations between the Mercury II encounter and Mercury III encounter were reduced even further. Again DSN commitment to other projects forced further reductions in tracking coverage of the Mariner spacecraft. DSN coverage was reduced to about 7 passes per week. This level of coverage is barely sufficient to collect minimum required radiometric data in order to determine an accurate orbit of a nominal spacecraft. It is also the minimum confidence level coverage to maintain the spacecraft in a healthy state. Shortly after Mercury II encounter, the spacecraft had problems remaining Canopus-acquired. The navigation problem and the spacecraft housekeeping problem then became critical. The spacecraft had lost its reference on the star Canopus several times due to dust particle interference in the Canopus tracker's field of view. This caused the spacecraft to use up a large amount of its attitude-control gas, making it nearly impossible to attain a third encounter if the spacecraft were to be allowed to maintain a three-axis reference.

A gas-saving technique was devised and implemented. The technique was to disable the roll attitude-control jets and allow the spacecraft to roll, maintaining two-axis pitch and yaw control only. This caused several operational problems, as follows.

- (1) The roll rate had to be maintained within certain limits. If it rolled too fast, cross coupling in the pitch and yaw axis caused high gas usage. If it rolled too slow, low-gain antenna nulls would cause long periods of no data (telemetry or radiometric) and the collection of radiometric data was essential. Operational personnel were required to support

on a nonregular shift basis. Days, nights, weekends, whenever a track by the DSN was available and when commanding was necessary.

- (2) The seven passes a week by the DSN had to be scheduled to allow two to three long passes per week on the order of 16 to 24 hours long. This required station coverage that was overlapping. These long tracks were required by navigation as their problem now was to converge an orbit on a rolling spacecraft. The net effect was that it was necessary to accept tracking gaps as long as 48 hours.
- (3) Prior to TCMs it was necessary to establish a very accurate roll rate as the technique used for the maneuver was to allow the spacecraft to roll to the desired TCM attitude without the use of gyros or the roll gas jets. This meant that two to three days prior to the TCM, continuous or near-continuous tracking and spacecraft monitoring was required. Adjustments to the spacecraft roll rate were made using the solar wind to provide roll torques, and the CC&S was loaded for the TCM when a good command uplink was available (i. e., when the roll position on the LGA was favorable).

These operational problems were handled quite effectively by the very small operations crew primarily because:

- (1) The personnel by this time had acquired a broad knowledge of all aspects of the mission; e. g., the ACMOs knew the Ground Data System, the Command System, the Data Processing System, and a great deal about the spacecraft. The spacecraft team members likewise had a very good understanding of the same systems.
- (2) Delegation of authority by the Project Manager, the CMO, and the Team Chiefs was more extensive.
- (3) Total and complete dedication by all team members was a very significant factor.

B. Recommendations

Recommendations for future projects that can be drawn from the MVM extended operation in the area of the Mission Control Team are as follows:

- (1) The Mission Control Team was understaffed. At least three ACE-1s trained in command system operation are needed. There always seem to be periods of more than 24 hours of relatively high activity that require both an ACE and a Command Operator to be on for at least 10 to 12 hours of the period. Also, vacations became a problem with too few staff members.

- (2) ACMOs can handle the Data Chief function but not the SOFCON and FLICON functions. The Data Chiefs could have been reduced to one assuming the SOFCONs and FLICONs could be called in to perform part of the Data Chief function, if required.
- (3) MSAs should be designed for extended mission operations. A small densely packed MSA is desirable as long as there is only a small staff. For example, the command console should be in very close proximity to the ACE-1 console. (In the MVM extended mission, the command console often served as the ACE console, as there was often only one man performing both functions.)

C. Command System

1. Command Operations. During the first ten weeks of the Extended Mission, a designated command operator was utilized for day shift command operations. During the off shift periods, the on-duty ACE-1 was also the command operator (as well as being the data chief). After that initial period, all command operations were performed by ACE-1; during the occasional high activity periods both ACMOs were on-duty, one primarily to operate the command system. If needed, a command operator from the prime mission (assigned to other tasks during the extended mission) was available, but was utilized infrequently.

This arrangement worked quite well. Both ACMOs had been ACMOs during the prime mission. Further, one was also the Command System cognizant engineer and the other was adequately trained in command system use and operations. There was no need to have a full-time command operator assigned.

Recommendation. Future missions which have extended cruise periods (or otherwise low-activity profiles) should utilize the on-duty ACE-1 as the command operator. At the very least, all ACE-1s should be qualified command operators.

2. Replacement of Command System. The ground command system utilized during the Prime Mission was also used during the Extended Mission until January 16, 1975. On that date, the entire ground command system software was replaced with what is known as the Redesignated Command System. During the three-month period preceding the switchover, training in the use of the new system was performed on an off-line basis.

There was an initial scare when the new system was used in flight operations for the first time: the first nine commands transmitted were not received by the spacecraft. However, the problem was resolved to be a ground hardware failure, which could have occurred under the old system just as easily. Thereafter, commanding via the new system was generally smooth and somewhat easier.

One feature of the new command system was the isolation of the Deep Space Station command initialization function into the NCS. Two significant problems arose with the advent of the NCS. One problem had to do with the partial development of the NCS: the project normally had to test whether the command system portion at a DSS and the portion in the MCCC were in agreement as to the GMT day. If a difference existed, a special one-time (per DSS per day) work around had to be exercised by the Project to resolve the conflict. The other problem was that the Project had absolutely no visibility into the state of DSS initialization or what operational parameter values had been set by the NCS. A blind faith acceptance of NCS actions was required.

Recommendation. Provide the Project command operator the capability to access (and modify, as necessary) in real time the operational parameter values set by the NCS; the Project should have complete control of the command system at a DSS.

Another problem area was encountered during the period when the new command system was in use, but was essentially independent of the new system. Hardware modifications (ECOs), were implemented at the DSSs in preparation for the Viking Project. Some of these ECOs caused MVM command anomalies (confirmed transmissions not received by the spacecraft), although the changes were not expected to affect Mariner 10. Occasionally, single commands were transmitted to the spacecraft to confirm proper DSS operation before a series of commands were transmitted, thus providing the spacecraft team with a higher level of confidence in the new command system.

Recommendation. Appropriate equipment should be installed at each DSS which may be

used to verify command throughput - intercept the DSS uplink signal as it leaves the antenna to verify that supposedly transmitted commands are actually radiated. The equipment need only be used pretrack during command system checkout.

3. **Reliability and Statistics.** Reliability of the command function during the Extended Mission was very high as measured by the number of attempted command transmissions which were actually received by the spacecraft: 99.49% (8942 of 8987). The comparable reliability for the Prime Mission was 99.82% (15307 of 15334). The apparently reduced reliability is due primarily to two major factors: (1) the spacecraft ability to receive ground commands was reduced by the existence of the low-gain antenna pattern nulls, and (2) the implementation of Viking Project ECOs. If the anomalies resulting from these two factors are discounted, the reliability during the Extended Mission was 99.87% (8942 of 8954).

The distribution of successful transmissions of the six types of ground commands during the two Extended Mission phases is given in Table 2, while the distribution of the command anomalies is given in Table 3. The corresponding distribution of successful commands allocated to the old and new command systems is given in Table 4. The anomaly distribution allocated to old and new system periods is identical with that given in Table 3.

4. **Manpower/Month Expenditures.** Figure 24 presents the actual manpower expended per month during the primary and extended missions.

Table 2. Successful commands by mission phase

Type of command	Extension I ¹	Extension II ²	Total
CC-1/2 pairs (CC&S loads)	1167	1032	2199
CC-3 (CC&S readout)	0	39	39
CC-4 (fixed sequencer)	377	354	731
CC-5 (FDS commands)	1327	430	1757
CC-6 (APS commands)	927	631	1558
DC (direct commands)	292	167	459
Total individual commands	5257	3685	8942
¹ Extension I is the period from April 15, 1974 to October 15, 1974.			
² Extension II is the period from October 15, 1974 to end of mission.			

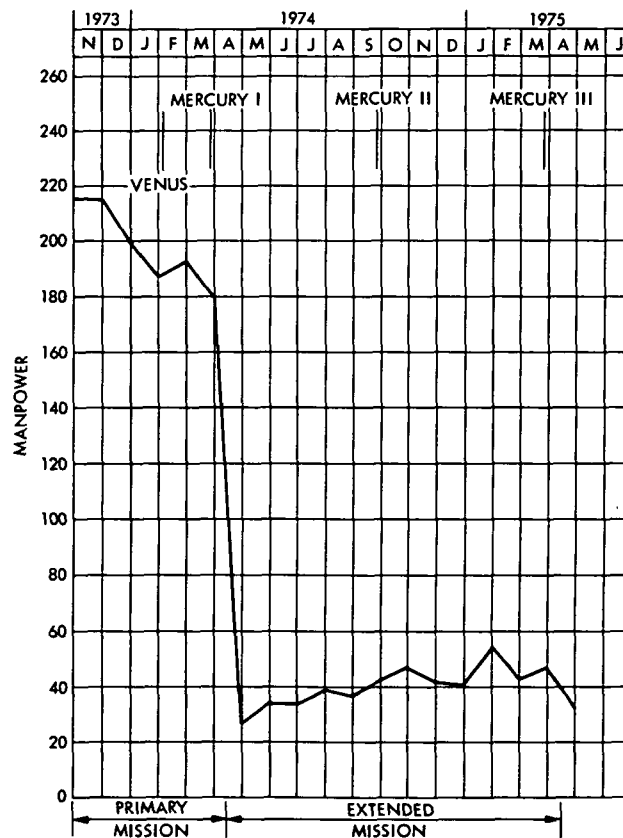


Figure 24. Monthly manpower chart

ORIGINAL PAGE IS
OF POOR QUALITY

Table 3. Command anomalies by mission phase

Type of anomaly	Extension I	Extension II	Total
Hardware aborts			
Exciter/transmitter failures	0	1	1
CMA/confirm loop	0	2	2
Unreceived commands			
Hardware anomalies	0	26	26
Procedure errors	8	0	8
Low-gain antenna null	0	7	7
Unresolved	0	1	1
	<hr/>	<hr/>	<hr/>
Totals	8	37	45

Table 4. Extended mission successful commands by command system

Type of command	Old system	New system	Total
CC-1/2 pairs (CC&S loads)	1281	918	2199
CC-3 (CC&S readout)	12	27	39
CC-4 (fixed sequencer)	418	313	731
CC-5 (FDS commands)	1428	329	1757
CC-6 (APS commands)	996	562	1558
DC (direct commands)	310	149	459
	<hr/>	<hr/>	<hr/>
Total individual commands	5726	3216	8942

A. Telecommunications Systems

During the Extended Mission, telecommunications systems performance was monitored in a wide variety of operational modes. These ranged from 117.6 kbits/s imaging data being transmitted over the high-gain antenna to 8-1/3 bits/s engineering data being transmitted over the low-gain antenna. Performance objectives were met or exceeded in all phases of operations. No anomalies or failures were recorded in this period. The following sections will summarize the characteristics and performance of the individual mission phases.

1. Mercury I to Mercury II Cruisea. Trajectory Correction Maneuvers (TCMs)

Two TCM's were performed during the cruise. TCM 4 took place in two parts on May 9 and 10, 1974. TCM 5 occurred on July 2, 1974. The same basic sequence was used on each. The spacecraft was commanded to Data Mode 21 (33-1/3 bits/s uncoded engineering data) and switched from the high-gain antenna to transmitting over the low-gain antenna. The roll and pitch turns were then performed. During the burns the data rate was 2450 bits/s block-coded engineering data. It was recorded by the Data Storage subsystem for playback at a later time. Real-time data reception was not possible at this data rate as the turns required for the TCMs placed the spacecraft in a minimum gain area on the low-gain antenna pattern, hereafter referred to as a LGA null. Figure 25 shows typical link performance during the maneuver periods. As can be seen performance was varied depending on the data mode. The period of no data is when 2450 bits/s data was being transmitted over the LGA during the burn. Although this plot of downlink AGC is of TCM 4A it is very representative of TCM 4B and TCM 5 performance.

b. Solar superior conjunction. Superior conjunction took place during May and June 1974. The Earth, Sun, and the spacecraft were most nearly aligned in a straight line, with the spacecraft on the opposite side of the Sun from the Earth, on June 6, 1974. Telecommunications performance was influenced primarily by: (a) the separation angle between the Sun and where the antenna is pointed, i.e., Sun-Earth-Probe (SEP) angle, (b) the level of solar activity, and (c) the communications mode. The SEP angle is measured with respect to the center of the Sun. A plot of the SEP angle during this period is shown in Fig. 26. Communications modes determine the relative amounts of power placed in the phase-modulated carrier, its sidebands, and also the bandwidths of the data channels.

This section will deal primarily with the effects of solar activity on the 33-1/3 bits/s uncoded rate. There is also some information provided on the X-band downlink AGC. However, due to the X-band failure during the prime mission the data is somewhat clouded.

Solar activity was predicted to be low for MVM'73 superior conjunction. The average

predicted solar activity is only an average, and it is the solar flares that are truly disruptive of S-band communications. Large flares occurred about one month after the MVM'73 conjunction (time relative to minimum SEP angle).

The characteristics of the solar conjunction period are:

- (a) Bit error rate increased as SEP decreased with no total loss of data during the entire period.
- (b) Usable two-way S-band doppler and S-band ranging was received though the noise level increased.
- (c) X-band downlink, X-band ranging, and X-band two-way doppler was too noisy for any use due to the multiplication of the S-band noise by the 11/3 X/S-band transmission ratio on the X-band downlink.

Because of manpower limitations and the pressure of other tasks, proper monitoring was not possible. In addition, because of severe computer processing limitations in terms of recording and display associated with the data taking itself, it was necessary to manually record most data in real time. The data observed was on a digital television monitor, and it consisted of the receiver AGC from the two Block III receivers at the station (and in the case of DSS 14, one of the Block IV receivers used for X-band). Also, there was SNR from one or two strings or chains of telemetry receiving equipment (subcarrier demodulator assembly, symbol synchronizer assembly, TCP, etc.)

As already indicated, most of the data consisted of cruise telemetry at 33-1/3 bit/s. Because of the need for real-time manual monitoring, observation periods were limited to between 20 min and 2 or 3 h per day, and this would be divided into one to three periods over the working day. The AGC and SNR readings were recorded once every 30 s with mean and standard deviation being calculated for each period.

Figure 27 represents all the data available from the time observation was begun (May 25, 1974) until five days after minimum SEP angle (June 10, 1974). Figure 28 continues the data through July 19, 1974 in a somewhat simplified manner.

Starting with the AGC in Fig. 27, the circled dots represent the mean of the AGC over 15-min periods each day, with the receiver in the wide loop bandwidth. If there were more than one such 15-min period on a given day, the AGC's were averaged. The dots surrounded by triangles are similar AGCs when the receiver was in narrow-loop bandwidth. Several days of questionable data was not included when the configuration was uncertain. The rest of the data shows that the narrow-loop bandwidth produced an indicated AGC about half a decibel higher than that wide-loop bandwidth. The data is generally, but not

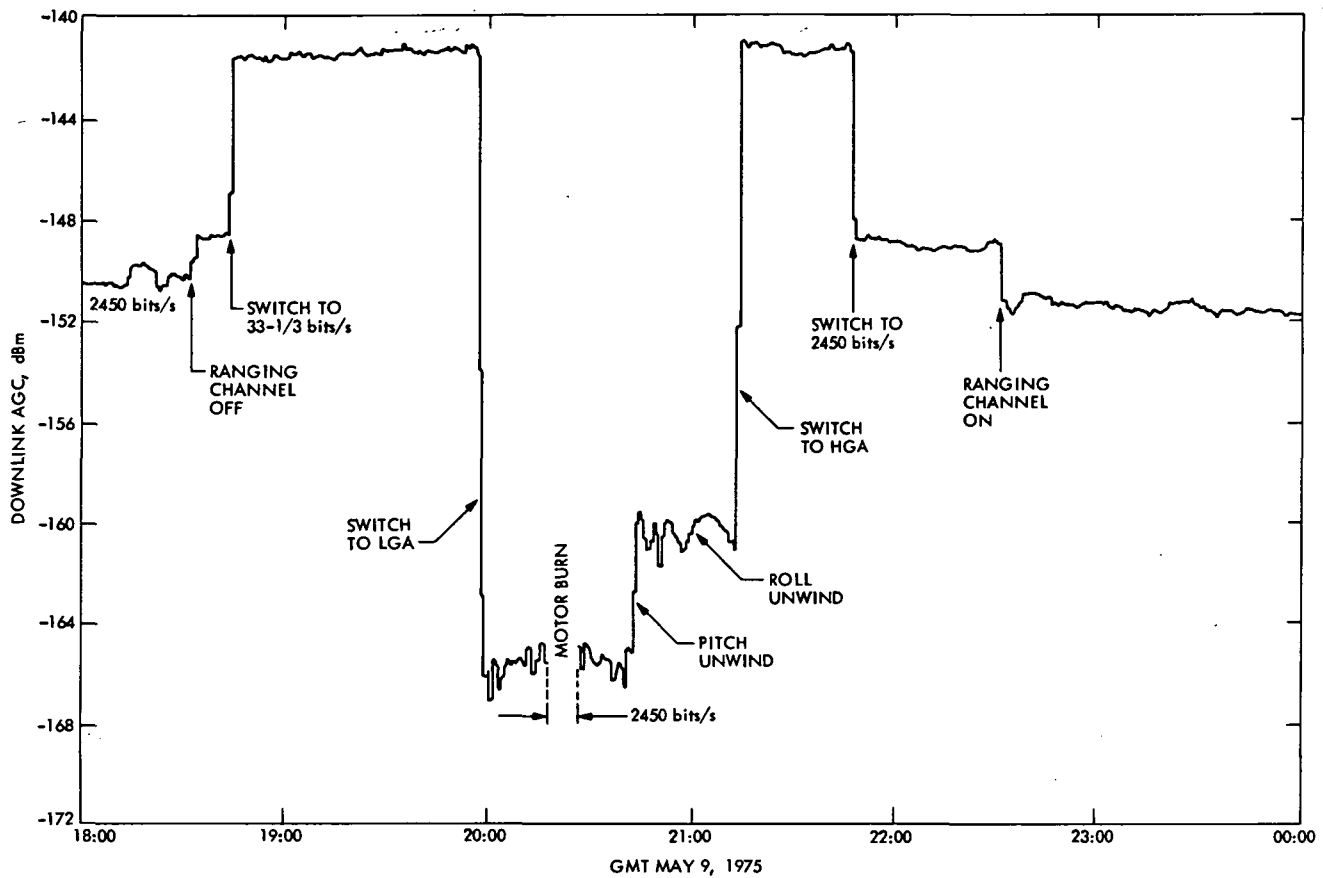


Figure 25. TCM 4A downlink AGC

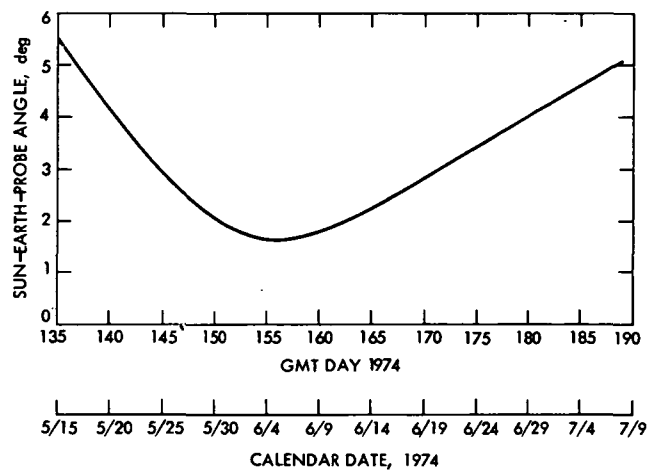


Figure 26. Sun-Earth-probe angle

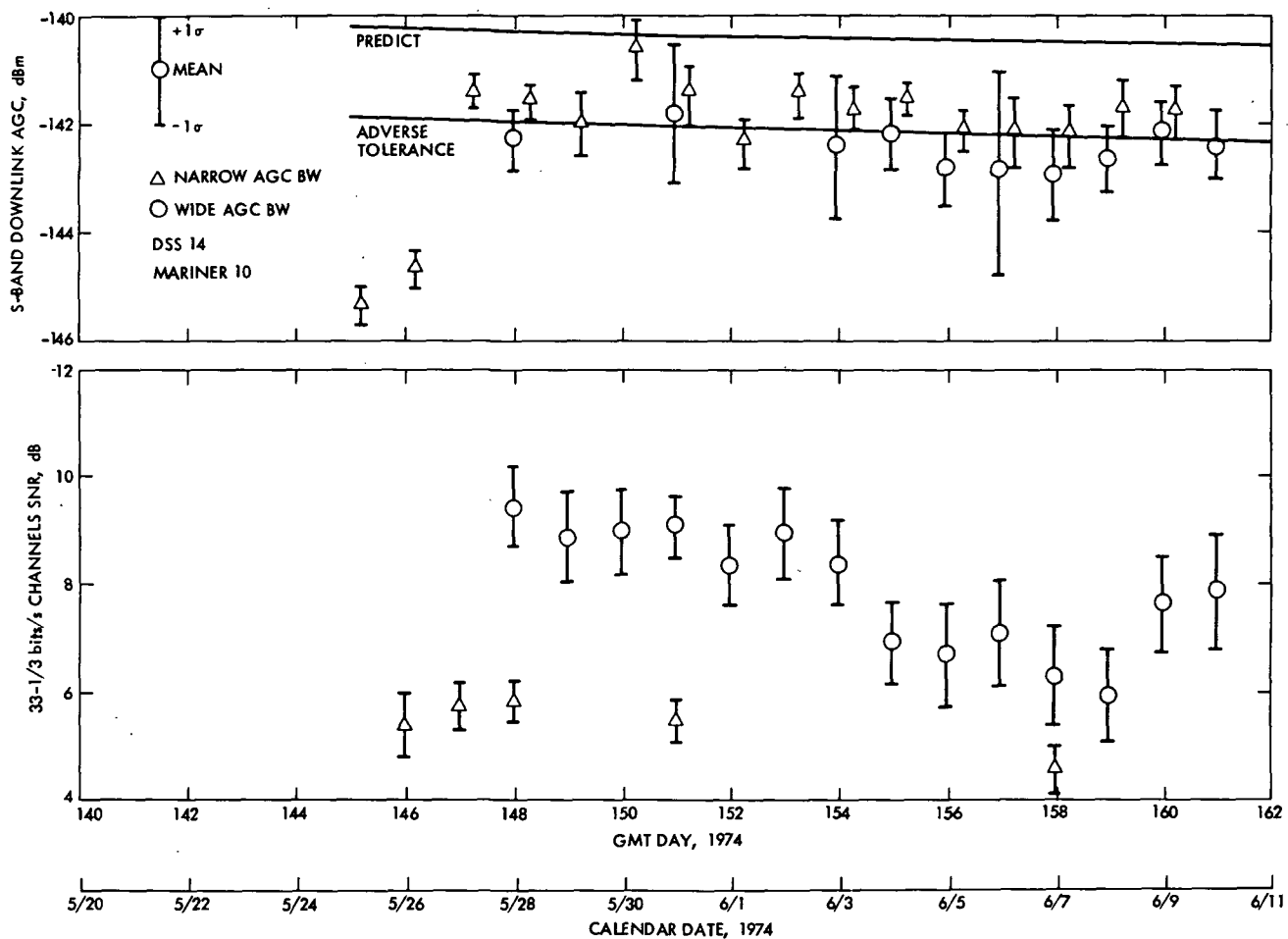


Figure 27. 33-1/3 bits/s SNR and AGC, May 22 to June 11, 1974

entirely, from DSS 14. The early data is from DSS 63.

The bottom half of Fig. 27 shows the 33-1/3 bits/s cruise mode SNR. Again, some of the data occurred with the loop bandwidth in the wide position (circled dots) and some in the narrow position (triangled dots). (In general, the wide bandwidth resulted in an indicated SNR that was 2 to 3 dB higher than when the narrow bandwidth was used.)

Minimum SEP angle occurred on June 5, 1974 (GMT Day 156). Maximum AGC degradation occurred two days later, on June 7, 1974. Maximum SNR degradation occurred three days later on June 10. However, AGC variation during the week, centered on June 5, was less than 0.5 dB and SNR variation was less than 1 dB. SEP angle was changing very slowly.

The standard deviation is indicated by the vertical line centered on the dot for each day. The reason for the extreme change in AGC variation on June 6, relative to the other days nearby, is not known unless the station Digital Instrumentation Subsystem AGC smoothing factor was set differently on that one day. This factor results in the current AGC output being affected by from 0 to 19 of the previous AGC outputs. The SNR standard deviation on June 6 is only slightly larger than on nearby days.

Figure 28 provides data only for the wide loop bandwidth. Once SEP angle had increased to 3 deg, there was a single DSS 14 pass weekly in which the 33-1/3 bits/s cruise mode was available. The data on Days 182 and 189 (July 1 and July 8, 1974) is interesting. "Importance 1" solar flares occurred on July 4 and 5, and high to very high solar activity occurred during the entire week. A large scatter, but small degradation, occurred on the indicated S-band AGC. The degradation of the SNR was larger on July 1 than on July 8, but the scatter was more than twice as much as July 8 than on July 1. After the July 8 observation, the Sun entered a quiet period of activity. By the time the SEP angle was 6 deg, the scatter in the data seemed to show that conditions were back to the way they were before the Sun had a perceptible effect on the downlink.

Because of various spacecraft problems during the mission, the X-band transmitter was not operating normally at all times. However, the degradations discussed in this paragraph are believed to be due mainly to the solar effects and not the X-band transmitter anomalies.

Figure 29 is a summary of the Block IV receiver AGC from the X-band downlink. Immediately apparent is the great difference between the one-way and the two-way signature. Compared to two-way, the one-way AGC has a much higher mean and a much lower standard deviation. The degradation in two-way AGC is caused by the effects on the S-band uplink caused by its passage close to the Sun. Phase jitter in the spacecraft S-band receiver is multiplied by the factor 11/3 before being applied to the X-band downlink carrier. The spacecraft S-band receiver can follow (to some degree) the phase transients. However, the ground receiver has much less success in following the phase transients which have been multiplied by 11/3.

One significant accomplishment was achieved when spacecraft telemetry was received throughout the superior conjunction period. MM'69 and MM'71 each had 20-day blackouts of telemetry. Therefore, for the first time the effects on the S-band uplink could be deduced directly by means of telemetry. Figure 30 shows that solar effects on the uplink were significant. There were some bit errors induced in the downlink telemetry; however, most of the data points shown in the computer-generated plot lie within the range of -128 to -136 dBm and are considered therefore to be valid. On the day shown, May 29, the SEP was 2.2 deg, and the amplitude fluctuations on the uplink AGC were about 8 dB peak-to-peak. Figure 31 is a summary plot of DSS 14 100 kW uplink AGC mean and standard deviation for the entire period. The use of DSS 14 100 kW transmitter was ended prior to loss of all solar effects.

When comparing the uplink and downlink AGC plots for this period it should be noted that the respective measurement quantizations are quite different. The uplink AGC measurement is taken from the spacecraft telemetry stream and each DN (data number) equals a quantization of approximately 1 dB. The downlink AGC measurement is received in the DSN monitor block data and each DN equals a quantization of -0.016 dB. Therefore, a greater scatter is seen in the uplink AGC data.

2. Mercury II Encounter. The second Mercury encounter was designed primarily as a TV pass. Therefore it was important to provide 117 kbits/s imaging data with the lowest possible BER. At Mercury I encounter the actual performance was a BER ranging from 2.35 per 100 to 2.63 per 100. However, Mercury II encounter was to take place at a greater range (i.e., higher BER) and with the tape recorder failure was restricted to either 117 kbits/s real-time coverage or 22 kbits/s quarter-strip pictures.

With DSS 14 in a listen-only configuration using the super-cooled maser a BER of 4.4 per 100 to 4.9 per 100 was expected. In order to improve the performance capabilities it was determined that by arraying the antennas (Fig. 32) of DSS 14, DSS 12, and DSS 13, each in a low-noise configuration, and by using a special signal combiner the BER could be lowered to 3.0 per 100 to 3.3 per 100. Additional antenna arraying details are discussed in Sections VIII-A-7 and VIII-C. In addition a further option was used, in that by using the Mercury I occultation analog recorders at DSSs 14 and 43 the BER could possibly be lowered to even 1.6 per 100. This would be accomplished by recording the SSA soft decision integral bit values. The analog tapes would be returned to JPL for processing in the Telecommunications Development Laboratory.

Figure 32 shows the DSN configuration used during the 117 kbits/s portion of the encounter. Figure 33 shows the predicted and actual BER achieved. The actual BER at 117 kbits/s during the prime encounter TV sequences ranged from 3.1 per 100 to 3.6 per 100. The predict for normal operation and the predict for combined operation reflect the improvement expected. An extrapolation for normal operation was taken from the actual combined data. This was verified

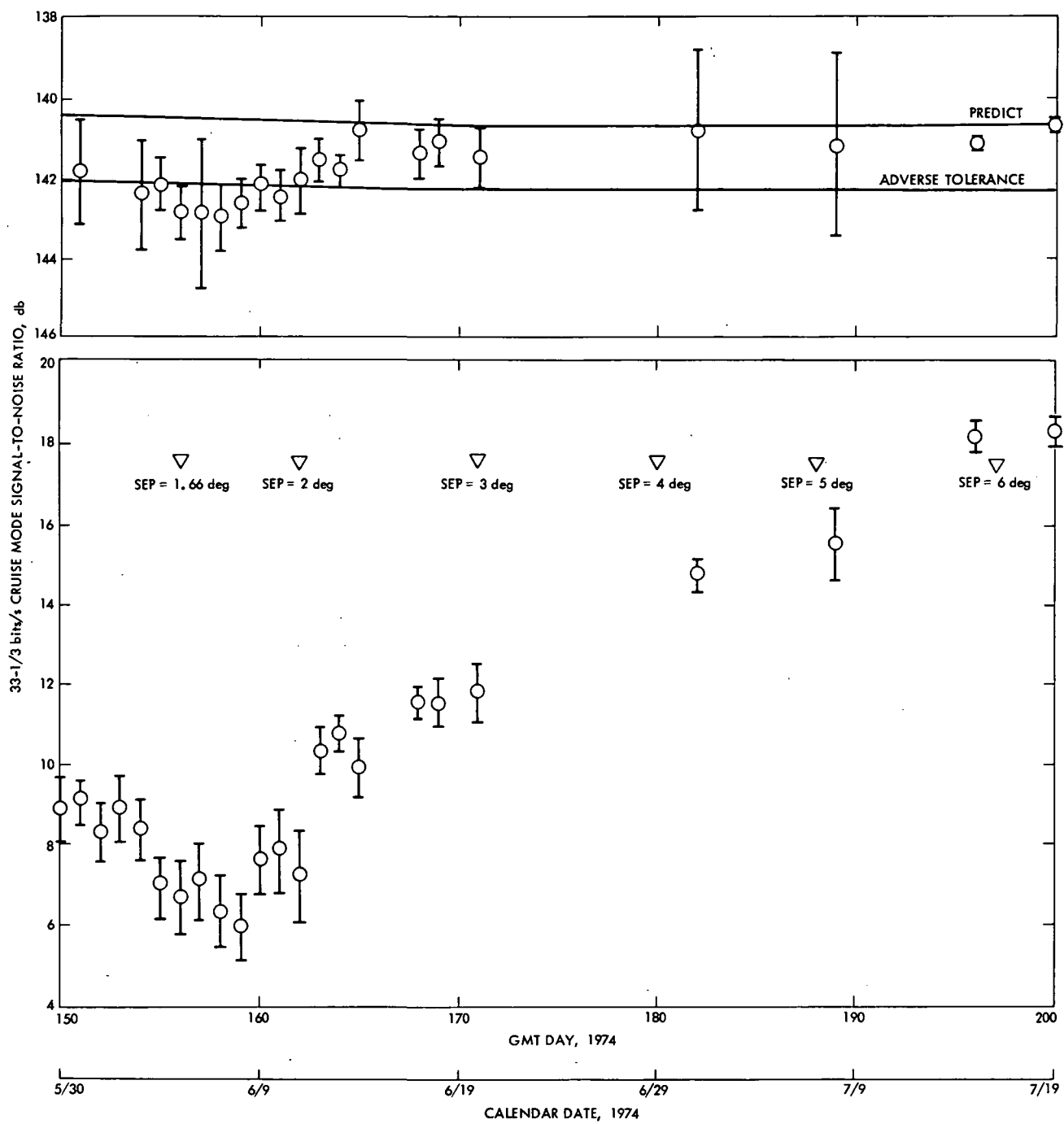


Figure 28. $33\text{-}1/3$ bits/s SNR and AGC, June 19-29, 1974

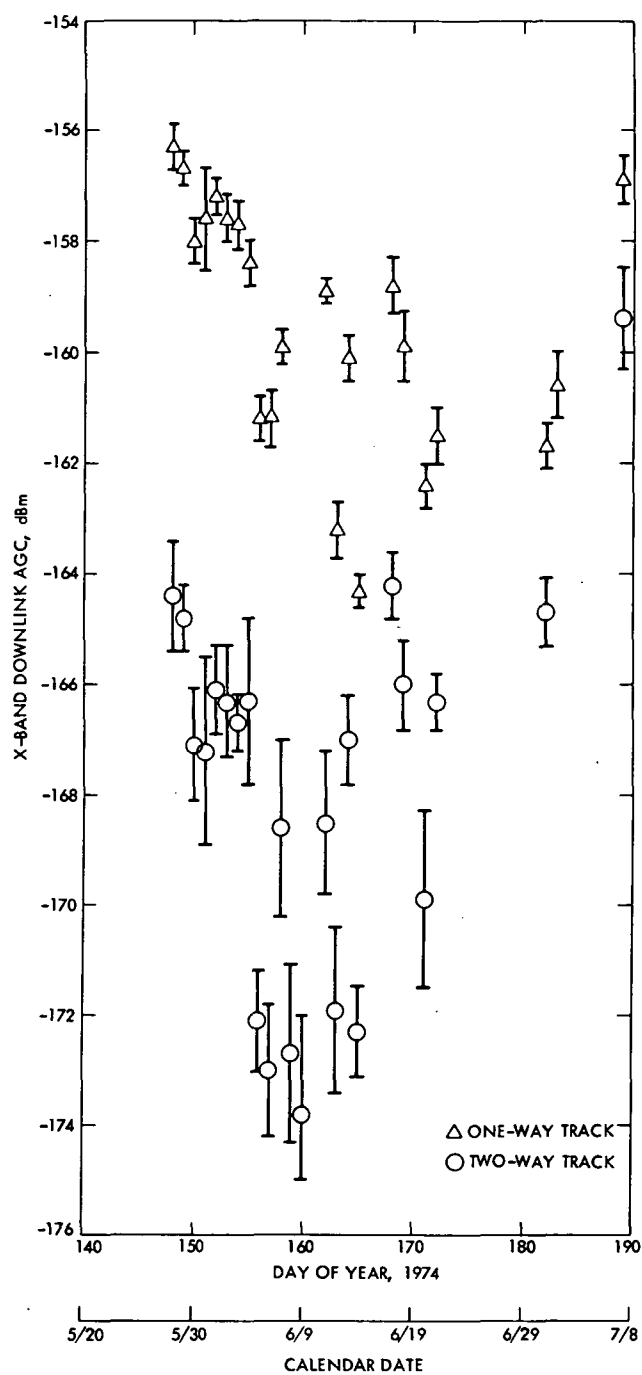


Figure 29. X-band downlink AGC mean and standard variation

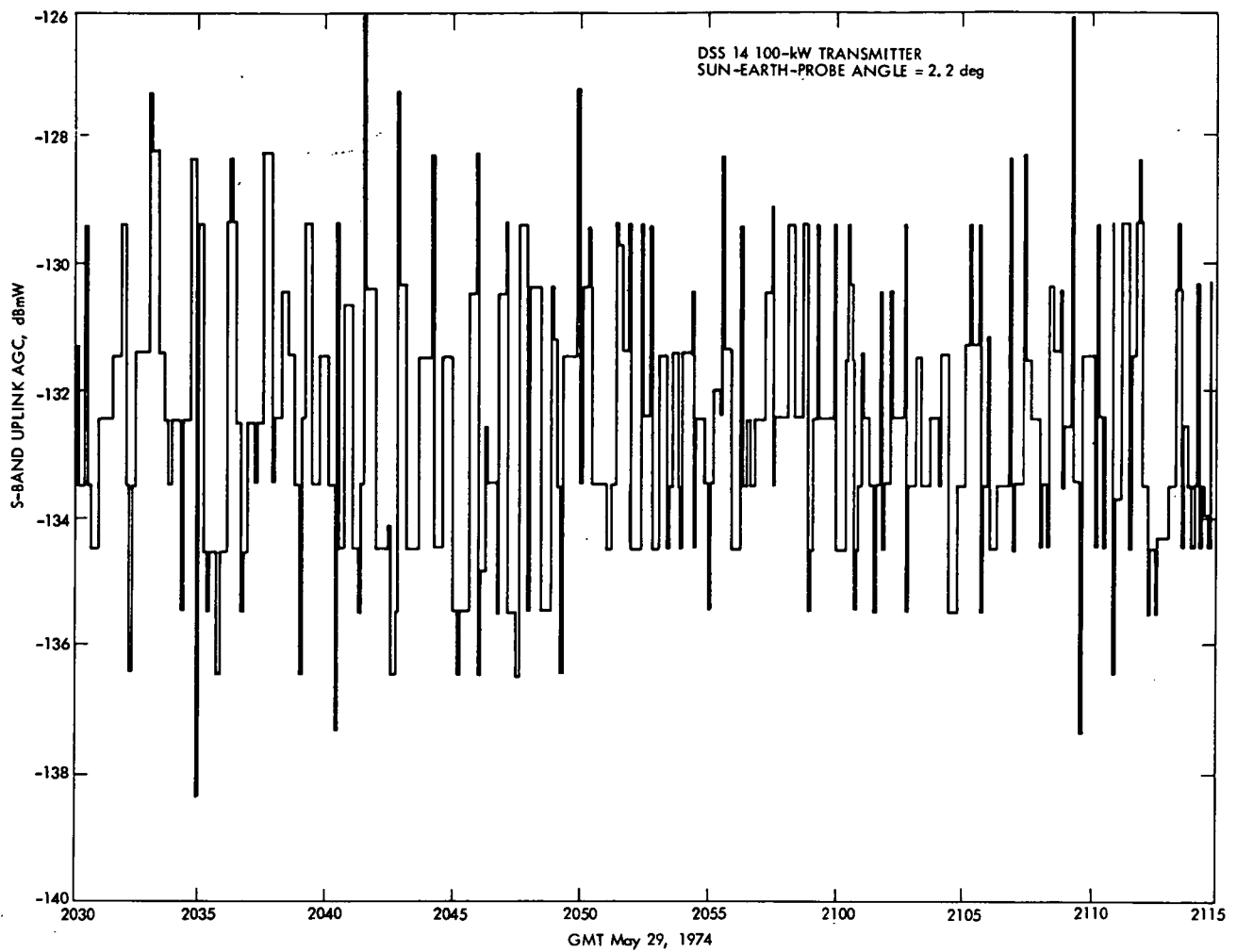


Figure 30. S-band uplink AGC

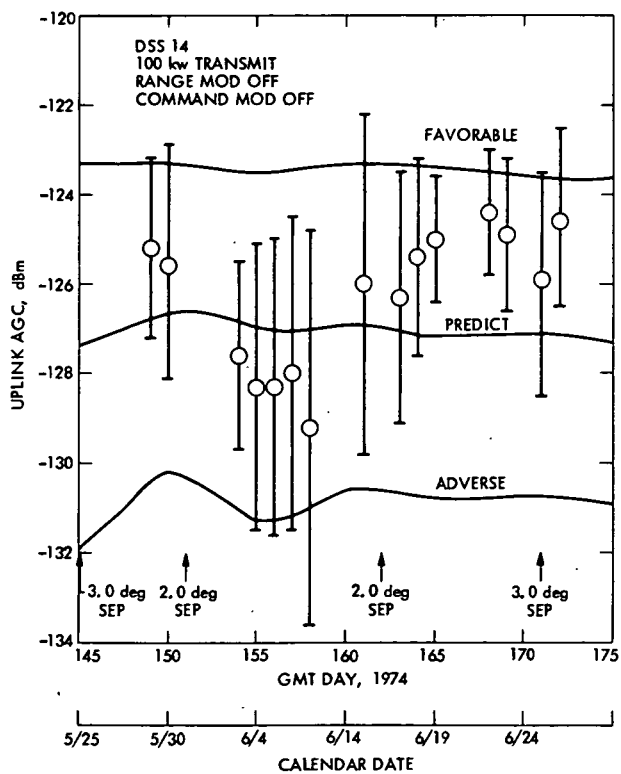


Figure 31. Uplink carrier power mean and standard variation

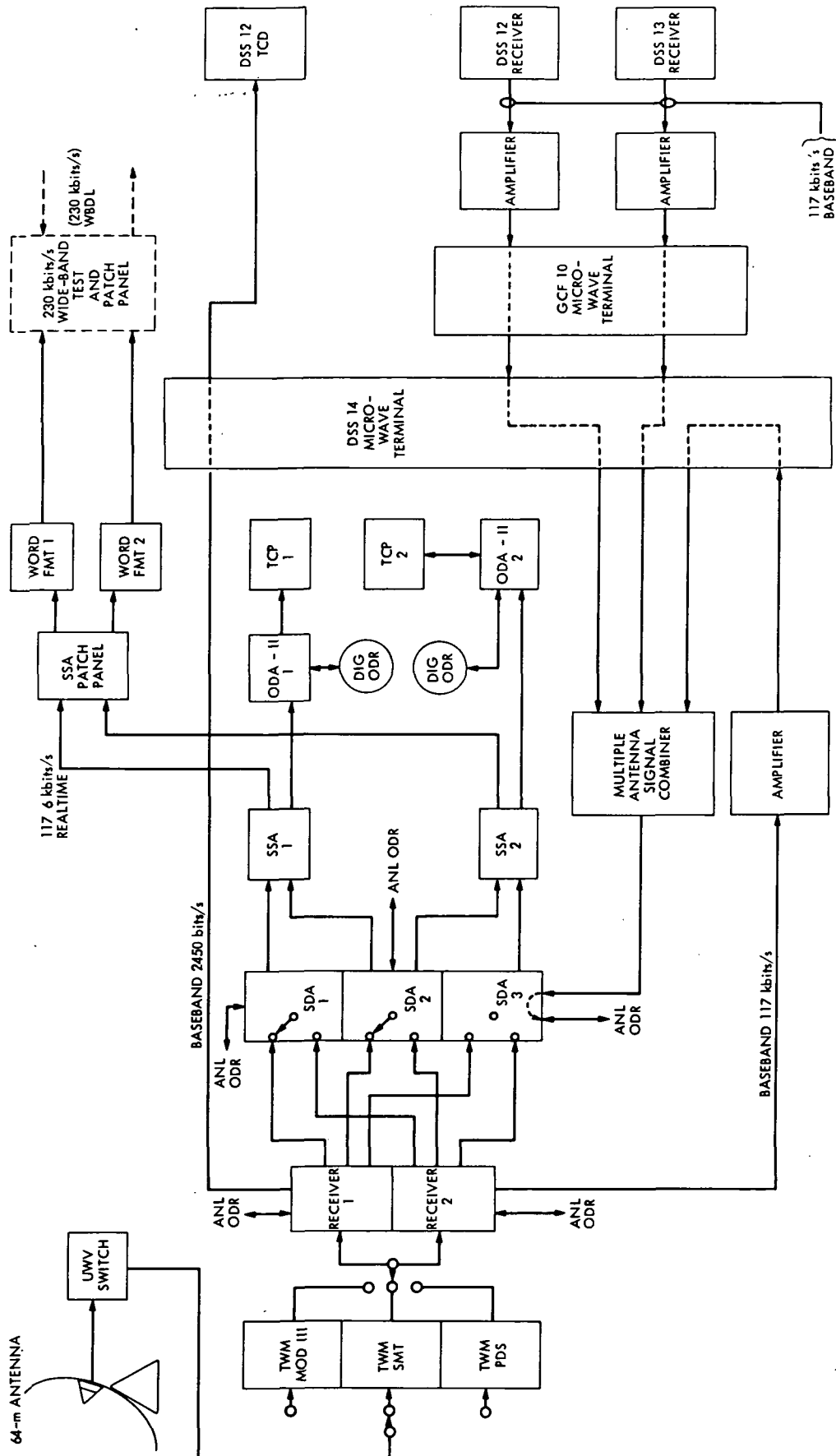


Figure 32. DSN antenna array configuration

to be accurate by the operation mode change shown as 1. in Fig. 33.

3. Mercury II to Mercury III Cruise

a. Link performance with a rolling spacecraft. In order to have a successful Mercury III encounter an extreme attitude-control gas conservation mode was required. On Oct. 5, 1974 the spacecraft went off Canopus and was allowed to roll using solar panel tilt angle and HGA position to control the rate and direction. Communications with the spacecraft was maintained by both transmitting and receiving via the LGA.

Up to this point the spacecraft has been Canopus acquired. With the use of a trajectory tape from the Navigation Team, TPAP (Telecommunications Prediction and Analysis Program) has been used to generate telecommunications performance predicts. This could no longer be done.

First, among other things, TPAP depended on a predictable Earth clock and cone angle for use in determining LGA gain. The Earth clock angle, however, was rapidly changing with unpredictable rate and acceleration changes in the roll drift. When the spacecraft was Canopus acquired the Earth clock angle changed from a fraction of a degree per day to as much as $1\frac{1}{2}$ deg per day. With a now possible rate as great as two or more degrees per minute, telecommunications performance predictions had to be done by hand.

Second, the shape of LGA pattern reduced the link capabilities. Being in the general shape of a doughnut the relative gain of the antenna changed with increments in clock and cone. Coupled with the increased range of the mid-cruise the LGA nulls created losses in downlink communications.

Figure 34 is a comparison of: (1) the TPAP prediction with Canopus acquired, (2) the theoretical LGA pattern through 360 deg of roll and, (3) actual spacecraft downlink AGC recorded over DSS 43 on Oct. 15, 1974. As can be seen, the TPAP predict is totally unusable, while the theoretical pattern is usable only in a general sense as a trend indication. The theoretical pattern had a resolution of 5 deg in clock which for a slow roll rate was inadequate. Discussion of TCM 7, TCM 8, and the Canopus acquisition sequence prior to Mercury III will bear this out further.

Figures 35 and 36 yield a comparison of spacecraft downlink AGC data under similar conditions but with different roll rates. The primary difference is in the data scatter. When the spacecraft is rolling at a more rapid rate much of the fine grain structure is smoothed over by the roll rate and AGC sampling time. The downlink AGC is recorded once per minute. This sample is an average of 12 5-s data samples from the station. If the roll rate is high then as much as two or more degrees could be represented by one sample. Also, if the roll rate is low then a higher resolution antenna pattern is obtained.

Through the unique nature of MVM'73 operations it was discovered that the antenna patterns included in TPAP were inadequate for the above situation. The solution would be to have a larger,

more accurate pattern. To accomplish this, TPAP should be expanded to accommodate a larger pattern matrix, or a series of grids, each covering a small area, developed for use when needed.

b. Trajectory correction maneuvers. In this portion of the Extended Mission three TCMs were performed to bring the spacecraft to its aim point. They were unique in that they were initiated while the spacecraft was rolling. The idea was to stop rolling at the end of the roll turn then pitch turn and burn.

TCM 6 and TCM 7 were standard maneuvers. TCM 8 was a sunline maneuver. TCM 6 telecom performance was as expected. The associated turns caused changes within ± 1 dB of steady state. TCM 7 presented a more interesting set of conditions. Due to a timing error the first attempt had to be aborted. However, the maneuver was successfully accomplished the next day, Feb. 13, 1975. The LGA pattern for the maneuver is shown in Fig. 37. Note the difference in the TPAP turn predict and the pattern predict. This is due to the difference in the resolution. TPAP uses a 10 deg clock \times 10 deg cone increment, whereas the LGA pattern uses a 5 deg clock angle \times 0.5 deg cone increment.

An expanded view of the area from Canopus through the pitch turn with the actual data added is shown in Fig. 38. The data scatter is quite large. To extract a shape overlapping 5 min means were plotted. The difference between the actual data and the predict is shown. The X's on the predict line are the 5 deg clock points. Compared to actual data points they exhibit the poor resolution of the predict pattern. TCM 8 being a sunline maneuver with, therefore, no pitch turn was uneventful for telecommunications. It was performed when the link signal strengths were at peak.

4. Mercury III Encounter. Prior to the initiation of the encounter sequences it was necessary to stop the roll drift and acquire Canopus with minimum gas usage. Standard acquisition procedures were no longer adequate due to possible roll gyro oscillations and the entrance into the particle area. The particle area was especially serious in that whenever the HGA position was changed there followed a short time later a large number of particles.

The acquisition sequence called for an extremely slow roll rate with position information coming from LGA pattern observations. At this time the LGA nulls coupled with increasing range covered 120 deg of the pattern. A new plan had to be devised. The spacecraft was commanded to transmit via the HGA after the roll was stopped. By slewing the antenna along the Earth line a signal was finally located. Spacecraft position was determined by comparing HGA position at peak signal strength to where the HGA should be pointed when Canopus acquired. Using this as a map, the HGA was repositioned and the spacecraft was rolled to a peak signal and stopped.

Data rates for the encounter were single channel 2450 bits/s block coded non-imaging science (NIS) data and 22 kbits/s block coded imaging data interplexed with the above 2450 bits/s

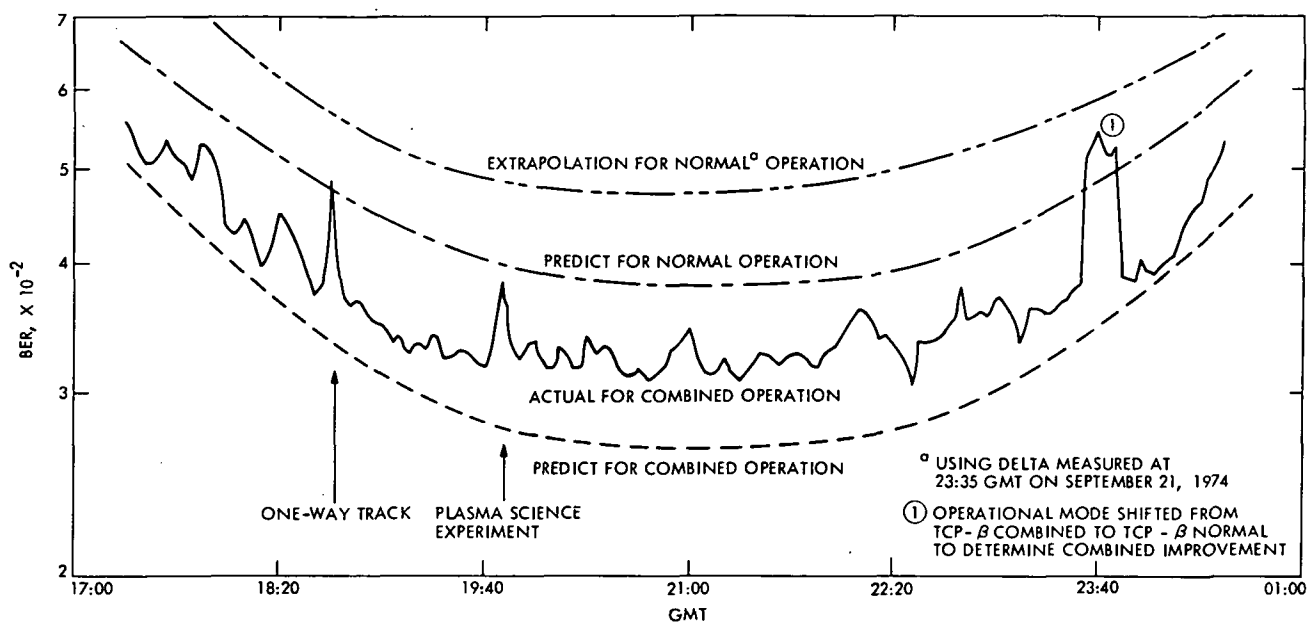


Figure 33. 117 kbits/s BER - Mercury II

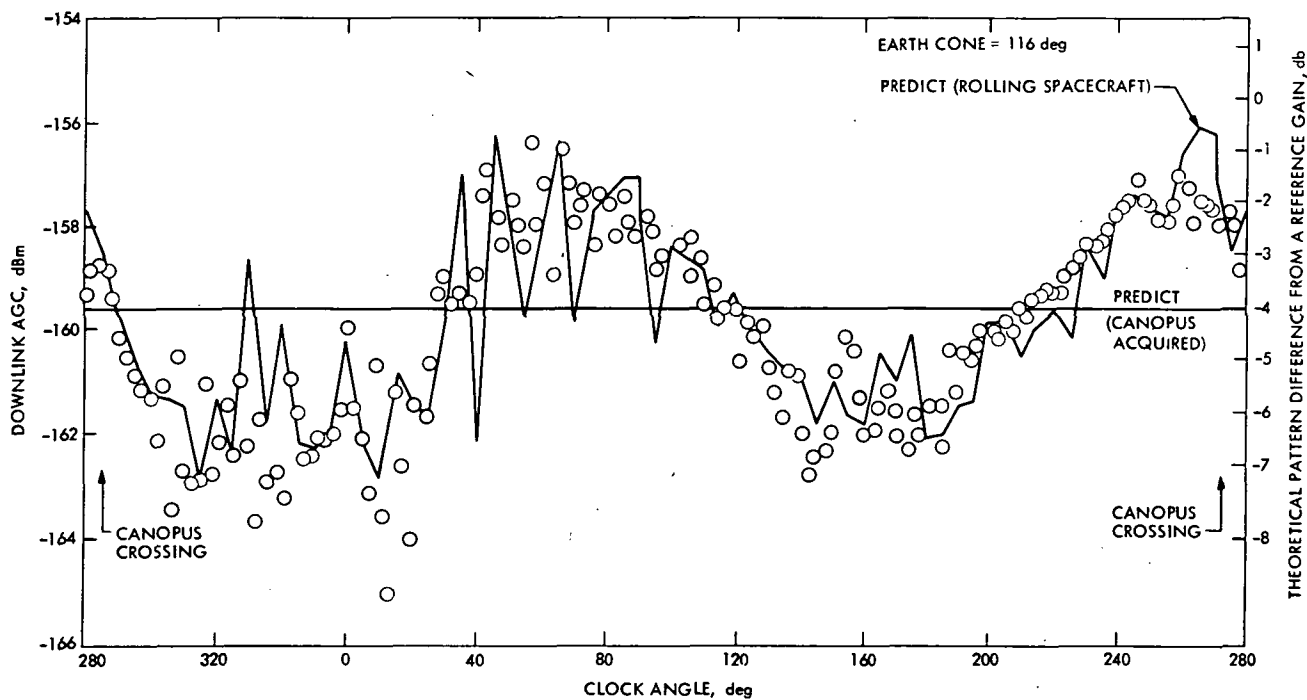


Figure 34. LGA performance comparison

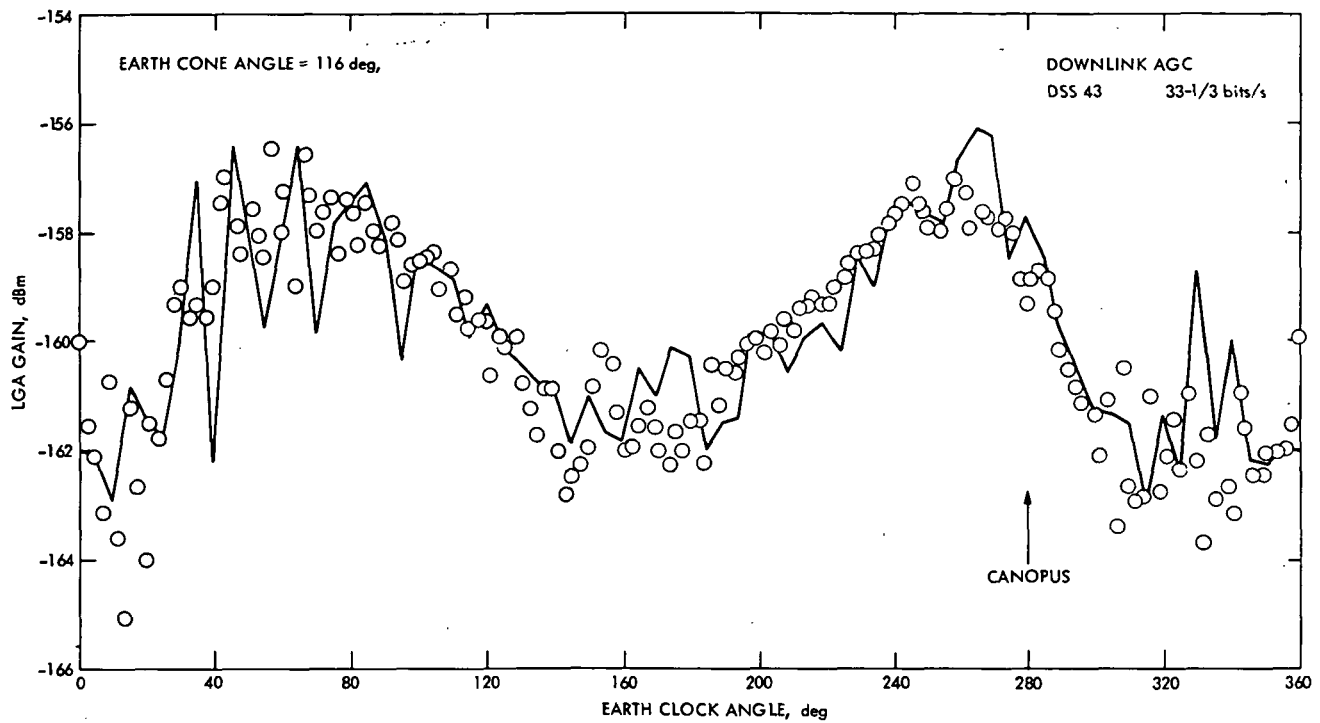


Figure 35. LGA performance, Oct. 15, 1974

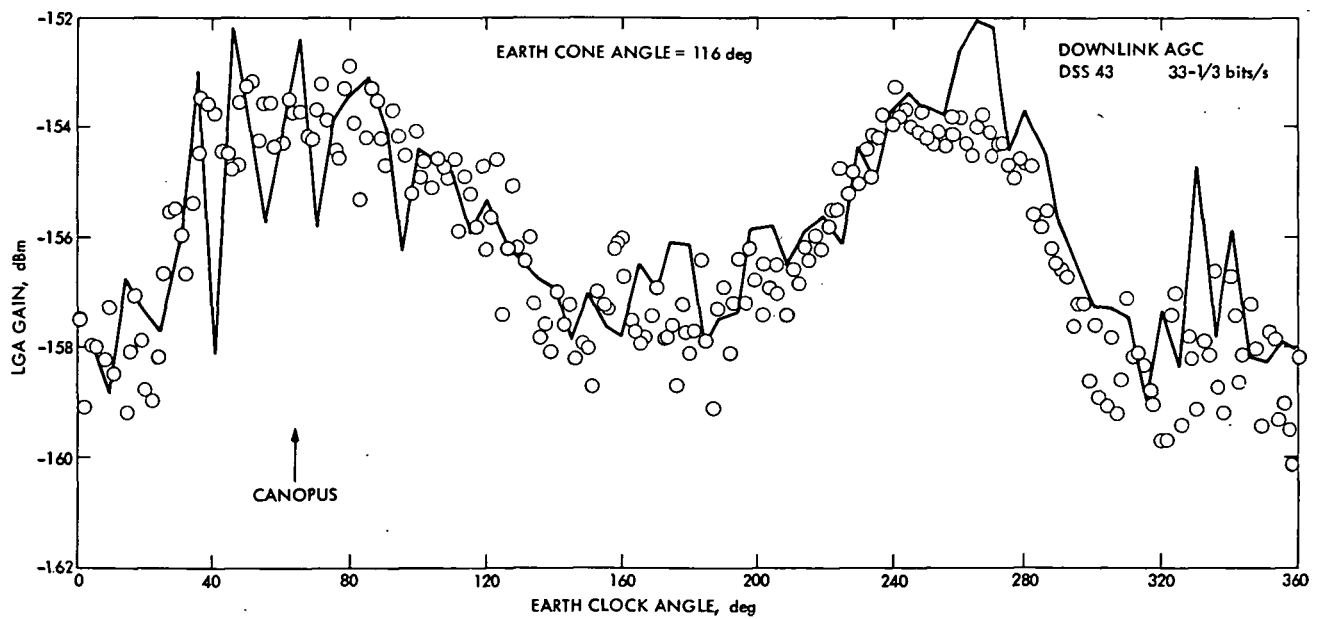


Figure 36. LGA performance, Jan. 8, 1975

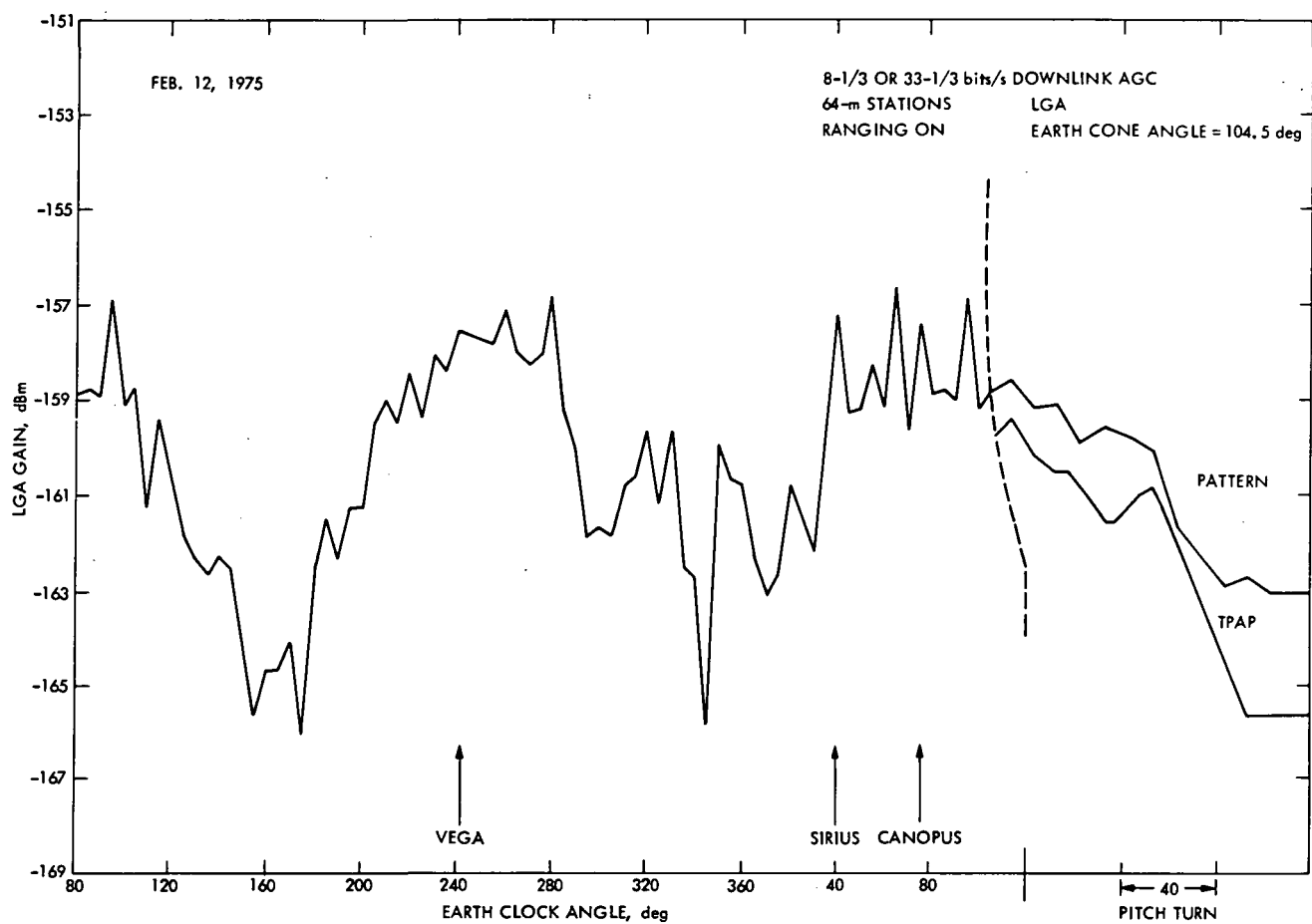


Figure 37. TCM 7 predict LGA pattern

NIS data. Real-time 117 kbits/s imaging data had been planned. However, due to some last minute difficulties it was cancelled. This is discussed further in Section VIII-D. The 22-kbits/s data bit-error-rate is shown in Fig. 39 for the prime encounter TV sequences. As can be seen it was somewhat higher than predicted. The average delta shown corresponds to an actual SNR degradation of 0.4 dB. The receiver AGC for this period averaged within ± 0.1 dB of predicts.

5. End-of-Mission Testing. No tests were performed that were strictly for telecommunications systems. The HGA feed test was canceled when it was determined that the attitude-control gas was close to being depleted. The TMU (Telemetry Modulation Unit) was switched to its redundant element, TMU II, as part of the FDS (Flight Data Subsystem) testing. TMU II had not been powered since before launch, as it has an unfused power supply. For twenty minutes it operated flawlessly before power was returned to TMU I. Also, the Radio Frequency Subsystem (RFS) TWT was cycled OFF/ON three times in the final three days before the final DC 55 TWT OFF command was transmitted. No anomalies were recorded.

6. Systems Operation Summary. During the 343 days of the Extended Mission no new anomalies were recorded which affected the RFS, MDS, X-band transmitter, or S/X-band antennas. The RFS was maintained in a TWTA 1, high-power mode throughout. All engineering channels and performance checks were normal and as expected. The Auxiliary Oscillator frequency was found to decrease more with temperature than original predicts indicated. The cause is unknown at this time.

The MDS remained steady state with the Flight Command Unit processing close to 9000 commands during the extended mission with over 24200 commands over the entire mission. The DC 42, DC 43 (TWT to high power, TWT to low power) interface problem of the prime mission was never investigated further. The TMU performed within specifications and was exercised repeatedly in all modes.

The X-band transmitter continued to toggle within its predicted anomalous modes from the prime mission. In July of 1974 the Block IV receiver system was removed from DSS 14 for modification. From that time on no estimate of X-band downlink AGC or S/X-band ranging performance can be given. Performance prior to then can be found in Section VI-A-1-b.

The S/X-band antennas performed within their acceptable margins. The HGA anomaly from the prime mission did not reappear. As was noted before, however, when the spacecraft entered the particle region a number of particles were observed after each HGA repositioning.

B. Guidance and Control

1. Attitude-Control Extended Mission report.

a. Introduction. During the MVM '73 system design phase, the possibility of multiple Mercury encounters was recognized, provided an adequate supply of attitude-control gas remained, to

maintain spacecraft Sun orientation for power and temperature control purposes.

During the Earth to Mercury I transit period, conservation of attitude gas for potential multiple Mercury encounters was a secondary consideration; the first priority was achieving a first Mercury encounter. MVM'73 was launched with 3.63 kg (8 lbm) of attitude control gas and ended the Mercury I encounter sequence with 1.36 kg (3 lbm). However, the many performance anomalies and operating characteristics identified during the primary mission provided the constraints and insights required in developing the attitude control operational modes which minimized Extended Mission gas usage.

This section will discuss the unique attitude-control modes, analysis techniques and insights used to achieve a remarkable one-year two-encounter extended mission.

b. Extended mission attitude-control modes. Using torque produced by solar pressure on spacecraft surfaces to reduce attitude-control gas usage is not a new concept. Mariner IV had movable solar vanes on the ends of its four solar panels which attempted to create a favorable gas usage torque in the pitch and yaw axes. However, there were some control problems with these devices, and active attitude control using solar pressure as a spacecraft control mechanism was abandoned on subsequent Mariners.

Mariner 10, illustrated in Fig. 40, was configured with four movable appendages: two tiltable solar panels, a two-degree-of-freedom HGA, and a scan platform. The two solar panels and the HGA had surfaces exposed to solar radiation and the forces produced on these surfaces produced torques on the spacecraft. As a result of observations made during the primary mission, it was determined that differentially tilting the solar panels produced torques in the control axes.

The solar panels absorbed approximately 78% of the incident energy. Figure 41 illustrates an end view of one solar panel and the forces which produced roll and yaw torques. Roll axis torque was approximately related to solar panel angles as follows:

$$\text{Roll torque} = K_1(SI)[\sin(2\theta_p) - \sin(2\theta_n)]$$

where

θ_p = the tilt angle of the +x solar panel

θ_n = the tilt angle of the -x solar panel

$K_1(SI)$ = a proportionality factor which is a function of solar intensity and absorptivity

Yaw axis torque was approximately related to solar panel angles as follows:

$$\text{Yaw torque} = K_2(SI)[\cos(\theta_p) - \cos(\theta_n)]$$

$K_2(SI)$ = a proportionality factor which is a function of solar intensity and reflectivity

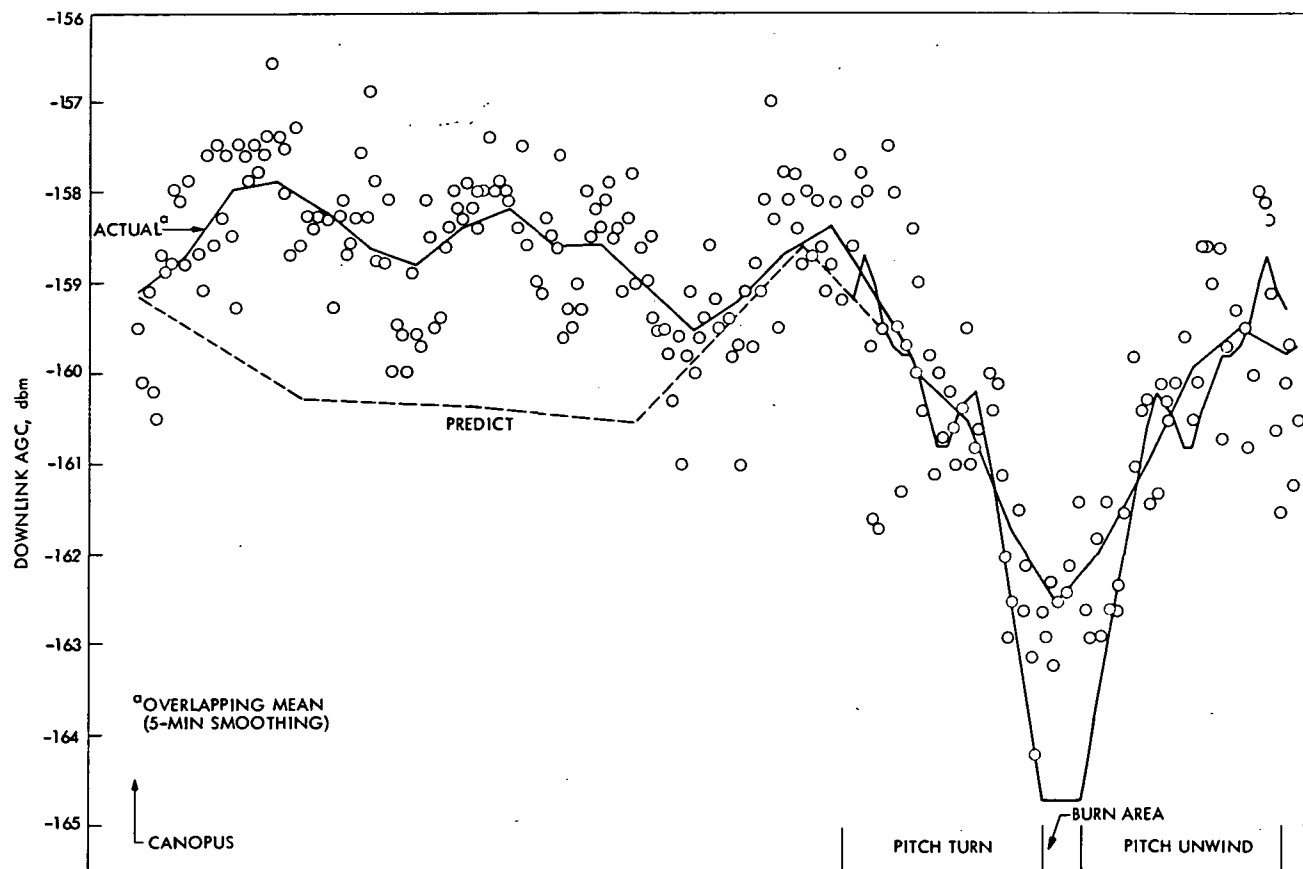


Figure 38. TCM 7 performance plot

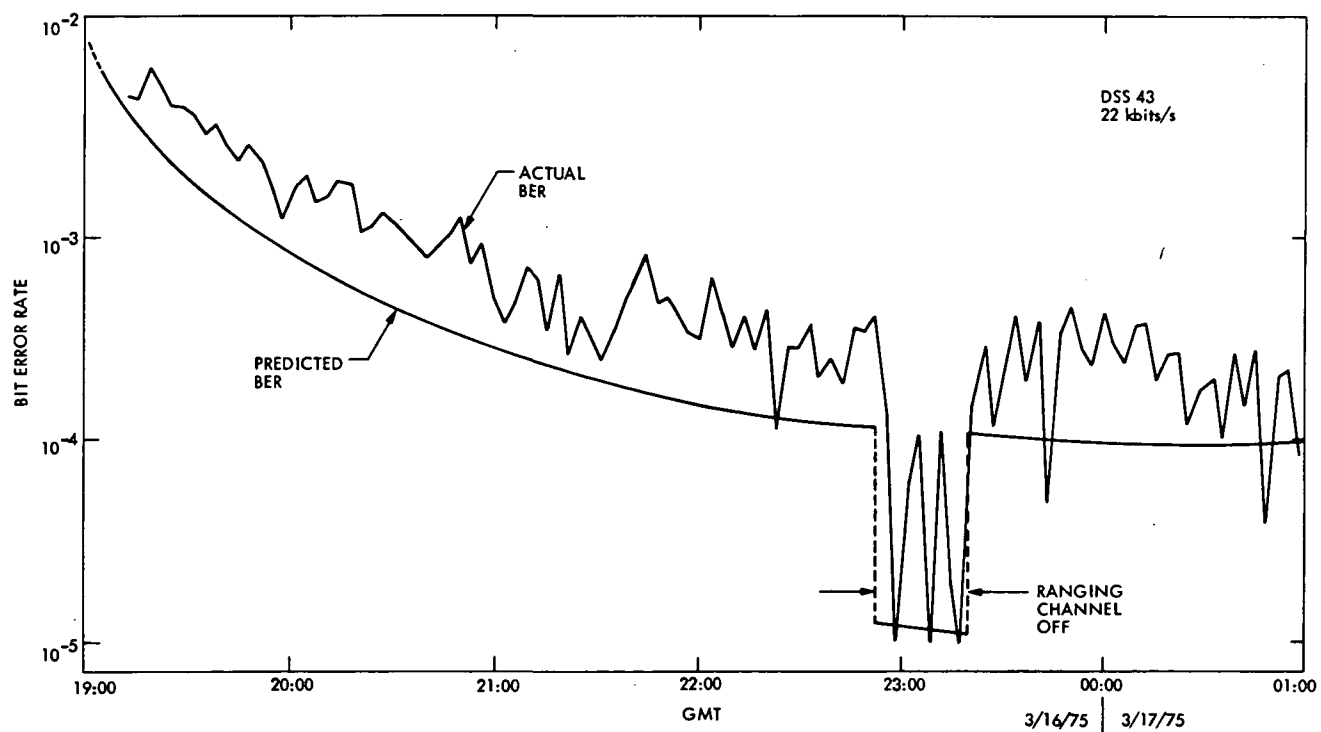


Figure 39. Mercury III 22.05 kbits/s bit error rate

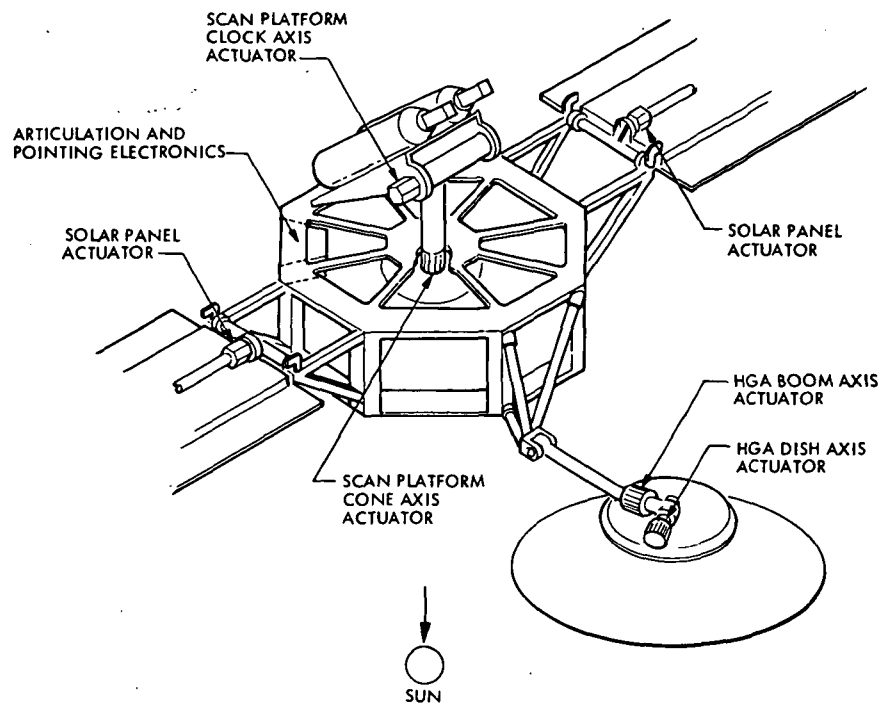
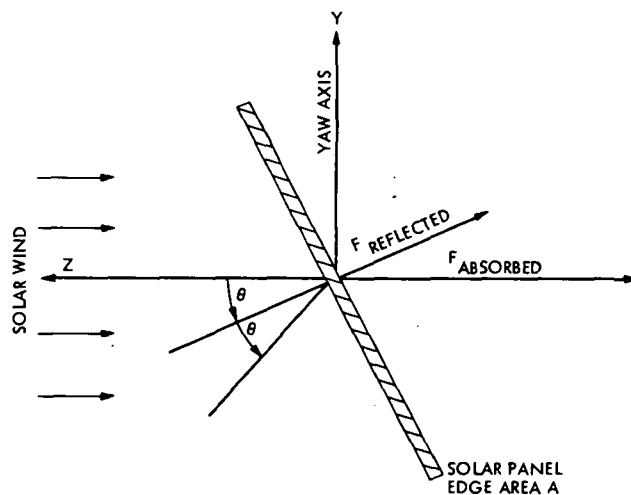


Figure 40. Mariner 10 articulated members configuration



$$F_Z = -K_1 A \cos \theta - 2 K_2 A \cos^2 \theta$$

$$F_Y = 2 K_2 A \cos \theta \sin \theta = K_2 A \sin 2\theta$$

A = AREA OF SOLAR PANEL

K_1 = FRACTION OF TOTAL RADIATION ABSORBED

K_2 = FRACTION OF TOTAL RADIATION REFLECTED

SINCE $K_2 \ll K_1$

$$\text{ROLL TORQUE} = K_2 (\sin 2\theta_P - \sin 2\theta_N)$$

$$\text{YAW TORQUE} = K_1 (\cos \theta_P - \cos \theta_N)$$

Figure 41. Solar pressure forces on solar panel

The net torque observed about the three spacecraft axes was also largely influenced by the HGA torque contributions. No simplified expression for HGA torques was ever developed; however, torque evaluations made during the primary mission demonstrated that when the HGA boresight axis cone angle was about 45 deg, the pitch and yaw torques were very small. This was discovered by correlating HGA boresight clock and cone angles during the primary mission to the spacecraft observed torques. Figure 42 illustrates the Earth track (HGA boresight angles) in a clock cone polar plot.

Gas usage predicts and actual usage for the Mercury I to Mercury III period are plotted in Fig. 43. Two predicts were made. The first predict assumed three-axis celestial control with successful torque control in all three axes and a limit cycle gas usage of about 2.7 g/day (0.006 lbm/day).

The second predict assumed an unsuccessful torque control usage of 5.9 g/day (0.013 lbm/day) until Mercury II, and then a roll drift mode (to be discussed later) usage of about 1.6 g/day (0.0036 lbm/day) until Mercury III.

c. Mercury I to Mercury II attitude control modes. From Mercury I to Mercury II, the spacecraft maintained 3-axis orientation and control. During this period the mean solar panel angles were selected to provide adequate power within temperature constraints and the HGA was positioned to maintain telecommunications link performance. Roll torques were brought to desired levels by differentially tilting the solar panels.

During this period, the evaluated average gas usage from limit cycle data was:

Axis		Gas/day, g(lbm)
Pitch	=	1.2 (0.0027)
Yaw	=	0.7 (0.0015)
Roll	=	0.8 (0.0018)
Total	+	2.7 (0.0060)

Gas usage from tank temperature and pressures was evaluated as follows:

GMT day	Gas weight, g(lbm)
107 (L + 165)	1360 (3.0)
242 (L + 300)	820 (1.8)
Total 135	540 (1.2)

Gas usage other than limit cycle in this interval was:

Event	Gas used, g(lbm)
TCM 4A/4B	73 (0.16)
Gyro test	9 (0.02)
TCM 5	36 (0.08)
Gyro test	9 (0.02)
Science	9 (0.02)
	136 (0.30)

The average daily limit cycle gas usage evaluated from tank temperatures and pressures is as follows:

$$\begin{aligned}\frac{\text{Average gas}}{\text{Day}} &= \frac{1.2 - 0.30}{135} = \frac{0.0067 \text{ lbm}}{\text{Day}} \\ &= \frac{540 - 136}{135} = \frac{2.99 \text{ g}}{\text{Day}}\end{aligned}$$

The excellent correlation between predicted gas usage and actual usage up to launch plus 305 is illustrated in Fig. 43.

On Sept. 4, 1974 (L + 305) a particle induced a roll axis star loss. During the reacquisition the gyros structural interaction occurred and resulted in the loss of 272 g (0.6 lbm) of gas. Another star loss and reacquisition occurred on Sept. 9, 1974 (L + 310) and resulted in the loss of another 113.4 g (0.25 lbm) of gas. Fortunately, no further star losses occurred until after the Mercury II encounter.

d. Mercury II to Mercury III attitude control modes. After Mercury II encounter, the hazard of a roll axis star loss and the large amount of gas required for reacquisition was being pondered versus going into the untried roll drift mode. In the roll drift mode, roll axis torque must be reduced to very small values to minimize roll spin-up and large gas usage (through the product of inertia terms) in the pitch and yaw axes. Additionally, pitch and yaw torques must be kept small to keep their usage small.

On Oct. 6, 1974 (L + 336) another roll axis Canopus loss occurred and initial acquisition attempts failed after the use of about 118 g (0.26 lb) of gas. At this point it was decided that Mercury III was only possible in the roll drift mode. After about two days of very high usage, searching for an acceptable spacecraft torque configuration, it was determined that positioning the HGA boresight at 45 deg cone and about 30 deg clock should produce a very low torque in all axes. For small changes around this point, the pitch, yaw and roll torques were nearly decoupled. Clock angle changes in HGA boresight controlled roll torque, cone angle changes controlled pitch torque and yaw torques could be controlled by differentially tilting the solar panels. The polarities of these control torque changes are illustrated in Fig. 42.

On the outgoing leg of the Mercury II to Mercury III transient phase, the average gas usage was about 1.4 g (0.003 lbm) per day and the average usage on the incoming leg was about 1.8 g (0.004 lbm) per day.

For short periods, limit cycle evaluation indicated gas usage as low as 0.23 g/day (0.0005 lbm/day) and some as high as 4.5 g (0.010 lbm/day). During this period spacecraft tracking was only four to six hours per day, three to four days per week. Had there been continuous tracking and a larger support team, the limit cycle usage could easily have been reduced to 0.45 to 0.90 g/day (0.001 to 0.002 lbm/day).

e. Analysis methods used during the extended mission. Analysis during the Mercury I to Mercury III period was principally confined to

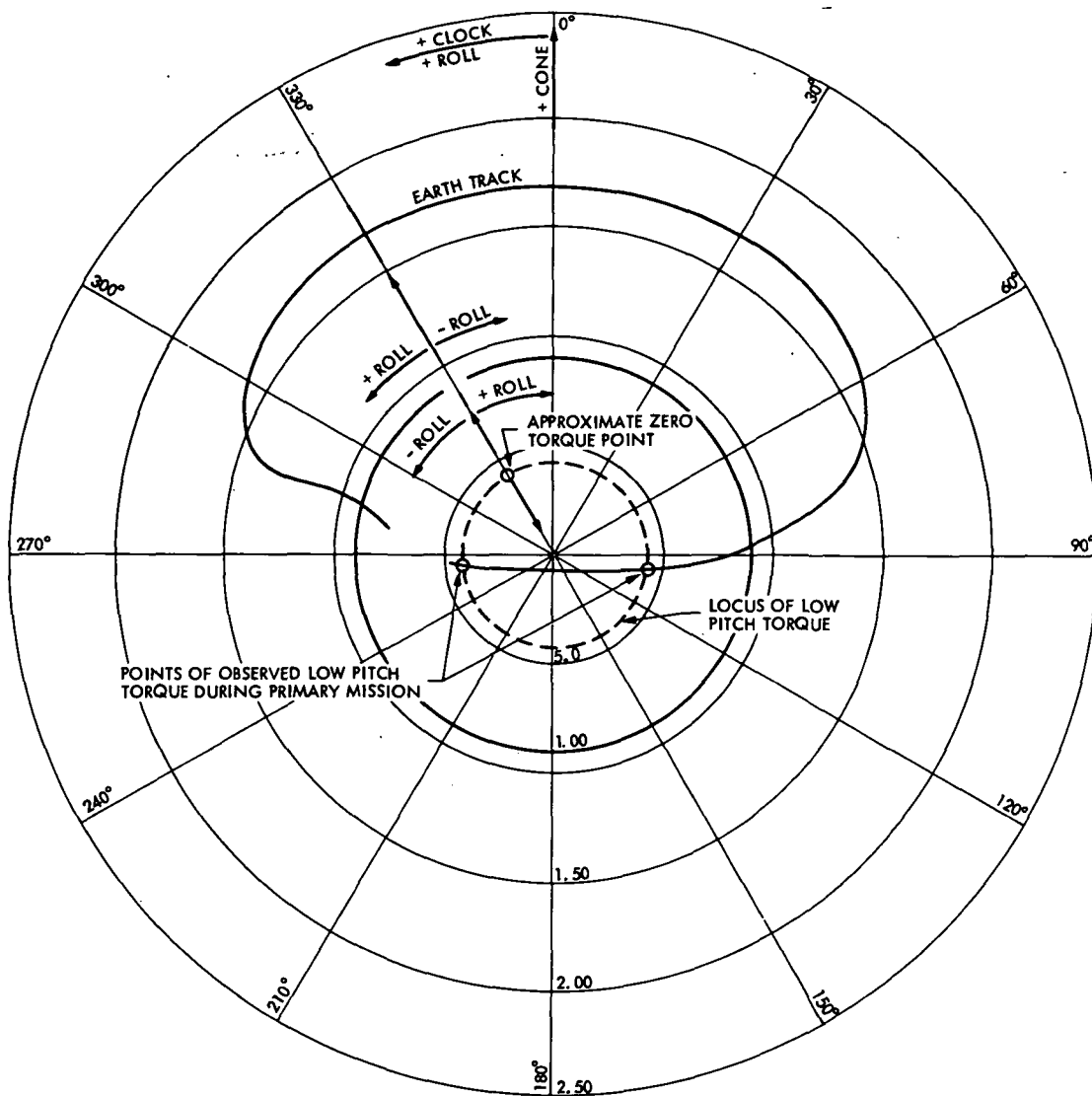


Figure 42. Earth track and HGA torque versus clock and cone angles

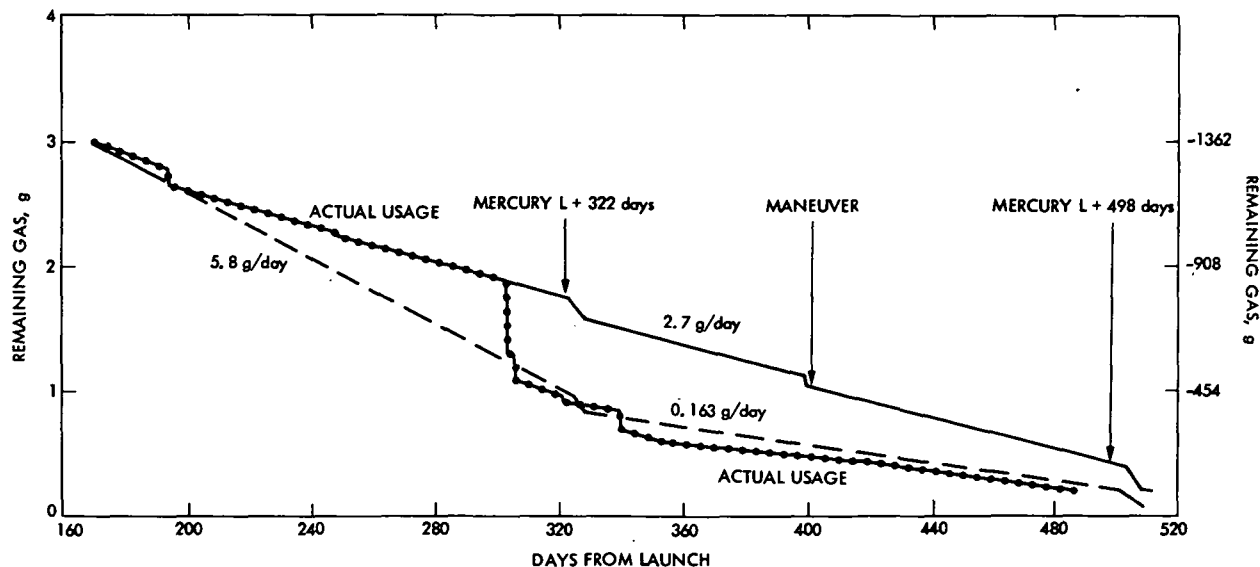


Figure 43. Extended mission gas predicts and actual usage

evaluating attitude control gas usage from limit cycle data, and revealed some startling facts about the effect of external spacecraft torques on gas usage.

(1) Daily gas usage evaluation from limit cycle data. Each axis controlled with reference to a specified celestial or inertial position produces a position versus time history (limit cycle) which will have a signature similar to one of the three signatures illustrated in Fig. 44.

Figure 45a illustrates a torque-free limit cycle; Fig. 44b illustrates a one-sided limit cycle due to a large torque; and Fig. 44c illustrates a limit cycle with a torque too small for a consistent one-sided limit cycle.

The gas used in the torque-free limit cycle case can be evaluated with the aid of Fig. 44a with the following expression:

$$\text{Gas (lbm)} = \frac{2 \cdot \text{WD} \cdot \theta_{\text{dB}}}{\alpha} \sum_{i=1}^n \frac{1}{\Delta t_i}$$

Gas = gas used in time interval Δt , lbm

θ_{dB} = width of position deadband (rad)

WD = gas value flow rate to produce angular acceleration α in lbm/s

α = gas system angular acceleration at gas flow rate WD, in rad/sec²

Δt_i = time to cross deadband, s

The gas used in the one-sided limit cycle case can be evaluated once the disturbance torque is known. The disturbance torque is determined with reasonable accuracy by averaging a series of single-point torque evaluations as follows:

$$\text{Tor} = \frac{8J}{M} \sum_{i=1}^M \frac{\Delta \theta_i}{\Delta t_i^2}$$

Tor = average torque, in ft-lbf

J = inertia in slug-ft²

M = number of samples

$\Delta \theta_i$ = height of position excursion, in rad

Δt_i = time between gas jet firings as illustrated in Fig. 44(b)

The gas used in one-sided limit cycle is evaluated with the following expression:

$$\text{Gas (lb)} = \frac{\text{Tor} (t_{\text{ST}} - t_{\text{SP}}) \text{WD}}{J\alpha} \quad (1)$$

$$(t_{\text{ST}} - t_{\text{SP}}) = \text{time interval of gas evaluation, s} \quad (2)$$

$$J \cdot \alpha = \text{gas jet torque in ft-lb} \quad (3)$$

The gas used in the small torque limit cycle case illustrated in Fig. 44(c) uses the Eqs. (1), (2), and (3) developed above as follows:

$$\text{Gas (lbm)} = \left[\frac{2\theta_{\text{DB}}}{\alpha} \cdot \sum_{i=1}^N \frac{1}{\Delta t_i} + \frac{\text{Tor} \sum_{K=1}^P t_K}{J\alpha} \right] \text{WD}$$

$$\sum_{K=1}^P t_K = \text{total one-sided limit cycle time, s}$$

The above expressions enabled rapid, accurate evaluation of each axes' gas usage without the tedious evaluation of individual rate increments.

(2) Gas usage versus disturbance torque. During the extended mission, the disturbance torque in each axis was adjusted using the solar panels and HGA. In the initial torque adjustment period, critical torque levels were sought. Critical torque and a torque-free limit cycle are illustrated in the phase plane in Fig. 45(a). Gas usage for a critical torque limit cycle is ideally 1/4 that of torque-free limit cycle.

Gas usage versus the ratio of observed torque to critical torque is plotted in Fig. 45(b). Also plotted in Fig. 45(b) is the actual Mariner 10 observed gas usage relative to the ratio of observed to critical torques. It was observed that a critical torque limit cycle could not exist under actual conditions, and guaranteed one-sided limit cycle did not exist until the disturbance torque was about three times critical torque levels. However, minimum gas usage was recorded at a disturbance torque slightly less than twice critical torque values. In addition, using derived rate and apparently subject to a small amount of noise, the torque-free limit cycle consumption was about 1.5 times the ideal value, and this state was observed only during periods when no electrical coupling could be detected.

f. Insights into roll gyro-structural interaction. During the primary mission the roll axis gyro structural interaction resulted in the consumption of about 680 g (1.5 lbm) of gas and about 390 g (0.85 lbm) just prior to Mercury II encounter. Analysis and simulation determined the frequency of the disturbance to be 3.6 Hz, but little was determined about the mechanism of exciting this roll gyro-structural resonant frequency.

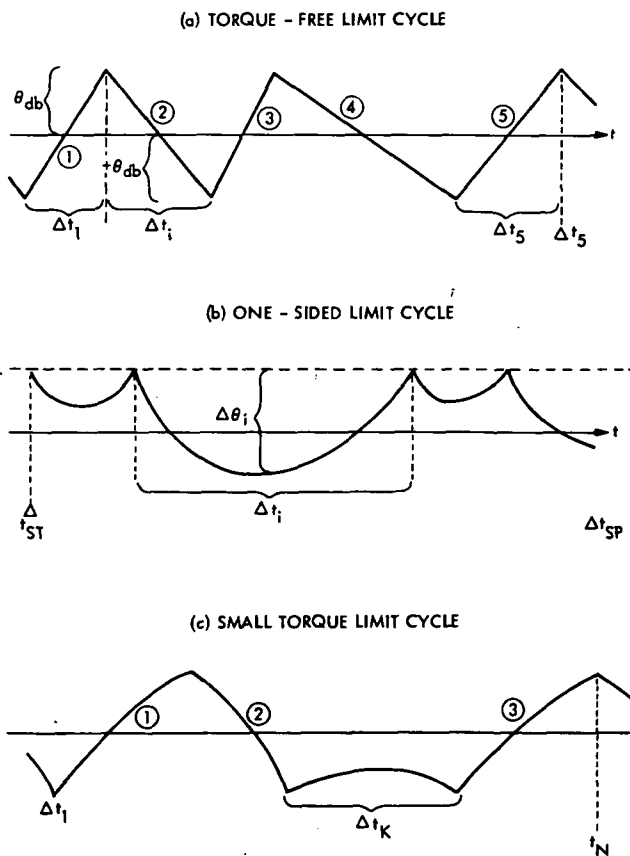


Figure 44. Limit cycle torques

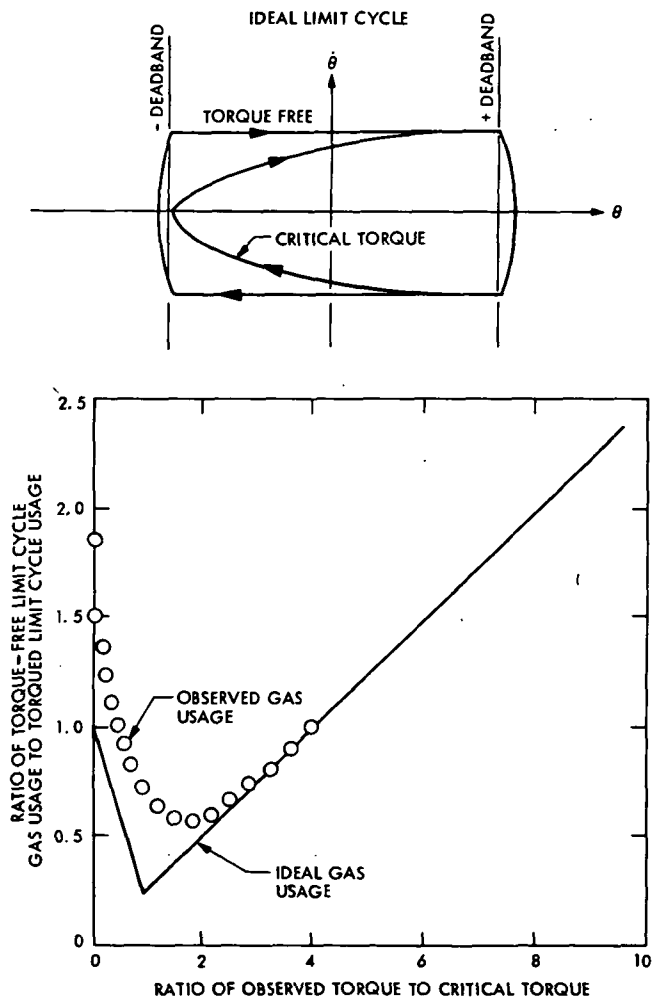


Figure 45. Limit cycle and torque versus gas consumption

It was discovered that while operating with the gyros on, a variable frequency of gas jet pulsing resulted as the spacecraft state moved up and down the combined rate plus position switching line. The time between gas jet pulsing can be calculated subject to the following assumptions illustrated in the phase plane in Fig. 46:

- (1) The gas jet rate increment $\Delta\dot{\theta}$ is about constant.
- (2) The rate plus position switching line is a straight line in the phase plane expressed as:

$$\left(\frac{\theta_{pb}}{\theta_{db}} \right) = C$$

θ_{pb} = position deadband

θ_{db} = rate deadband

Figure 47 illustrates the time between gas jet pulses versus spacecraft rate in the roll inertial mode, and Fig. 48 illustrates the time between gas jet pulses in the celestial plus gyro rate mode. It was concluded that this model explained all occurrences of gyro structural interaction and that if spacecraft roll rate has kept below 150 $\mu\text{rad/s}$, there was little danger of exciting the roll axis gyro structural interaction.

This policy was enforced during the Mercury II to Mercury III period and no incidents of the interaction were observed.

2. Roll Drift. The period of roll drift mode for attitude-control gas conservation extended from 04:30 GMT on Oct. 6, 1974 until 05:00 GMT on March 15, 1975. This was a total of 160 days using solar pressure for spacecraft attitude-roll control which was interrupted for small periods of all axis inertial control during TCMs 6, 7, and 8. The average attitude-gas consumption during this period was 1.6 g/day (3.5 mlbm per day).

The attitude-gas conservation problem became more complex in the roll drift mode. Because of large inertia cross-products, especially in the roll axis to pitch axis, a low value for the roll rate had to be maintained. The solar panels directly controlled yaw solar torque; so for best performance in yaw only two solutions were available around a mean position, dictated by power considerations. These two positions were as follows:

- (1) +X panel at the greatest pitch angle and the -X panel at a position for producing between 50 and 100 dyne-cm negative yaw torque, positive roll torque for panel angles less than 45 deg and negative roll torque for panel angles greater than 45 deg.
- (2) -X panel at the greatest pitch angle with a similar opposite torque affect.

The HGA was found to control pitch adequately at a cone angle of 45 to 50 deg with the variance due to solar intensity changes. With these constraints for attitude-gas conservation, the roll drift torque had to be controlled primarily with the HGA clock angle torque component. Another factor concerning the roll drift modes was the navigation team request for knowledge of the roll position of the spacecraft for doppler data modification for orbit determination. This constraint required a negative roll direction above a certain rate dictated by DSN tracking, because the star tracker must have a negative sweep to track a star across its field of view. Even with these many constraints, the roll drift mode of attitude-control operation was successful and made a third encounter with Mercury a reality.

During the roll drift mode the longest time period between two articulation and pointing subsystem configurations was 23 days with an average rate of .340 $\mu\text{rad/s}$ and an average negative rate increase of 8 $\mu\text{rad/s}$ each day. The average period was more than 3 days between configuration changes. The minimum gas consumption for a 10-day period was less than 6.8 g (0.015 lbm).

The major problem with the operational aspects of this control mode is the DSN tracking required. After a configuration change a minimum period of 20 hours of continuous spacecraft tracking was necessary to see the new torque level in the roll direction. Probably an optimum spacecraft tracking schedule for this mode should have been two 24-hour continuous coverage periods per week which may have reduced the configuration change frequency to one change every 8 to 12 days.

3. Trajectory Correction Maneuvers (TCM's). Five TCM's were completed during the MVM Extended Mission. These maneuvers varied considerably in procedure and scope especially during the later mission phases. Desired parametric values for these TCM's are shown in Table 5. For each TCM, a priori 3-sigma uncertainty pointing errors were calculated, based upon an analysis of spacecraft hardware error sources. Similarly, a posteriori estimates of the pointing errors associated with each TCM were determined, using spacecraft engineering telemetry data. Table 6 consists of a summary of the results of these analyses.

A description of the operational procedure used in each TCM is given in the remainder of this section. TCM 4 was divided into two parts, 4A and 4B, because of thermal constraints on the jet vane actuator potentiometers. The engine burn duration of 195.014 sec for TCM 4A preceded by a negative roll turn of 181.431 deg and a positive pitch turn of 25.607 deg was initiated at 20:05 GMT on May 9, 1974. The burn stop was followed by a normal celestial acquisition with a gyro power inhibit to prevent attitude gas loss due to gyro oscillation. TCM 4B was accomplished in a similar manner using an engine burn duration of 139.014 s initiated at 20:06 GMT on May 10, 1974. This engine burn was preceded by a negative roll turn of 178.481 deg and a positive pitch turn of 36.028 deg with a

Table 5. Summary of Extended Mission TCM parameters

TCM No.	Date	Commanded ΔV , s	Commanded	
			Roll turn, deg	Pitch turn, deg
4A	May 9, 1974	49.998	-181.431	25.607
4B	May 10, 1974	27.554	-178.481	36.028
5	July 2, 1974	3.321	56.100	57.828
6	Oct. 30, 1974	14.543	-100.800	86.344
7	Feb. 13, 1975	2.021	-21.364	114.494
8	Mar. 7, 1975	0.483	a	a
^a Not applicable; sunline (no turn) maneuver.				

normal acquisition after the engine burn completion.

TCM 5 was accomplished using the normal procedure with a burn duration of 18.8 sec initiated at 19:55 GMT on July 2, 1974. The spacecraft turns for thrust vector pointing were a positive roll turn of 56.100 deg and a positive pitch turn of 57.828 deg. This was the final TCM used before the second Mercury encounter.

Because of gyro oscillations during reacquisition sequences before the second Mercury encounter, the attitude-control gas was approaching a negative margin for a third encounter using a normal cruise attitude-gas conservation mode. A roll drift gas conservation mode was adopted upon the loss of Canopus acquisition on Oct. 6, 1974, with only 272 g (0.60 lbm) of attitude gas remaining in the tanks. This mode of operation changed the strategy for the remaining TCM's significantly.

TCM 6 was completed on Oct. 30, 1974, using the new operation strategy required by the roll drift mode. The negative roll turn of 100.8 deg was accomplished by timing a minimum duration (0.156 s) positive roll turn from the null center

of the last tracker Canopus crossing. The interval between the Canopus null crossing and the spacecraft inertial stop was calculated based upon the roll rate and roll acceleration determined by previous Canopus crossings. Four consecutive spacecraft revolutions were tracked before the last Canopus crossing which determined an average rate of $-197.56 \mu\text{rad/s}$ for the roll turn. This rate determined a roll turn interval of 8905 sec followed by a conventional positive pitch turn of 86.344 deg. The engine burn duration of 83.15 s was initiated at 21:53 GMT and was followed by a pitch unwind plus a return to the roll drift mode. Some roll turn error may have been introduced because of moving the solar panels during the roll drift turn.

TCM 7 used the same procedure as the previous maneuver. Limited spacecraft tracking due to the DSN reconfiguration for Viking created a situation where the roll rate had to be calculated based on one Canopus tracker star crossing. The roll turn magnitude of 21.47 deg dictated a reaction time of less than 10 min after the Canopus crossing to the first critical command. The TCM was originally planned for Feb. 12, 1975, but an unexpected early arrival of the Canopus crossing made a cancellation necessary. The TCM was

Table 6. Attitude control estimates of TCM pointing errors-TCM pointing error estimate (bias $\pm 3\sigma$ deg)

TCM No.	A Priori			A Posteriori		
	Pitch	Yaw	Resultant	Pitch	Yaw	Resultant
4A	0 ± 1.207	0 ± 1.313	0 ± 1.985	0.164 ± 1.303	0.176 ± 1.122	0.241 ± 1.720
4B	0 ± 1.482	0 ± 1.285	0 ± 1.962	0.426 ± 1.296	0.081 ± 1.147	0.434 ± 1.731
5	0 ± 1.373	0 ± 1.330	0 ± 1.789	0.074 ± 1.272	0.155 ± 1.220	0.172 ± 1.762
6	0 ± 1.597	0 ± 2.206	0 ± 2.723	-0.127 ± 1.593	0.194 ± 1.566	0.232 ± 2.234
7	0 ± 1.375	0 ± 1.855	0 ± 2.310	-0.198 ± 1.300	-0.106 ± 1.413	0.199 ± 1.920
8	0 ± 0.892	0 ± 0.891	0 ± 1.261	-0.086 ± 0.580	0.293 ± 0.579	0.305 ± 0.820

completed the next day, Feb. 13, using a negative roll drift turn of 21.364 deg at a roll rate of -161.0 μ rad/s and a positive pitch turn of 114.494 deg. The engine burn duration of 12.5 sec was initiated at 10:00 GMT followed by the return to the roll drift mode. The inaccuracy of the spacecraft thrust vector pointing during this maneuver caused an overcorrection in the orbit. The error was mainly created by the error in the roll turn which was caused by inadequate spacecraft tracking for roll rate determination.

TCM 8 was a sunline maneuver completed on March 7, 1975. Since this maneuver was initiated without any pitch turn, TCM 8 was not constrained by the roll drift attitude control mode. An engine burn duration of 3.2 sec preceded by all-axis inertial attitude mode targeted the spacecraft very close to the nominal aim point for TCM 7. During the last two TCMS, a slight instability in the autopilot control was noticed; but since these were short duration engine burns, no major effects were noticed.

With the exception of a general tendency shown by tracking-data-based orbit determination for roll turn error to be somewhat larger than expected from a priori statistical predictions (giving indication of an unidentified bias effect), no performance anomalies occurred in TCM attitude-control operations. Overall pointing accuracies achieved were considered to be adequate for attainment of all extended mission objectives.

4. Acquisitions. Although the normal cruise configuration of the spacecraft is Sun and Canopus acquired, it was necessary to cruise for an extended period (from Mercury II to Mercury III) in a non-Canopus acquired state (the modified roll drift/solar sailing mode) in order to achieve a level of attitude-control gas consumption that would ensure a Mercury III encounter. This section deals with the reacquisitions of Canopus during the extended mission.

On April 16, 1974, after the first tracking gap in the Mariner 10 mission, it was discovered that the FDS had suffered an analog-to-digital converter failure that resulted in the loss of nearly half of the engineering analog telemetry. Some of the measurements had been redundantly input to the other ADC, but the primary measurement used for star acquisitions was not; the function of Canopus intensity had been lost. In addition, the tracker cone angle position and adaptive gate telemetry was also lost. Recognition of the star acquired now depended upon a priori knowledge of the approximate roll position of the spacecraft, keeping track of the last commanded cone angle and adaptive gate settings, and, as a final confirmation, the received signal strength from the high-gain or low-gain antenna. Telemetry on the pointing direction of the high-gain antenna had also been irretrievably lost, but the high-gain antenna calibrations performed during the primary mission coupled with the position command capability of the Articulation and Pointing Subsystem were sufficient to point the high-gain antenna to any desired position.

The first loss of Canopus acquisition was deliberate; on April 26, 1974 a gyro test was performed to evaluate the possibility of the roll

axis structural interaction occurring in the spacecraft configuration proposed for TCM 4. The gyros were enabled with DC-19, turned on with 7M1, and two DC 18 commands were sent to roll the spacecraft +4 deg. DC 19 then allowed the spacecraft to roll search back to Canopus. Canopus was acquired normally, and the gyros automatically turned off after acquisition. Command DC 40 was then sent to prevent a roll search in the event of accidental loss of Canopus acquisition.

TCM 4 was split into two parts due to temperature constraints on the TVCA. TCM 4A was performed on May 9, 1974 and TCM 4B on May 10. Both maneuvers involved loss of Canopus acquisition; TCM 4A was a -181.19 deg roll turn, TCM 4B a -178.14 deg roll turn. In each case, the roll unwind turn was 4.98 deg longer than the roll turn, to allow acquisition of Canopus without a roll search. The reacquisitions after the unwind turns were normal.

It was necessary to periodically update the tracker cone angle position, as the cone angle of Canopus varied with spacecraft position in the heliocentric orbit. Updating was invariably done by programming the CC&S to issue the required number of 7D commands at the proper time. Throughout both the primary and extended missions, the cone angle updating was completely routine; no anomalies associated with an update were ever observed.

The next reacquisition of Canopus occurred on June 24, 1974 when a gyro test similar to that performed on April 26 indicated that no roll axis oscillation would be expected to occur in the TCM 5 spacecraft configuration. Canopus acquisition after the +4 deg roll turn produced by the two DC 18 commands.

TCM 5 was performed on July 2, 1974. The roll turn was +56.1 deg; the roll unwind resulted in normal reacquisition of Canopus.

From time to time during this Mercury I to Mercury II cruise, flyback and sweep sequences had been observed in the tracker roll error signal. Since the intensity telemetry was no longer available, there was no method of deducing the severity of the disturbances other than by the number of flyback and sweep sequences observed at each disturbance. The bright particles that were apparently causing the temporary loss of acquisition, followed by the flyback and sweep sequences, were expected to increase in intensity and frequency as the spacecraft heliocentric range decreased. The standard cruise mode was modified by utilizing DC 40, the unconditional gyros off command, to prevent a roll search in the event loss of Canopus acquisition did occur, thus preventing the roll axis structural oscillation that could possibly occur during the roll search. However, on Sept. 4, 1974, a stream of bright particles caused loss of Canopus acquisition, and reacquisition did not occur on the flyback and sweep.

The attitude-control subsystem is mechanized such that when a negative roll gas jet valve has commanded ON for 30 seconds, roll axis control is removed. When the flyback and sweep sequence failed to reacquire Canopus, the Canopus tracker field-of-view moved to the roll search

position, causing the negative roll gas jet valve to fire, accelerating the spacecraft in the (negative) roll search direction. With the gyros inhibited from coming on upon loss of acquisition, only the 30-second roll search inhibit prevented the spacecraft from spinning uncontrollably.

With Canopus not acquired, with the roll axis uncontrolled, and with the spacecraft spinning in roll, the ground station acquired the signal every time the high-gain pattern swept across the Earth. About one to two minutes of data were available before the station lost lock. Transmission over the low gain antenna at 33-1/3 bits/s was attempted, but the signal strength was too low for good data reception, so the spacecraft transmitter was switched back to the high-gain antenna, at 2450 bits/s engineering. This "lighthouse" data mode was sufficient to obtain all the data needed to assess the state of the spacecraft. The spacecraft roll rate was measured by timing the Canopus crossings (i. e., the times between zero roll error readings on the roll error signal as the tracker acquired Canopus each time the spacecraft rolled through zero clock angle; with roll axis control removed, the roll error signal was not enabled to the attitude control, so that spacecraft acquisition of Canopus could not occur). The spacecraft roll rate was -0.47 deg/s (-8.2 mrad/s). Since 30 s of acceleration would result in a rate of -0.75 deg/s (-13 mrad/s), the bright particles had most likely caused the tracker to lose acquisition at a spacecraft rate of +0.28 deg/s (+4.8 mrad/s) after tracking the particle(s). After about six hours of observing the spacecraft, a DC 19 ground command was sent to enable the gyros to come on and reduce the roll rate to dead-band values, followed by a DC 21 to reset the roll search inhibit and start a roll search to Canopus. The commands were timed to occur such that the roll axis control would be enabled 6 deg before Canopus entered the field of view of the tracker, so that acquisition would be immediate and the gyros would be on for a minimum amount of time; thus, if the roll axis oscillation occurred during the search, the amount of attitude-control gas expended would be minimized. The commands were received properly by the spacecraft at the correct time, but acquisition of Canopus did not occur, and the spacecraft executed a 360-deg roll search, acquiring Canopus approximately 24 min later. The roll axis oscillation was present during the search, and approximately 250 g (0.55 lbm) of the remaining attitude-control gas supply was used.

The reason for the failure to acquire Canopus on the initial opportunity may be one of two reasons: (1) the gyros did not come up to speed as quickly as expected (the gyro scale factor is directly proportional to gyro wheel speed) so that when the DC 21 command was received, the resultant spacecraft rate was too high to allow acquisition; (2) the spacing between the DC 19 and DC 21 commands was too small, such that the same effect was achieved—the gyro scale factor resulted in a spacecraft rate high enough to prevent acquisition. The corrective action for future incidents of this type is to turn on the gyros earlier in relative time, separate the DC 19 and DC 21 commands by 90 to 120 s, and take the risk of using more than the minimum amount of attitude-control gas required to acquire the star with the roll axis oscillation present.

The reason for the occurrence of the roll axis oscillation during the search was also not clear; it was felt that the spacecraft configuration had a bearing on the presence or absence of the oscillation, but the configuration at the time the gyros were enabled was very close to the TCM 4A configuration (the high-gain antenna was different by a few degrees in boom and dish).

Two days later, on September 6, an identical incident occurred. A bright particle, or a stream of bright particles, caused loss of acquisition, with a resultant spacecraft roll rate of -0.19 deg/s (-3.3 mrad/s). This time, the spacecraft was placed in the exact configuration used for TCM 4A, and the DC 19/DC 21 command pair separated by 90 s. Canopus was acquired immediately, but the roll axis oscillation was present, resulting in attitude-control gas usage of approximately 77 g (0.17 lbm).

Not all of the attitude-control gas used was used by the roll axis oscillation. During the Sept. 4th incident, the spacecraft roll rate, coupling through the products of inertia into the pitch and yaw axes, caused attitude-control operation at the edge of the deadband, resulting in gas usage rate of 10 g/h (0.022 lbm/h) for a total gas usage of 50 g (0.110 lbm); the roll axis oscillation used 193 g (0.425 lbm), and the rate reduction process used 2.6 g (0.0057 lbm). For the Sept. 6 incident, the scan platform was positioned to minimize the products of inertia; with the much smaller roll rate resulting after the loss of acquisition, the gas usage rate was 2.7 g (0.006 lbm/h) for a total of 0.120 lb; the roll axis oscillation used 18 g (0.040 lb), the rate reduction 2.6 g (0.0057 lbm).

Although bright particles continued to be observed in the roll limit cycle, no further losses of Canopus acquisition occurred through the time of the Mercury II encounter, on Sept. 21, 1974. The encounter attitude-control mode was the cruise mode: Canopus acquired, gyros off and inhibited from coming on with command DC 40.

After the encounter, the cruise plan was to forego cruise science data and use the high-gain antenna to generate torques from solar radiation pressure to minimize gas consumption in the pitch, yaw, and roll axes. The solar panels had been used during the Mercury I to Mercury II cruise to generate torques in the roll axis, but torques in the other two axes could not be controlled by the panels alone. It was felt that only this cruise mode would allow the attitude-control gas usage to be minimized enough to have enough gas left for the last encounter. Therefore, immediately after the encounter, the spacecraft was placed in the 33-1/3 bits/s engineering only data mode, and a series of empirical determinations of the position of the high-gain antenna positions that would produce the desired torques in the pitch and yaw axes was begun. After this calibration had been completed, roll axis control would be removed, and the spacecraft allowed to drift in roll, with the proper torques maintained in the pitch and yaw axes. This would reduce roll axis gas usage to zero and minimize gas usage in pitch and yaw.

Since tracking was not continuous, and since torque analysis of limit cycle behavior took an

appreciable amount of data, the calibration period was estimated to be a few weeks. However, on Oct. 5, 1974, another bright particle incident caused loss of Canopus acquisition, with a resulting roll rate of $+0.32 \text{ deg/s}$ ($+5.6 \text{ mrad/s}$). The fact that the roll rate was positive indicated that this was the most severe particle incident to date. After attempting to evaluate the data at $8\text{-}1/3$ and $33\text{-}1/3 \text{ bits/s}$ over the low-gain antenna, it was decided to move the high-gain antenna from its solar sailing torque generating position to the Earth-pointing direction, in order to go to the lighthouse data mode to assess the state of the spacecraft, confirm the positive roll direction, and measure the rate. After this was accomplished, an attempt was made to acquire Canopus without turning on the gyros by resetting the roll search inhibit when Canopus was in the field of view of the tracker. The command was timed such that the spacecraft rate would be reduced to zero when the spacecraft clock angle was very near zero; this should result in acquisition. Data was available when the command was received, but there was no indication of acquisition. The failure to acquire meant that the negative roll gas jets would be on for thirty seconds, resulting in a spacecraft rate of -0.45 deg/s (-7.9 mrad/s).

At this time, it was decided not to attempt further to acquire Canopus, but to reduce the roll rate to deadband values by turning on the gyros for 3.5 min. This action would place the spacecraft in the backup gas conservation mode—uncontrolled in roll, with torques generated as a function of high-gain antenna position and solar panel position in all three axes. This mode had been studied, but enough empirical data on the positions of the high-gain antenna had not been obtained to be able to predict what torques would be generated. However, for long-term cruise, there appeared to be no alternative; if bright particle incidents were going to occur periodically, some method of negating them was required. Accordingly, the gyros were turned on for the minimum amount of time possible (3.5 min) and then turned off. The high-gain antenna was returned to the only known torque configuration established, and the data rate returned to $8\text{-}1/3 \text{ bits/s}$.

During the next few weeks, it became clear that the best use for the torque generating capability of the high-gain antenna was to control pitch torques. The criticality of the pitch torque was that the pitch axis control was now the largest user of gas. Yaw and roll torques were affected by the high gain, and the solar panels were used to trim these torques.

TCM 6 was performed on Oct. 30, 1974; a -100.80 deg roll turn was required. The roll turn was accomplished by turning on the gyros and placing the spacecraft in the all-axis inertial state after the spacecraft had rolled the required amount past Canopus, as determined by the time and rate observed when the Canopus crossing occurred. After the maneuver, the spacecraft was returned to the roll drift mode.

During the cruise period, the roll rate was determined by observing the acquisitions of Canopus (and whatever other stars were acquirable by the tracker) as the spacecraft rolled through the clock angle of the star. With roll

axis control removed, the tracker was able to electronically acquire and track the star without effect on the spacecraft. The high-gain antenna and solar panels were then adjusted to produce the required amount and polarity of roll torque, while maintaining the required amount and polarity of pitch and yaw torques.

TCM 7 was performed on Feb. 13, 1975. It had originally been scheduled for Feb. 12, but was aborted when the Canopus crossing occurred approximately 20 min earlier than expected. The roll rate had been reduced to about a nine-hour period, so that the spacecraft rate when the gyros were turned on would not be high enough to excite the roll axis structural interaction. As a consequence, Canopus crossings did not fit the tracking schedule, and enough information was not available to accurately predict position, rate, and acceleration in the roll axis. The maneuver implementation sequence was modified so that the maneuver could proceed immediately upon detecting a Canopus crossing, and the maneuver then rescheduled for the next day. The roll turn required was -21.47 deg ; the turn was accomplished in the same manner as the TCM 6 turn, with the exception being that the Canopus tracker had to be turned off prior to turning on the gyros (because the roll search inhibit had been set prior to TCM 6, but the loss of Sun gate during the TCM 6 pitch turn had reset it). Again, after the maneuver, the spacecraft was returned to the roll drift state.

The final maneuver prior to Mercury III, TCM 8, was performed on March 7, 1975. This maneuver was a sunline maneuver; no roll or pitch turns were required. Accordingly, the spacecraft was simply stopped in roll by turning on the gyros and placing the spacecraft in the all-axis inertial state, and executing the engine burn. Again the spacecraft was returned to the roll drift mode.

One more Canopus acquisition was required for Mariner 10. The Mercury III encounter sequence required the spacecraft to be Sun- and Canopus-acquired in order to return high-rate science data over the high-gain antenna. The method of acquisition proposed was to slow the spacecraft rate to a value that would permit the acquisition commands to reach the spacecraft while Canopus was still in the field of view, when the acquisition commands were sent when Canopus entered the field of view. A sequence was devised that would place the spacecraft in a safe state even if the acquisition commands were late, and Canopus had passed through the field of view. The direction of roll could then be reversed, the spacecraft "backed up" beyond Canopus, and the process repeated until acquisition had occurred.

The first opportunity for acquisition was predicted to occur during a tracking gap on March 12, 1975. Although the spacecraft roll period was approximately 24 h, an attempt was made to slow the rate even further, so that the Canopus crossing would occur after the tracking gap (which was about three hours in length). However, the station had trouble in acquiring the spacecraft after the gap, and no Canopus crossing was evident. Determination of the roll rate and position was complicated by the fact that no other stars were acquirable by the tracker in the encounter cone

angle setting, and by the fact that there were two sizable low-gain antenna nulls, causing loss of data for nearly 180 deg of the 360 deg of roll. Real-time plotting of the low-gain antenna transmitted received signal strength gave an approximation of spacecraft position, as well as knowledge of the position of the nulls.

The first attempt at acquisition was made on March 13, 1975. However, the command arrived at the spacecraft after the spacecraft had passed through Canopus, and the tracker had lost acquisition. The Flight Data Subsystem was reprogrammed to increase the number of tracker roll position samplings, and the polarity of the roll torque reversed. The spacecraft was then placed in the roll drift mode, and backed up across the star. After about an hour and a half, several flyback and sweep sequences were noted in the roll position measurement. This was taken to mean that Canopus had been passed through (rolling in the positive direction will not produce an acquisition until the star is at the edge of the field of view; the acquisition will be immediately followed by a loss of acquisition, producing a flyback and sweep). The spacecraft was then stopped, the direction of the roll torque again reversed to produce a negative roll, and returned to the roll drift mode.

Astoundingly, Canopus was not acquired, and the spacecraft continued rolling into a low-gain antenna null, resulting in the loss of telemetry data. The only possible reason for not crossing Canopus was that the spacecraft had not been rolled far enough in the positive direction to cross the star, which meant that the flyback and sweep sequences observed were not Canopus, but a bright particle incident. The occurrence of this incident at this particular time was disastrous; had it not occurred, Canopus would have almost surely been acquired.

Although the telemetry was lost in the low-gain antenna null, it was still possible to command the spacecraft. Therefore, the spacecraft was stopped once again, the polarity of the roll torque changed to produce a positive roll, and the spacecraft returned to the roll drift mode to back out of the null. After several hours of backing up, it appeared the spacecraft had reached the other low-gain antenna null, about 140 deg from Canopus. The spacecraft was stopped, and the Earth-pointing direction of the high-gain antenna calculated. The high-gain antenna was then pointed toward the Earth, and spacecraft transmission over the high gain commanded. Receipt of the signal then gave a positive confirmation of spacecraft position. The solar panels were then differentially tilted to give the maximum amount of negative torque (since leaving the high-gain antenna in the near-Earth pointing direction produced a positive roll torque) and the spacecraft allowed to roll drift to Canopus. The high-gain antenna was positioned such that it would point toward Earth 40 deg prior to Canopus and the spacecraft was allowed to drift to a position 7.5 deg from Canopus where it was stopped, then allowed to roll toward Canopus. With the high-gain antenna pattern being tracked in real time and the spacecraft rate deduced from the pattern,

a time was determined to send the acquisition commands. Canopus was acquired at a net roll error of -1.5 deg. The spacecraft was placed in the roll axis inertial mode after the roll error had been updated to about +0.20 deg to provide an inertial reference. The use of the roll axis inertial mode guaranteed that no bright particle incidents would cause loss of acquisition for the encounter.

The acquisition of Canopus occurred on March 15, 1975 about 30 h before closest approach at Mercury III. One far-encounter mosaic sequence was lost, due to not acquiring Canopus earlier, but the significant encounter sequences were now enabled. A routine was devised to update the inertial roll reference when needed (roll gyro drift was about -0.54 deg/h, requiring an update about once per day).

Attitude-control gas usage during the Mercury II to Mercury III cruise in the non-Canopus acquired state averaged about 0.59 g/day (0.0013 lbm/day) for attitude control, and about 0.45 g/day (0.001 lbm/day) of system leakage. Usage in the Mercury III encounter mode, roll axis inertial control, averaged about 0.45 g/h (0.001 lbm/h).

6. Post Mercury III. During the Mercury II to Mercury III transient phase, it was demonstrated that at certain spacecraft configurations very low torques existed in all axes. This implied that the spacecraft center of mass and center of pressure were linear. If the distance between the center of mass and center of pressure was sufficient and the center of pressure was behind the center of mass, a stable spacecraft Sun-oriented configuration should result without any active attitude control. Unfortunately, this principle could not be verified since an attempted derived rate acquisition from a cone angle of less than 1 deg resulted in consuming all the remaining attitude-control gas and imparted a large spacecraft pitch axis rate, causing the spacecraft to tumble.

C. Thermal control.

During the extended mission, the spacecraft was predominantly in a cruise mode. The major events of thermal significance were: (1) the two Mercury encounters and (2) the five trajectory midcourse maneuvers. Thermal control of the spacecraft was maintained by turning on the supplemental heaters as required. Also the solar panels were tilted as required for temperature and power considerations. During this period, the solar flux has cycled between 211.5 W/ft² (1.68 Suns) and 602.2 W/ft² (4.78 Suns). The total accumulated solar exposure through L+500 days was approximately 30,000 equivalent Sun hours (ESH). A plot of ESH versus time from launch is shown in Fig. 49

1. Mercury Encounters. The thermal performance of the spacecraft at the first, second, and third Mercury encounters can be compared, since the solar intensity is the same (4.61 Suns). Table 7 shows the data for Mercury I, II, and III. The data shows a significant increase in temperature with the exception of the TV optics.

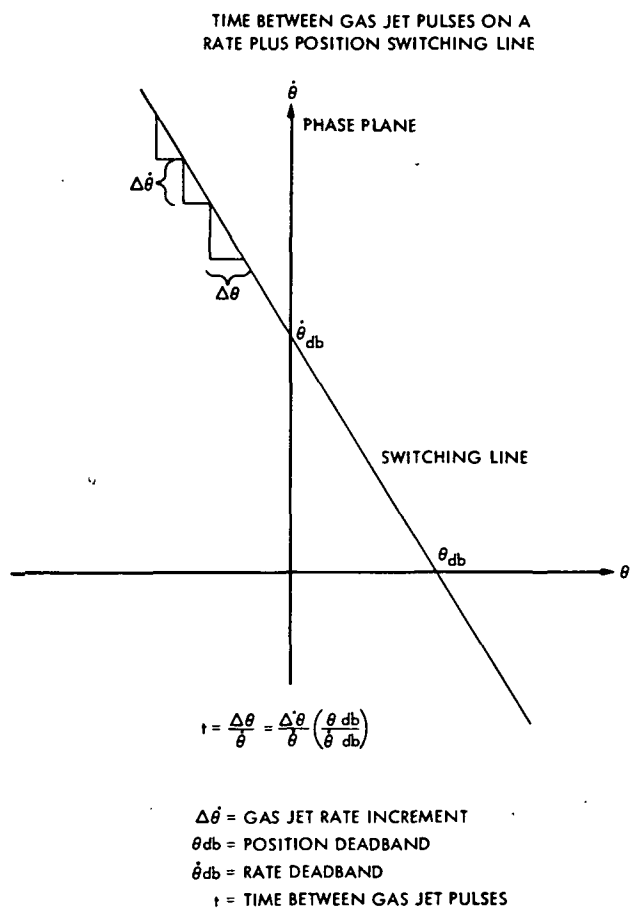


Figure 46. Gas Jet pulse rate

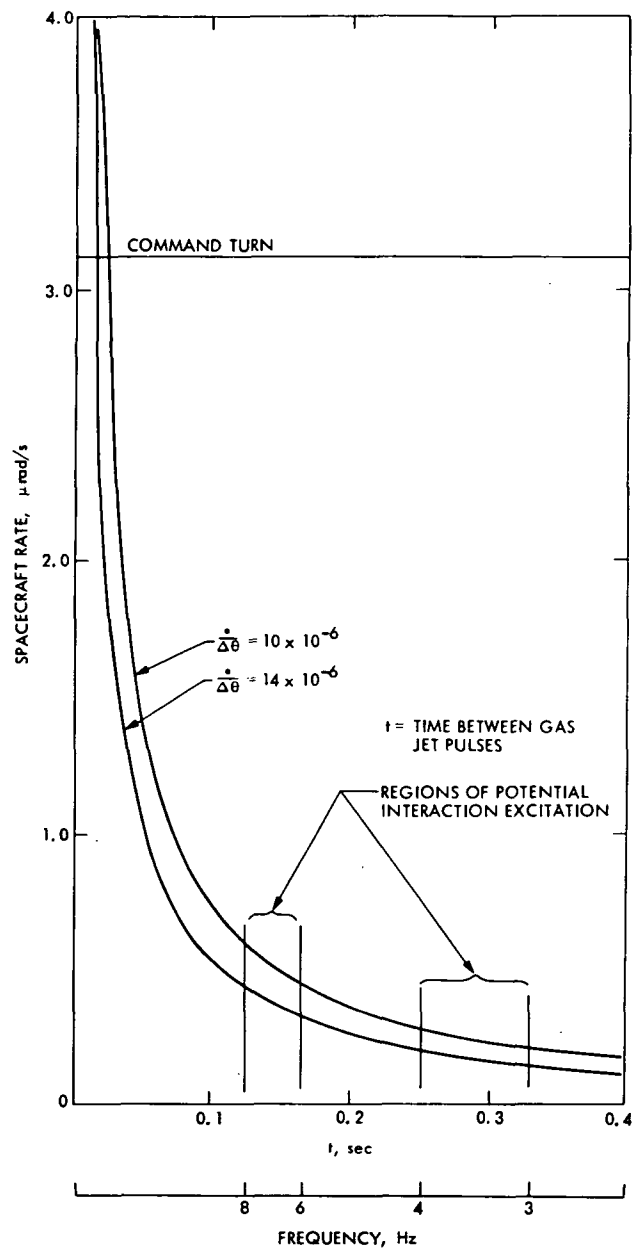


Figure 47. Roll axis gyro - structural interaction excitation - celestial (roll inertial)

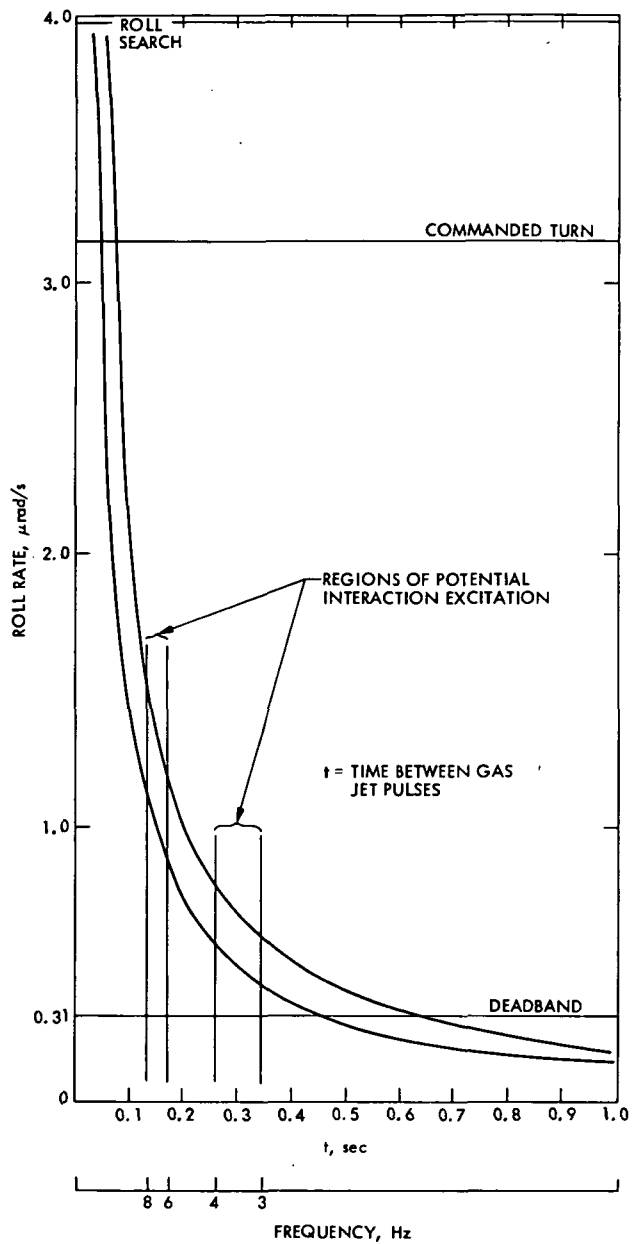


Figure 48. Roll axis gyro - structural interaction excitation - celestial (gyro rate)

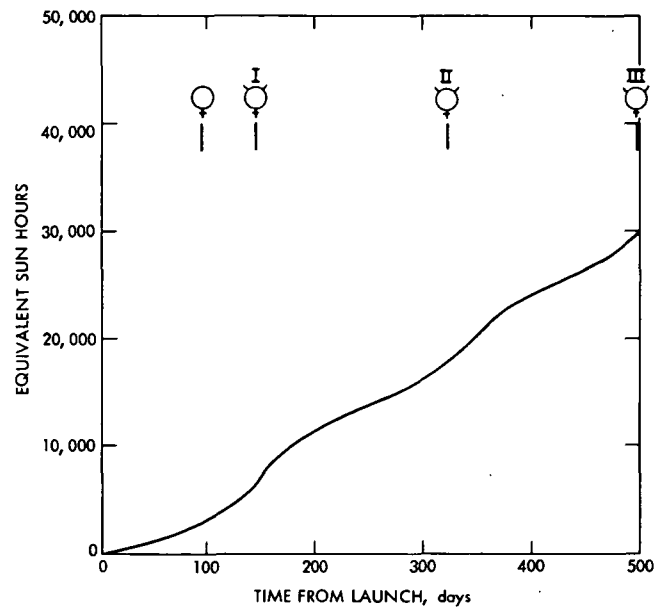


Figure 49. Equivalent Sun hours from launch

Table 7. Temperatures at Mercury I, II, and III

Mission and test computer channel No.	Temperature measurement description	I	II	III
		Temperature, °F		
065	Canopus tracker	40	58	65
066	Gyro control assembly	78	84	127
067	Sun sensor	105	116	119
068	+X/-Y N ₂	69	88	95
069	-X/+Y N ₂	74	a	a
070	Thrust vector control assembly	168	180	186
106	PSE electronics	86	a	a
107	PSE plat.	85	89	129
301	CPT charged particle telescope	38	45	51
408	Ultraviolet spectrometer airglow	51	a	a
409	Ultraviolet occultation	76	92	88
454	Propellant N ₂	86	a	a
455	Propellant	88	106	112
456	Valve	138	a	a
457	Thrustplate	140	151	155
500	IRR	85	96	102
602	Magnetometer A	-4	5	8
603	Magnetometer B	10	a	a
604	Magnetometer electronics	95	101	106
605	Magnetometer processor	97	a	a
663	Auxiliary oscillator	88	98	106
664	TWT 1	112	a	a
665	TWT 2	95	107	113
666	VCO	84	a	a
667	Dish 1	177	14	91
668	Dish 2	22	a	a
669	Dish 3	61	178	227
670	S/X Feed	222	a	a
671	X-band transmitter	74	a	a
750	Bay 1	69	115	122
751	Bay 2	69	a	a
752	Bay 3	72	85	92
753	Lower blanket	17	44	44
754	Bay 5	77	83	87
755	Bay 6	74	a	a
756	Bay 7	72	77	84
757	Sunshade	411	a	a
758	HGA boom	203	a	a
800	TVA optics F	42	0	
801	TVA optics R	49	a	a
802	TVA video	66	24	23
803	TVB optics F	42	a	a

^aTelemetry channels lost due to FDS-ADC 2 failures.

Table 7. (contd)

Mission and test computer channel No.	Temperature measurement description	I	II	III
		Temperature, °F		
804	TVB optics R	51	9	9
805	TVB vidicon	66	a	a
806	Auxiliary electronics	46	5	6
869	Battery	68	a	a
870	+X solar panel 1	126	129	115
871	+X solar panel 2	145	176	166
872	+X solar panel 3	194	214	210
873	+X solar panel 4	149	169	160
874	-X solar panel 1	128	a	a
875	-X solar panel 2	180	a	a
876	-X solar panel 3	155	a	a
877	-X solar panel 4	198	a	a

^aTelemetry channels lost due to FDS-ADC No. 2 failures.

The higher temperatures are the result of the thermal surface degradation of the Alzak and silvered Teflon surfaces. Of particular interest is the PSE platform temperature. It exceeded the upper temperature allowable limit at the third Mercury encounter. The TV optics temperatures were lower at the second and third encounters since the optics heaters were on at Mercury I and off at Mercury II and III. The power anomaly caused an increase in Bay 1 and 3 temperatures. It was necessary to tilt the solar panels to 71 deg at Mercury III. This was done so as not to exceed the upper allowable temperature limit.

2. Trajectory Correction Maneuvers. There were five trajectory correction maneuvers performed during the extended mission. The fourth TCM of the mission (first of the extended mission) was divided into two maneuvers, TCM 4a and TCM 4b. This was necessary for the long burn duration required for the maneuver. All of the thermal predictions made for the TCM's were based on previous MVM data and Edwards Test Station data. The soakback temperatures were generally lower than the predictions and no temperatures exceeded the upper allowables. Table 8 lists the TCMs with the solar intensity and burn duration. Plots of soakback temperatures for TCMs 4-8 are included in Ref. 4.

3. Thermal Control Staffing Requirements.

Thermal control responsibilities during the extended mission included: (1) monitoring and recording spacecraft temperatures on an almost daily basis, (2) providing temperature predicts for maneuvers and encounters, and (3) recommending changes to the supplemental heater power state as required to maintain adequate temperatures.

Plots of each telemetered temperature were generated and maintained throughout the mission. These plots are included in Refs. 3 and 4.

Table 8. Trajectory correction maneuvers

TCM	Solar intensity, Suns	Burn duration, sec
4a	2.85	195.014
4b	2.80	139.014
5	1.70	18.813
6	2.97	83.17
7	2.60	12.52
8	4.08	3.12

A constant staffing level of men was required throughout the extended mission to fulfill the responsibilities listed above. Additional support (~1 man) was occasionally required for very brief periods of time to support the maneuver and encounter periods.

This level of effort was considered adequate for the successful completion of the extended mission.

D. Data Control and Processing

1. Flight Data Subsystem. The FDS which collects all science and engineering data, encodes it for radio transmission and controls the science instruments processed all commands it received properly. It also issued all commands to the science instruments properly.

Unfortunately, however, at approximately 18:00 GMT on April 16, 1974, the FDS lost half of

its analog data collecting capacity due to a failure of analog-to-digital converter number two. This failure had no effect on the ability to transmit the data that could be collected. The failure caused the loss of all analog engineering measurements processed by that ADC. No digital measurements were affected. Eighty-nine active telemetry channels were lost. Of those 89, 17 were redundant to both ADC 1 and 2. For a more thorough discussion of this failure and its consequences, refer to Refs. 1 and 2.

To circumvent this failure as much as possible, the FDS was extensively reprogrammed to eliminate sampling of the lost measurements and to optimize information returned by the remaining measurements. After the DSS failure (refer to Sect. VI, D, b) reprogramming of the FDS became quite common, as it was often necessary to improve spacecraft team visibility of specific measurements during critical periods such as trajectory correction maneuvers.

The ability of the FDS to substitute one predetermined block of measurements for another block (block substitution) was also used to advantage several times during the mission. The possibility of an FDS power on reset (POR) in which the FDS reinitialized itself in response to transients in its power source was accounted for by backup data mode commands whenever gyro activity was planned; so the POR presented no problems during the extended mission.

a. End-of-Mission tests. This test consisted of exercising the major blocks of redundant hardware in the FDS. TMU number 2 was turned on in order to obtain more information relative to the failure of FDS-ADC number 2. Five separate tests were conducted, including switching power converters. Data analysis consisted of real-time verification of proper FDS responses. A detailed test sequence is presented in Ref. 12.

b. End-of-Mission test results. Proper FDS operation for each step was verified. The four internal voltages measured during operation of the redundant power converter (B) were the same levels as those for power converter A. The FDS clock error was measured over the 37-min interval of operation on oscillator B. This clock error, $+5.5$ Hz at 307°K (93°F), fell in line with prelaunch subsystem test data. The switch to TMU number 2 did not cure the failed ADC number 2. These test results can be summarized as "perfectly normal response."

2. Data Storage Subsystem (DSS). The DSS failed completely on Aug. 14, 1974. After much testing and investigation, it was determined that the failure was most likely due to a mechanical problem with the tape itself. Possibilities are that the tape is stuck to the head or that it came off its guides. For a thorough analysis of this failure, refer to Refs. 9 and 13. The net result of the failure was a serious reduction in the data-gathering ability of the spacecraft and a considerable simplification of sequence design exercises. Unfortunately, the most serious data losses occurred at the times of greatest need. For example, during a TCM, the high-gain antenna is

usually not Earth pointed and therefore engineering data was normally recorded by the DSS. Without the DSS, maneuvers were done essentially in the blind.

The simplification of sequence design was quite dramatic because the DSS is a difficult device to work with. It is flexible enough to create many options to its use in a sequence, but not flexible enough to permit easy use. As an example, note that none of the control sources (CC&S, FDS, and radio receiver) has complete control over the DSS. Also the inability to reliably determine tape position at any given time during a tape pass is a severe restriction on sequence design.

a. DSS End-of-Mission test. A DSS end-of-mission test was conducted to attempt to reactivate the tape recorder. The test comprised of two parts. The first was an attempt to move the tape by means of maximum torque tape direction charges. This was unsuccessful. The second was an experiment to discover the consequences of leaving the tape in a maximum motor torque state with the motor stalled for a long period of time. Three results were possible: (1) nothing would happen, (2) the motor driver transistors would burn out, and (3) the heat generated by the motor and transistors would unstick the tape and the tape would move to its end and stop. Unfortunately, the mission ended before any results were obtained from this portion of the test.

3. Central Computer and Sequencer. For the extended mission, various changes were made in programming the Central Computer and Sequencer (CC&S). The changes were due to changes in requirements and philosophy, and failures or malfunction in spacecraft equipment.

The first candidate for change was the trajectory correction maneuver routine. The routine was rewritten to be quite general in application. Although this approach uses more words than a specifically tailored routine, it was very useful for the five TCMs that followed. With no modifications, the routine performed maneuvers that went from a full-scale maneuver all the way down to a motor-burn only maneuver. By a two-word addition to the routine, it was also possible to initiate a minute counting chain with DC 32 which started the maneuver sequence. The minute counting chain was used to issue events on minute centers.

Since the maneuvers were computer-only maneuvers, a scheme had to be devised to guarantee the maneuver durations. A tandem maneuver using both the sequencer and the computer would automatically abort a maneuver if there were timing differences between the two. However, this mode was not used due to attitude-control gas conservation activities. To protect against the possibility of infinite turns should a noise glitch reset the program counter in the CC&S, the routine was written so that once a turn starts, it was guaranteed to stop as programmed.

Another feature used in the extended mission was the clock calibration routine. This made it possible to obtain clock calibration points independent of the down-link data bit rate.

For the two extended mission encounters, most of the routines remained essentially the same. Except for the TV mosaic routines, all changes made were to effect simplification and, therefore, word savings. The encounter loads were the most troublesome because the sequences required more memory words than were available in the spacecraft computer. In the extended mission, no restrictions were placed on the types of mosaics, i.e., the mosaics were not restricted to be rectangular, single strip, step strip, or parallelogram in form. The mosaic parameters such as pictures per row and scan platform step sizes were not constrained, although imposing restrictions would have saved considerable memory words. For example, if the step size in the main slew axis had been fixed for several mosaics, a single table entry could have been used repeatedly.

A feature that was desired for Mercury I but could not be incorporated due to lack of time and memory space was included in the extended mission. This was the corrections to the APS data word to account for backlash in the scan platform. To do this, the tailored mosaic routines were rewritten into a fairly general mosaic routine. To operate in conjunction with this routine, backlash correction routines were also written. At Mercury III, for example, out of the thirty-one mosaics, ten different types of backlash corrections were required. This consumed twenty-five words of memory. The determination as to where backlash corrections were required was a time-consuming task. The direction of movement of each scan platform position had to be reviewed. Then the clock and cone steps for the first movements in each mosaic were determined. If the movement was in the opposite direction, backlash correction had to be applied. The second row of each mosaic had to be studied in relation to the flyback position and corrections applied where necessary.

During the period when the acquisition of Canopus was being attempted prior to the final encounter of Mercury, extensive use was made of the coded command-direct command (CCDC) capability of the CC&S. This function causes the CC&S to issue a command upon receipt of the execute command by ground transmission. The CCDC was used to issue 7B and 7B/R (Canopus tracker ON and OFF). Since the encounter sequence was already loaded in memory, and since it was desirable not to disturb the sequence, the one spare word in memory was used to load the data word. This eliminated the necessity of having to reload any memory words connected with the encounter sequence. This guaranteed a CC&S controlled automatic sequence if a problem had occurred in command transmission.

For the first time in the MVM '73 mission, an update to the CC&S was made before the beginning of the automatic encounter. This, too, was done to maintain the philosophy that once the automatic sequence had started, no intervention by ground command was necessary to ensure a successful encounter. The update consisted of one word that changed the programmed FDS data

mode command. Without this change, highly degraded video signals would have been received.

The successful programming of the sequences was to a large measure due to the small, but close, knit working group where the communication line was always open. Solutions were quickly achieved by free discussion and interchange of ideas. The CC&S functioned without fault throughout the extended mission. Fifty-three programming loads were made using over 2,000 load commands. The CC&S issued almost 4,500 commands to other spacecraft subsystems during the extended mission.

4. Support Software. Very extensive use was made of four ground support software programs; COMGEN, OPSCOP, MOVTIM, and FDSMEM. Some use was made of a fifth program, RAMAP.

a. Command Generation (COMGEN). In all the programs and routines written, validation is required. A software package called COMGEN is used to do this. COMGEN produces a simulation of the program and provides a detailed listing of all events and their timing. It also checks the coded words to the APS and FDS. In the case of the APS word, COMGEN will check for valid addresses and magnitudes. It will also indicate conditions where one slew command overlaps another.

The program COMGEN, which contains a CC&S assembler; a merge capability, a command generation capability; and an extensive simulation ability of the CC&S, the FDS, the APS, and the DSS, was the most used program. It was run through over 50 operational cycles. In general, a new cycle was started after each period of high CC&S execution or loading activity in order to eliminate having to continually resimulate what was, by then, history. As each cycle was completed, the complete status of COMGEN was recorded on magnetic tape as a backup against any possible data file losses on the computer. COMGEN was always run in a sequence with the file packing routine AMPACK and several utility routines designed to ease data file maintenance problems. This was all done in one operating card deck by using the capabilities of the utility program OPSCOP.

During the sequence preparation work for the two encounter sequences, COMGEN was used in an additional mode. The purpose of this mode was to allow inputs from three sources; namely, TSOST, SPOP, and the Data Systems Engineer to be merged without having to physically mix the three decks. This mode also permitted delaying FDS timing decisions until nearer encounter when frame starts could be better predicted.

This special mode of COMGEN was also run in conjunction with the program OPSCOP and in fact made use of all of OPSCOP's capabilities. Had it not been for this method of COMGEN use, situations such as correcting for unexpected FDS frame start drift several days before encounter would have required changing hundreds of COMGEN inputs instead of just six.

COMGEN's time ordered merge of inputs from several sources plus the ability to work in a relative time base made it possible to keep up

with the rapidly changing command periods that resulted from sporadic station coverage and the roll drift mode of spacecraft operation. It was especially useful during TCMs which were timed based on star sightings instead of wall clock time.

COMGEN did have several shortcomings, some of which cost many manhours of effort in solving. Among the more serious of these were the infinite loop problem and the merge-assembly incompatibility problem. The infinite loop problem occurred when COMGEN was asked to simulate a CC&S execution that crossed over one of the CC&S's hours marks. The result was that the COMGEN run went into an infinite loop and had to be cancelled. Cancelling the run, of course, lost the output and helped obscure the problem. The merge assembly problem was worse. Its causes and cures are not yet completely understood. Another problem was one of output delivery. There were many occasions where the time between the conclusion of a COMGEN run and the receipt of the printed output from that run was an hour and a half. Such a delay makes response to dynamic situations very difficult.

b. OPSCOP. The utility program, OPSCOP, was almost always used to run COMGEN because it enabled the automating of several file maintenance functions associated with the operation of COMGEN and thereby saved much time and presented many errors. Occasionally, OPSCOP's file update capability was used to correct minor errors in COMGEN-generated output files.

The only serious OPSCOP problem that was encountered was with the file update capability. Under certain conditions, update lines ended up in surprising places. Another serious problem which was a procedural problem involved OPSCOP writing on a magnetic tape that belonged to another group. The only real solution to a problem such as this is for the computer's operating system to be set up to use standard system labels on all tapes.

c. MOVTIM. The program MOVTIM was a latecomer on the scene. Its purpose was to allow a user to move a specified block of COMGEN inputs by some specified amount of time. The concept is very useful, but it was quickly implemented (less than one day), with such severe limitations as fixed column format inputs. The program did, however, assist greatly in the complete reorganization of the Mercury III sequence in less than two days beginning just three days before encounter. This was done in order to adjust for the star acquisition difficulties and uncertainties in the aimpoint due to the late execution of TCM 8.

A program such as MOVTIM should be developed to a high level and made available to mission sequence implementation groups.

d. FDSMEM. All of the extended mission FDS reprogramming was done using a FDS memory maintenance and command generation program called FDSMEM. This program saved many manhours and eliminated many mistakes by producing all of the spacecraft commands, all of the Mission Test Computer (the telemetry decommutating computer) inputs, and most of the documentation for the changes. FDSMEM was also

capable of supporting block substitutions with commands and MTC inputs. The MTC inputs were necessary for block substitutions because of a serious deficiency in the MTC programming that prevented the automatic handling of block substitutions.

e. RAMAP. The DSS simulation program, RAMAP, was occasionally used as sequence preparation work, but the program had several restrictions that discouraged its use. Among these was a fixed column field input that made hand preparation of inputs difficult. An inability to reject DSS commands was very inconvenient. The fact that RAMAP was not on the same computer as its prime source of inputs, COMGEN, seriously discouraged its use. Data identification after a RAMAP run was not easy as there was no provision for titling the stored data. RAMAP had no continuous mission run capability such as COMGEN's cycling ability. Certain control functions were not changeable during the course of the RAMAP run thus producing too little information or way too much.

With respect to errors, though, RAMAP was very good. Only one was found, and it was minor.

E. Propulsion Subsystem Performance

Table 9 summarizes the performance of the Propulsion Subsystem during the eight TCMs. TCMs 4a through 8 were performed during the extended mission. Initial tank pressure was not known for the maneuvers subsequent to TCM 4a due to the FDS failure of April 16, 1974. However, it proved to be possible to compute the initial tank pressure with sufficient accuracy that the burn errors did not significantly increase.

TCMs 4a and b were so-called because they were considered to be two parts of one maneuver. They were performed approximately 24 h apart to prevent possible damage to spacecraft components from the temperature increases due to a single long burn. The burn time for TCM 4b was computed before TCM 4a. It was not readjusted based on observed TCM 4a performance.

Table 9 shows that the ΔV errors attained were well within the basic subsystem 3σ accuracy requirement of 8%. At the time of preparation of the table, ΔV error estimates were not available from navigation for TCMs 7 and 8. A propulsion TCM 8 ΔV error estimate is not possible due to the lack of telemetry.

A more detailed discussion of the extended mission maneuvers, including plots of the telemetry data, is given in Refs. 5-8.

In general, the propulsion subsystem performed satisfactorily during the Mariner 10 Mission. No malfunctions occurred, and the burn errors were less than 1σ after TCM 1. The subsystem gradually increased in thrust a few percent during the mission due to decreasing catalyst bed pressure drop and higher than predicted thrust coefficient, but even these phenomena were not unexpected.

Table 9. Mariner 10 TCM summary

TCM	Burn time, s	Predicted ΔV , m/s	Percent of 3 σ A priori ΔV error	Percent of 3 σ A posteriori ΔV errors ^a	
				Propulsion	Navigation
1	19.90	7.778	4.3	+0.9 \pm 2.32	+1.81 \pm 0.39
2	3.70	1.359	5.2	+1.55 \pm 1.2	+1.25 \pm 0.04
3	51.153	17.831	4.6	-0.9 \pm 0.7	-0.72 \pm 0.10
4A	195.014	49.998	6.2	-0.82 \pm 0.75	-0.27 \pm 1.03
4B	139.014	27.554	6.1	+0.32 \pm 0.90	+0.67 \pm 2.80
5	18.813	3.321	7.1	+0.96 \pm 1.07	+1.46 \pm 0.20
6	83.17	14.543	7.2	+0.72 \pm 1.21	+1.86 \pm 0.21
7	12.52	2.022	7.9	+0.5 \pm 1.77	
8	3.12	0.486	10.2		

^aIncludes errors due to propulsion performance prediction, temperature prediction and burn time.

F. Mariner 10 Power Subsystem

The Mercury I encounter on March 29, 1974 was very successful in spite of the deteriorated condition of the spacecraft. The power subsystem had sustained anomalies causing transfer to the standby chain (redundant boost regulator and 2.4 kHz inverter) and partial reduction in one solar panel power string output. Because of excessive control gas usage, the solar panel tilt capability was used for attitude control of the spacecraft by varying the effective solar pressure resulting from the differential tilt angles.

Immediately after the successful Mercury I encounter on March 31, 1974, the power subsystem experienced an electrical failure in Bay 1 which manifested itself as a 90-W load at the input to the boost regulator and a measurable bay temperature increase. After many attempts to adjust and reduce the spacecraft electrical loads, it was determined that the power system had sufficient power margin to support normal operations plus the parasitic anomalous load. Operating modes were adopted so that the Bay 1 temperature would not become excessive. The far encounter science sequence was not compromised.

The following week contained several more anomalies in other subsystems, i.e., the tape recorder power (2.4 kHz) turning on and off without commands and the loss of direct command capability to change the TWT from low to high mode. No correlation could be established between the boost regulator "parasitic load" and these other subsystem events.

On April 16, 1974, the Flight Data Subsystem (FDS) experienced a failure which eliminated many of the engineering data channels. The power subsystem was left with only the following

data after FDS was reprogrammed to maximize the data return from the operating channels:

E-750	Bay 1 temperature
E-853	30 V regulator voltage
E-854	30 V regulator current
E-861	+X solar panel 1 current
E-862	+X solar panel 2 current
E-866	Irradiated cell current (I_{scr})
E-867	Standard cell voltage (V_{oc})
E-868	Standard cell current (I_{sc})
E-870	+X solar panel 1 temperature
E-871	+X solar panel 2 temperature
E-872	+X solar panel 3 temperature
E-873	+X solar panel 4 temperature
E-660	X-band transmitter current (power switching and logic voltage indicator)

All of the information about the -X solar panel power performance was lost. The V_{oc} - I_{sc} transducer data from the -X panel provided the only indication of tilt angle change and temperature. The power output of the -X panel was assumed to be proportional to the +X panel performance. The four +X panel temperature transducers provided data to permit -X panel temperature assumptions. It was fortunate that the Bay 1 temperature data remained available so that the boost regulator parasitic load could be monitored. The 30-V regulator current and voltage channels were not useful because the regulator was never turned on after the power chain transfer to standby. The X-band transmitter load is constant power on the raw dc bus. Therefore, its input current varies inversely proportional to the bus voltage. Channel E-660 thus provided an excellent indication of the raw bus (PS&L) voltage. Because all battery telemetry channels were lost, the X-band transmitter current measurement provided the only data on battery performance when

the solar panels were off Sun or during the solar panel/battery share mode. The performance of the battery charger was monitored by noting the change in +X solar panel currents when the charger was commanded ON/OFF. This limited power system telemetry data provided a sufficient information base from which the power system performance could be implied.

After the anomalies were analyzed and understood, work-around procedures were developed so that the remainder of the mission was conducted in a near normal manner. TCMs 4A, 4B, and 5 were performed without incident allowing the spacecraft to again encounter Mercury on Sept. 21, 1974 and provide excellent return of science data.

The six-months cruise period between Mercury II and Mercury III was filled with solar panel differential tilts so that maximum conservation of control gas could be realized. Without control gas, a third Mercury encounter would be useless. TCMs 6, 7, and 8 were performed successfully, making Mercury III encounter a significant science and engineering accomplishment.

After Mercury III encounter, the spacecraft was dedicated to engineering tests. One of the tests involved tilting the + and - solar panels from 71 to 78 deg and return in 1 deg or less increments. (The largest tilt angle used during the mission was the design limit of 76 deg.) The results of this exercise were twofold. First, the

steady-state data plotted in Fig. 50 permits assessment of the solar panel performance after 500 days in space at Sun intensities never before experienced (0.4 AU). The solar panel performance data includes calibration at large tilt angles and the evaluation of degradation due to ultraviolet and hard particle irradiation. Second, the MVM '73 solar panel design and near Sun performance could be evaluated for use in the MVM Encke Comet study. Preliminary analyses indicates a significant ultraviolet degradation of the thermal properties and solar cell coverglass transmission. Comparable data at equal Sun intensities and tilt angles indicate a 11°C increase in solar panel temperatures. The resulting solar panel power loss due to thermal degradation and coverglass transmission loss was approximately 12 to 14%. Hard-particle damage does not appear to be significant, e. g., 1% or less.

During the Mercury III encounter sequence, the power system provided 470 W from the solar panels at the bus voltage of 43.25 V. The panels were both at 71 deg tilt, and the zener diodes were not dissipating any power. The average solar cell temperature was estimated at 85°C. This performance, assuming operation at the maximum power point, would imply that the solar panels had a capability in excess of 600 W at launch and near Earth. The power subsystem performed well throughout the entire mission. The design proved to be reliable enough to sustain the failures and anomalies without compromising the mission objectives.

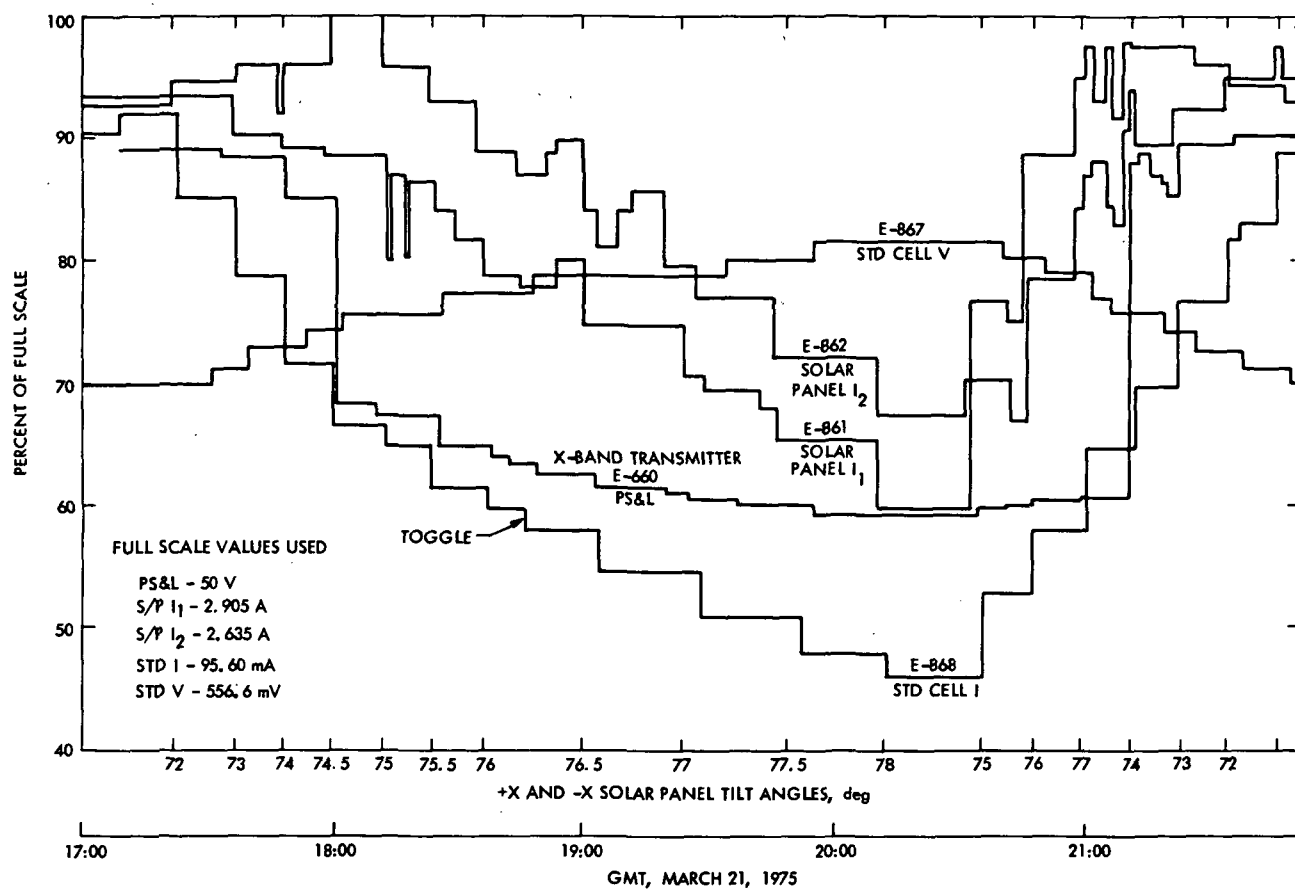


Figure 50. Solar panel degradation

VII. NAVIGATION

A. Introduction

The navigation activities during the Extended Mission were a natural extension of the activities during the baseline mission in the sense that both the personnel, and to a major extent the software, were carried over from the baseline mission. However, due to both spacecraft anomalies and the Extended Mission science requirements, the details of the navigation effort between the two phases were distinctly different.

After the first Mercury encounter an evaluation of the science requirements along with the remaining capability for controlling the spacecraft orbit showed that the maximum science return would be obtained by targeting the spacecraft for a far Sun-side flyby on the second Mercury encounter and for a close dark-side flyby on the third encounter. The far Sun-side flyby was designed to complete the TV coverage and the close dark-side flyby to investigate the magnetic field properties.

Following the first Mercury encounter the uncorrected trajectory would have taken the spacecraft to a closest approach point approximately 800,000 km below Mercury on the second encounter. The navigation activities required to achieve the desired closest approach distance of 50,000 km included two trajectory correction maneuvers (TCMs 4 and 5) and three periods of orbit redetermination. The first TCM (TCM 4) was designed to correct the major portion of the error during a period when the ΔV requirements were low and the second (TCM 5) to correct any residual errors and achieve an accurate flyby. The orbit determination activities involved reconverging the orbit prior to each of these maneuvers plus a final reconvergence after the TCM 5 to support the encounter sequence planning.

Navigation between the second and third Mercury encounters became much more challenging than on the previous leg. This was due to two opposing factors. On one hand, the science return improved as the closest approach distance decreased, provided the spacecraft did not impact the planet. Thus the need for highly accurate navigation. On the other hand, the reduced supply of attitude-control gas forced the project to adopt the "solar sailing" mode (in this mode the roll-orientation of the spacecraft is not controlled) which, in turn, severely degraded both the doppler and range data. This data degradation had a potentially catastrophic effect upon the orbit determination accuracy and a major portion of the navigation effort on this leg was applied to correcting and working around this problem. As with the maneuver strategy on the previous leg, it had been hoped to achieve the final flyby trajectory with two maneuvers (TCMs 6 and 7). However, due to a combination of large execution errors on the last planned maneuver and the degraded orbit redetermination capability, the probability of Mercury impact was unacceptably high after TCM 7 which forced the execution of TCM 8 in order to decrease the impact probability. Even with all of the problems the spacecraft was delivered to a closest approach point only 327 km above the surface. This distance

was less than half the closest approach distance on the first Mercury encounter.

The Extended Mission was supported by roughly one third the personnel supporting the baseline mission. The full-time support included a team chief, an orbit determination analyst, a data editor, and a maneuver analyst. There was also regular part-time support for the orbit determination, targeting, and reconnaissance areas. Additionally, when particular problems arose that required either specialized support or a short-term effort exceeding the capability of the navigation team, further manpower was provided by the Mission Analysis Division.

The reduction in the manpower level was possible because of a number of factors. First, the software and operational procedures had, for the most part, been thoroughly developed and debugged during the baseline mission and were used during the Extended Mission without a further expenditure of effort. Secondly, the entire operational staff was much smaller, which greatly reduced the time required for coordination of the inter-team activities. The availability of the outside support for the solution of special problems eliminated the necessity of maintaining the capability to handle these problems from within the normal navigation team. Finally, the pressure to rapidly process the received tracking data and maintain an updated orbit was reduced which allowed an extended schedule for orbit redetermination.

The transition from prime mission status to Extended Mission status had some negative effects in terms of increasing the workload during the extended mission. The most noticeable effect was the loss of priority in the use of the 1108 computer. Due to the large size of the navigation software, especially in the orbit determination area, it is not possible to execute these programs when the general computer user is also using the 1108. This incompatibility forces the scheduling of periods where the 1108 is used exclusively by the navigation team (block time). During the baseline mission block time was normally scheduled during normal working hours. However, during the Extended Mission block time was available only after the normal hours (typically 5:00 pm to 3:00 am during the week). This forced the personnel executing these programs (primarily the orbit determination analyst and the data editor) to work a very abnormal shift and greatly increased the communication problems between these functions and the remainder of the project. While this situation was acceptable for short periods of time, it became increasingly evident that over-extended periods of time this arrangement was reducing the efficiency of the navigation team.

The reduction in priority also increased the effort associated with obtaining the required tracking coverage. During the baseline mission both the priority of the project and the DSN workload allowed sufficient tracking coverage to be easily scheduled. During the Extended Mission the reversal of both of these factors required that the tracking requirements be carefully generated

and coordinated with the DSN. In various portions of the Extended Mission the tracking coverage became critical to the success of the mission and the scheduling effort imposed a considerable workload on the navigation team.

B. Radiometric Tracking

1. Introduction

The MVM '73 Extended Mission was constrained to use only about half the tracking coverage time available to the prime mission. This sparser coverage by itself naturally complicated the navigation of the Extended Mission. Additional difficulties arose from the comparative degradation of much Extended Mission tracking data due to (1) solar plasma corruption around superior conjunction June 6, 1974, (2) rolling spacecraft data signatures during the period of solar sailing from Mercury II to Mercury III, and (3) increasing reliance on 26-m stations for coverage.

The goals of this subsection are to provide more detail of the manner in which MVM '73 accumulated and prepared tracking data for the orbit determination process and to outline several unique difficulties facing the navigation team in the accomplishment of its task.

2. Creation of Radiometric Tracking Data

In order to create doppler data types (to measure range rate) a synthesizer frequency (F_T)¹ of approximately 22 MHz (Block III S-band) was multiplied by a factor of 96 to produce a carrier tone of about 2200 MHz (see Table 10 for list of Deep Space Stations), and transmitted to the MVM '73 spacecraft. The received signal was then retransmitted at an S-band frequency 240/221 times higher and returned to Earth. (An X-band transponder also returned the carrier at a frequency adjusted by 880/221, but this could only be received by a Block IV receiver located at DSS 14. The X-band data was not used to support navigation.) When the receiving DSS is the same as the transmitting deep space station, the data is labeled F2 (two-way doppler), but if the receiving deep space station is different, the data is labeled F3 (three-way doppler). When the spacecraft did not receive a carrier signal from Earth, it would transmit a constant beacon tone of about 2300 MHz. When this was received by a deep space station, it was labeled F1 (one-way doppler).

The cycles of the received signal are counted by a doppler counter at the DSS. The cycle counter is then interrogated at a specified sample interval, and the count is transmitted along the high-speed data line to the MCCC. The radial spacecraft velocity is a function of the measured

Table 10. Deep Space Stations used to support Mariner 10

DSS	Station No.	DSCC	Antenna size, m	Comments
Echo	12	Goldstone, Calif.	26	PLOP ranging during prime; PRA removed during Extended Mission
Venus	13	Goldstone, Calif.	26	Used to track ATS-1 and ATS-5 for ionospheric charged particle calibration
Mars	14	Goldstone, Calif.	64	First usage of a Block IV receiver during prime; Block III installed during Extended Mission with PLOP ranging
Weemala	42	Tidbinbilla, Australia	26	Conjoint PLOP ranging during Extended Mission with DSS 43 PRA
Ballima	43 ^a	Tidbinbilla, Australia	64	PLOP ranging
Robledo	61	Madrid, Spain	26	Conjoint PLOP ranging during Extended Mission with DSS 63 PRA
Cebreros	62	Madrid, Spain	26	No ranging capability
Robledo	63 ^a	Madrid, Spain	64	PLOP ranging
^a Used for the first time by MVM '73.				

¹The exact value of the synthesizer frequency for optimal spacecraft communication is established by PREDIX runs. Deep Space Station operations personnel dial this value into the station hardware.

doppler shift in the received signal. (See Fig. 51 for a diagram of F2 creation.)

Measurements of spacecraft range are obtained by transmitting a series of coded pulses via sidebands of the main carrier frequency to the spacecraft which are then retransmitted by the spacecraft back to Earth. The Earth-received code is matched against the transmitted code. The spacecraft range is a function of the phase shift between the two signals. In practice, the range measurements are influenced by daily variations in the spacecraft and deep space station hardware timing delays, as well as local weather conditions at the station. Calibrations of local ranging delays must be taken at each station during its ranging pass, which must be combined with the current spacecraft delay to produce ranging adjust values as described in Section VII-A-5. These calibrations are added to the measured value in order to obtain the proper range measurement.

Table 11 summarizes all navigation data types used in the MVM '73 mission. Figure 52 summarizes the flow of tracking data and the relationships of personnel and interfaces involved in the navigation process. Reference 19 further

describes the manner in which the DSN accumulates tracking data.

3. Data Conditioning

All incoming data must be evaluated for quality and validity before the orbit determination fit. Calibrations and recovery procedures are employed whenever possible to correct deficiencies, but much data is not recoverable and must be removed from the final data file. This was a formidable task, since about 1000 data points were received each day.

Radio metric data measurements of spacecraft range and range rate are corrupted by error sources classified into three groups:

(1) Spacecraft error sources

Spacecraft rotational motion
Spacecraft nongravitational accelerations
Spacecraft electronic irregularities

(2) Earth-based error sources

Ground facility hardware malfunctions and irregularities

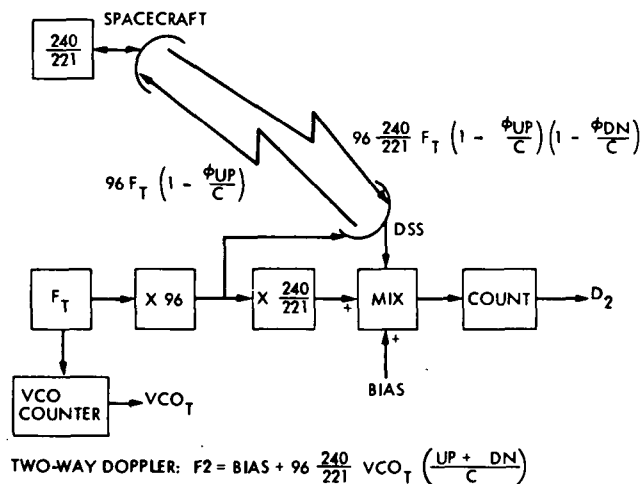
Table 11. DSN data types used to support navigation

Designation	Definition	Band ^c	Comments
F1	One-way doppler	S, X	Primarily used for radio science
F2 ^b	Two-way doppler	S, X	S-X band dual doppler also used to calibrate charged particles
F3	Three-way doppler	S, X	Requires use of two deep space stations simultaneously
PLOP ^{a b} (PRA)	Discrete planetary operational ranging	S	Primary range type used in extended mission
MU2 ^a	R&D planetary ranging (discrete)	S, X	Used only with DSS 14 Block IV receiver
MARK 1A	Near-Earth ranging	S	Post-launch ranging system; originally designed for lunar distances
DRVID	Differenced range versus integrated doppler	S	Used to calibrate charged particles
F3C ^a	F3-F2	S	A pseudo-data type which eliminates spacecraft stochastic accelerations
CHPART	Faraday rotational data	—	Used to calibrate charged particle content of Earth's ionosphere

^aData types used for the first time by MVM '73.

^bPrimary data types used to navigate MVM '73.

^cX-band data from DSS 43 was available, using the Block IV receiver, until July 1, 1974, at which time the Block IV receiver was replaced by the Block III receiver.



ϕ_{UP} = SPACECRAFT RADIAL VELOCITY (km/sec) RELATIVE TO TRANSMITTING STATION

ϕ_{DN} = SPACECRAFT RADIAL VELOCITY (km/sec) RELATIVE TO RECEIVING STATION

C = SPEED OF LIGHT (km/sec)

F_T = SYNTHESIZER FREQUENCY OF TRANSMITTING STATION (NOMINALLY 22 mHz FOR BLOCK III RECEIVER AND 44 mHz FOR BLOCK IV RECEIVER)

VCO_T = COUNTED VCO FREQUENCY OF TRANSMITTING STATION, NOMINALLY 22 mHz

BIAS = 10^6 Hz FOR BLOCK III AND 5 TIMES 10^6 FOR BLOCK IV RECEIVER

Figure 51. Block diagram to generate two-way doppler (F2)

ORIGINAL PAGE IS
OF POOR QUALITY

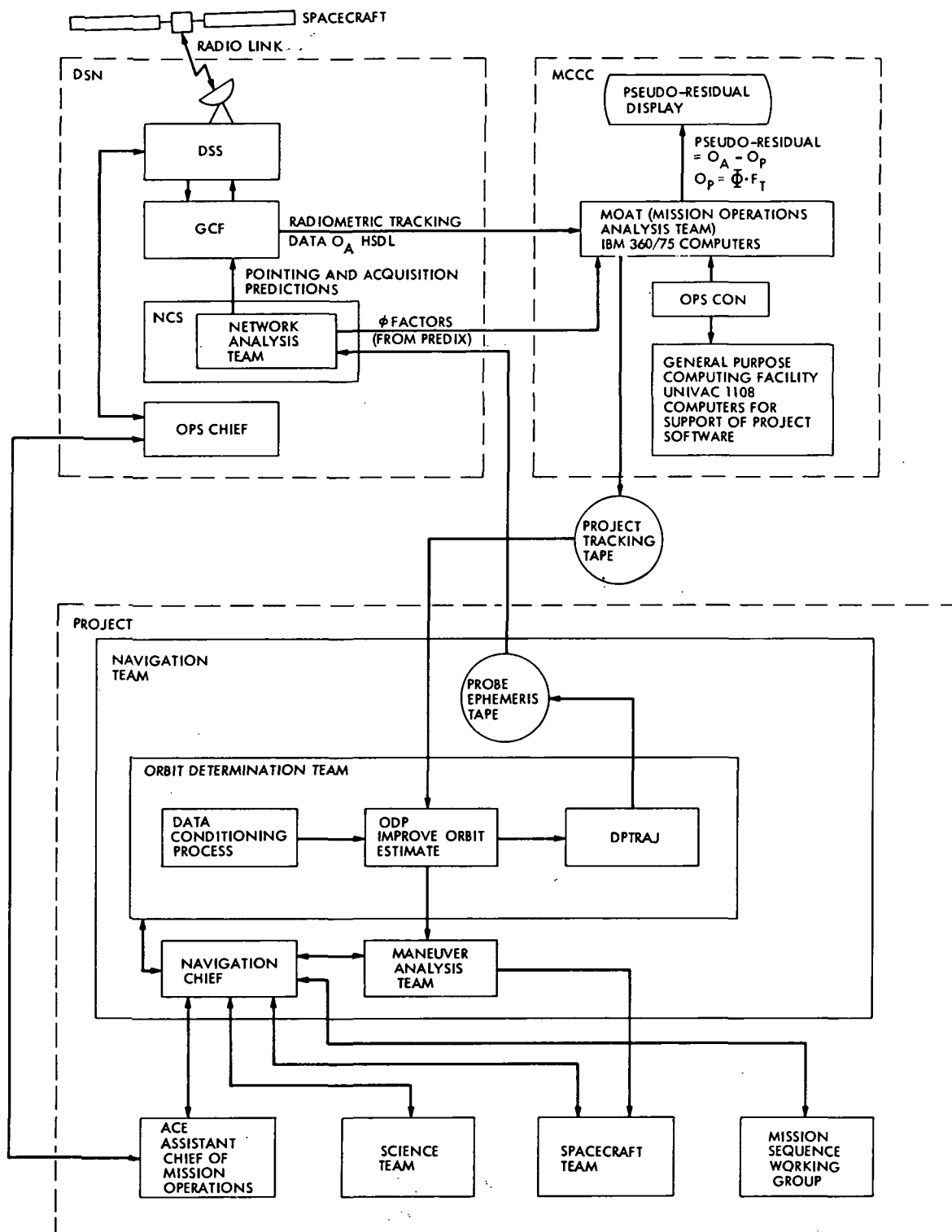


Figure 52. Tracking data flow block diagram

Human error
Tracking station motion (polar motion and irregularities in Earth rotation rate)

(3) Intervening tracking mediums

Tropospheric refraction
Ionospheric charged-particle influences
Space plasma charged-particle effects.

The data editing procedure employed by MVM '73 is shown schematically in Fig. 53. At specified times a tracking tape, containing recently received data consisting primarily of doppler counter samples, is transferred to a Univac 1108 computer. Here the Orbit Data Editor (ODE), a general-purpose data file manipulation program, first converts the tracking data file into an 1108 compatible format (decode process), and subsequently creates an orbit data file containing differenced, time-normalized values of the doppler counter samples. The doppler shift in this frequency is a function of the spacecraft velocity. The orbit data file was next processed by the Tracking Data Editor (TRKED) which creates a file of residuals based on an assumed a priori orbit. The residual file permits an evaluation of the data quality.

MVM '73 was the first interplanetary mission to make use of a computer interactive graphics system as a data quality analysis aid. Previously, support personnel have been constrained to first create hard-copy data residual plots, and then refer back to hard-copy listings of the data in order to manually produce edit control cards. MVM '73 implemented an Interactive Orbit Data Editor (IODE)² for use on JPL's Univac 1108 computers in conjunction with a Univac 1557/1558 interactive graphics display device (Fig. 54).

Using the graphics system, data residuals for each tracking pass can be immediately displayed on the face of a cathode ray tube. Although the interactive orbit data editor employs automatic scaling features within each tracking pass, any interval of data can be quickly replotted to any desired scale. Data can be flagged for rejection, and the entire pass replotted and rescaled minus the rejected data. The image on the CRT may be stored at any point for subsequent production of hard-copy records.

It is estimated that the use of computer video graphics reduced the time required to produce edit control cards by a factor of from 10 to 20. At the same time reliability had been improved by removing the human error in the traditional manual techniques. Interactive graphics also allowed

the analyst great flexibility to make qualitative evaluations of subtle data signatures.

The resultant file of edit control card images was used to form the final data file. Intervals of data not rejected were averaged into compressed points, thus reducing the process time necessary to determine the Mariner 10 trajectory.

Much activity was devoted to calibrate or further understand error sources that affect tracking data. These activities are briefly described as follows:

- (1) Calibrations of the variations in the Earth's rotational rate and polar motion were updated weekly³ and incorporated into the orbit fits.
- (2) Tropospheric refraction was modeled to include an observed seasonally varying component as described in Ref. 2.
- (3) Calibrations of the charged-particle content of the total intervening tracking mediums were made using S/X dual doppler data,⁴ available mostly during the prime mission. These measurements were compared against calibrations of the ionospheric charged particle content from Faraday rotation data. The charged particle calibrations, however, were performed as a demonstration only, and were not incorporated into the orbit fits used to support navigation.
- (4) Calibrations of the spacecraft and DSS hardware delays were factored into the range measurements as described in VII-A-5.

4. Ranging Parameters⁵

Discrete Planetary Operational Ranging (PLOP) from the Planetary Ranging Assembly (PRA) was the primary range data type used during the extended mission. For a PLOP point of N components, the final range value is ambiguous by multiples of 2^{10+N} range units (1 range unit $\sim 1/7$ m). Thus to properly interpret a range point of 10 components, the spacecraft orbit positional uncertainty must be no greater than about 150 km.

The ranging system effectively divides the solar system into concentric shells, each shell being 2048 ranging units thick. The spacecraft position is determined with respect to this measuring system. The T_0 time is the second when the range code first returns to the ranging deep space station from the spacecraft. Then follows an interval of $(T_1 + 1)$ sec during which the

²Programmed by B. M. Cooper of JPL.

³Supplied by M. Dodds and J. Humnicky of JPL as "STOIC" decks.

⁴Performed by B. Winn and K. Yip of JPL. References 20 and 22 describe this topic in greater depth.

⁵Refer to Ref. 21 for a more comprehensive discussion of the Planetary Ranging Assembly.

spacecraft location is defined within one of the ranging shells. Following the T1 interval are (N - 1) T2 intervals, each (T2 + 1) seconds in duration, which successively define the particular shell containing the spacecraft. After the last T2 interval, a series of T3 intervals (each T3 seconds long) define DRVID data.

The range parameters were calculated as follows:

Clock acquisition time parameters

$$T_1 = 12.5 \left(\frac{15}{\sigma} \right)^2 \frac{N_0}{P_R} \text{ sec}$$

where

$$\frac{N_0}{P_R} \text{ (watts/watt)} = 10^{-\rho/10}$$

σ is the desired range accuracy in meters

N_0 is the system noise spectral density

P_R is the power in the ranging channel

$\rho = \frac{P_R}{N_0}$ (dB), signal-to-noise ratio, available from dumps of project tracking tapes or telecommunications predictions.

Constraint

$$T_1 = J T_s - 1 \text{ sec}$$

where T_s is the Tracking and Data Handler sample rate and J is an integer.

Probability of False Acquisition Parameter

$$T_2 = 10^{(9-\rho)/10} \text{ sec}$$

provides for $PE < 1/1000$

Constraint

$$T_2 = 20K - 1 \text{ sec (K an integer)}$$

DRVID Post Range Acquisition Integration Time

$$T_3 = \frac{1}{8} 12.5 \left(\frac{15}{\sigma} \right)^2 \frac{N_0}{P_R} \text{ sec}$$

Constraints

$$T_3 = L(T_2 + 1) \text{ sec (L an integer)}$$

$$T_3 = M T_s \text{ sec (M an integer)}$$

Optimal values of N, T1, T2, T3 and the suggested interval between successive T0 times were periodically transmitted from the navigation team to the ACE and the OPS CHIEF, who would communicate the values to the individual DSS. During the MVM '73 extended mission, the capability was developed to take conjoint ranging from the 26-m facilities DSSs 42 and 61. The technique involves borrowing the planetary ranging assembly of the adjacent 64-m facility. Due to its smaller antenna size, the P_R/N_0 for a 26-m facility will be almost 16 dB weaker than a corresponding P_R/N_0 at a 64-m facility. Consequently, longer range integration times are required for conjoint ranging. In one instance, when the spacecraft was in the solar-sail mode and communicating to Earth via its low-gain antenna, more than 3-1/2 hours were required to integrate a single 7-component $\sigma = 15$ m conjoint range point. However, when the spacecraft ranging signal-to-noise ratio was favorable, range point parameters were generally adjusted to provide $\sigma \leq 5$ m and $N \geq 10$.

5. Ranging Calibrations

The raw range reading provided by the planetary range assembly at a deep space station is not the final desired range measurement. As seen in Fig. 55, the raw PRA range value will contain an unwanted round-trip through path ABC plus a station hardware delay (as electronic impulses pass through cabling and are processed by the ranging equipment). In order to calibrate the unwanted component (which may vary daily due to local meteorological conditions at the station), a signal is transmitted from a zero delay device (ZDD) through the station feed horn and electronics and then returned to the ZDD. The round-trip through path DEF and the station equipment duplicates the travel of the actual spacecraft signal, so that when the ZDD calibration and the current spacecraft delay are subtracted from the raw PRA reading, the range measurement PQ (Fig. 55) results. Since the desired range measurement is PR (the distance from the spacecraft to the deep space station axis), the Z-height value (the distance between the ZDD and DSS axis) is then added to the intermediate result.

In practice, the ZDD measurement for each ranging pass was transmitted to the Network Analysis Team (NAT) in the form of a post-track report, which then became available to the navigation team. Ranging adjust cards for the Orbit Determination Program during the MVM '73 Extended Mission were produced by G. Pease using the 1108 computer program GORC.⁶ The

⁶(Generate ordinary range calibrations) programmed by G. Sievers and S. Reinhold for use on a real-time computer demand device.

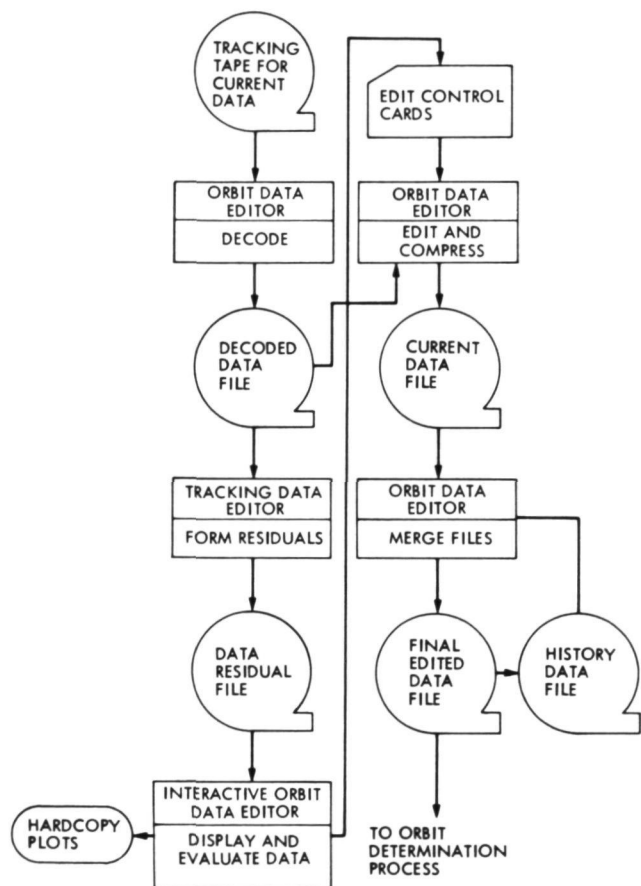


Figure 53. Data quality analysis edit procedure



Figure 54. Univac 1557/1558 display device

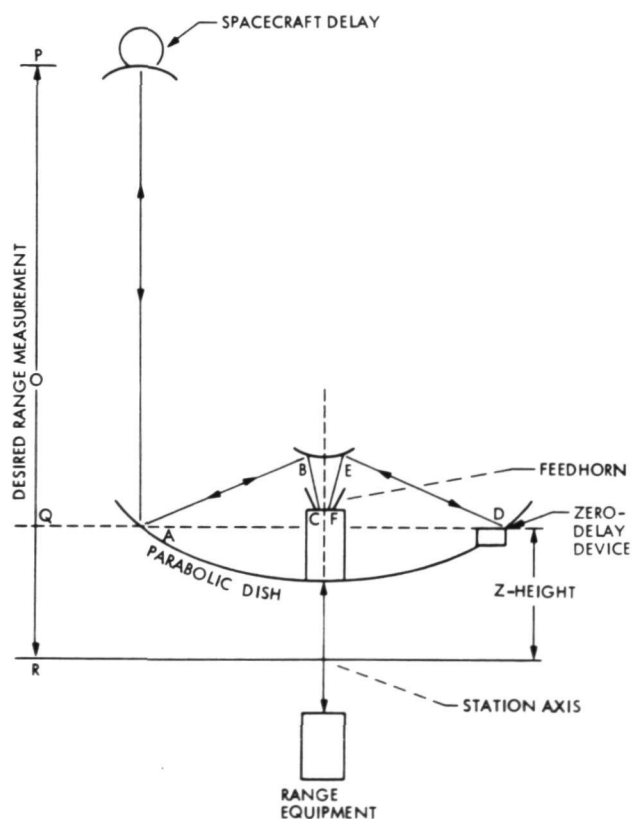


Figure 55. Theory of range calibration at a deep space station

user inputs range data type, station ID, pass ID, transmitter-receiver frequency, band, spacecraft delay, and station delay and the program computes the range adjust value (using a stored table of Z-height values for each deep space station). The internal calculations are performed in terms of a naturalized measurement system composed of range units (1 RU ~ 1/7 m; 1 RU ~ 1 ns).

In the course of the mission it was observed that the consistency of valid range measurements at a particular deep space station was on the order of a few meters. This minor variation could in part be due to the limitation on the clock acquisition time parameter, T1. However, there still remain serious biases on the order of 20 m between individual deep space station facilities, which apparently arise due to inconsistencies in the calibration procedures within the DSN, as well as survey errors in the deep space station location (Fig. 56).

6. Superior Conjunction Data

As expected, near superior conjunction the doppler data was seriously corrupted by interactions with solar plasma (Fig. 57). It was not, however, anticipated that serious charged-particle corruption would be apparent as soon as or for as long as it in fact was observed. Plasma interactions in the form of spurious wavy signatures were developing in early March of 1974 when the Sun-Earth-probe angle was greater than 30 deg (Fig. 58). Consistently serious corruptions were observed from mid-April through late August of 1974. Figure 59 shows an example of the characteristically poor data received during this period which may be contrasted against the clean data received for most of the prime mission as in Fig. 60.

7. Calibration of Rolling Spacecraft

In order to conserve attitude-control gas, the spacecraft roll correction jets were inhibited from Oct. 6, 1974 to March 15, 1975. The roll period was controlled by the spacecraft team to be between several hours and about one day. This was accomplished by adjusting the high-gain antenna position and tilting the solar panels periodically to manipulate solar radiation torques. During this period, communication was through the low-gain antenna. Circulatory motion in the transmission point of the low-gain antenna introduced a sinusoid in the doppler tracking data (Fig. 61).

Since it was not known at the outset of the solar sailing period how an irregular sinusoid in the doppler tracking data would affect the orbit estimation process, it was decided to code new software to model the physical process taking place and remove the extraneous signature from the data. This resultant program, ROLL/TORQUE,⁷ used a current probe ephemeris tape to model the spacecraft-Earth salient geometry.

⁷ Coded by G. Rinker of JPL.

⁸ A time when Canopus is visible in the star tracker, only accurate to within several minutes.

A series of Canopus-crossing-time⁸ observations (values provided by the spacecraft team) were input on punched cards, and fit in a least-squares manner to provide a simple second-order polynomial expression for the spacecraft roll motion during intervals of nearly constant acceleration. Every time a new high-gain antenna adjustment or panel tilt occurred, a new calibration interval had to be begun. ROLL/TORQUE then produced a series of DRVID adjust cards for the ODP to remove the unwanted roll signature. Unfortunately, it appears that the actual physical process taking place on the spacecraft was much more complicated than just a simple single point source on the end of a 3.763-m rotating pipe. Indeed, by inspecting corrected Orbit Determination Program residuals (such as in Fig. 62), it appears that the radio signal underwent interactions with the spacecraft assembly (high-gain antenna, Sun shield, solar panels, TV cameras, etc.), creating a very difficult situation to model exactly. The calibrated residuals seemed to vary in appearance as the Earth-spacecraft geometry changed in time. Deviations of the roll signature from a true sinusoid support the hypothesis of signal/structure interactions.

Another problem experienced was that the correction tended to go out of phase somewhat over longer intervals, indicating that perhaps a higher order polynomial fit to the Canopus crossings was needed. Thus, ROLL/TORQUE only removed between 60 and 90% of the total roll signature. Fortunately, at least over a long data arc, it was found that the uncorrected data solutions were very close to the calibrated data solutions.

C. Orbit Determination

1. Introduction

The Mariner 10 mission was one of the most successful interplanetary projects in history. All scientific objectives were met or exceeded with the first Mercury encounter in March of 1974. Additionally two bonus encounters with Mercury were achieved in September 1974 and March 1975, under the budgeted cost.

The Mariner 10 spacecraft demanded more accurate navigation than any other interplanetary spacecraft in history, and can boast of several navigational firsts. It was the first spacecraft to successfully fly by two planets, using the gravity assist of the first to aim it toward the second; it was the first to fly by Mercury; it was the first to accomplish repeated flybys of the same planet. Large delivery errors at any of the earlier encounters would have imposed abnormal corrective propellant costs, jeopardizing the later encounters. Thus, highly accurate trajectory estimates were paramount to mission success. This subsection will discuss the orbit determination (OD) activities and results in support of each phase of the extended mission. The OD effort for the primary mission is discussed in Ref. 21.

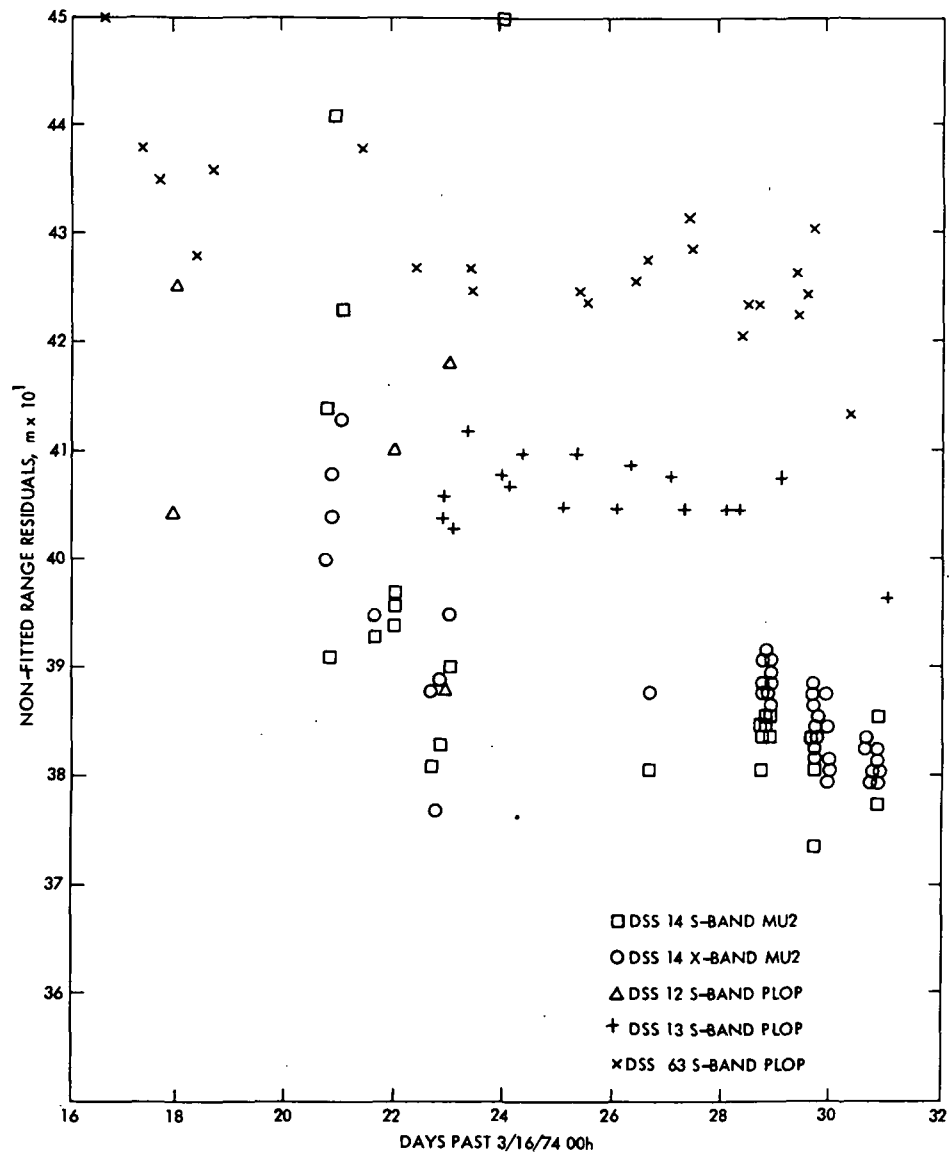


Figure 56. DSS range residuals

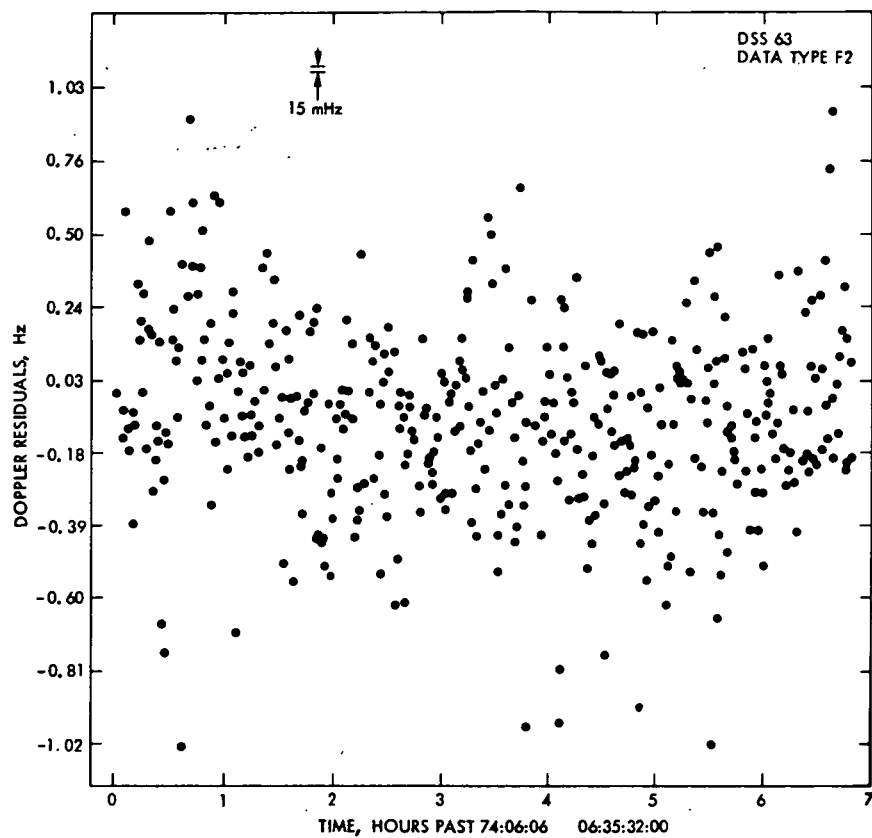


Figure 57. F2 data on day of superior conjunction

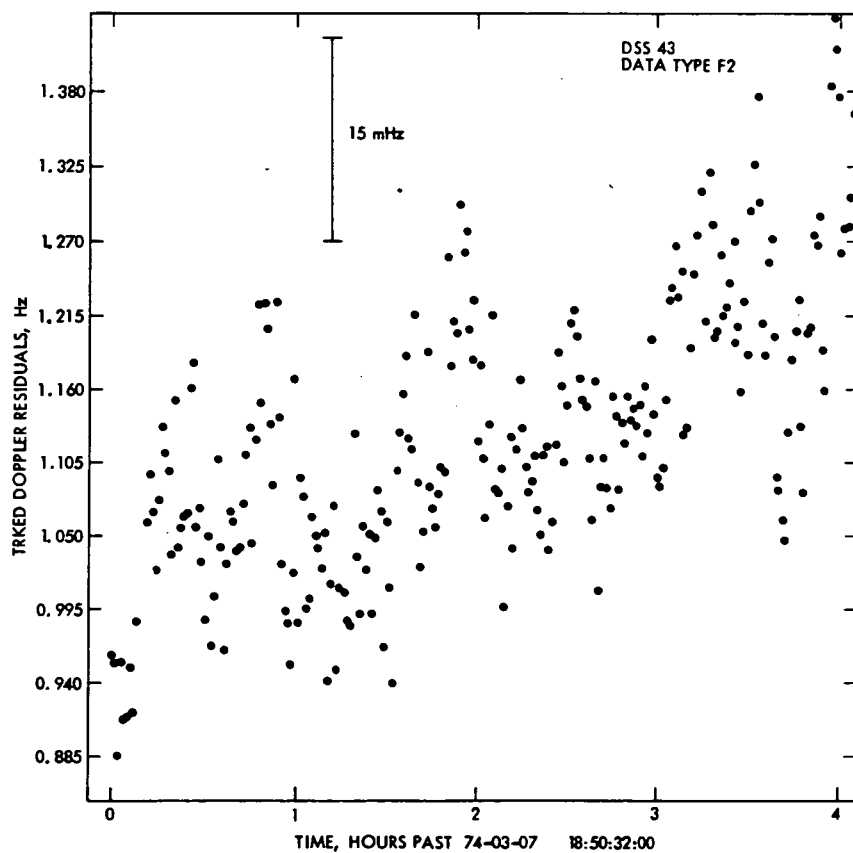


Figure 58. Assumed plasma-corrupted F2 residuals

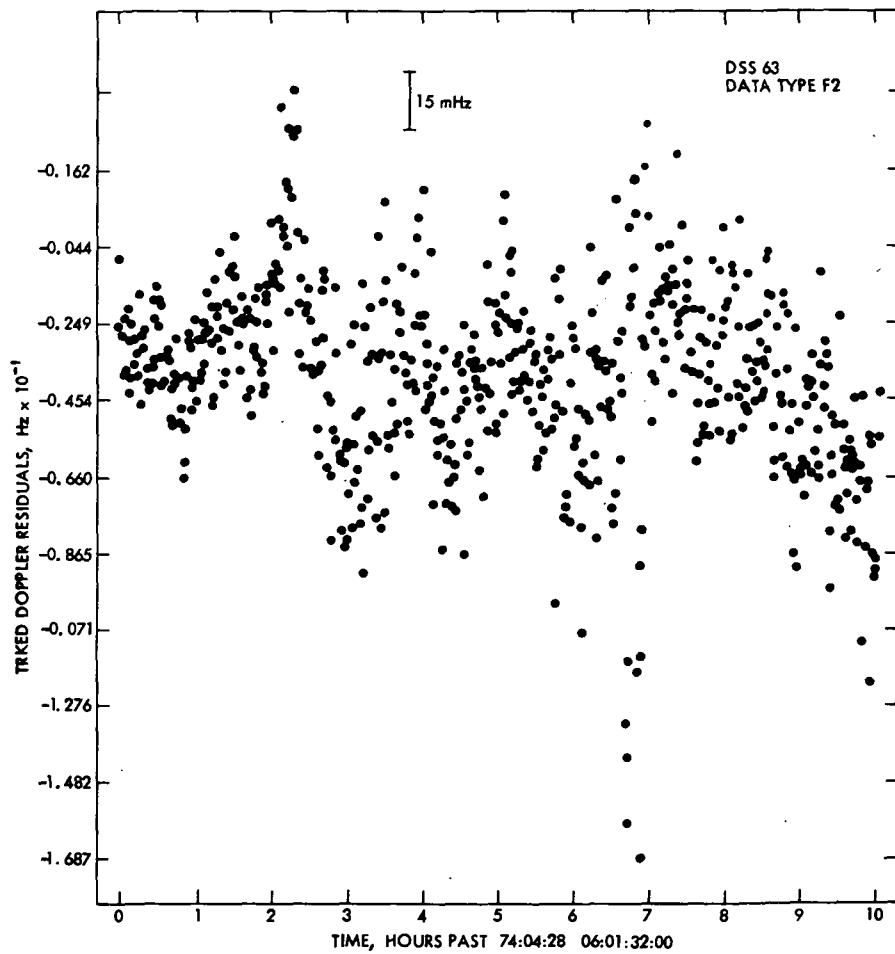


Figure 59. Plasma-corrupted F2 residuals

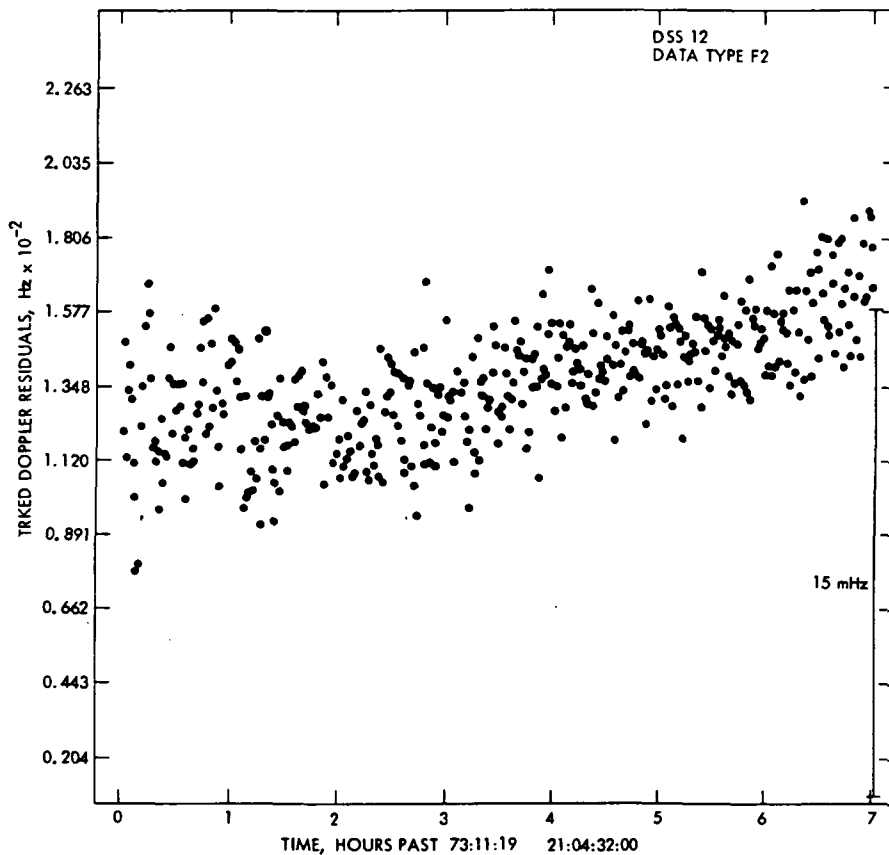


Figure 60. Clean F2 residuals data

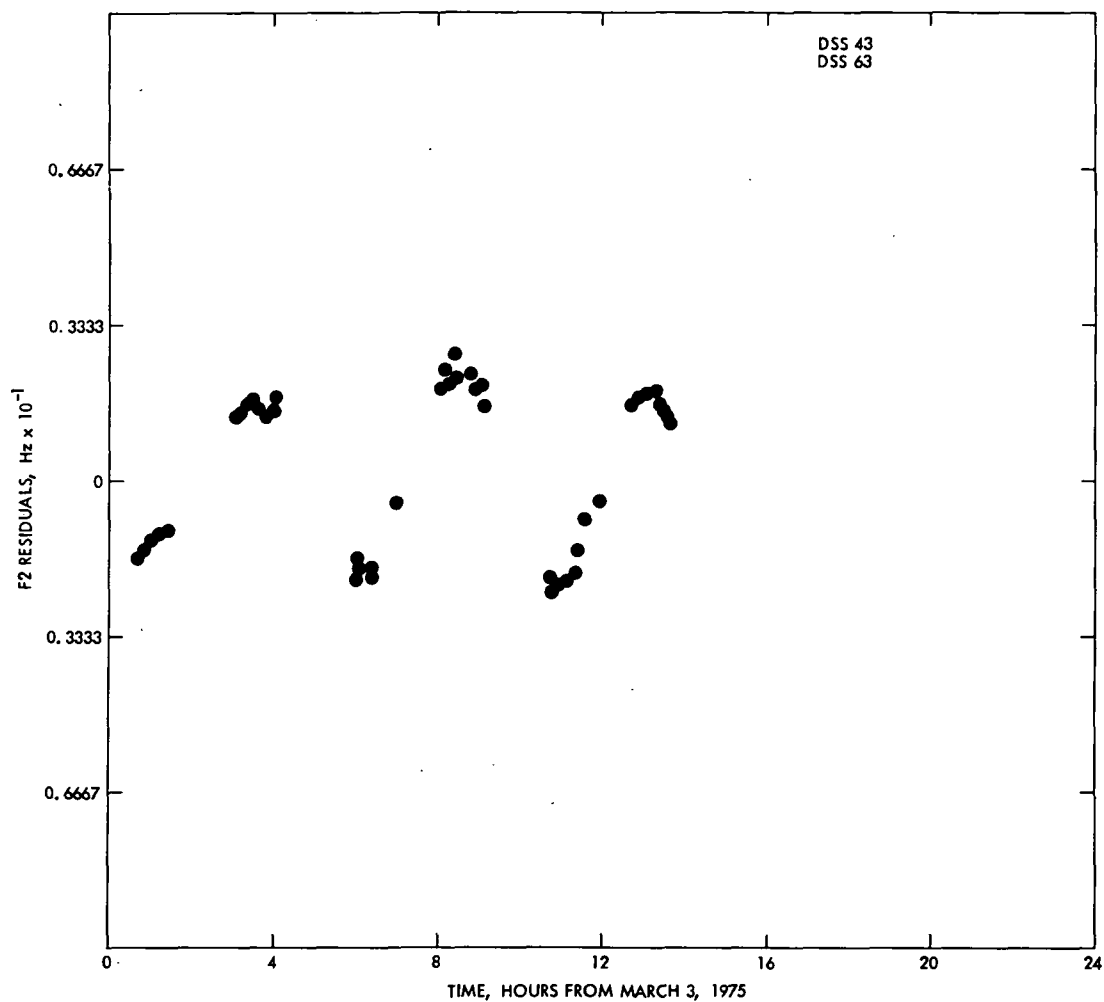


Figure 61. Uncorrected F2 residuals

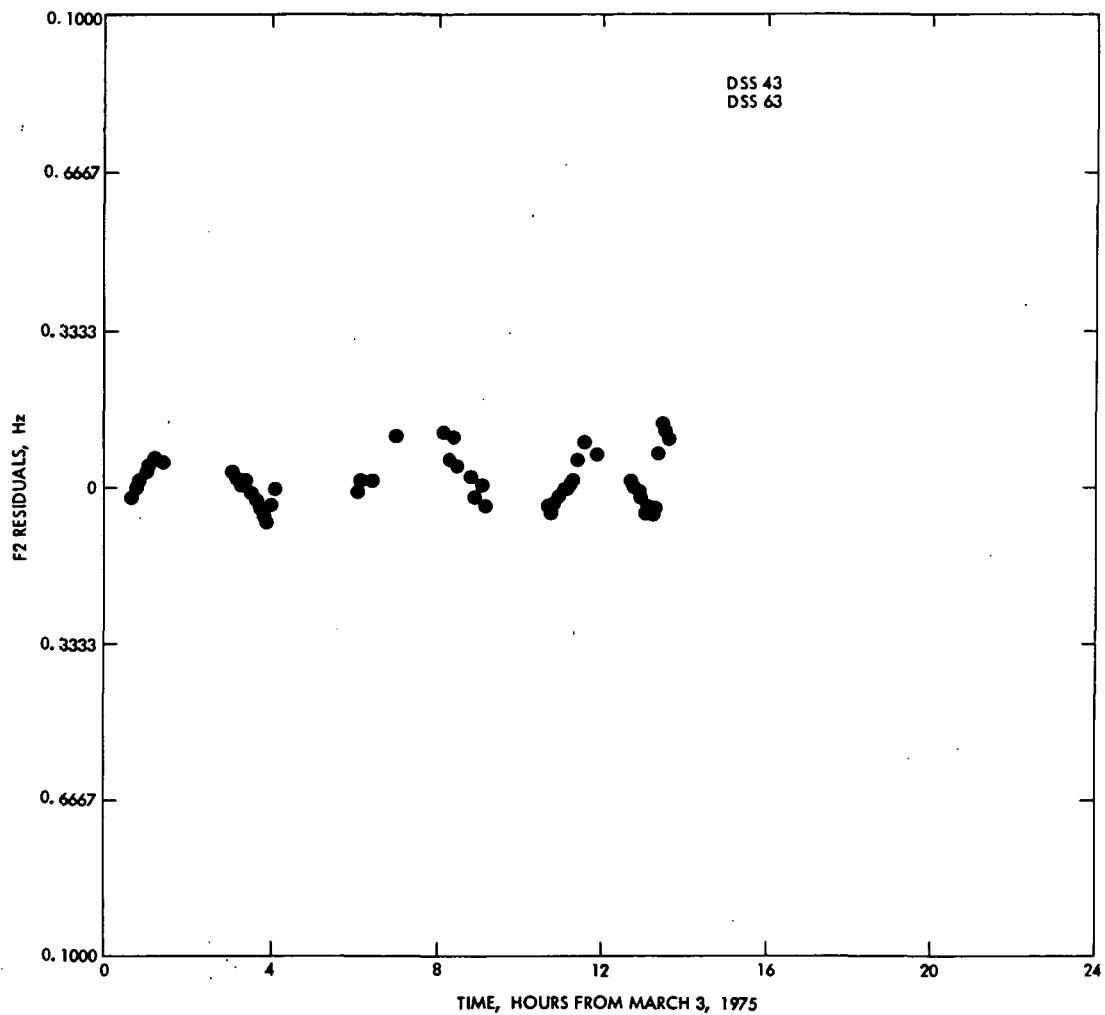


Figure 62. Roll-corrected F2 residuals

2. Philosophy

It was standard practice during the Extended Mission to run a series of orbit determination runs once a week during cruise phases. During critical phases such as preparation for TCMs and encounters, OD fits were done more frequently. Normally the data was updated and validated every Monday as described in the tracking section. The resultant current data file would then be fit on Tuesday night with the Orbit Determination Program. Block time on the 1108 B-string was necessary in order to process the many large ODP cases required.

3. Procedures

a. Software. Orbit determination was performed with two filters: (1) a classical least-squares batch filter, and (2) a batch sequential filter. The batch filter has been the standard orbit determination tool for interplanetary missions in the past. The sequential filter was designed and implemented specifically for use in the Mariner 10 Mission. This effort was undertaken because of the critical orbit determination requirements of Mariner 10. The concern was that the Mariner 10 spacecraft would pass relatively close to the Sun, and the action of solar pressure upon the complicated spacecraft structure might produce nongravitational force signatures that could not be modeled in the batch filter, perhaps confusing its estimation process. Also there was concern regarding the amount of leakage and uncoupling in the attitude-control system and leakage in the propellant system which would contribute to the total stochastic nongravitational force signature (Ref. 16).

A major advantage of the sequential filter is its capability to estimate stochastic parameters as piecewise constant functions during each batch. (The data arc is divided into batches of typically one-day duration. A particular stochastic parameter is treated as being exponentially correlated between batches with correlation time τ . For a further discourse on the theory of sequential estimation see Ref. 17. The mathematical formulation of the Orbit Determination Program is discussed in Ref. 18.

Although the sequential filter was used heavily during the prime mission, the Extended Mission emphasized the batch filter. This condition was largely due to the length of the solar sailing period, when the Orbit Determination Program could not model the rolling spacecraft in order to estimate stochastic forces in the pitch and yaw directions. Previous experience had also shown that the batch filter was relatively insensitive to the levels of stochastic nongravitational accelerations experienced by the spacecraft. Also, there was little danger that the batch filter would misidentify Mercurial gravity harmonics in an encounter phase. The batch filter provided stable solutions adequate for navigation, while reducing manpower demands, cost, and quantity of computer runs.

b. Data. The tracking during the Extended Mission was approximately one-half continuous

coverage and was described in the previous subsection. The primary navigation data types were two-way doppler (F2), nominally sampled at 60-sec intervals, and PLOP ranging. The doppler data was edited and then compressed to a count time of either 300, 600, or 1200 sec, depending on the data arc length and phase (very close to encounter, the count time was retained as 60 sec).

Throughout the Mariner 10 Mission, solutions were made using three data sets: doppler only, doppler and range, and range only. Consistency in the solutions increased the confidence in their validity. Generally, the doppler and range solutions were regarded as being the most powerful.

c. Solution Sets. Each OD solution was in reality a large set of solutions, each estimating a particular parameter set. For the batch filter the following constant parameter sets were estimated:

- (1) Spacecraft state plus other parameters
- (2) Spacecraft state plus station locations
- (3) Spacecraft state plus solar pressure
- (4) Spacecraft state plus attitude control forces
- (5) Spacecraft state plus station locations plus solar pressure
- (6) Spacecraft state plus station locations plus solar pressure plus attitude control
- (7) All parameters including J2

Other parameters include the Mercurial mass and ephemeris when in an encounter phase, and motor burn parameters following a TCM.

Parameter sets for the sequential filter consist of all but (4) and (6) above. The attitude-control forces, i. e., spacecraft accelerations along the three spacecraft axes, were treated as estimative stochastic parameters in each sequential filter run. A priori sigmas of 10-12 km/s² and 10-11 km/s² were used for stochastic parameters, with a batch size of one day and a correlation time of from one to five days.

d. Method. The first Orbit Determination Program run generated during a session would integrate an updated spacecraft trajectory using the best estimate of spacecraft state obtained from the last session. The second run produced a file of data residuals based upon this current trajectory, plus partials of each observable with respect to the total parameter set. This run provided a precise evaluation of all data, particularly the range, and any remaining poor quality points could be removed before proceeding further. Subsequent runs yielded specific trajectory estimates as various functions of data set, parameter set, filter type, and filter a priori parameter uncertainty. Each run was assigned a unique catalog number, recoded and summarized.

Every Orbit Determination Program run required about 65K of computer core. Thus three runs in the 1108B (approximately 170K to 200K of user-available core) would effectively use all of the machine's capacity. Considering the large volume of data to be processed, the number of runs needed, and the large program size and software processing time for each run, it became apparent that this critical work could only be completed using regularly scheduled computer block time. Even so, the entire set of required runs generally consumed between seven and twelve hours of computer time. (The block time was scheduled during evening hours, so as not to impact the general laboratory user significantly.)

4. Results

A calendar of major mission events is shown in Fig. 3 in Sect. II. The spacecraft orbit is shown in Fig. 63 from Mercury I to Mercury III. Orbit determination activities can be broken up into phases and described separately. It is customary to express results in terms of the B-plane parameters, described in Fig. 64.

a. Mercury I to TCM 4. It was decided by the science team to go for a bright-side pass at Mercury II, which would allow a good probability for a dark-side Mercury III pass. The bright-side Mercury II would be excellent for TV, whereas the dark-side Mercury III would be excellent for the magnetic field experiment and celestial mechanics and good for TV.

The determination of the orbit for TCM 4 was aided by the large spacecraft acceleration experienced during the first Mercury flyby. This advantage was somewhat negated, however, by the long mapping time of an entire spacecraft revolution to the next encounter. Another problem was presented by the gradual degradation of the doppler data as the spacecraft was approaching superior conjunction (for example, see Fig. 59). Although the actual doppler gaussian data noise about the mean was not extreme; wavy signatures were developing for quite some time as far back as early March (for example, see Fig. 58). These signatures were correlated with the spacecraft's proximity to the Sun in the sky, perhaps indicating an interaction of the radio signal with charged particles from a solar plasma arm. The danger of such wavy signatures is that they are difficult to edit properly, and they may cause important parameters to be misestimated by the orbit determination filters. Orbit determination accuracy was not, however, a major concern in preparing for TCM 4, since the maneuver would most likely be dominated by execution errors.⁹

Two primary data arcs were examined to prepare for TCM 4: (1) EM - 4 days to EM + 4 days; and (2) EM + 2 days to the latest data

available. The solution finally chosen was from (2). (1) was not especially good for OD due to large associated mapping errors. A 1-km uncertainty in the Mercury I B-plane mapped to a 3000-km uncertainty in the Mercury II B-plane. Thus even a plausible error of 1/2 km at Mercury I mapped into a 1500-km error at Mercury II. Solutions from (1) did, however, serve as useful comparators.

Figure 65 plots the final set of OD solutions available to compute TCM 4. Only data to April 22 was contained in these solutions due to the time constraints imposed by the project to compute, design, and load the maneuver sequence. Solutions among the various parameter sets were quite consistent, and the most faith was placed in the state-only solutions. The final solution chosen was for the sequential filter, F2 + range, 10-12 km/s² a priori uncertainty on stochastic forces (Case 370013) and had the following Mercury II B-plane parameters:

$$B \cdot R = 584,225 \text{ km}$$

$$B \cdot T = 545,020 \text{ km}$$

$$TCA^{10} = 9/19/74 \quad 20^{\text{h}}6^{\text{m}}21^{\text{s}} \text{ GMT}$$

This solution changed very little when data up to TCM 4 became available (Case 400002):

$$B \cdot R = 583,978 \text{ km}$$

$$B \cdot T = 545,119 \text{ km}$$

$$TCA = 9/19/74 \quad 20^{\text{h}}5^{\text{m}}46^{\text{s}} \text{ GMT}$$

Inconsistencies among the various OD runs and 1 σ OD uncertainties were well within the expected 1- σ maneuver execution error of 10,000 km. Figure 66 shows TCM 4 in the Mercury II B-plane.

b. TCM 4 to TCM 5. Superior conjunction occurred midway through this phase, degrading the orbit determination capability by causing high data noise and spurious data signatures. Figure 67 plots the observed 1- σ data noise (for one-minute doppler samples) as a function of time during the superior conjunction phase. Also plotted is the Sun-Earth-probe angle, and the predicted data noise based upon the results of the Mariner 9 superior conjunction. The agreement with the observed noise was good at the limbs of the curve, but not at its peak.

It had been expected that charged particles in the solar corona would affect a radio signal passing through it. The amount of corruption would be proportional to $1/R^4$, where R is the Sun-radio signal distance. The Sun's corona is thought to extend to a SEP angle of about 4 deg. However, the Mariner 10 radio signal was

⁹ TCM 4 would move the spacecraft on the order of 800,000 km in the Mercury II B-plane. In fact TCM 4 was so large, that it was divided up into two segments, TCM 4A and TCM 4B, to avoid engine overheating. See Sect. VII-C-6.

¹⁰ Time of closest approach (Ephemeris Time).

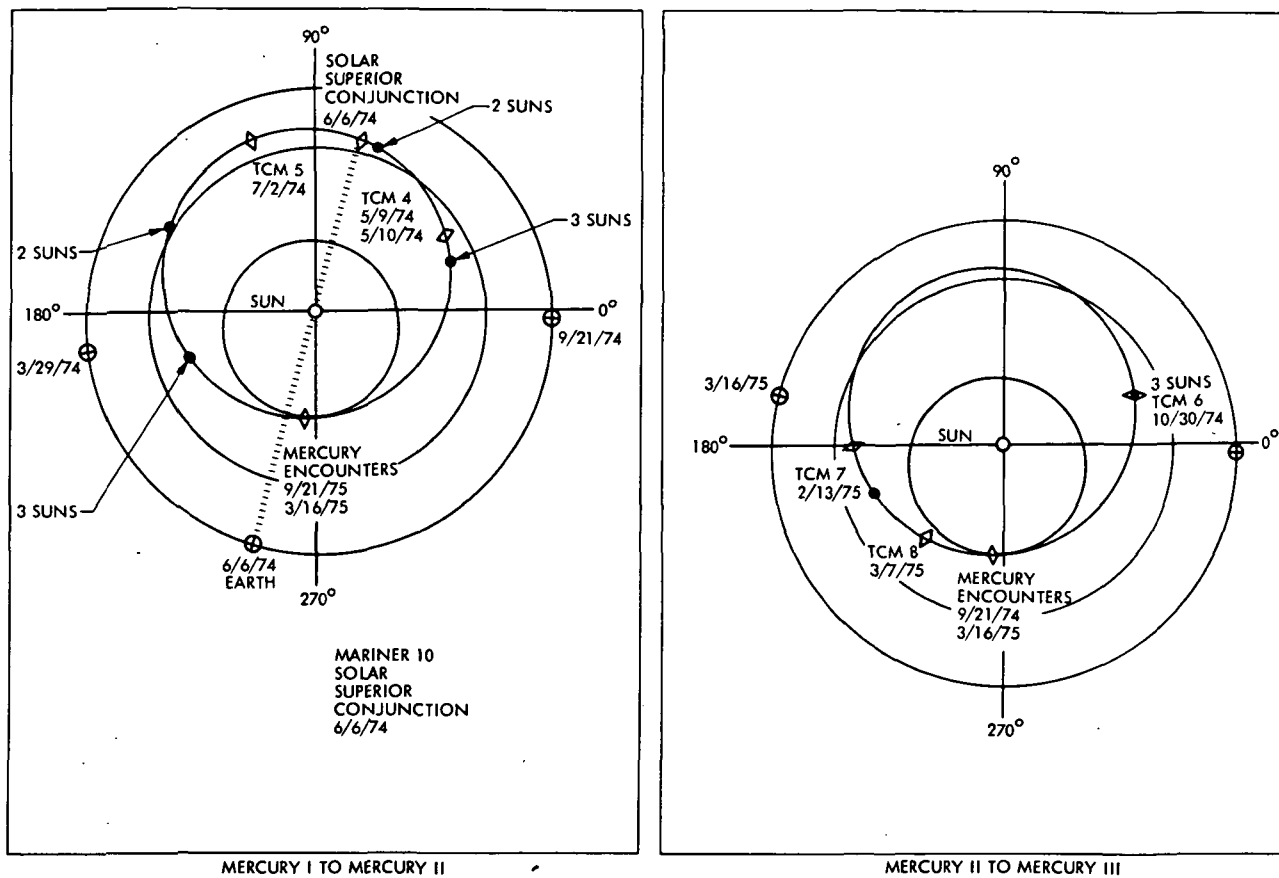
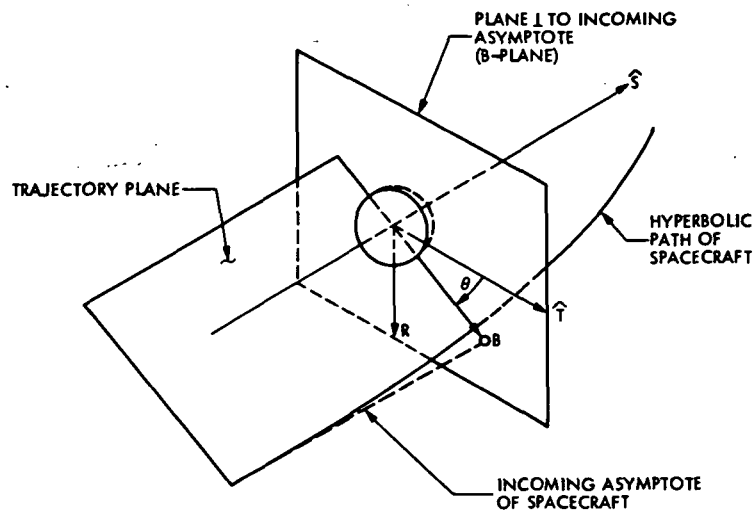


Figure 63. Significant navigation events

ORIGINAL PAGE IS
OF POOR QUALITY



- B MISS PARAMETER ($B \perp \hat{S}$), DISTANCE IN B-PLANE FROM CENTER OF PLANET TO INCOMING ASYMPTOTE
 S PARALLEL TO INCOMING ASYMPTOTE
 T PARALLEL TO ECLIPTIC PLANE AND \perp TO S
 $R = \hat{S} \times \hat{T}$
 θ ORIENTATION OF B WITH RESPECT TO T

Figure 64. Definition of B-plane

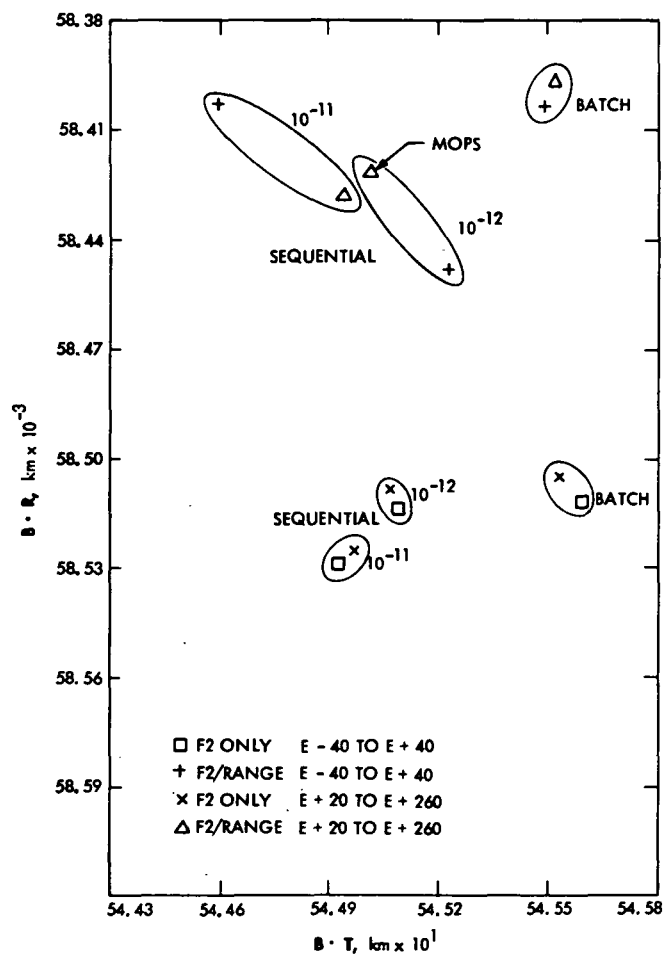


Figure 65. Mercury II B-plane solutions

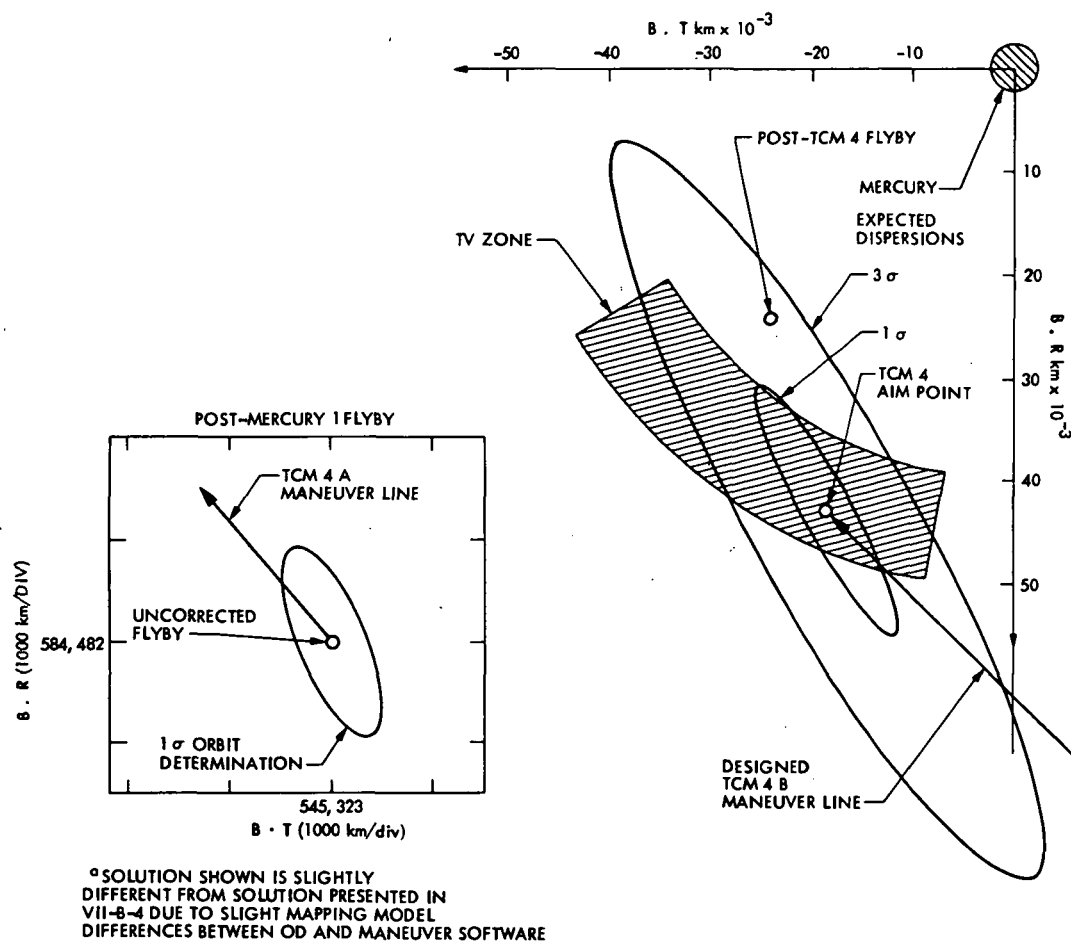


Figure 66. TCM 4 in Mercury B-plane

seriously corrupted at SEP angles greater than ten degrees.

TCM 5 in the Mercury II B-plane is shown in Fig. 68. The solution passed on to the Maneuver Operations Program System (MOPS) to calculate TCM 5 was limited to about one month of tracking data (from TCM 4 to June 6, 1974). Although the associated OD error ellipse was fairly large, on the order of 1200 km x 400 km, this was not a critical consideration, since the acceptable science zone was extremely large. The ODP case passed on to MOPS used the batch filter, F2 + range data, and estimated state only. The Mercury II B-plane parameters (pre-TCM 5) were (Case 450015):

$$B \cdot R = 24,061 \text{ km}$$

$$B \cdot T = -24,024 \text{ km}$$

$$TCA = 9/21/74 \quad 21^{\text{h}}46^{\text{m}}16^{\text{s}} \text{ GMT}$$

This solution proved to be extremely close to the best solution eventually available, which was based on data up to TCM 5 (Case 490001):

$$B \cdot R = 24,112 \text{ km}$$

$$B \cdot T = -23,983 \text{ km}$$

$$TCA = 9/21/74 \quad 21^{\text{h}}48^{\text{m}}37^{\text{s}} \text{ GMT}$$

c. TCM 5 to Mercury II. This was a long cruise phase, relatively undemanding for orbit determination. The OD group's major responsibility in this period was to provide the science team with a trajectory prediction with which to plan the TV camera pointing strategy. Because of the large encounter distance at Mercury II, a precise estimate of trajectory was not needed. An acceptable trajectory estimate was passed on to the Science Team, based on data (F2 and range) from TCM 5 to August 5, 1974. State only was estimated using the batch filter. This case (530003) showed good stability among its various estimated parameter sets and good consistency with other data arcs examined, having Mercury II B-plane parameters of

$$B \cdot R = 32,753 \text{ km}$$

$$B \cdot T = -38,585 \text{ km}$$

$$TCA = 9/21/74, \quad 20^{\text{h}}59^{\text{m}}46^{\text{s}}.9 \text{ GMT}$$

This solution is quite close to the current best estimate of the flyby point which was based on data (F2 only) from EM 3 - 4 days to EM + 4 days. For this run the batch filter was used, estimating state, station locations and Mercurial mass. The Mercury II B-plane parameters are found to be (Case 600010):

$$B \cdot R = 32,779 \text{ km}$$

$$B \cdot T = -38,690 \text{ km}$$

$$TCA = 9/21/74, \quad 20^{\text{h}}59^{\text{m}}44^{\text{s}}.9 \text{ GMT}$$

d. Mercury II to TCM 6. Orbit determination for TCM 6 was complicated by the solar

sailing mode, which began on Oct. 6, 1974. As described earlier, the rolling spacecraft introduced an extraneous sinusoidal signature into the data. It was not clear at this point how such an unmodeled signature would affect the orbit estimation process (subsequently the program ROLL/TORQUE was developed to model the roll signature as described in Sect. VII-A-7). Thus increased reliance was placed upon solutions containing only near Mercury II encounter data, since (1) planetary bending of the spacecraft trajectory would act as an orbit determination aid, (2) the large encounter distance minimized mapping errors - 1 km error at Mercury II mapped to only about 250 km at Mercury III, and (3) these data sets did not contain any roll signatures. Also TCM 6 would be a large maneuver, dominated by maneuver execution errors, and pinpoint OD was not needed. Thus the safest OD estimates would be more desirable.

Many different data arcs were examined, but the most confidence was placed in the arc from EM 3 - 4 days to EM 3 + 4 days. Figure 69 shows the Mercury III B-plane solutions presented at the TCM 6 maneuver conference. The EM 3 - 4 days - EM 3 + 4 days solutions all show good consistency as well as good agreement with a case containing data to Oct. 7, 1974. The solution chosen as the best (Case 600010) estimated state, station locations and Mercurial mass, and had Mercury III B-plane parameters of

$$B \cdot R = 244,583 \text{ km}$$

$$B \cdot T = 102,718 \text{ km}$$

$$TCA = 3/16/75, \quad 2^{\text{h}}13^{\text{m}}31^{\text{s}} \text{ GMT}$$

Figure 70 shows TCM 6 in the Mercury III B-plane.

e. TCM 6 to TCM 7. The purpose of TCM 7 was to correct the maneuver and OD errors associated with TCM 6 to bring the spacecraft to an optimal flyby point for science at Mercury III. The magnetic field experiment had top priority, and since the value of its return was proportional to $1/B^3$, it was desired to come as close to Mercury as possible without actually impacting.

The introduction of the solar sailing mode caused a major modification to the precision trajectory program, DPTRAJ, used by both the ODP and the maneuver analysis program, MOPS. Two distinct modifications were required. First the existing solar pressure model was not capable of modeling the forces acting on the spacecraft with a continuous roll rate. Due to the configuration of the spacecraft, in particular the tiltable solar panels, solar pressure produces forces which are both along and normal to the spacecraft sun-line. When the spacecraft is stabilized in roll, the normal forces act on inertial direction which changes slowly due to the orbital motion of the spacecraft. However, with a continuous roll rate, the normal forces change direction sinusoidally. Since the motion was fast with respect to the orbital motion, the normal forces tended to cancel. Thus the solar pressure model was modified to allow the normal forces to be set to zero during specified periods. With this modification, trajectories containing

both rolling and non-rolling periods could be handled.

The second modification involved the tables specifying the orientation of the solar panels and the high-gain antenna. Under normal operating conditions the orientation of these appendages changed only infrequently and, accordingly, only limited tables had been provided within DPTRAJ to describe the various positions. However, the process of controlling the roll rate in the solar sailing mode demanded that these orientations be changed more frequently, and a major effort was required to increase the size of the tables. Due to the structure of DPTRAJ, this turned out to be a more complex change than the change to the solar pressure model.

There was considerable concern that the rolling spacecraft signature introduced into the data by solar sailing might seriously affect the OD capability. As mentioned earlier, the program ROLL/TORQUE was developed to remove this signature as best as possible. However, the extremely long data arc available during this phase, describing 180 deg of central angle travel, reduced OD errors to a very small level (Fig. 71). Both long-arc simulations and actual data solutions showed very small perturbations between uncalibrated and roll-calibrated data — few tens of kilometers at most.¹¹

A separate effort was also undertaken to estimate the orbit using differenced doppler data with a technique known as QVLBI (quasi-very long baseline interferometry).¹² The technique differences two-way and three-way doppler data being received simultaneously and hence has the advantage of removing short-term nongravitational accelerations affecting the spacecraft. The results of this effort agreed favorably with the results of the OD team (using F2 and range).

Thus an OD solution of high confidence could be passed on to the Maneuver Analysis Team. The solution regarded as the best was for the batch filter, uncalibrated data (F2 + range) from TCM 6 to January 26, 1975, estimating state only. This case (750006) had the following Mercury III B-plane parameters:

$$B \cdot R = -6926 \text{ km}$$

$$B \cdot T = 3644 \text{ km}$$

$$TCA = 3/16/75, 22^{\text{h}}44^{\text{m}}35^{\text{s}} \text{ GMT}$$

f. TCM 7 to TCM 8. This period was the most challenging one of the mission for the orbit determination team. TCM 7 had malfunctioned somewhat, and many orbit solutions shortly after TCM 7 were predicting impacts with Mercury (Fig. 72). Hence it appeared that another maneuver might be needed to back the spacecraft away

from the planet. Orbit determination was critical, and very difficult, during this phase due to (1) the short data arc available, (2) the roll signature in the data, (3) limited coverage due to the high priorities of competitive missions (as well as deep space station reconfigurations), (4) absence of ranging during much of this period due to equipment reconfigurations and malfunctions at DSS 63, and (5) Mariner 10's weakening signal strength while on its low-gain antenna. Real-time negotiations were carried out with the DSN to supplement the tracking coverage during this critical phase.

When the decision point was reached whether or not to perform TCM 8, many orbit solutions were actually impacting, or showing an unacceptably high probability of impact (several of these solutions are shown in Fig. 72). Thus, although TCM 8 implied some risk to the spacecraft, it was necessary to move the orbit farther from the planet so as to reduce the impact probability.

The estimate thought to be the best at this time was for the batch filter, data from TCM 7 to March 4 (F2 plus range), estimating state only. This solution was roughly in the middle of the group of solutions then available and also clustered with several others. The estimate predicted a probability of impact of about 31 percent and had the following Mercury III B-plane parameters (Case 870003):

$$B \cdot R = -2600 \text{ km}$$

$$B \cdot T = -680 \text{ km}$$

$$TCA = 3/16/75, 22^{\text{h}}39^{\text{m}}42^{\text{s}}.8 \text{ GMT}$$

g. TCM 8 to Mercury III. TCM 8 is shown in the Mercury III B-plane in Fig. 75. TCM 8 appeared to have been executed nominally. The science team had an adequate trajectory for science sequence planning. The mission of the navigation team was not complete. All that remained was to process routine orbits, and to evaluate the effectiveness of navigation after the Mercury III encounter.

The navigation team received a brief scare on the morning of the third encounter with Mercury, as several Orbit Determination Program cases were indicating impacts (the solutions were on the order of a few tens of kilometers below the surface at closest approach). At this time only data to EM - 9 hours was available (roughly 300,000 km from Mercury). The spacecraft still had not undergone appreciable perturbation from Mercury's gravity field to help determine the orbit and the available data arc was very short. The great dispersions in the solutions — about 250 km — plus the large statistical uncertainty ($\sigma_{B \cdot R} \sim 150 - 200 \text{ km}$) caused the Orbit

¹¹In practice, a disadvantage of roll-calibration was that during periods with frequent high-gain antenna and solar panel redeployments or high spacecraft roll period, not enough Canopus crossings were observed to model the spacecraft roll motion. Also as mentioned earlier in Sect. VII-A-7, due to the complexity of the real model, ROLL/TORQUE generally removed only 60 to 90% of the total signature.

¹²This study was performed by H. Siegel and C. Chao of JPL.

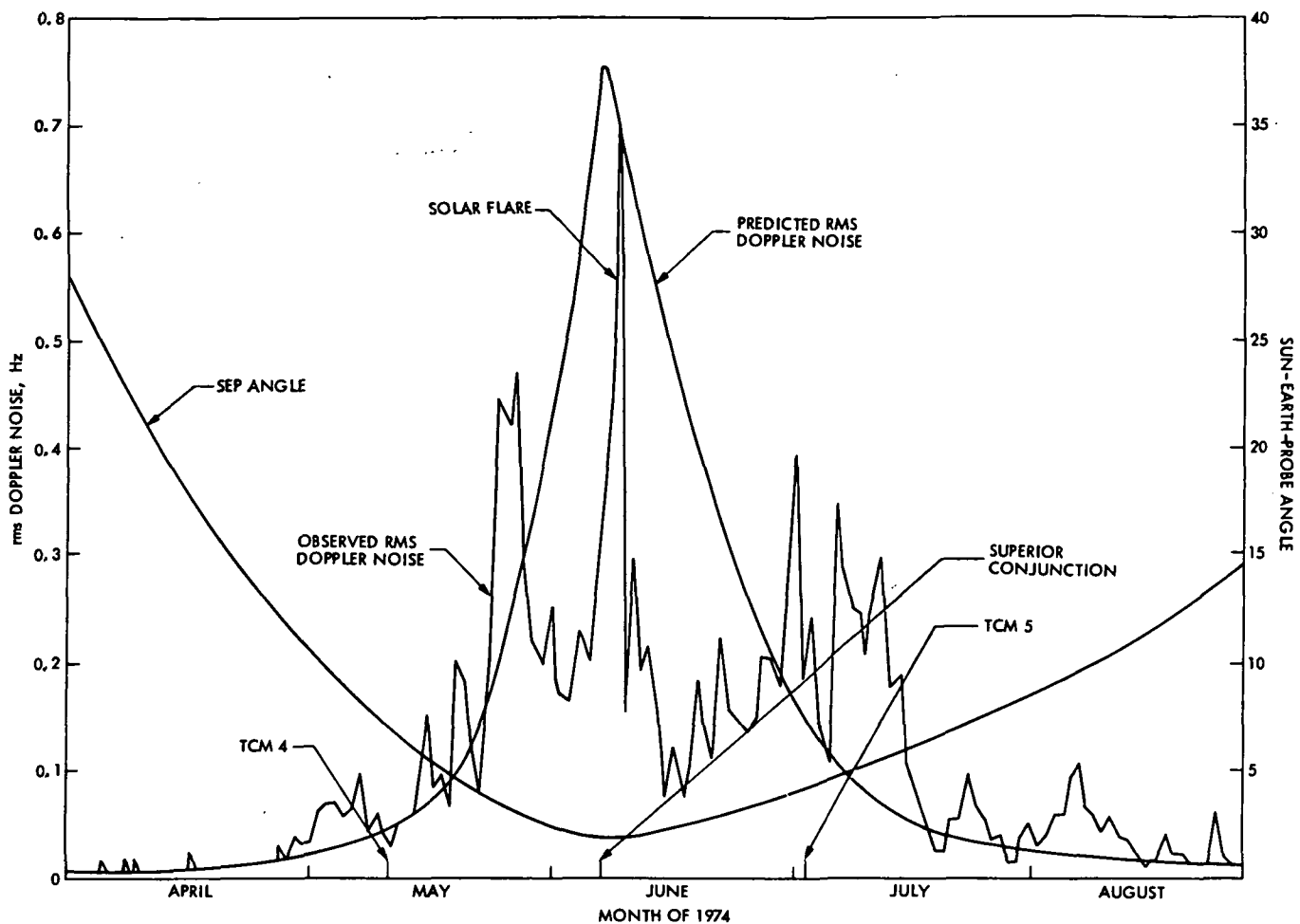


Figure 67. Doppler noise versus Sun-Earth-probe angle

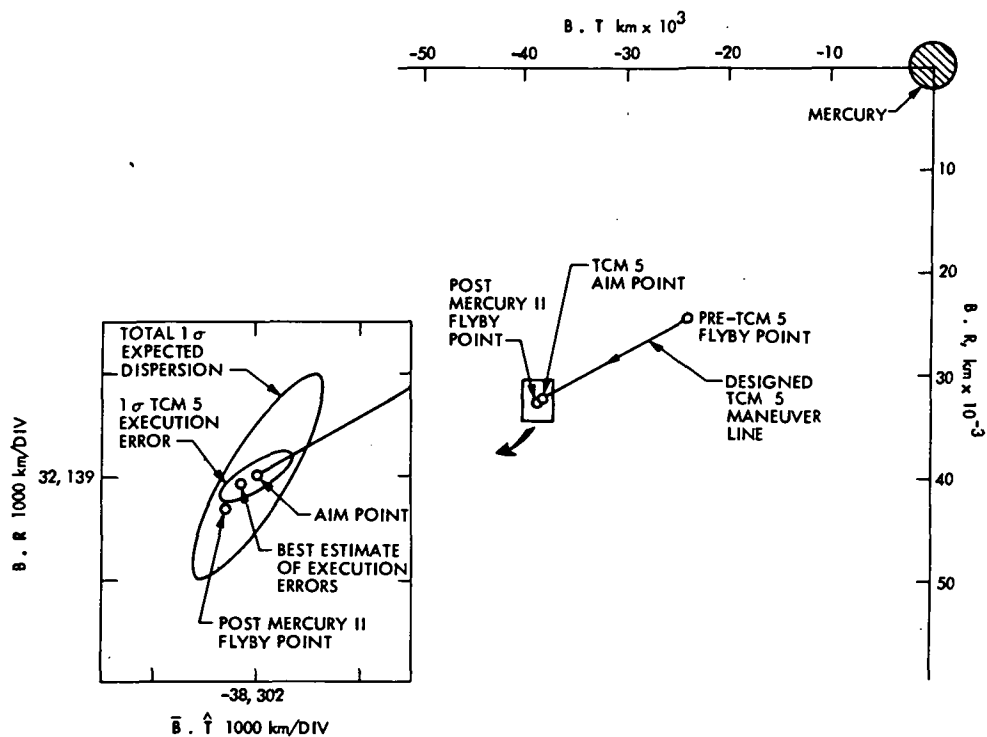


Figure 68. TCM 5 in Mercury II B-plane

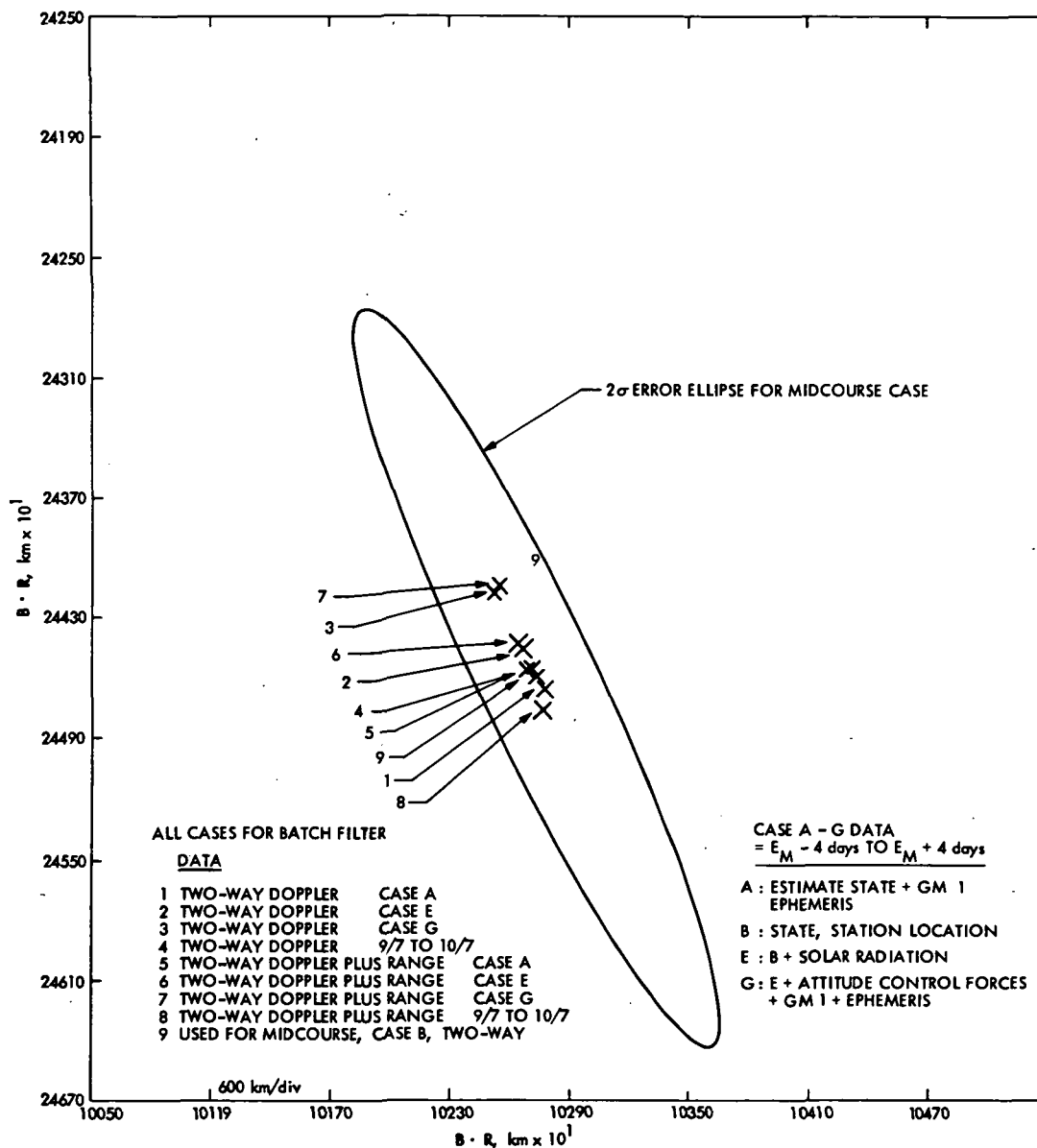


Figure 69. Pre-TCM 6 Mercury B-plane

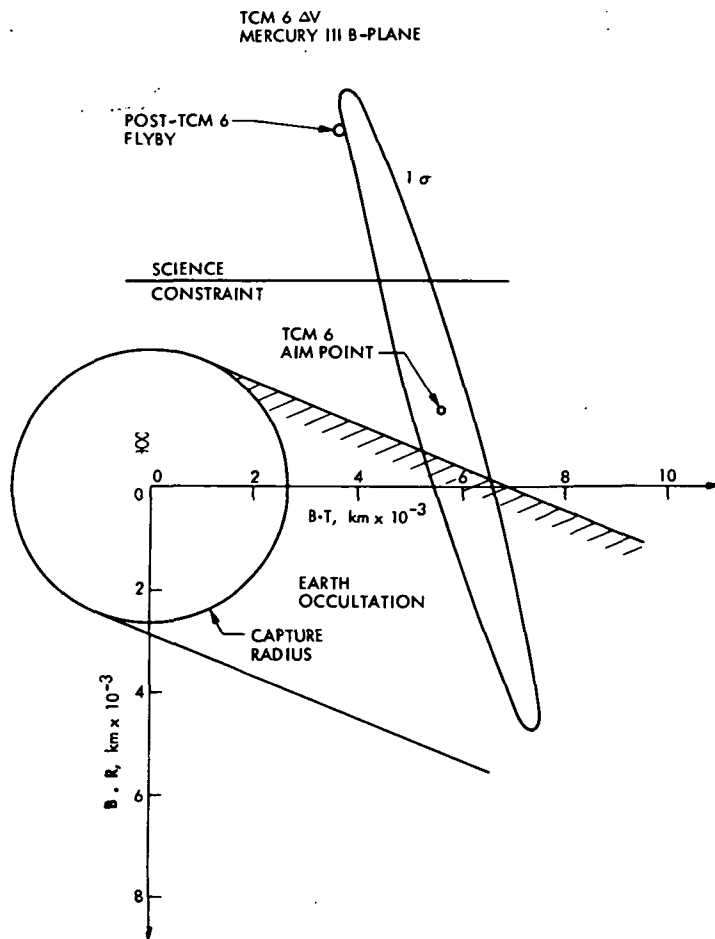


Figure 70. TCM 6 in Mercury III B-plane

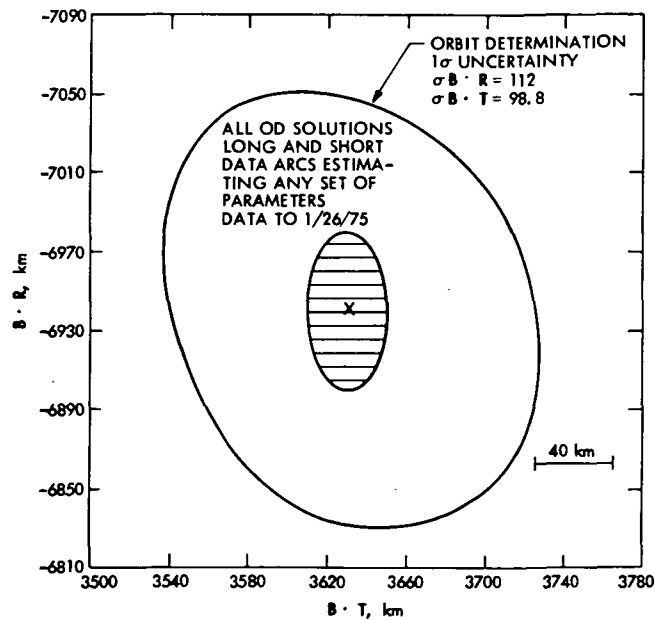


Figure 71. TCM 7 orbit determination in Mercury III B-plane

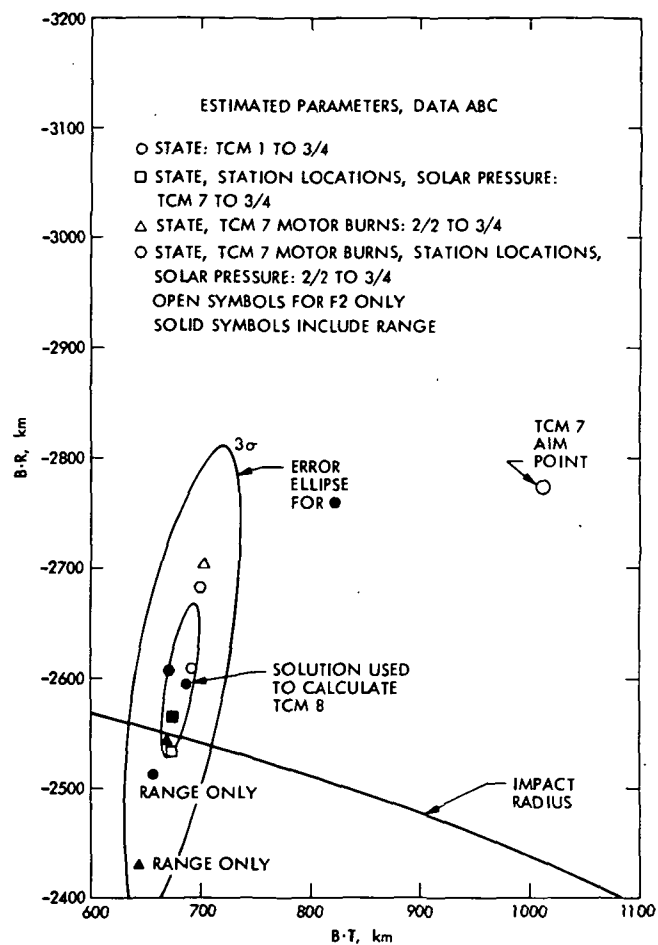
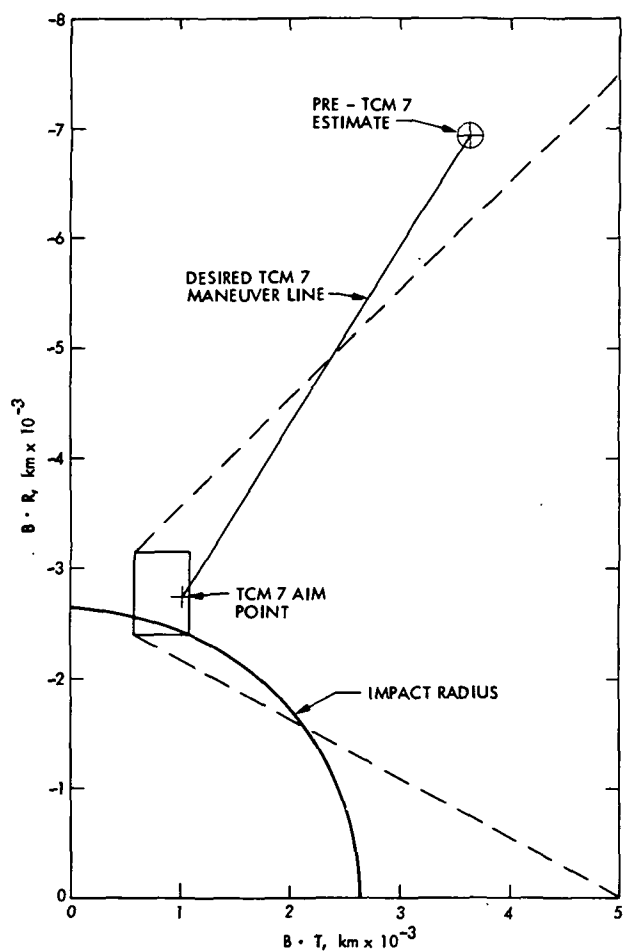


Figure 72. TCM 7 post-maneuver estimates in Mercury III B-plane

Determination Team to place little confidence in them.

After the encounter was successfully completed, near-encounter data was used to obtain an accurate flyby point. The current best estimate for this point in the Mercury III B-plane is (Case 980002):

$$\left. \begin{array}{l} B \cdot R = -2780.0 \text{ km} \\ B \cdot T = 1016.0 \text{ km} \end{array} \right\} B = 2959.8 \text{ km}$$

$$TCA = 3/16/75, 22^{\text{h}}40^{\text{m}}10.02^{\text{s}} \text{ GMT}$$

This batch filter run contained data from EM 3 - 1 day to EM 3 + 4 days (F2 only) and estimated state, station locations, ephemeris and Mercurial mass. All solutions with this data set are within a few tenths of a kilometer of each other.

5. Operational Recommendation for Real Time Range Evaluation

Highly accurate range fits were only possible with the Orbit Determination Program. Since orbit fits with the Orbit Determination Program were generally done on a weekly basis, subtle failures in the ranging equipment at a particular deep space station, or errors in the ranging calibration procedures, could go unnoticed for some time. It would be of great benefit to the Navigation Team to have available a software program which could fit and evaluate range points in real time. The program should operate from the current probe ephemeris tape. It should have the capability to include range calibrations, and to plot all desired range residuals both before and after calibrations. The user should have the flexibility of using the software from a demand device or in a batch processing mode. The primary user inputs would be "to" times, range observable values (available immediately after end of acquisition from MOAT) and the number of components. If calibrations are to be included, they would be handled as in the program GORC, described in Sect. VII-A-5.

D. Maneuver Analysis

1. Introduction

The completion of the primary mission culminated in the gathering of a wealth of scientific data, the quality of which exceeded all expectation. Attention was then focused on an extended mission for additional encounters with Mercury which would serve to enhance and/or verify the scientific data collected at the first encounter. The science objectives for the Extended Mission were, by necessity, determined in flight, since these objectives were largely dependent on both the science return of the primary mission and the state of the spacecraft after the Mercury I

encounter. In the discussion to follow, a maneuver strategy is developed in light of the demands imposed by prevailing engineering constraints and the science objectives for the extended mission.

2. Maneuver Constraints

Two constraints played a primary role in the development of maneuver strategies for the Extended Mission. The first and most demanding constraint was imposed by the necessity to avoid conditions where the roll gyro oscillation would reoccur, since the resultant loss of attitude-control gas would reduce the supply below the level required for attitude stabilization during cruise and encounter. This constraint required that all trajectory correction maneuvers made at heliocentric ranges less than 2 suns would be limited to Sun-line (radial) maneuvers which have only limited correction capability.¹³ Maneuvers at heliocentric ranges greater than 2 suns could be unconstrained. The rationale for relaxing this constraint was based on the results of TCM 2, performed in the vicinity of 2 suns, which showed no roll gyro oscillation.

The second constraint was the available ΔV capability of the spacecraft propulsion subsystem. Prelaunch estimates of the total corrective capability was 122 m/s. However, inflight estimates showed that an additional 4 m/s could be made available. Since 27 m/s had been used to achieve the first Mercury encounter, 100 m/s were available for the remainder of the mission.

Although not a hard constraint, it was deemed highly desirable to target each maneuver such that a productive Mercury flyby would result. This precautionary strategy was adopted in order to compensate for any additional anomalies that might have precluded the execution of subsequent maneuvers. As a result of this strategy, the maneuvers were targeted to fly by points which maximized the delivery probabilities into acceptable regions as opposed to flyby points which minimized the overall ΔV requirements.

3. Science Objectives

Based on an evaluation of the science return from the first Mercury encounter, two mutually exclusive target zones were defined. The zones were:

Zone I: Television Experiment. This zone required a southern latitude bright side passage at $40,000 < B < 50,000 \text{ km}$ and $150 \text{ deg} > \theta > 105 \text{ deg}$. Aim points in this region provided coverage of the unphotographed region between the portions of Mercury seen on the incoming and outgoing legs on the first encounter. Further, these trajectories would improve detail in various regions where the existing photographs were highly foreshortened.

¹³ In the cruise attitude, the thrust vector of the spacecraft is directed toward the Sun. Thus, without a pitch turn, only radial velocity changes could be applied. Radial maneuvers are restrictive due to the reduced set of flyby errors that can be corrected. The only controls available are the magnitude of the maneuver and the time of engine burn.

Zone II: Fields and Particles Experiment.

This zone required a dark-side passage at $B < 5,000$ km and $-30^\circ < \theta < 30^\circ$. Aim points in this zone would provide expansion and/or confirmation of fields and particles observations obtained during the first encounter.

4. Sunline Maneuver Strategy

Based on the definition of the two mutually exclusive science zones, a maneuver strategy was designed to achieve either of the two zones with the stipulation that the TV experiment would be given first priority at Mercury II. However, in the event of a camera failure, for example, trajectories targeted for aim points in the TV zone could be retargeted for the fields-and-particles zone. This strategy adhered to the sunline constraint for early maneuvers in regions where the solar intensity was greater than two suns. Total attitude freedom was allowed for maneuvers where the solar intensity was less than two suns.

Based on these targeting objectives and maneuver constraints, the most efficient Sun-line strategy in terms of minimum propellant cost required at least two maneuvers. The Sun-line maneuver (TCM 4) would provide the majority of the B-plane correction required to reach the vicinity of the TV zone. A second unconstrained maneuver (TCM 5) would then provide the remaining correction to achieve a flyby in either the TV zone or the fields and particles zone. Analysis of this strategy showed that aim points in the television zone could be achieved with two maneuvers for a mean velocity of not more than 95 m/s. However, aim points in the fields-and-particles zone would require a third maneuver in order to reduce the delivery dispersions to an acceptable level. The resulting three-maneuver strategy required a mean ΔV in excess of 100 m/s. The two maneuver strategy to the TV zone satisfied all of the science requirements with the exception of arrival time. A requirement for the TV experiment was to arrive at Mercury II over the Goldstone DSCC in California near the time for maximum elevation angle 20:30 GMT on Sept. 21, 1974, in order to provide the highest possible data quality during the encounter period. However, the sunline maneuver strategy would allow an arrival time no later than 17:00 GMT. The resulting 3.5-h discrepancy would have seriously compromised the quality of the received data.

5. Unconstrained Maneuver Strategy

In light of the limitations imposed by constraining TCM 4 to be along the sunline, a parallel study was conducted to develop a maneuver strategy assuming that the sunline restriction could be removed for a period of time in the vicinity of 3 suns. This study showed that the removal of the sunline constraint allowed the achievement of all the science objectives at Mercury II, including the capability to retarget from the TV zone to the fields and particles zone. A separate attitude-control gas analysis showed that a proposed conservation scheme would provide enough gas for a Mercury III encounter assuming that gyro oscillation did not occur during the unconstrained maneuver.

The maneuver and attitude-control gas studies provided the impetus for conducting a roll-attitude structural interaction test. This test consisted of performing a small roll turn with the solar panels in the maneuver configuration. The outcome of this test showed no gyro oscillation in roll, and it was decided to attempt TCM 4 unconstrained.

6. TCM 4

TCM 4 was performed in two segments with the solar panels in the gyro test configuration. The first segment, TCM 4A, was performed on May 9, 1974, 41 days past Mercury I encounter, at a solar intensity of approximately 3.1 suns as shown in Fig. 63. The second segment, TCM 4B, was performed the next day, May 10, 1974. The requirement to segment the maneuvers was imposed by a hardware soakback temperature constraint, limiting the allowable engine burn time for the first segment.

Selection of the TCM 4 epoch had large impact on the ΔV requirements for the Extended Mission. The final selection was based on two considerations. First was the desire to provide some safety margin in satisfying the three suns thermal constraint, and second was the desire to minimize the required velocity. Fortunately, the epoch imposed by the thermal constraint (May 5, 1974) and the epoch for minimum velocity were nearly coincident. Consequently, negligible propellant penalty resulted from this choice.

Aim-point selection for TCM 4 was based on the desire to maximize the probability of an acceptable return from the television experiment in the event that a second maneuver could not be performed. Thus the aim point was chosen to maximize the intersection of the previously defined TV zone and the expected post-maneuver dispersions. This aim point did not preclude the retargeting to the field and particles zone on the next maneuver.

Table 12 presents a summary of the B-plane conditions for all maneuvers on the Extended Mission, including flybys. These data present the Mercury encounter conditions on the uncorrected trajectory (premaneuver nominal) and the predicted (postmaneuver nominal) flyby conditions, based on perfect execution of the commanded maneuver. The commanded maneuver differed from the ideal maneuver due to quantization errors in the two turns and the thrust duration. The mechanization of the spacecraft was such that the turns and thrust duration were controlled by a digital timer which restricted the turn angles and thrust duration to discrete values. In order to reduce the effect of the resulting maneuver error, values of the turns and thrust duration were chosen to minimize an error criterion. Typical criterion were errors in the miss at the forthcoming encounter and the projected ΔV at the next maneuver epoch.

Also presented on Table 12 are the standard deviations in the parameters describing the Mercury encounter postmaneuver. The premaneuver statistics reflect only the uncertainty in the orbit determination at the time of the maneuver while the post-maneuver a priori statistics

Table 12. Trajectory correction maneuver and flyby summary for the Extended Mission

Event	B-plane conditions	Premaneuver ^b		Postmaneuver ^{a,c}	
		Nominal ^a	Standard deviation	Nominal ^a	Standard deviation
TCM 4	B · T	545,323 km	408 km	-18,631 km	6894 km
	B · R	584,482 km	961 km	42,965 km	12438 km
	TCA	9/19/74 20:05:12	240 sec	9/21/74 20:19:41	3798 sec
TCM 5	B · T	-24,024 km	230 km	-38,308 km	616 km
	B · R	24,061 km	920 km	32,143 km	1067 km
	TCA	9/21/74 21:46:16	122 sec	9/21/74 20:58:17	150 sec
Flyby Mercury II	B · T			-38,690 km	14 km
	B · R			32,779 km	7 km
	TCA			9/21/74 20:59:45	0.8 sec
TCM 6	B · T	102,727 km	953 km	5557 km	2017 km
	B · R	244,578 km	2044 km	-1446 km	6208 km
	TCA	3/16/75 2:13:31	540 sec	3/16/75 22:20:52	1740 sec
TCM 7	B · T	3644 km	130 km	1010 km	123 km
	B · R	-6926 km	72 km	-2767 km	147 km
	TCA	3/16/75 22:43:50	22 sec	3/16/75 22:39:51	23 sec
TCM 8	B · T	680 km	18 km	992 km	18 km
	B · R	-2600 km	100 km	-2665 km	100 km
	TCA	3/16/75 22:38:56	16 sec	3/16/75 22:40:11	16 sec
Flyby Mercury III	B · T			1016 km	1.0 km
	B · R			-2780 km	1.0 km
	TCA			3/16/75 22:39:24	0.10 sec

^aTCA in GMT. Small differences between these results and the results presented in Sect. VII-B are due to mapping techniques.

^bRepresents nominal encounter conditions for the uncorrected trajectory at the time of the maneuver. Statistics contain uncertainties in orbit determination only.

^cRepresents targeting conditions for the maneuver. Statistics contain uncertainties in both orbit determination and maneuver execution. Flybys represent postmaneuver conditions obtained from tracking data through planet encounter.

**ORIGINAL PAGE IS
OF POOR QUALITY**

include this uncertainty plus the statistical errors in the maneuver execution.

Table 13 presents a summary of the parameters (roll, pitch, turn, and magnitude of the maneuver) for all maneuvers on the Extended Mission. Quantities associated with the nominal parameters are, the computed values, the commanded values (which differ from the computed values by the quantization errors previously mentioned), and the best estimate of the actual parameter.

The best estimate of the parameter was obtained using the Orbit Determination Program and estimating the maneuver parameters along with the orbit using tracking data on both sides of the maneuver. The fourth column of Table 13 lists the a priori standard deviations which were assigned to the various maneuver parameters based on system models and preflight testing. The fifth column relates the difference between the best estimate of the maneuver and the commanded maneuver in terms of the a priori standard deviations in the previous line. Column six gives a measure of the uncertainty in line 3.

Table 12 presents a summary of the flyby conditions for TCM 4 at Mercury II. Figure 66 shows TCM 4 in the Mercury II B-plane relative to the TV zone. Shown are the post-maneuver aim point and a priori statistics. Also shown in Fig. 66 (see inset) is the uncorrected flyby point and associated 1- σ orbit determination statistics. As may be seen from Table 12 and Fig. 66, the accuracy of TCM 4A and TCM 4B were limited by execution errors. This assessment is verified in the discussion of TCM 5 results.

Table 13 presents a summary of the maneuver parameters for TCM 4A and TCM 4B. Comparing the errors in the parameters with those of previous unconstrained maneuvers, it may be seen that both the ΔV and pitch errors were 1 σ or less. However, the roll error was dominant at about 1.5 σ .

The impact of the Mercury I flyby on the ΔV requirements for the Extended Mission is reflected in the magnitude of TCM 4 (77.5 m/s). Prior to Mercury I encounter, it was shown that aim points in the vicinity of the TV zone at Mercury II could be targeted in two unconstrained maneuvers for a mean velocity of no less than 25 m/s. However, the maneuver sequence for this strategy was based on the assumption that the aim point at Mercury I would be located near the free return contour. Based on the best estimate of the Mercury I flyby point immediately following TCM 3, the magnitude of the post Mercury I maneuver was found to be in excess of 65 m/s. However, it was a project decision not to jeopardize the success of the baseline mission in favor of the ΔV requirements for the extended mission by performing a fourth maneuver prior to Mercury I encounter.

7. TCM 5

The selection of the aim point for TCM 5 involved a tradeoff between the coverage for the TV experiment on the Mercury II encounter and the propellant required to achieve a fields and

particles zone on the Mercury III encounter. While the premaneuver flyby point (see Table 12 and Fig. 66) at $B = 34,000$ km, $\theta = 135$ deg satisfied the scientific objectives of the TV experiment, a Monte Carlo analysis showed that the ΔV required to accomplish 99% of the sample missions exceeded the 22 m/s remaining.

Further analysis showed that the maximum return from the television experiment required an aim point at $B = 50,000$ km, $\theta = 135$ deg and that the 99% ΔV requirement would be less than 22 m/s for $B = 50,000$ km, if the orientation was changed to $\theta = 140$ deg. This compromise was made and the aim point at Mercury II was chosen to be $B = 50,000$ km and $\theta = 140$ deg.

TCM 5 was performed on July 2, 1974, 95 days after Mercury I encounter as shown in Fig. 63. Selection of TCM 5 epoch reflected the following considerations:

- (1) The desire to minimize propellant cost
- (2) The requirement to redetermine the orbit following TCM 4
- (3) The requirement to satisfy the 2 suns constraint (this constraint was satisfied in the period May 30 to Aug. 1, 1974)
- (4) The desire not to interfere with experiments being conducted during the solar conjunction period from May 23 to July 1, 1974.

Considering the two weeks of tracking required to redetermine the orbit following TCM 4 and the negligible propellant penalty as a function of epoch in the interval from May 23 to July 7, it was decided to perform TCM 5 as soon as possible after the exit of solar conjunction.

Table 12 presents a summary of the flyby conditions for TCM 5 at Mercury II. Based on the a priori delivery dispersions at the time of TCM 4, the difference between the flyby point prior to TCM 5 and the predicted flyby point after TCM 4 represents a 2- σ B-plane miss at Mercury II as shown in Fig. 66. This result compares favorably with the best estimate of TCM 4 as shown in Table 13, indicating that orbit determination errors at the time of TCM 4 were small compared to TCM 4 execution errors.

The maneuver parameters for TCM 5 are summarized in Table 13. Table 13 shows that the errors in all parameters were less than 1 σ .

Figure 68 shows TCM 5 in the Mercury II B-plane. Shown are the post-maneuver aim point, the premaneuver flyby point and the Mercury II flyby computed from tracking data through Mercury II encounter. Based on initial engineering telemetry observations of the doppler shift during the maneuver and the results of the first two weeks of tracking following the maneuver, the flyby at Mercury II was deemed successful and a final trim maneuver was not considered.

8. Mercury II Flyby

The encounter parameters for the Mercury II flyby are presented in Table 12. The flyby was

Table 13. Trajectory correction maneuver parameter summary for the Extended Mission

Event	Parameter ^a	Computed value	Commanded value	Best estimate of actual value		Maneuver execution σ (A priori)		Maneuver execution σ A posteriori $ (3) - (2) / (4)$		σ In estimate of actual value
		(1)	(2)	(3)		(4)		(5)		(6)
TCM 4A	Roll	-181.34	-181.43	49.542		1.090 deg		1.70		0.057 deg
	Pitch	25.600	25.607	127.597		0.471 deg		0.30		0.331 deg
	ΔV	50.000	49.998	49.865		1.130 m/s		0.1		0.172 m/s
TCM 4B	Roll	-178.51	-178.48	-177.22		0.809 deg		1.50		0.052 deg
	Pitch	36.056	36.028	35.589		0.471 deg		0.90		0.178 deg
	ΔV	27.546	27.554	27.738		0.625 m/s		0.30		0.257 m/s
TCM 5	Roll	56.061	56.100	56.626		0.556 deg		0.95		0.06 deg
	Pitch	57.813	57.828	57.826		0.471 deg		0.004		0.12 deg
	ΔV	3.3151	3.3210	3.3696		0.080 m/s		0.60		0.01 m/s
TCM 6	Roll	-100.11	-100.80	-99.021		0.501 deg		3.56		0.046 deg
	Pitch	86.284	86.344	85.608		0.471 deg		1.56		0.018 deg
	ΔV	14.536	14.543	14.813		0.333 m/s		0.811		0.0063 m/s
TCM 7	Roll	-21.264	-21.364	-18.480		0.517 deg		5.58		0.275 deg
	Pitch	114.553	114.494	111.946		0.471 deg		5.41		0.264 deg
	ΔV	2.0139	2.0217	2	2.0841	0.053 m/s	2	1.17	0.016 m/s	
TCM 8	Yaw	0	0	-0.0652		0.370 deg		0.176		0.3084 deg
	Pitch	0	0	0.1225		0.370 deg		0.331		0.3084 deg
	ΔV	0.4842	0.4863	0.4952		0.016 m/s		0.556		0.0027 m/s
^a Roll and pitch, deg; ΔV , m/s										

within 740 km of the aim point and within 32 s of the desired closest approach time. Figure 68 (see inset) shows the flyby in relation to the post-TCM 5 statistics. Shown are the a priori statistics on the predicted flyby, the contribution to the a priori statistics from execution errors and the best estimate of the execution error vector mapped to Mercury II encounter. A comparison of the total error ellipsoid with the execution error ellipsoid shows that orbit determination errors provided the largest contribution to the total a priori statistics. However, a comparison of the perturbations (about the nominal aim point) from execution errors with the total error shows that orbit determination and execution contributed equally to the total error.

9. Mercury III Encounter

The third and final encounter of Mariner 10 was the most ambitious ever attempted, requiring precision navigation in the presence of many and varied anomalies. While the previous flybys of Venus and Mercury had each presented their own navigation problems, this mission phase presented a new and unique set of problems due to a combination of low ΔV capability, adverse spacecraft configuration, and stringent science requirements. In particular, the science return at Mercury III was highly dependent on navigation capability because the scientific value of the encounter was extremely sensitive to closest approach (periapsis) altitude. It is subsequently shown that orbit determination uncertainty was the major criterion for aim-point selection since it was a science objective to minimize periapsis altitude, maintaining impact probability acceptably small. The navigation strategy was further complicated by the requirement to track a variable period rolling spacecraft with a critical shortage of station coverage.

10. TCM 6

Soon after the second Mercury flyby it was determined that, on the uncorrected trajectory, the spacecraft would pass about 275,000 km below Mercury and, since less than 20 m/s were available, it was necessary to execute the next trajectory correction maneuver as soon as possible. Accordingly, on Oct. 30, 1974, 38 days after the Mercury II encounter (TCM 6) was performed as shown in Fig. 63.

The purpose of TCM 6 was to synchronize the orbital period of the spacecraft to approximately twice that of Mercury, thereby assuring a flyby point in the near vicinity of the planet at the third encounter. The epoch for TCM 6 was chosen to minimize the ΔV required in the presence of the 3-suns thermal constraint. Fortunately, the epochs for minimum ΔV and 3 suns were nearly coincident and negligible propellant penalty resulted from the selected epoch.

The target for TCM 6 was selected to maximize the return from the fields and particles experiment in the presence of the Earth occultation constraint, which arose due to the loss of the tape recorder shortly after the first Mercury encounter. The target for TCM 6, the Earth occultation zone and the total post maneuver

errors are shown in perspective in Fig. 73. Also shown in Fig. 73 are the total a priori 1- σ uncertainty about the nominal aim point and the orbit determination (see inset) uncertainty about the uncorrected flyby point.

TCM 6 was unique from previous maneuvers in terms of implementing the roll turn. Due to the occurrence of a bright particle acquisition on Oct. 5, 1974, resulting in the loss of approximately 109 g (0.240 lb) of attitude-control gas it was decided to inhibit the roll channel of the attitude-control system thus rendering the spacecraft to a roll attitude drift mode. The desired roll angle for the maneuver was obtained in the roll drift configuration by timing the turn from known Canopus crossings. The turn was terminated by an all-axis inertial ground command. Relative to the calibrated roll turn normally employed, the roll drift acquisition mode was considered to offer the least probability of exciting the structural interaction in the roll channel with resultant excessive loss of attitude control gas.

Table 13 presents a summary of the maneuver parameters for TCM 6. The fourth column of Table 13 lists the a priori standard deviations which were assigned to the parameters based on system models and preflight testing with the exception of the roll-turn uncertainty. This quantity was assessed by a consideration of the error sources in the implementation of the roll-drift turn.

The roll-drift acquisition offered some adaptive capability normally unavailable with the calibrated computer turn. This capability was utilized in the final selection of the commanded roll turn. During the sequence of events that led to final stabilization of the roll rate (by ground commanded solar panel and high-gain articulation) to a final value of approximately 180 μ r/s, it was found that the design maneuver at 19:00 GMT would be postponed by 2.7 h. Since the pitch turn and burn duration were to be activated through computer commands, only the roll turn adjustment was available as a means of minimizing the effect of the epoch lag, which was approximately 235 km in the B-plane. Neglecting time of flight error, a lag of 2.7 h indicated that the roll turn should be altered by -0.5 deg from a nominal value of -100.3 to a final commanded value of -100.8 deg. The result of the adjustment was to lower the B-plane error due to lag from 235 km (principally along ΔB) to 90 km normal to ΔB .

Table 12 presents a summary of the flyby conditions for TCM 6 at Mercury III. The first two columns of Table 13 show that the predicted accuracy of TCM 6 was limited by execution errors. This assessment is verified in the discussion of TCM 7 results.

11. TCM 7

Since the expected post-TCM dispersions were large with respect to the size of the target zone, the overall maneuver strategy was dependent upon the actual outcome of this maneuver. If the maneuver errors were large, then to remain within the available ΔV , a maneuver near aphelion would be required with a possible trim

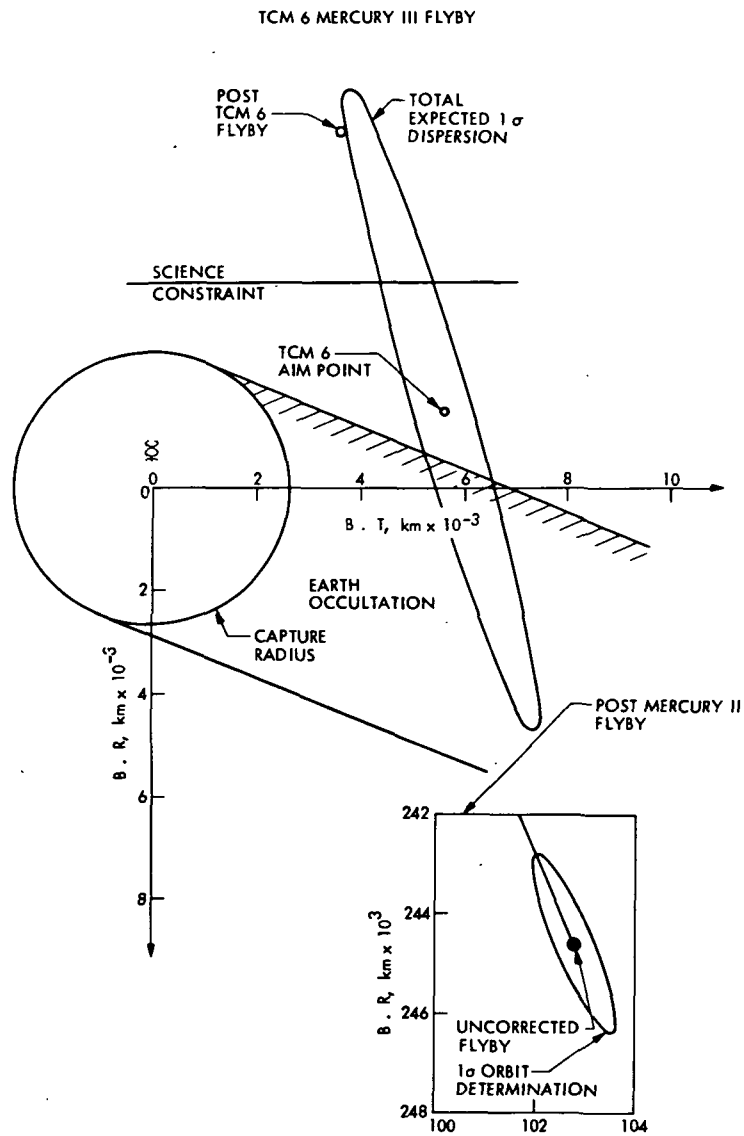


Figure 73. TCM 6 Mercury III flyby

ORIGINAL PAGE IS
OF POOR QUALITY

maneuver near the incoming 3 sun's thermal constraint boundary. If the maneuver errors were small, then a single maneuver near the incoming thermal boundary would yield the minimum closest approach distance.

After approximately one month of tracking it became clear that an excellent maneuver¹⁴ had been achieved and that the new flyby point was within 5,000 km of the target zone. Accordingly, plans for an aphelion maneuver were abandoned and the emphasis was placed on precise orbit determination for a mid-February maneuver.

On February 13, 1975, 144 days after the second Mercury encounter and near the inbound 3-suns thermal constraint boundary the seventh Trajectory Correction Maneuver (TCM 7) was performed as shown in Fig. 63. The purpose of TCM 7 was to retarget the TCM 6 flyby at Mercury III in order to maximize the return from the fields and particles experiment in the presence of the prevailing constraints. The principal engineering constraint boundaries affecting the selection of a target for TCM 6 were the capture circle (the desire to avoid impact) and the Earth occultation zone (the desire to maintain real-time communication during the flyby).

The science objectives were directed primarily toward the verification of magnetic field measurements taken at Mercury I encounter. These measurements indicated the unexpected and scientifically exciting possibility that Mercury may very well have an intrinsic magnetic field. Based upon theoretical models of the field characteristics deduced from Mercury I encounter data indicated that the third Mercury encounter should be targeted for high latitudes and minimum achievable periapsis altitude. The target for TCM 7, capture circle and total expected post-maneuver errors are shown in Fig. 74. This choice of flyby reflects an Earth occultation probability of 9% and an impact probability (after correction and no subsequent maneuvers) of 2%.

The epoch for TCM 7 reflected three principal considerations. First was the desire to provide a tracking arc of maximum length in order to reduce the TCM 7 orbit determination error to a minimum (i. e., to the same relative size as the execution errors). This consideration arose due to modeling uncertainties associated with the knowledge of the system of forces acting on the spacecraft in the rolling mode. Second was the desire not to violate the 3-suns thermal constraint. The third consideration was the available propellant at the time of TCM 7 which was estimated to be 4.4 m/s. Fortunately, the 3-suns epoch allowed a tracking arc of adequate length and in addition provided enough residual corrective capability for a "backaway sunline" maneuver in the event of an anomalous TCM 7.

Table 12 presents a summary of the flyby conditions for TCM 7 at Mercury III.

Based on the total uncertainty at the time of TCM 6 the difference between the flyby point prior to TCM 7 and the predicted flyby point after TCM 6 represents a one sigma B-plane miss at Mercury III, as shown in Fig. 73. However, when the total error (including time of flight) is considered, TCM 6 outcome was 3.6σ . This result is in close agreement with the a posteriori execution errors derived from the best estimate of the parameters as shown in Table 13. An analysis of the velocity error in terms of the total a priori maneuver uncertainty has shown that the resultant 3.6σ error was due to large turn errors which map primarily into time of flight.

Initial planning called for the execution of TCM 7 on February 12, 1975; however, due to a problem in acquiring the proper roll reference prior to the maneuver, the maneuver was delayed one day. The delay required recalculation of the entire set of maneuver parameters in a period of roughly 5 hours. TCM 7 was executed the next day on schedule; however, the doppler data received during the maneuver indicated that the burn was anomalous. This initiated an intensive period of orbit redetermination (see Sect. VII-B) which culminated in the decision to perform an additional maneuver. Concurrently efforts were made to estimate the maneuver errors during TCM 7 in order to isolate the cause of the large doppler errors and establish confidence in the ability of the spacecraft system to execute another maneuver. While this analysis effort did confirm the basic stabilizing of the spacecraft during a maneuver, the accuracy was not sufficient to isolate the TCM 7 maneuver errors. The estimates of the actual maneuver presented in Table 13 was obtained after the third Mercury flyby by mapping back from the known flyby point and including the uncertainties in TCM 8.

12. TCM 8

On March 7, 1975, nine days before the third Mercury encounter, the eighth trajectory correction maneuver was performed as shown in Fig. 63. The purpose of TCM 8 was to retarget the anomalous post-TCM 7 flyby point (30% probability of impact pre-TCM 8) using a sunline maneuver to obtain a post-maneuver impact probability of 2%.

Table 12 presents a summary of the flyby conditions for TCM 8. Based on the statistics at the time of TCM 8 a comparison of pre- and post-maneuver statistics shows that the predicted accuracy of TCM 8 was limited by orbit determination errors.

Figure 75 presents the flyby point upon which TCM 8 was computed (A), the aim point for TCM 8 (B) along with the predicted TCM 8 delivery dispersions. In addition, the actual Mercury III flyby point is shown (C) along with the reconstructed post-TCM 7 flybypoint (D). Due to both the small magnitude of the maneuver

¹⁴The maneuver was successful in terms of the B-plane flyby achieved, turn errors notwithstanding. It is subsequently shown in the discussion of TCM 7 results that large turn errors were sustained. However the trajectory dynamics and maneuver geometry were such that turn errors had virtually no range in the B-plane.

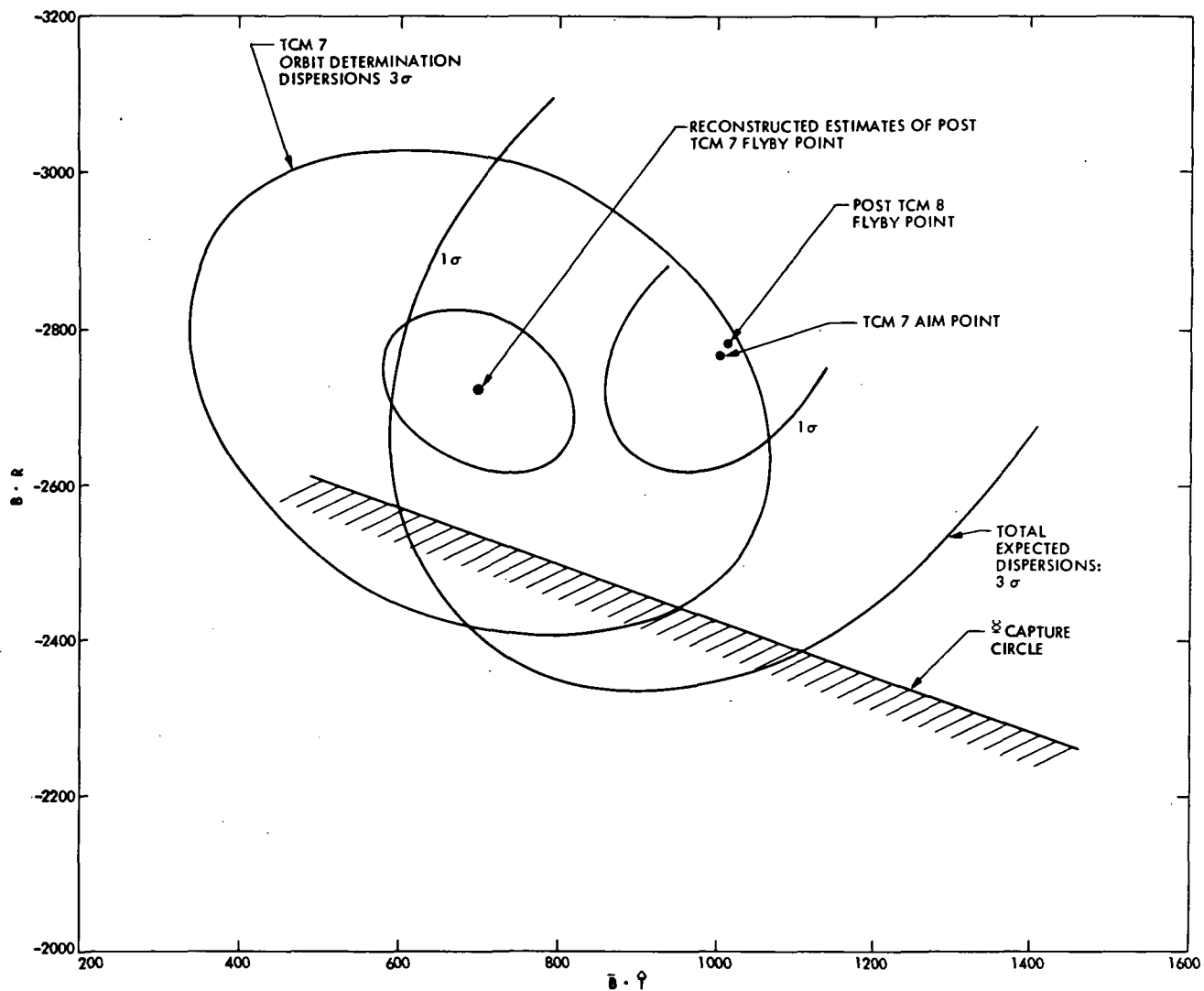


Figure 74. TCM 7 Mercury III flyby

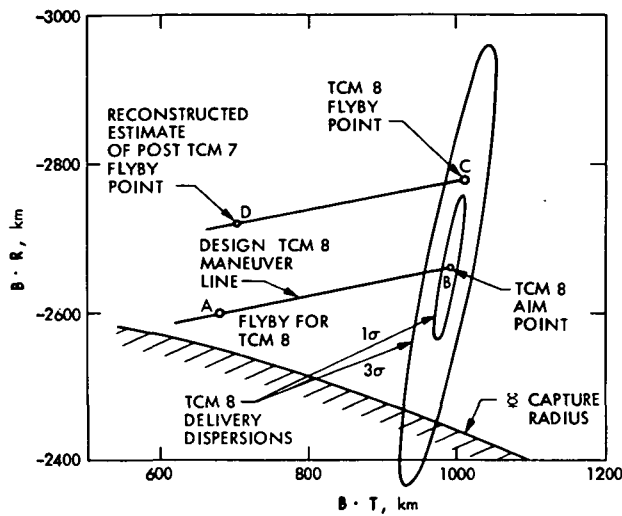


Figure 75. TCM 8 Mercury III flyby

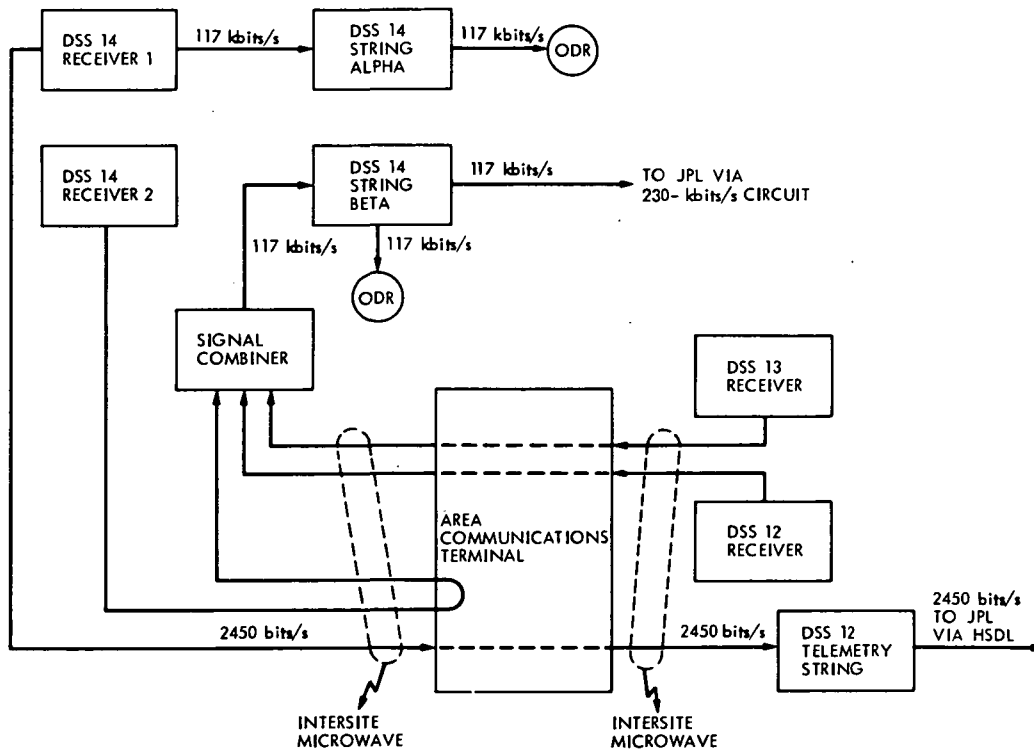


Figure 76. Goldstone DSSC antenna array block diagram

and the sunline orientation (which eliminates the pre-maneuver turns) the predominance of the error resulted from orbit determination errors. The a posteriori estimates of the maneuver are presented in Table 13.

13. Mercury III Flyby

The encounter parameters for the Mercury III flyby are presented in Table 12. The flyby was within 10 km of the TCM 7 aim point and within

1.0 s of the closest approach time for the post TCM 7 flyby. A comparison of the total error with the execution errors shows that orbit determination errors provided the largest contribution to the total a priori statistics. Based on the total error at the time of TCM 8 the best estimate of the maneuver was 1.1σ including time of flight. This result further indicates that the orbit determination statistics pre-TCM 8 were realistic and provides some confidence that the TCM 8 execution errors were nominal.

A. The Period April 15 to Oct. 15, 1974

This section covers the period from April 15, 1974 through October 15, 1974. April 15, 1974 marked the end of the MVM '73 Project and the beginning of the Mariner 10 Extended Mission Project. In addition to the Mercury second encounter (Mercury II), DSN support during this report period included other major events, such as superior conjunction and two trajectory correction maneuvers. The special antenna arraying experiment that the DSN conducted to enhance the video data quality at Mercury II is also summarized.

1. Planning Activities

Only after completion of the primary mission in early April 1974 was any significant Project or DSN attention given to Extended Mission planning. This late start, combined with the number of required critical events and the occurrence of additional spacecraft problems, placed a heavy load on DSN planners during the short six-month interval between the first and second Mercury encounters. Detailed planning was, however, satisfactorily accomplished in advance of each major event, which included the following: (1) TCM 4, (2) cruise support, (3) superior conjunction radio science, (4) TCM 5, and (5) Mercury second encounter.

2. Documentation

During April 1974, the Mariner 10 Extended Mission Project Support Instrumentation Requirements Document (SIRD) was prepared and approved by JPL. In response to this SIRD, the NASA Support Plan (NSP) was prepared and approved by JPL in June 1974. These documents covered requirements and commitments only through Mercury second encounter. The Network Operations Plan for MVM '73 was revised to incorporate new configurations and capabilities.

3. TCM 4

First priority was given to supporting the Project in planning for TCM 4. The primary concern in the DSN was in arranging for required 64-m DSS support once the date and time of TCM 4 were fixed. The Project had many factors to consider: spacecraft constraints, science return, encounter aim point, and third Mercury encounter, before finalizing the TCM design. On April 26, 1974, the DSN supported a special spacecraft gyro test conducted to determine if the roll axis oscillation would occur with the solar panels and the scan platform set in the planned maneuver configuration. No oscillation resulted. Also, spacecraft propulsion subsystem thermal constraints precluded one engine burn of the required duration; therefore, the maneuver was planned to be conducted in two parts. It was pointed out that real-time telemetry data would not be possible during the TCM unless the spacecraft high-gain antenna was adjusted to point at

Earth. However, the Project opted to give up these data in order to maintain the high-gain antenna in the April 26, 1974 test configuration during the actual TCM. These data would be recorded on the spacecraft recorder for post-TCM playback.

4. Cruise Support Plan

The Mariner Venus/Mercury 1973 primary mission had enjoyed essentially continuous tracking coverage from November 3, 1973 through April 15, 1974, via a combination of the 26- and 64-m deep space stations. This level of support could not be continued throughout the extended mission due to the higher priorities of other flight projects and DSN implementation requirements. Basically, the plan was for Mariner 10 to receive approximately two-thirds continuous coverage by a combination of full or partial passes each day. The daily coverage gap would normally occur over the Australian longitude since each of these stations was planned to be down for upgrade and repair, in a serial manner, throughout the extended mission. Therefore, it was planned that the Mariner 10 spacecraft would record non-imaging science data during coverage gaps and then play back these data via a 7.35-kbits/s dump during the next scheduled 64-m pass.

During the very first such coverage gap on April 16, 1974, analog-to-digital converter number two in the spacecraft flight data subsystem apparently failed, causing a loss of 50 of the 134 analog engineering measurements. This spacecraft failure, unlike some others, had no direct effect on the DSN. It did, however, raise some concerns regarding continuation of the partial coverage plan, but circumstances dictated a continuation in this mode. Unfortunately, the spacecraft was not long in putting an end to the record-playback plan.

On August 14, 1974, the spacecraft recorder was to serve as the data source for a ground telemetry test; however, no tape start occurred. It appeared that the recorder tape was stuck in the parking window and could not be freed. Trouble shooting continued through August 19. Some tape movement was achieved, but it then apparently became permanently jammed. The recorder was declared inoperable and turned off on August 21, 1974. This, of course, meant complete loss of data during DSN coverage gaps. Of more concern, however, was the increased potential for loss of critical event data even while tracking due to inadequate telecommunications link performance (e.g., during TCMs) or failures at the deep space stations. As a result of this loss, the DSN gave added attention to redundant configurations and backup recordings to assure recovery of data on Earth.

5. Superior Conjunction Support Plans

Mariner 10 superior conjunction activities occurred during the period May 24-June 21, 1974. Recovery of dual-frequency S/X-band doppler, range, and open-loop receiver data types was

required. In addition, it was desired that calibration tracks be provided beyond the stated interval. Since Mariner 10 provided the first opportunity for spacecraft dual-frequency analysis of solar corona and gravity effects, the DSN gave considerable emphasis to arranging proper support at DSS 14. Originally, DSS 14's Block IV S/X-band receiver was scheduled for removal and rework in preparation for Viking test support in mid-June 1974 following superior conjunction on June 6, 1974. The expanded observation period required negotiation of the removal date and was subsequently set for July 1, 1974. Support of the special Block IV receiver trouble-shooting team was planned to continue in effect until July 1, 1974.

6. TCM 5

In parallel with superior conjunction activities, the DSN assisted the Project in planning support for TCM 5. The TCM was planned to occur on July 2, 1974 over DSS 14, preceded by a gyro roll test on June 24, 1974. To avoid possible impact on DSS 14's support of the TCM, removal of the Block IV receiver was negotiated to occur on July 5 rather than July 1, 1974 as previously planned.

7. Mercury II Support Planning

Following the Project's decision in May 1974 regarding the second encounter aim point, detailed encounter support plans were able to rapidly progress. Initially, the second encounter differed in two significant ways from the first encounter: (1) the second encounter would be a Sun-side pass having no solar or Earth occultations with emphasis on additional TV coverage of Mercury; and (2) the Earth-spacecraft distance would be greater than that at first encounter, resulting in a 1-dB lower signal level in the telecommunications link.

The aim-point difference in fact made second encounter planning easier for the DSN than that for first encounter since there were no occurrences of radio science occultation and rapid signal reacquisition requirements. The spacecraft could be continuously tracked near the planet in a listen-only mode. However, the lower signal level due to the increased distance posed some critical questions and support considerations. Would real-time 117-kbits/s video still be possible at Mercury II? Or would the reduced rate of 22 kbits/s be necessary to stay above the maximum allowable bit error rate of one in thirty? Could some improvement in the DSN deep space stations be implemented to regain the "lost" decibels?

Telecommunications link analyses indicated that the bit error rate would be, at best, one in twenty and somewhat worse during much of the encounter pass at the 117-kbits/s rate. It appeared as if TV experimenters had a choice between a large number of TV frames of poor quality or a small number of high quality.

In June 1974, engineers of the DSN Communications Systems Research Section proposed that DSS antenna-arraying and signal-combining techniques might be employed to gain 0.6 to 0.7 dB.

The feasibility of this approach was pursued in a number of meetings, and the decision was made to implement an arrayed antenna capability for Mercury II. It was understood that data via this source would be provided on an engineering experiment basis in parallel with the standard configuration at DSS 14.

Tests were planned which would evaluate the array performance using actual spacecraft data during far-encounter TV sequences. The Project would decide between the standard configuration and the array on the basis of these tests. Theoretically, the arraying gain was expected to produce a bit error rate of between one in thirty and one in fifty over most of the Goldstone DSSC near-encounter passes. If achievable, this would exceed minimum requirements and provide picture quality nearly equal to that of the first encounter. This would represent a significant increase in TV science data return; consequently, priority attention was given to the experiment.

The subsequent failure of the spacecraft tape recorder in August 1974 added a significant third difference to Mercury II. There would be no preservation of high-quality TV frames on board for later playback; only what was recorded on the ground in real time would be available to experimenters. The optional record-playback mode was no longer available, and this added more importance to the arraying implementation.

DSS 43 support was also employed as a part of the second encounter TV data acquisition plan. To provide for reasonable data quality, the low-noise ultra cone was retained at DSS 43 through second encounter.

B. Program Control

The DSN continued to provide monthly inputs to the Project Management Report throughout this period. With the decision to implement the antenna arraying capability, the DSN held weekly status meetings to review progress. These meetings continued until encounter. A DSN encounter readiness review was conducted on Sept. 6, 1974, and all action items were closed prior to encounter.

C. Implementation Activities

Very little implementation activity was anticipated between Mercury first and second encounters. However, this proved to be a busy period, primarily as a result of antenna arraying and the possibility of real-time 117-kbits/s video data.

To provide tracking coverage flexibility in the Spain longitude, DSS 61 was, for the first time, configured and checked for Mariner 10 support. This also gave access to DSS 61's 20-kW transmitter for commanding during spacecraft loss-of-Canopus emergencies.

The 230-kbits/s super group communications service between DSS 14 and JPL was reinstalled and checked for encounter support. The service had been removed in the belief that real-time 117 kbits/s would not be possible during the

second encounter. The 28.5-kbits/s wideband communications service to the overseas 64-m stations was reactivated after being down in cruise for cost avoidance reasons. The DSS 14 to JPL 28.5-kbits/s circuit had been converted to 50 kbits/s in preparation for Viking test support.

Improvements were made in DSS 14's backup antenna cone-maser performance by relocation of the maser nearer the feed horn in the cone. This provided an acceptable backup to DSS 14's standard cone-maser in the event of failure. Special configurations were implemented at DSSs 14 and 43 for analog recording of integral values of video data bits at the symbol synchronizer assembly output for possible post-encounter processing and enhancement.

The proposed antenna array and signal combining experiment was successfully implemented at Goldstone and tested for encounter support. Tests with the spacecraft demonstrated achievement of the expected 0.6-0.7-dB improvement, and the decision was made to use this configuration for real-time handling of encounter data. The key characteristics of the array experiment are given in Table 14 and Fig. 76. It should be noted that DSS 13, which is not normally a flight support station, was employed as one of the arrayed stations to take advantage of its lower system temperature.

D. The Period Oct. 15, 1974 To Feb. 15, 1975

This section covers the period from Oct. 15, 1974 through Feb. 15, 1975. The primary objectives during this portion of the Extended Mission were to assure survival of the spacecraft for a third Mercury encounter through conservation of attitude-control gas and to conduct trajectory correction maneuvers as necessary to target the spacecraft for a solar occultation zone pass. Special support activities included TCMs 6 and 7 conducted on Oct. 30, 1974 and on Feb. 12-13, 1975, respectively. During this period the DSN interface organization was involved in (1) the allocation of sufficient coverage to assure accurate orbit determination solutions, (2) monitoring of DSN implementation for Viking to assure maintenance of compatible interfaces and capabilities required for Mariner 10, and (3) the development of encounter coverage, sequences, and readiness test plans.

1. Planning and Operations

During October 1974 the DSN participated with the Project in planning and preparing for TCM 6. A major effort went into obtaining sufficient tracking coverage for Mariner 10 in the face of higher priority tasks: Pioneer 10 and 11, Helios A prelaunch tests, Viking implementation, and Deep Space Station upgrades. During this period, DSS 44 was converted from the STDN to DSN configuration; DSS 14 was implemented for Viking; and DSS 63 underwent gear box repairs. Limited but adequate coverage was provided for Mariner 10. TCM 6 was accurately performed on Oct. 30, 1974, and there were no DSN support problems.

Table 14. Goldstone antenna arraying experiment key characteristics and comments

Three-station array, two 26-m and one 64-m, DSSs 12, 13, and 14, all listen-only.

DSS 12 and 13 receiver baseband output microwaved to DSS 14 for arraying experiment.

DSS 14 receiver 1 output to DSS 14 string alpha for normal 117-kbits/s processing recording.

DSS 14 receiver 2 baseband output microwaved to Goldstone area communications terminal and looped back to DSS 14 via microwave to induce signal delay nearly equivalent to DSSs 12 and 13.

Signal combiner device located in DSS 14 at microwave interface. Receives parallel input from microwave of DSSs 12, 13 and 14 baseband signal.

Signal combiner correlated and phased signals providing a combined output to the DSS 14 SDA-string beta for processing, real-time transmission to JPL, and recording.

DSS 14 string alpha did a little better than expected on the non-arrayed data.

DSS 14 string beta performed a little worse than expected on the arrayed data.

String beta appeared to be about 1/2 dB down from alpha. Arraying was hard-wired into beta; a switch would have been ideal but no time to implement. Even so, arraying gave 0.3 to 0.4 dB better performance. Had arraying been on alpha, the expected 0.8-dB gain would have been realized or exceeded.

Signal combiner worked well, no difficulties.

Promised and delivered pictures at BER of ≤ 3 in 100 for 2-1/2 h near encounter.

Low-rate data (2450 bits/s) microwaved from DSS 14 to DSS 12 for processing and transmission to JPL.

Due to spacecraft attitude-control problems and high usage of attitude control gas in October, Project placed the spacecraft in a roll-drift mode with the high-gain antenna and solar panels positioned to produce torques in the pitch, yaw, and roll axes that would minimize gas consumption. This required communications to be conducted over the spacecraft low-gain antenna and lowering of the data rate to 8-1/3 bits/s. Furthermore, the spacecraft roll mode seriously impacted the navigation accuracy achievable with the previously negotiated DSN tracking time. Project requested additional radio-metric data, particularly three-way doppler data to understand roll signatures in the doppler data and additional ranging points. Special efforts were required to

resolve the tracking coverage conflicts among the various users.

Planning for TCM 7 continued through November and early December 1974. In order to allow for a single maneuver strategy and to avoid coverage conflicts during the Helios A launch and Pioneer 11 encounter periods, TCM 7 was rescheduled from early January 1975 to Feb. 12, 1975. This permitted allocation of adequate coverage for Mariner 10 pre- and post-maneuver orbit determination activities. During this time the spacecraft continued its flight in the solar torque, roll-control mode. Following resolution of the December 1974 to February 1975 tracking allocations, full attention was given to development of a compromise plan for the March 1975 period.

On Dec. 16, 1974, the DSN met with the Mariner 10 Project to develop an understanding of essential encounter requirements, as well as the requirements of other flight projects during the March 1975 period. This meeting resulted in a significant reduction of Mariner 10's initial requirement for 8 days of continuous 64-m subnet coverage at encounter. This reduction was a key factor in permitting the DSN to draft a recommended solution to the problem. In summary, the problem was as follows:

- (1) Helios and Mariner view periods were almost entirely overlapping during March 1975.
- (2) Helios A perihelion, an event of prime interest, would occur March 15, 1975, requiring 64-m subnet coverage during the period March 5-25, 1975.
- (3) Mariner 10's Mercury encounter would occur on March 16, 1975, requiring 64-m subnet coverage during the period March 12-20, 1975.
- (4) Pioneer 11 and 10 solar conjunction would occur on March 24, 1975 and April 4, 1975, respectively, requiring 64-m subnet coverage during the period March 19 to April 4, 1975.

The problem was significantly reduced by the following:

- (1) Helios A would not use DSS 63 since coverage in this longitude is provided by the German tracking station.
- (2) Mariner 10 agreed to schedule pre-encounter critical events to occur over DSS 63. These included: (a) central computer and sequencer load for encounter (March 11, 1975), (b) Canopus reacquisition (March 13, 1975), and (c) far encounter TV calibrations and tests (March 14-15, 1975), thus leaving DSS 14 and 43 free to support other projects.
- (3) Mariner 10 reduced the encounter 64-m subnet coverage requirements to the minimum essential to recover near-encounter imaging and non-imaging data, three consecutive passes on March 16-17, (GMT).

Meetings and negotiations continued between the Flight Projects throughout January 1975 to reach agreements on detailed tracking schedules based on the proposed compromises.

By early February 1975, plans for TCM 7 were completed, and the required DSS coverage was allocated. Since the spacecraft continued in the roll-drift mode, timing of the roll by monitoring Canopus and other star crossings was critical to proper execution of the maneuver. Coverage from 64-m stations was required to acquire these data at 33-1/3 bits/s since link conditions were inadequate for communications via the 26-m stations. However, shortly before start of the maneuver sequence on Feb. 12, 1975, a change in time of the Canopus crossing was noted and the TCM was postponed until February 13.

Excellent support was provided by DSS 63. Recovery of data was continuous throughout the TCM even though a dropout had been expected due to the planned adverse pitch angle. DSS 63 accomplished two post-TCM replays of telemetry data acquired during the burn to fill gaps caused by difficulties at the data processing facility. As evidenced by greater than planned changes in the doppler data, TCM 7 was other than planned. Early indications indicated a 20% error as a result of either engine overburn, roll error, pitch error, or a combination of all of these error sources.

2. Implementation Activities

The low-noise ultra cone was maintained at DSS 43 for third encounter support. This required negotiation of the DSS 43 RF cone reconfiguration work scheduled in preparation for Viking 75. During January 1975, the SMT cone was replaced with the S-band Polarization Diversity (SPD) cone. The DSN, however, later installed the SMT maser in the SPD cone to improve system performance.

With Project agreement, it was necessary to terminate the Block III planetary ranging capability at DSS 14 in order to meet the Viking schedule for completing the Block IV configuration. If this configuration is not verified and operational by early March 1975, the Block III configuration will be restored for Mariner 10 encounter support.

The 230-kbits/s super group communications service between DSS 14 and JPL was reactivated for the third encounter. The circuit has been deactivated during cruise to avoid lease costs.

E. The Period Feb. 15 to April 15, 1975

This section covers the period from Feb. 15, 1975 through April 15, 1975, Mercury II being on March 16, 1975. Other special support activities included trajectory correction maneuver No. 8 conducted on March 7, 1975 and restabilization of the spacecraft via acquisition of the reference star Canopus. During this period the DSN was also involved in (1) assisting the Project in obtaining adequate tracking coverage, (2) monitoring DSN implementation for Viking to assure maintenance of capabilities required for

Mariner 10, and (3) conducting pre-encounter data flow tests to verify network support readiness.

1. Mission Support

a. TCM 8. Trajectory correction maneuver No. 7, conducted on Feb. 13, 1975, was not of the required accuracy. The DSN interface organization assisted the Project in negotiating additional Deep Space Station tracking time in order to rapidly and accurately determine the post-burn orbit.

Trajectory correction maneuver number eight was planned and supported on March 7, 1975. In keeping with coverage conflict resolution agreements described in paragraph D-1, TCM 8 was timed to be supported by DSS 63. This minimized impacts on other flight project support, particularly Helios A, which obtained zero-longitude support from the German tracking station. DSN support of the maneuver, as well as special post-burn radio metric data generation activities, were very satisfactory, leading to rapid verification that the required aim point had been achieved.

b. Canopus acquisition. Canopus acquisition, the next critical event prior to encounter, proved to be a delicate and difficult operation. Uncertainty in the spacecraft roll rate and less than continuous 64-m subnet coverage contributed to the acquisition problem.

Scheduled DSS 63 passes on 10, 11, and March 12, 1975 were devoted to spacecraft roll timing, and the Project's calculations indicated that the best time for an acquisition attempt fell at a time when no 64-m DSS coverage could be made available. Therefore, the Project took action to slow the spacecraft roll such that the Canopus crossing would be delayed to occur over DSS 43 where partial-pass coverage could be scheduled. However, the ensuing acquisition attempt on March 12, 1975 was not successful.

The next acquisition attempt on March 13, 1975 was also unsuccessful since the spacecraft roll rate was apparently higher than expected. Concern grew and a spacecraft emergency was declared. The DSN negotiated with the JPL Helios Project representative for release of DSS 14 and 43 for Helios A to support two Mariner 10 passes. Although Helios agreed in this one case, there was strong opposition to any further reduction in 64-m subnet coverage; to do so would seriously impact Helios prime mission objectives at perihelion on March 15, 1975. At one point, in the absence of 64-m DSS support, DSS 12 employed an experimental tracking loop of 3-Hz bandwidth in the Block III receiver to improve signal detection capabilities. This effort was successful in providing the Project critical signal level information which indicated that the spacecraft was, in fact, rolling toward a position of improved signal rather than toward a deep null. It became clear that the low-gain antenna mapping technique was not an adequate tool for Canopus acquisition.

It was decided that the spacecraft high-gain antenna, with its narrow beam and precisely

calibrated pattern, offered the best means of determining the spacecraft's position and, consequently, Canopus acquisition. This required pointing the high-gain antenna at Earth. The plan was put into effect, and DSS 42 was employed to first get a precise calibration on the roll position. Then, using the received signal level and the pattern to confirm roll position, the spacecraft was allowed to roll-drift toward Canopus. This process took place in carefully controlled steps to assure success. Signal level readouts from DSS 63 were provided every five seconds as the spacecraft rolled the last 7 deg. The reported signal levels tracked very precisely along the predicted plot. At the proper time, allowing for one-way communications, the roll-drift stop commands were sent to be received at the spacecraft while Canopus was still acquired by the Canopus tracker. The technique worked and Canopus was acquired. The spacecraft was stabilized to celestial reference, and the encounter sequence was initiated shortly thereafter.

c. DSN encounter readiness tests. As described previously, a brief but adequate test plan was designed to revalidate DSN 64-m subnet encounter support configurations and data flow capabilities. As planned, this test plan was executed in early March 1975 but not without some difficulties. Very limited DSS time was available for tests due to the higher priority activities of other projects as well as Mariner 10's critical events described above. By March 6, 1975, the situation had become critical, and special steps were taken to gain additional test time for a concentrated effort on March 7 and 8, 1975. Stations were instructed to give priority to completion of internal system performance tests. Negotiations with the Viking Project resulted in cancellation of one Viking systems integration test in order to provide DSS 14 test time for Mariner 10.

All test objectives were met by March 10, 1975, and the DSN held a brief encounter readiness review on March 13, 1975. Although the review verified that DSN preparations for encounter were adequate and complete, concern continued to be expressed regarding the limited number of test and training exercises and regarding use of the newly implemented Block IV receiver-exciter configuration at DSS 14.

In addition, it was also planned that end-to-end data flow tests would be conducted with the spacecraft following Canopus acquisition on March 12, 1975. The availability of actual spacecraft data rather than simulated data would have provided a precise demonstration. Unfortunately, these tests were canceled due to Canopus acquisition difficulties. Consequently, the DSN supported the third encounter having had the benefit of only one successful test with each supporting 64-m station.

d. Mercury III. The encounter sequence was initiated on March 15, 1975 with turn-on of the TV cameras over DSS 63. Ground commanding was required to accomplish the color TV mosaic over DSS 14. Problems at the DSS 14 Block IV exciter-transmitter interface caused command aborts during the second command of

this sequence. Action was taken to reestablish DSS 14 command capability via the Block III exciter. Although this was subsequently accomplished, the color mosaic sequence was too far behind the time line and had to be aborted.

Before further discussing DSN support for encounter and another problem associated with that support, it is important to first understand the objectives and situation. The primary objective of Mercury III was the investigation of Mercury's magnetic field and particles. The aim point was optimized to provide acquisition and return of these non-imaging data. Also, as reported previously, the third encounter offered excellent geometry for the celestial mechanics experiment through the continuous acquisition of two-way doppler data and ranging points. As a secondary objective, TV data were to be acquired at the full resolution, 117 kbits/s rate. The non-imaging 2450 bits/s science was the prime data type having priority over data for accomplishment of other objectives. Consequently, the DSN configuration was such to assure the acquisition, recording, and real-time handling of 2450 bits/s data rather than video data as on previous encounters. This meant that redundant DSN equipment and data paths were assigned to the nonimaging science rather than to video. Attention was, however, also given to the generation of radio metric data for celestial mechanics purposes and to the acquisition of TV data but not at the expense of the prime data type.

As with previous Mercury encounters, acquisition of full-resolution video data at 117 kbits/s depended upon proper operation of an experimental R&D supercooled maser ultra cone at DSS 43. This R&D ultra cone was installed at DSS 43 prior to Mercury first encounter to provide for mission enhancement well beyond that which could be gained via the standard 22 kbits/s mission. Successful use of the ultra cone on the first two Mercury encounters resulted in TV science returns well beyond expectations. R&D devices are only occasionally used in the DSN for operational support with the understanding that they are for mission enhancement purposes, for experimental tests in parallel with operations, and are provided on a best-efforts basis with spares, documentation, testing and training much less than that normally associated with operational commitments. Use of such equipment carries a higher risk of failure which must be weighed against the potential increase in returns. On MVM '73, the returns were well worth the gamble. The foregoing is offered to point out that failures in R&D equipment should not be unexpected and that such failures should not be considered as having a serious effect on primary objectives.

The DSN had problems with the R&D ultra cone supercooled maser at DSS 43 during third encounter. On March 14, 1975, word was received that the maser was not cooling down as expected. DSN maser cognizant design engineers were assigned to work with DSS 43 via voice circuit in an all-out effort to effect repairs. The maser was removed, equipped with new cross head and cleaned. JPL engineers continued coordination with DSS 43 throughout March 14-16, 1975 and provided special recommendations regarding cool-down procedures. This effort was not successful and the maser remained warm.

This activity was reported to the Project and frequent progress reports were provided in order that the Project could be ready to make a decision as encounter approached. Even with the standard cone and maser at DSS 43, two options were still open: (1) acquire 117 kbits/s video containing a high bit error rate (6 to 10 bits in error per 100) while gaining area coverage or (2) change the data rate to 22 kbits/s to acquire very high quality but quarter-frame pictures. The Project opted in favor of quality rather than quantity and flew the 22 kbits/s mission.

The DSN provided continuous, high-quality acquisition and real-time handling of the 2450 bits/s non-imaging data throughout the third encounter. Also, continuous two-way S-band doppler data were generated and periodic ranging points were acquired as required for celestial mechanics. DSS 43 performed in an excellent manner for acquisition and transmission of all 22 kbits/s video data in real time to JPL. Therefore, overall DSN support for this encounter was very satisfactory.

Following encounter, the DSN supported a number of science calibration and spacecraft engineering tests through March 24, 1975. On March 24, data received reflected that the spacecraft had depleted its attitude gas supply. Shortly thereafter, at 12:00 GMT, the command was sent to turn off the spacecraft transmitter. DSS 63 observed loss of signal one round-trip light time later indicating that the mission indeed had ended.

Table 15 summarizes some of the significant Project and DSN accomplishments and firsts which were associated with the very productive MVM '73 Mission.

Table 15. Significant project/DSN mission achievements

First multi-planet gravity assist mission
First spacecraft to photograph Venus
First spacecraft to approach and photograph Mercury
First spacecraft to have multiple encounters with target planet
First spacecraft to effectively conserve attitude control gas by the solar sailing technique
First spacecraft to successfully complete 9 TCMs
First JPL spacecraft to transmit full-resolution pictures in real time from planetary distances
First mission to use dual-frequency radio transmission
First mission to use arrayed ground station antennas to improve SNR

IX. MISSION CONTROL AND COMPUTING CENTER

A. Extended Mission Planning

MCCC planning for the extended mission started in December 1973. An examination of the Viking requirements for mission support space, computer facilities and computer time was conducted and compared to similar review of assumed MVM '73 Extended Mission project requirements for the time period of the extended mission. This was complicated by guidelines generated by the Project regarding the number of Extended Mission encounters varying in number from 1 to 3. The MCCC December plan for mission support area was reviewed by the Mission Operations System Manager and approved. Subsequent to that, Project requirements were drastically revised and within a week of that revision the MCCC had a revised MSA plan. The Extended Mission period was characterized by significant MSA perturbations as discussed below and occasional conflicts with Viking for computer resources.

B. MCCC Extended Mission Support

The MCCC provided support in the form of an MTC 1230/1219 string for telemetry processing, a single 360/75 with (occasionally) a second 360/75 for hot backup, and 1108 support.

The software in the MTC 1219 system remained unaltered during the extended mission, as it had reached a level of good stability during the prime mission. Primary concern in the 1219 support was the availability of equipment for extended missions. The primary limitation for long-term support was the availability of 1219 computers. The Viking MCCC missions operations' commitment is for all existing MCCC 1219 computers. Discussions with Viking indicated that once software development was completed, little impact between MVM '73 and Viking would occur until the start of heavy Viking integration and MOS testing. The Viking test plan indicated heavy testing would start with the mission support area beneficial occupancy date of March 15, 1975 (one day before Mercury III). An agreement was negotiated with Viking which would allow MVM '73 total usage of the 1219, 24 hours/day for a period immediately surrounding Mercury III ending on March 20 and one shift/day support to April 1.

Prior to Mercury III, judicious scheduling was necessary to minimize interaction between MVM '73 and Viking. A principal consideration in MTC support was to avoid frequent and rapid shift changes since the MTC budget covered only 1 shift/day operations. This represented a considerable problem during the early Extended Mission, but as the DSN tracking coverage became well determined, this problem disappeared.

During the period of cruise to Mercury II and III, the Project made use of a 360/75 computer for tracking data handling support and for the operation of the command sequence generation programs. During Mercury II cruise, Helios software was loaded into the 360/75 mission build and a series of Mariner/Pioneer/Helios

cohabitation tests took place. The Pioneer and Mariner Projects were concerned that a true understanding of the 360/75 software system performance could only be obtained when all projects were running under heavy simulated or real load conditions — a situation very difficult to achieve during data system integration testing.

The Helios cohabitation testing which occurred during the months of May and June 1974, was performed with only one resulting lien. It was observed that the 360/75 system backlogged when the Helios 2048 bits/s telemetry data stream was running and in addition the 360/75 was being heavily used by Pioneer Project. Support from a single 360/75 was made available to MVM 24 hours/day, 7 days/week with an additional hot backup computer during short periods of time near TCMs and encounters. 1108 computer support was similarly available 24 hours/day, 7 days/week. MVM '73 chose to schedule block time once a week on Tuesday swing shifts. On a number of occasions during the mission the Project requested prime time 1108 block time. Since it is GPCF policy to avoid prime shift block scheduling of the 1108s, MVM '73 was requested to use swing-shift time instead. The Project's requirements were satisfied by mutually negotiated compromise time periods.

C. MCCC Operations

The Extended Mission support to MVM '73 was made during the heaviest single period of activity in the history of the MCCC. During the fourth quarter 1974, for example, the MCCC supported Viking integration testing, Helios A launch, Pioneer 11 Jupiter encounter, and Extended Mission operations, including a TCM.

Prior to Mercury II and III encounters, the MCCC and the DSN conducted readiness tests to validate end-to-end data flow. The principal concern during these tests was to refresh the Operations Team capability to validate and operate the wide-band data lines and the super group data lines. These were only used during the immediate encounter periods, and inevitably it was these areas that represented the principal trouble spots during pre-encounter testing. One major MCCC readiness test was conducted prior to each encounter.

D. Mission Support Area

By the time the prime Mariner 73 mission was completed, sufficient planning for Pioneer and Viking had proceeded to the point where the MSA space occupied by Mariner had been committed to Viking and Pioneer. What resulted was the formulation of a strategy requiring Mariner to move their operations team a number of times (6) to accommodate the Pioneer and Viking MSA construction schedule. Figure 77 shows the area occupied by the Mariner 10 Extended Mission Operations teams for the majority of the Extended Mission. In some instances (TVSA Channels) reduced capability resulted because the equipment was recommitted to other projects. These

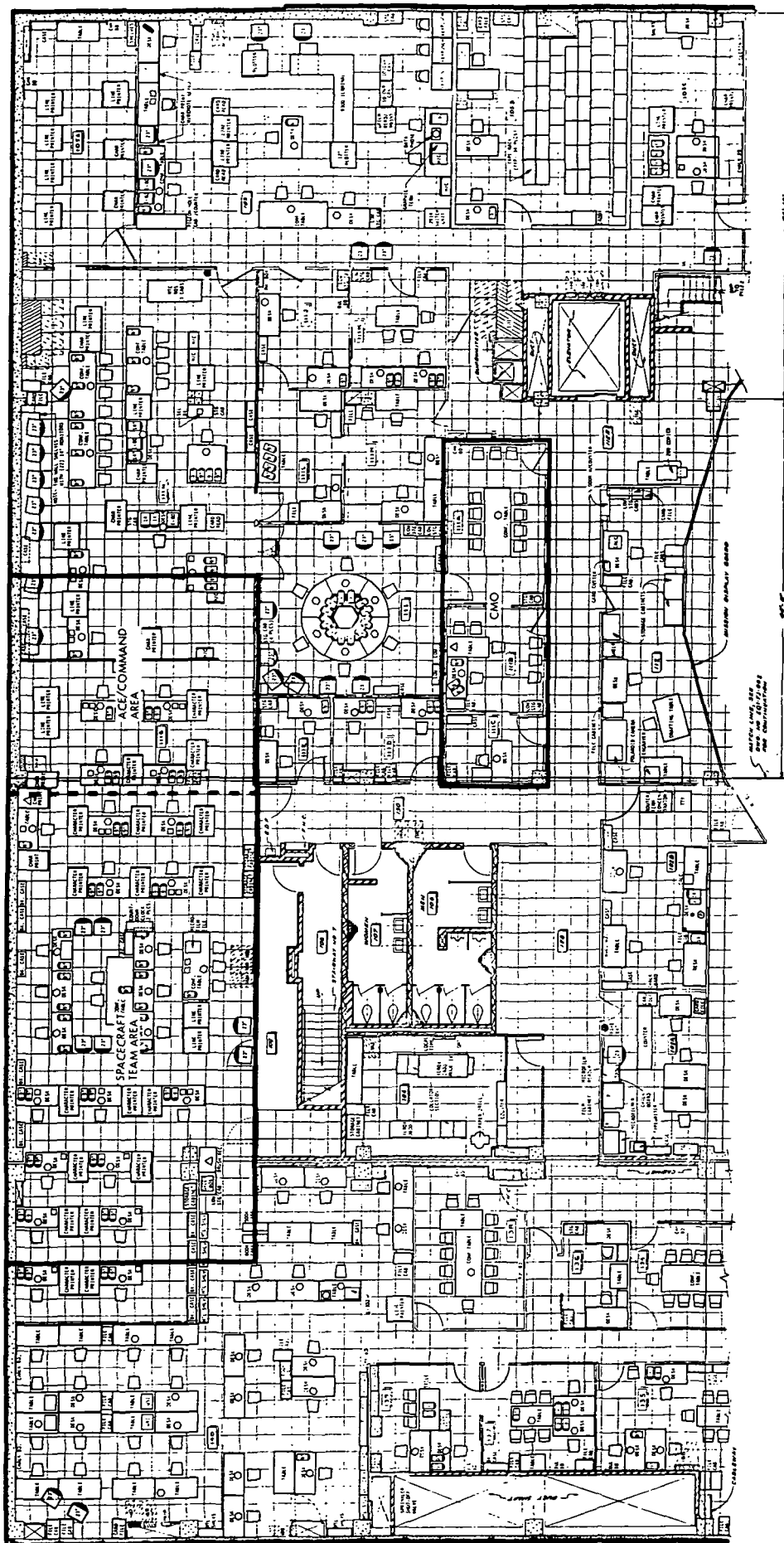


Figure 77. Mission support area layout

moves involved people, furniture, records equipment, recabling, and cable patching and eventually resulted in Mariner time-sharing the same MSA area with Viking. This was accomplished during an era when the facility was in a state of flux due to MSA occupation and utilization. Many manhours were spent in the physical moving of people and equipment together with the additional time required to revalidate the configuration after each move.

With hindsight it can be said that the expenditure of the additional manhours and the resulting increases in cost could have been avoided and a more cost-effective use of this resource brought about by sufficient premission planning for an extended mission/missions. Had this planning taken place early enough, Extended Mission MSA space and equipment requirements could have been factored into the overall laboratory plan for accommodating all the flight projects competing for laboratory resources.

E. MSA for Extended Missions

With cost effectiveness (manpower and resources) of prime consideration for the future, it would seem axiomatic to carefully consider a facility wherein extended mission activities could be performed. The functions which must be performed are known, and past experience gives us insight to what has been accomplished by a rather small dedicated team with limited resources. This facility need not be dedicated solely to performing extended mission functions. For example, software development would be a logical choice when the area was not utilized for an extended mission.

In conclusion, it is quite evident that the premission planning, not only for the prime mission, but for possible extended missions that may follow has far-reaching consequences with regard to the cost-effective use of manpower and laboratory resources.

X. DATA RECORDS

A. Science Data Team Activities

The major activities for the Science Data Team during the Extended Mission portion of the flight of Mariner 10 were the following: validation and shipment of Experimenter Data Records (EDR's); production, validation, and shipment of Supplementary Experimenter Data Records (SEDR's); development of utility programs and modification of existing data records production software to aid or make possible the production of valid SEDR's; and preparation of predicts data for and real-time support of the Mercury II and III encounters. At this writing all primary mission and Mercury II encounter data records have been processed and shipped to their respective principal investigators. Production of data records for the Mercury III encounter is dependent upon the delivery of EDRs from the MTC. Data record production activities will be complete approximately one month after receipt of the final EDR.

B. EDR Activities

These activities involve the receipt and logging of EDR magnetic tapes from the MTC, the running of EDRVAL to validate the contents of each tape, the coordination with MTC personnel for the reproduction, if possible, of EDR's with unrecoverable data content or invalid data gaps, the manufacture of individual tape logs describing EDR data content and the shipment of these data to the PI's. In addition to these activities, further processing of the magnetometer (EPIM) EDR received from the MTC must be accomplished. This tape contains not only all required EPIM data but a full complement of decommutated spacecraft engineering telemetry data as well. The tape must be input to the EDRGEN program which outputs the following three items: 1) a new EPIM EDR without the extraneous engineering data, 2) a Celestial Mechanics and Radio Science (CMRS) EDR consisting of CMRS engineering data only, and 3) a Scan Platform Telemetry (SPT) tape consisting of Guidance and Control engineering channels, which is used in the production of SEDR's. During the Extended Mission period most (all but the Venus encounter and some Earth to Venus cruise) of the primary mission and all Mercury II EDR's were handled and shipped. This amounted to approximately 2400 EDRVAL and 850 EDRGEN computer runs and the shipment of 3478 EDR's.

C. SEDR Activities

The production of SEDR's involves the accumulation of required input data and the processing of these inputs plus control information through several computer programs to obtain the desired outputs. The input data consists of spacecraft telemetry data, navigation data and command/event data files which are acquired throughout the mission based upon actual spacecraft history.

The following software is utilized to generate the input data: spacecraft telemetry data - EDRGEN, navigation data - DPTRAJ and command/events data - COMGEN. Once the

input data is accumulated, two methods of generating SEDR's are used. For CPT, PSE, magnetometer and UVS (low scan platform activity periods) SEDR's, SPOP, FIP, RFMT and COPY are run to produce the desired product. These SEDR's all have the same data content and are generally referred to as PAFUVS SEDR's. TV, UVS (high scan platform activity periods) and IRR SEDR's are produced by running SPOP, LIBPOG, and RFMT. Once the SEDR's have been produced and validated, tape logs are prepared and the tapes shipped to the appropriate principal investigators.

During the primary mission essentially no production SEDR's were produced due to the slow development of the data records portion of SPOP (processing mode) which derives limit cycle and scan platform parameters. However, during the transition period between primary and extended mission, a version of SPOP was delivered to the Science Data Team and was used to generate approximately 50% of the primary mission SEDR's. Production of the SEDR's was halted at this time to investigate some abnormal time differences between the navigation and spacecraft derived data that are merged together by RFMT to produce the PAFUVS SEDR's. The source of these time differences was traced to the fact that the navigation data was time tagged based on ephemeris time (ET), a time-base system referenced back to the epoch of 1950.0, while the spacecraft data was referenced to GMT or universal time (UTC). The time difference between these two systems (~45 s) was contained within the navigation data and a minor modification to RFMT was required to use this time difference to convert the ET to UTC so that proper merging of navigation and spacecraft data could be accomplished. While investigating this anomaly, two other errors related to timing were uncovered. First, the RFMT algorithm which converts navigation time (total seconds from the epoch of 1950.0) into units of year, day, hour, minute, second and millisecond was incorrect and all time tagging of navigation data in this manner was invalid. Second, inconsistent timing of spacecraft clock values on the SEDR was discovered and traced back to both the MTC and SPOP. The MTC based all of its engineering data time tagging upon spacecraft clock values (FDSC) and minor frame counter in the science frames (SCI).

During periods of spotty or invalid data the science frame was often incorrect and led to incorrect time tagging by the MTC resulting in minor frame time duplications and regressions. SPOP was programmed to receive and process data on a FDSC basis rather than a minor frame basis (4 minor frames/FDSC) and the time tagging of partial FDSC's (less than 4 minor frames) was often incorrect. A decision was made at this point in time that all SEDR's produced to date should be reproduced after accomplishing modifications to RFMT to amend its timing problems and the development of a utility program designed to rectify MTC and SPOP timing problems. Utilizing this new utility program (STUFF) and the new version of RFMT, all primary mission SEDR's were produced and sent to the principal investigators. However, toward the end of this

production phase, it became apparent that more serious problems in SPOP concerning scan platform pointing angles existed.

An investigation in this area was conducted by the Science Data Team and the result was that approximately 50% of the TV and UVS SEDR's that had been produced contained scan platform pointing errors. It was apparent that to correct these problems, a modification to SPOP would have to be made. Therefore, all known problems with SPOP were tabulated and were systematically corrected and tested with Division 91 programming support. A similar approach was then taken with the PAFUVS SEDR production portion of RFMT. The RFMT modification was undertaken due to the almost certainty of a Mercury III encounter in 1975 and the fact that the RFMT time algorithm for navigation data would not handle the year 1975. During the modifications of SPOP and RFMT, the utility program, STUFF, was expanded to include a representation for each FDSC of data. FDSC's in data gaps would be represented by four (4) minor frames of filler data with correct time tags, while the missing portions of partial FDSC's would also be represented by correctly time-tagged filler data. This would insure that SPOP would not have to perform any time tagging during data gaps and for partial FDSC's.

Utilizing the new program set, the SEDR's containing scan platform pointing errors (TV and UVS) were reproduced and all Extended Mission SEDR's were produced through Mercury II encounter. This same program set is expected to be adequate to produce all the SEDR's required for the Mercury III encounter. In all, for the Extended Mission period from April 16, 1974 until present, the Science Data Team made the following approximate number of runs, including an estimate for reruns, of the SEDR production software: 300 SPOP, 150 FIP, 200 LIBPOG and 500 RFMT.

D. Mercury II and III Predicts

These activities involved obtaining predicted navigation data for the encounter and processing these data to produce navigation data dumps, SEDR's containing navigation data only and predicted fixed instrument (all but TV and UVSA) pointing vectors in the Earth Mean Equatorial (EME) epoch of 1950.0 coordinate system. For Mercury II predicts 3 data dumps and 3 SEDR's were produced. Due to a loss of expertise in the transition from primary to extended mission, the Science Data Team was unable to produce any meaningful EME pointing data for this encounter. However, due to the similarity between these data from encounter to encounter, and the fact that

this encounter was mainly for the TV experiment, the principal investigators were able to use the Mercury I data for their purposes. During the production of predicts for the Mercury III encounter, the SDT regained EME pointing vector prediction capability and for this encounter the PI's were supplied with a full complement of predicts data based upon the applicable predicted navigation data. These data amounted to 2 navigation data dumps, 2 SEDR's and two EME pointing vector listings.

E. Real-Time Support of Mission Activities

The Science Data Team provided real-time support of the Mercury II and III encounters. The activities in this area included checkout and verification of data links to provide real-time encounter data to PI's at remote sites, the scheduling of computer time for PI near real time processing at JPL, the validation of quick look EDR's received from the MTC and the generation of quick-look magnetometer EDR's as required. These services were also provided during other portions of the mission as required by the PI's. Other real-time or near real-time activities included the generation of daily science data logs and command logs, maintaining a list of significant spacecraft science events and the generation of spacecraft clock value (FDSC) versus spacecraft event (SCE) time tables for the entire mission.

F. Recommendations

- (1) Flexibility should be built into non-critical mission software such as the SEDR production program set so that the programs involved can be updated and made available for production on a short turn-around basis without having to go through the bureaucracy of a mission build concept system.
- (2) The project should require maintenance support for interdivision software (software that is developed by one division and used by another) so that the user division will have an effective means of updating software as required during the mission.
- (3) Software users should be educated at least to the functional level as to the operation of his software tools and be able to absolutely verify the validity of the software execution by quickly analyzing the outputs.

REFERENCES

1. Whitehead, P. B., "Consequences of Failure of FDS ADC No. 2," IOM MVM 73-2-280, April 19, 1974 (JPL internal document).
2. Whitehead, P. B., and Messner, A., "Possible Causes of FDS ADC No. 2 Failure," IOM MVM 73-2-282, May 20, 1974 (JPL internal document).
3. Becker, R. A., "Mariner 10 Temperature Control Performance, L + 110 Days Through L + 165 Days," IOM 3533 MVM-74-046, June 18, 1974 (JPL internal document).
4. Garcia, R. D., "Mariner 10 Temperature Control Performance, L + 166 Days Through L + 500 Days," IOM 353 MVM-75-48, May 13, 1975 (JPL internal document).
5. Cowley, R. T., "Mariner 10 Propulsion Subsystem Performance During TCM 4a and b," July 19, 1974 IOM MVM 73-74-839 (JPL internal document).
6. Cowley, R. T., "Mariner 10 Propulsion Subsystem Performance During TCM 5," MVM 73-74-840, July 18, 1974 (JPL internal document).
- *7. Cowley, R. T., "Mariner 10 Propulsion Subsystem Performance During TCM 6," IOM MVM 384-74-850, Nov. 13, 1974 (JPL internal document).
- **8. Cowley, R. T., "Mariner 10 Propulsion Subsystem Performance During TCM 7 and 8," IOM MVM-73-851, March 31, 1975 (JPL internal document).
9. Bullock, G., "MVM '73 Tape Recorder Failure," IOM 3631-74-224, Dec. 6, 1974 (JPL internal document).
10. Turk, W., Ranger Program Attitude Control - Block III, Technical Report 32-663, Jet Propulsion Laboratory, Pasadena, Calif., Dec. 11, 1964.
11. Schumacher, L., "MVM 73 Extended Mission Gas Usage and Strategy," April 30, 1974 (JPL internal document).
12. Messner, A., and Whitehead, P. B., "MVM 73-FDS End-of-Mission Test," IOM MVM 73-2-285, Nov. 6, 1974 (JPL internal document).
13. Hooke, A., "Mariner 10 Tape Recorder Failure," IOM 3645-75-164, Sept. 5, 1974 (JPL internal document).
14. Christensen, C. S. and Reinbold, S. J., "Navigation of the Mariner 10 Spacecraft to Venus and Mercury," AIAA Paper No. 74-844, presented at Anaheim, California Conference, Aug. 5 to 9, 1974.
15. Bantell, M. H., and Jones, J. B., "Navigation Results of the Mariner Venus/Mercury 1973 Mission," AIAA Paper No. 74-84, presented at Pasadena, California Conference, Jan. 20 to 22, 1975.
16. Christensen, C. S., et al., "Final Orbit Determination Strategy and Accuracy, Mariner Venus-Mercury," 1973 (JPL internal document).
17. Bierman, G. J., "Computation Aspects of Discrete Sequential Estimation," 1974 (JPL internal document).
18. Moyer, T. D., "Mathematical Formulation of the Double-Precision Orbit Determination Program (DPODP)," Technical Report 32-1527, Jet Propulsion Laboratory, Pasadena, Calif., May 15, 1971.
19. "DSN System Requirements, Detailed Interface Design," Document 820-13, Rev. A, (JPL internal document).
20. Kock, R. E., et al., "Conditioning of MVM '73 Radio-Tracking Data," AIAA Paper 74-832, presented at Anaheim, Calif., Aug. 5 to 9, 1974.
21. Spradlin, G., and Schlaifer, R., "The Planetary Operational Ranging Subsystem (PRA)," IOM 4216-75-019, Jan. 30, 1975 (JPL internal document).
22. Yip, K. W., et al., "Dual Frequency Demonstration During Superior Conjunction," EM 391-619, Feb. 7, 1975 (JPL internal document).
23. Howard, H. T., et al., "Mercury: Results on Mass, Radius, Ionosphere, and Atmosphere from Mariner 10 Dual-Frequency Radio Signals," Science, Vol. 185, 1974.
24. Sturms, F. M., Polynomial Expressions for Planetary Equators and Orbit Elements with Respect to the Mean 1950.0 Coordinate System, Technical Report 32-1508, Jet Propulsion Laboratory, Pasadena, Calif., 1971.

*These numbers are those actually typed on the memo. The correct number is MVM 73-74-850.

**The correct number is MVM 73-75-851.

BIBLIOGRAPHY

- Anon, "Mercury Revisited by Mariner 10," Sky and Telescope, Vol. 49, No. 5, May 1975.
- Beatty, J. K., "Mariner 10's Second Look at Mercury," Sky and Telescope, Vol. 48, No. 5, Nov. 1974.
- Danielson, G. E., Jr., "Our Present View of Mercury and Venus," Reviews of Geophysics and Space Physics, Vol. 13, No. 3, Aug. 1975.
- Dunne, J. A., "The Mariner 10 Venus Encounter: A Review," Endeavor, Vol. 109, 1975.
- Dunne, J. A., "Mercury," The 1976 McGraw-Hill Yearbook of Science and Technology.
- Giberson, W. E., and Cunningham, N. W., "Mariner 10 Mission to Venus, XXV Congress, International Astronautical Federation, Amsterdam, Oct. 1974.
- Guest, J., "Mercury," The Solar System, New Scientist Special Review, pp. 12-16, 1975.
- Klaasen, K. P., "Mercury's Rotation Rate," Journal of Geophysical Research, July 1975.
- Murray, B. C., "First Look at Mercury," Engineering and Science, Vol. 38, pp. 30-33, Oct./Nov., 1974.
- Murray, B. C., "Mercury," Scientific American, Sept. 1975.
- Ness, N. F., et al., "Magnetic Field of Mercury Continued," Nature, Vol. 255, pp. 204-205, 1975.
- Ness, N. F., et al., "The Magnetic Field of Mercury, Part I," Journal of Geophysical Research, Vol. 80, pp. 2708-2716, 1975.
- O'Leary, B., "Venus, Vertical Structure of Stratospheric Hazes from Mariner 10 Pictures," Journal of Atmospheric Science, June 1975.
- Prinn, R. G., "Venus: Composition and Structure of the Visible Clouds," Science, Vol. 182, Dec. 14, pp. 1132-1135, 1973.
- Strom, R. G., "The Planet Mercury as Viewed by Mariner 10," Sky and Telescope, Vol. 47, No. 6, 1974.
- Weaver, K. F., "Mariner Unveils Venus and Mercury," National Geographics, Vol. 147, No. 6, June 1975.
- Various authors, "Conference on the Atmosphere of Venus," Journal of Atmospheric Physics, special issue, Vol. 37, June 1975.
- Various authors, "Mariner 10 Mercury Encounter," Science, Vol. 185, July 12, pp. 141-188, 1974.
- Various authors, "Mariner 10 Venus Encounter: Results," Science, Vol. 183, Mar. 29, pp. 1289-1321, 1974.
- Various authors, "The Planet Mercury," Journal of Geophysical Research, special issue, Vol. 80, June 10, pp. 2341-2514, 1975.

1. Report No. 33-734, Vol. II	2. Government Accession No.	3. Recipient's Catalog No.	
4. Title and Subtitle MARINER VENUS-MERCURY 1973 PROJECT FINAL REPORT EXTENDED MISSION -- MERCURY II AND III ENCOUNTERS		5. Report Date December 1, 1975	6. Performing Organization Code
		8. Performing Organization Report No.	
7. Author(s) JPL Staff		10. Work Unit No.	
9. Performing Organization Name and Address JET PROPULSION LABORATORY California Institute of Technology 4800 Oak Grove Drive Pasadena, California 91103		11. Contract or Grant No. NAS 7-100	
		13. Type of Report and Period Covered Technical Memorandum	
12. Sponsoring Agency Name and Address NATIONAL AERONAUTICS AND SPACE ADMINISTRATION Washington, D.C. 20546		14. Sponsoring Agency Code	
15. Supplementary Notes			
16. Abstract This report describes the Mariner Venus/Mercury 1973 mission operations Extended Mission. Prepared by the Mission Operations Team, this report encapsulates the activities from shortly after Mercury I through the end of mission. The operational activities are reported by Mission Operations Systems functions providing a brief summary from each discipline. Based on these experiences, recommendations for future projects are made.			
17. Key Words (Selected by Author(s)) Mariner Venus/Mercury 1973 Project		18. Distribution Statement Unclassified -- Unlimited	
19. Security Classif. (of this report) Unclassified	20. Security Classif. (of this page) Unclassified	21. No. of Pages 115	22. Price

HOW TO FILL OUT THE TECHNICAL REPORT STANDARD TITLE PAGE

Make items 1, 4, 5, 9, 12, and 13 agree with the corresponding information on the report cover. Use all capital letters for title (item 4). Leave items 2, 6, and 14 blank. Complete the remaining items as follows:

3. Recipient's Catalog No. Reserved for use by report recipients.
7. Author(s). Include corresponding information from the report cover. In addition, list the affiliation of an author if it differs from that of the performing organization.
8. Performing Organization Report No. Insert if performing organization wishes to assign this number.
10. Work Unit No. Use the agency-wide code (for example, 923-50-10-06-72), which uniquely identifies the work unit under which the work was authorized. Non-NASA performing organizations will leave this blank.
11. Insert the number of the contract or grant under which the report was prepared.
15. Supplementary Notes. Enter information not included elsewhere but useful, such as: Prepared in cooperation with... Translation of (or by)... Presented at conference of... To be published in...
16. Abstract. Include a brief (not to exceed 200 words) factual summary of the most significant information contained in the report. If possible, the abstract of a classified report should be unclassified. If the report contains a significant bibliography or literature survey, mention it here.
17. Key Words. Insert terms or short phrases selected by the author that identify the principal subjects covered in the report, and that are sufficiently specific and precise to be used for cataloging.
18. Distribution Statement. Enter one of the authorized statements used to denote releasability to the public or a limitation on dissemination for reasons other than security of defense information. Authorized statements are "Unclassified-Unlimited," "U.S. Government and Contractors only," "U.S. Government Agencies only," and "NASA and NASA Contractors only."
19. Security Classification (of report). NOTE: Reports carrying a security classification will require additional markings giving security and downgrading information as specified by the Security Requirements Checklist and the DoD Industrial Security Manual (DoD 5220.22-M).
20. Security Classification (of this page). NOTE: Because this page may be used in preparing announcements, bibliographies, and data banks, it should be unclassified if possible. If a classification is required, indicate separately the classification of the title and the abstract by following these items with either "(U)" for unclassified, or "(C)" or "(S)" as applicable for classified items.
21. No. of Pages. Insert the number of pages.
22. Price. Insert the price set by the Clearinghouse for Federal Scientific and Technical Information or the Government Printing Office, if known.